Modulation of PrP Aggregation and Cellular Prion Transfer

Fontaine, Sarah

Award date:
2010

Awarding institution:
University of Bath

Modulation of PrP aggregation and cellular prion transfer

Sarah Nicole Fontaine

A thesis submitted for the degree of Doctor of Philosophy

University of Bath

Department of Biology and Biochemistry

March 2010

Table of Contents

Table of Figures 6

Table of Tables 10

Acknowledgements 11

Abstract 12

Abbreviations Used 14

1. Introduction 17

1.1 Transmissible spongiform encephalopathies 17

1.2 The cellular prion protein, PrP^{C} 19

1.3 Functions of PrP^{C} 21

1.3.1 PrP^{C} functions in cellular signalling, processing, and survival 21

1.3.2 PrP^{C} and metals 22

1.4 PrP^{Sc} 26

1.5 Conversion of the prion protein to the disease-associated form 28

1.5.1 Kinetic theories of prion conversion 28

1.5.2 Prion aggregation models 28

1.5.3 Structural changes of conversion 29

1.5.4 Mutations to PrP and conversion 30

1.5.5 Additional factors affecting conversion 32

1.6 Transmissibility, neuroinvasion, and neurodegeneration 33

1.7 Aims 37

2. Materials and Methods 39

2.1 Materials 39

2.2 Molecular Biology Techniques 39

2.2.1 Preparation of DNA 42

2.2.2 Polymerase chain reactions 43

2.2.3 Agarose Gel Electrophoresis 44

2.2.4 Gel Purification 44
2.2.5 Restriction Enzyme Digests 45
2.2.6 Vector preparation 45
2.2.7 Phosphorylation of PCR products 46
2.2.8 Preparation of intermediate vector for blunt-ended ligations 46
2.2.9 Ligation Reactions 47
2.2.10 Preparation of calcium competent cells 48
2.2.11 Transformation of DNA into *Escherichia coli* 48
2.3 Cell Culture Methods 50
2.3.1 General cell culture: routine maintenance of cell lines 50
2.3.2 Cryopreservation of cell lines 51
2.3.3 Transfection 52
2.3.4 MTT Assay for cell viability 53
2.3.5 MTS Assay for cell viability 54
2.3.6 Preparation of Chelex Treated Media 54
2.3.7 Infectious inoculate preparation 55
2.3.9 Cell Blot Assay for detection of proteinase K resistant PrP 57
2.3.10 Preparation of samples for SDS-PAGE analysis 58
2.3.11 Bio-Rad method for protein concentration determination 59
2.3.12 SDS-PAGE 59
2.3.13 Western blot 61
2.3.14 Coomassie Blue staining 63
2.3.15 Densitometry analysis of Western blots 63
2.4 Recombinant Protein Techniques 64
2.4.1 Expression of recombinant mPrP constructs 64
2.4.2 Bacterial Cell Lysis 64
2.4.3 Purification of recombinant PrP 65
2.4.4 Refolding 67

2.4.5 Dialysis....69
2.4.6 Concentration Determination....70
2.4.7 Preparation of recombinant samples for SDS-PAGE analysis....71
2.4.8 Aggregation Assays....71
2.4.9 Transmission Electron Microscopy....72
2.4.10 Isothermal Titration Calorimetry....72
2.4.11 Computation peptide analysis....75
2.5 Statistical Analyses....76
3. Metals and cellular prion infection....77
3.1 Introduction....77
3.2 Method Development....79
3.2.1 Infected brain homogenates as infectious source....79
3.2.2 Infection by live cell co-culture....82
3.2.3 Infection by infected cell homogenates....85
3.2.4 PrP null cell line expressing mPrP....89
3.3 Role of metals in transfer of prion infectivity in cell culture....91
3.3.1 Viability of cells in Chelex media....91
3.3.2 Cellular infectivity assay and metals....92
3.4 Metal transporter proteins in prion disease....95
3.5 Discussion....97
3.5.1 Development of prion infectivity assays....97
3.5.2 Metals and prion infectivity....99
4. Metals and PrP Aggregation....102
4.1 Introduction....102
4.2 Results of cloning, expression, and purification of PrP constructs....103
4.3 Method Development....106
4.4 Aggregation of mPrP(23-231)....109
4.4.1 Self-seeding capabilities of mPrP(23-231)....111

4.4.2 Effect of metals on mPrP(23-231) aggregation 112
4.5 Aggregation of truncated and deletion mutant mPrP 114
4.5.1 Computational analysis of mPrP aggregation propensity 115
4.5.2 Aggregation of mPrP(23-231) versus truncated and deletion mutant mPrP 117
4.5.3 Aggregation of truncated mPrP(89-231) with metals 119
4.5.4 Aggregation of deletion mutants of PrP with metals 121
4.6 Aggregation of metal binding point mutations of mPrP 128
4.6.1 Computational analysis of metal-binding point mutations 129
4.6.2 Aggregation of mPrP(Null+H95), mPrP(Null+H110), mPrP(Null+H95, H110) and mPrP(Null) 129
4.6.3 Aggregation of mPrP(H95A+H110) 130
4.7 Conclusion and Discussion 132
5. Glycosaminoglycans in PrP aggregation and cellular infection 137
5.1 Introduction 137
5.2 Heparin binding to mPrP 138
5.2.1 ITC binding results for mPrP(23-231) 139
5.2.2 ITC binding results for mPrP(Δ51-89) 142
5.2.3 ITC binding results for mPrP(89-231) 143
5.2.4 Heparin binding to mPrP(H95A+H110A) and mPrP(Null) 147
5.2.5 Effect of copper on heparin binding to mPrP 150
5.2.6 Binding of other glycosaminoglycans to mPrP 152
5.3 Heparin and PrP aggregation 153
5.3.1 Deletion and truncation mutations of PrP 155
5.4 Heparin and cellular prion infection 156
5.5 Discussion 160
5.5.1 GAGs and PrP binding 160
5.5.2 GAGs and PrP aggregation 162
5.5.3 GAGs and prion infectivity 162

5.5.4 Future directions....163
6. Discussion....164
6.1 Summary of results....164
6.3 PrP aggregates, metals, and glycosaminoglycans....165
6.2 Oligomeric PrP, Toxicity and Infection....165
6.3 Mechanisms of Oligomer Toxicity and Neurodegeneration....167
6.4 Future directions and conclusions....170
References....174
Appendix I....224

Table of Figures

Figure 1.1. Schematic representations of murine *Prnp* gene and murine PrP^C.....20

Figure 2.1 Schematic representation of pcDNA3.1+-mPrP(1-254).....39

Figure 2.2. Schematic representation of mPrP constructs used for recombinant protein expression.....42

Figure 3.1 Western blot of Proteinase K resistant PrP in infected brain homogenates.....80

Figure 3.2 Western blot of PrP^C expression in N2a cells.....81

Figure 3.3 PK-resistant PrP in N2a(mPrP) and SMB cells.....82

Figure 3.4 Cell blot from brain homogenate infectivity assay, analysed 4 passages post infection.....82

Figure 3.5 Western blot of co-culturing assays with SMB-PS(mPrP) cells.....83

Figure 3.6 Live cell co-culture infectivity assays.....85

Figure 3.7 Infection by SMB homogenate.....87

Figure 3.8 Cell blot analysis of ScN2a(mPrP) infectivity assay.....88

Figure 3.9 Cell blot of infectivity assay with un-transfected N2a cells as target cells and ScN2a(mPrP) homogenate.....89

Figure 3.11 Cell blots of Zpl(mPrP) and Zwl infectivity assays.....90

Figure 3.12. Viability of N2a(mPrP) cells in Chelex-treated media determined by MTS assay.....91

Figure 3.13. Viability of N2a(mPrP) cells in Chelex-treated media with 100 µM $CuSO_4$, $MnSO_4$ or $ZnCl_2$ added determined by MTT assay.....92

Figure 3.14 Effect of Chelex-treated media on transfer of prion infectivity.....93

Figure 3.15 Representative cell blots of infectivity assays with metals.....94

Figure 3.16 PrP expression is unaffected by over expression of copper transporting proteins.....96

Figure 3.17 Cell blot of infectivity assay of N2a cells over-expressing ATOX1, CCS, CTR1, and CTR2 in a FLAG-tagged vector.....97

Figure 4.1 Expression trial showing induction of mPrP expression in BL21 *E.coli*....104

Figure 4.2 Examples of mPrP(23-231) purification and refolding.....105

Figure 4.3 Coomassie staining of SDS-PAGE analysis of refolded mutant mPrP proteins.....105

Figure 4.4 Western blot analysis of post-refolded mPrP proteins.....106

Figure 4.5 Optimisation of mPrP aggregation as assessed by ThT fluorescence.....108

Figure 4.6 Variability in mPrP(23-231) maximum fluorescence values.....109

Figure 4.7 Representative graph of recombinant mPrP(23-231) aggregation.....110

Figure 4.8 Negatively stained TEM image of mPrP(23-231) aggregate end products from aggregation reactions.....111

Figure 4.9 Aggregation of seeded mPrP(23-231) reactions.....112

Figure 4.10 Aggregation of mPrP(23-231) with 100 µM metals as monitored by ThT fluorescence.....113

Figure 4.11 Western blots of aggregate end products of mPrP(23-231).....114

Figure 4.12 WALTZ-predicted amyloidgenic regions in mPrP.....116

Figure 4.13 TANGO-predicted values for mPrP deletion and truncation mutant aggregation.....117

Figure 4.14 Initial rate and maximum fluorescence of no-metal mPrP aggregation...118

Figure 4.15 Aggregation of mPrP(89-231) with 100 µM metals as monitored by ThT fluorescence.....120

Figure 4.16 Representative Western blot of aggregate end products of mPrP(89-231) aggregation with and without metal.....121

Figure 4.17 Aggregation of mPrP(Δ51-89) aggregation with 100 μM metals as monitored by ThT fluorescence.....123

Figure 4.18 Western blots of aggregate end products of mPrP(Δ51-89).....124

Figure 4.19 Aggregation of mPrP (Δ67-90) aggregation with 100 μM metals as monitored by ThT fluorescence.....125

Figure 4.20 Western blots of aggregate end products of mPrP(Δ67-90).....126

Figure 4.21 Aggregation of mPrP(Δ106-126) with the addition of 100 μM metals as monitored by ThT fluorescence.....127

Figure 4.22 Western blots of aggregate end products of mPrP(Δ106-126).....128

Figure 4.23 TANGO-predicted values for metal-binding point mutation mPrP aggregation, compared to wild type mPrP(23-231).....129

Figure 4.24 Representative aggregation reaction of mPrP(Null) monitored by ThT fluoresescence.....130

Figure 4.25 Rate and maximum fluorescence of no-metal mPrP(H95A+H110A) aggregation as monitored by ThT fluorescence.....131

Figure 4.26 Western blot analysis of aggregation end products without metals.....132

Figure 5.1 Heparin binding of mPrP deletion and truncation mutations overlaid with previously published heparin binding regions.....139

Figure 5.2 Representative ITC binding isotherm for mPrP(23-231) and heparin.....141

Figure 5.3 Representative ITC binding isotherm for heparin binding to mPrP(Δ51-89).....143

Figure 5.4 Representative heparin binding isotherm for mPrP(89-231).....144

Figure 5.5 Comparison of binding isotherms of mPrP(23-231), mPrP(Δ51-89) and mPrP(89-231).....145

Figure 5.6. Heparin binding of mPrP histidine to alanine mutations overlaid with previously published heparin binding regions.....147

Figure 5.7 ITC isotherm of heparin binding to mPrP(H95A+H110A).....148

Figure 5.8 Representative ITC isotherm of mPrP(Null) binding to heparin sodium sulphate.....149

Figure 5.9 Charge distribution of mPrP(23-231), mPrP(H95A+H110A) and mPrP(null).....150

Figure 5.10 Effect of copper on heparin binding to mPrP(23-231).....151

Figure 5.11 Representative ITC isotherms of dextran sulphate binding to mPrP.....153

Figure 5.12 Aggregation of mPrP(23-231) with heparin.....154

Figure 5.13 Western blots of aggregate end products of mPrP((23-231).....155

Figure 5.14 Initial rate and maximum fluorescence of mPrP(Δ51-89) aggregation in the presence of varying concentrations of heparin.....156

Figure 5.15 Cell blot of infectivity assay of N2a(mPrP) with heparin.....157

Figure 5.16 Effect of heparin sulphate on PrP^{C} expression.....159

Table of Tables

Table 2.1 Mammalian protein expression constructs.....39

Table 2.2. Bacterial mPrP constructs.....41

Table 2.3 G418 concentrations required for stably transfected cell lines.....53

Table 2.4 Starting seeding densities for infection assay experiments.....56

Table 2.5 Antibody dilutions used in Western blotting.....62

Table 2.6 Yeilds of mPrP protein preparations..... 68

Table 2.7 Recombinant PrP parameters.....70

Table 5.1 Log K_a and number of binding sites for mPrP binding to heparin.....142

Acknowledgements

First I wish to thank my supervisor, Professor David R. Brown, for the opportunity to work in his laboratory, and his supervision and guidance throughout this Ph.D.

Next I would like to thank the members of the Brown Lab, both past and present. Special thanks to Dr Jo Wright for all her help, support, and unfailing encouragement throughout my Ph.D. Also, I wish to thank Dr Sarah Webb for help and support during the first year, and special thanks to Dr Cathryn Haigh for help, support, and brain storming despite distant locales. Thank you also to Kay, Paul, Scarlet and Dima, all of whom offered help and support whenever needed. I definitely enjoyed working with you during my time at Bath.

I'd also like to thank the great people I've met within the department who have helped to make my experience at Bath memorable and enjoyable, while there are too many to name special thanks need to go to Lab 1.33 not just for help and support but for drinking coffee with me and letting me borrow things! I would like to thank Dr Karl Payne in particular for his unfailing help, support and advice throughout, and for always cheering me up when I needed it. Thanks also to Mike Cowley, not only for putting up with me in our first year but also for being a great friend.

I would like to add a special thanks to Sara Poorfarhani and Dr. Joel Ybe for their help with the finishing stages of the thesis. Their help was generously offered and greatly appreciated.

I could not have come this far without the constant support and love from my family. I cannot thank you enough for your encouragement, your faith in me and for loving me despite how far away I am. Thank you for visiting me and for bringing me home to visit as well! It has not been easy being away, but without your support I would not have been able to do it. Special thank you to Mom and Dad for all your computer expertise! So thank you to Mom, Dad, Beccah, Bob, Grandma, and Grandpa.

Last but certainly not least, many, many thanks to Tom. Actually listing everything you've helped me with, from computer problems to driving me to and from work, even at weekends, would surely take far too many pages. I can only say thank you for all

your support, encouragement, and constant reassurance, and for putting up with me when I was a grumpy moo.

Abstract

Transmissible spongiform encephalopathies are fatal neurodegenerative diseases which affect many mammals, including humans. A unique feature involves the conversion of the prion protein (PrP) to an abnormal isoform. Previous studies indicate interconversion of PrP is associated with the binding of metals and glycosaminoglycans (GAGS) such as heparin. However, the impact of metals or heparin on the formation of disease-related PrP forms is not well understood. To determine whether metals and GAGs play a role in transfer of prion infection, a cell culture infection model was developed. Data from these studies show that prion infectivity was reduced with depletion of metals, but enhanced with the addition of heparin. Isothermal titration calorimetric experiments, a novel method to study heparin-PrP interactions, were performed to further classify heparin binding regions of PrP. Four sites were identified, and mutation analysis confirmed that at least two sites are located within the first 90 residues of the N-terminus. Finally, to address whether the effects seen in the cellular infection model were due to PrP-metal or PrP-GAG interactions, a aggregation method was developed to characterise recombinant PrP under physiologically relevant conditions. This is important to do as many *in vitro* prion conversion studies are performed in conditions not seen *in vivo* including extreme temperature or pH or in the presence of denaturants. The results of these studies showed that metals are able to significantly increase the conversion of PrP mutants containing deleted regions within the octameric repeat domain. In contrast, no significant promotional effect was seen with the heparin aggregation experiments. This result suggests a possible explanation of the cell culture data is that other cellular interactions besides PrP-heparin associations must be considered to fully account for these findings. This body of work establishes that PrP interactions with metals and glycosaminoglycans play a role in transmissible spongiform encephalopathies through prion conversion.

Abbreviations Used

bovine serum albumen (BSA)

bovine spongiform encephalopathy (BSE)

calcium chloride ($CaCl_2$)

carbon dioxide (CO_2)

cellular prion protein (PrP^C)

Celsius (C)

centimetre (cm)

central nervous system (CNS)

chronic wasting disease (CWD)

circular dichromism (CD)

Congo Red (CR)

copper (II) sulphate ($CuSO_4$)

Creutzfeldt-Jakob Disease (CJD)

dendritic cells (DC)

deoxynucleotide (dNTP)

deoxyribonucleic acid (DNA)

divalent metal transport protein 1 (DMT-1)

Dulbecco's Modified Eagle Medium (DMEM)

Eagle's Minimum Essential Medium (EMEM)

endoplasmic reticulum (ER)

ethanol (EtOH)

ethylenedinitrilotetraacetic acid (EDTA)

fatal familial insomnia (FFI)

follicular dendrite cells (FDC)

Fourier-transform infrared spectroscopy (FTIR)

Gerstmann-Sträussler-Scheinker disease (GSS)

glycosaminoglycan (GAG)

glycosylphosphatidylinositol (GPI)

gut-associated lymphoid tissues (GALT)

hour/hours (h)

immobilised metal affinity chromatography (IMAC)

isothermal titration calorimetery (ITC)

Kelvin (K)

kilodalton (kDa)

litre (L)

Luria-Bertani broth (LB)

magnesium (II) chloride ($MgCl_2$)

magnesium (II) sulphate ($MgSO_4$)

manganese (II)sulphate ($MnS0_4$)

messenger ribonucleic acid (mRNA)

microgram (µg)

microlitre (µL)

micrometre (µm)

micromolar (µM)

milligram (mg)

millilitre (mL)

millimetre (mm)

millimolar (mM)

minutes (min)

molar (M)

molecular weight (MW)

murine prion protein (mPrP)

nanogram (ng)

nanometre (nm)

Neuro2a cell (N2a)

Neuro2a over-expressing mPrP (1-254) (N2a(mPrP))

neuronal cell adhesion molecules (NCAMs)

nuclear magnetic resonance (NMR)

octameric repeat (OR)

open reading frame (ORF)

phosphate buffered saline (PBS)

polymerase chain reaction (PCR)

prion protein (PrP)

prion protein gene (*Prnp*)

proteinase K (PK)

pentosan sulphate (PS)

revolutions per minute (rpm)

ribonucleic acid (RNA)

scrapie infected Neuro2a cells over-expressing mPrP(1-254) (ScN2a(mPrP))

scrapie mouse brain cell (SMB)

scrapie prion protein (PrP^{Sc})

seconds (s)

signalling molecule stress-inducible protein 1 (STI1)

scrapie mouse brain cells cured with pentosan sulphate (SMB-PS)

sodium chloride (NaCl)

sodium dodecyl sulphate (SDS)

sodium dodecyl sulphate polyacrylamide gel electrophoresis (SDS-PAGE)

sodium hydroxide (NaOH)

sporadic Creutzfeld-Jakob Disease (sCJD)

Thioflavin T (ThT)

transmissible mink encephalopathy (TME)

transmissible spongiform encephalopathy (TSE)

transmission electron microscopy (TEM)

ultraviolet (UV)

un-translated region (UTR)

variant Creutzfeldt-Jakob Disease (vCJD)

volume/volume (v/v)

weight/volume (w/v)

zinc (II) chloride ($ZnCl_2$)

1. Introduction

1.1 Transmissible spongiform encephalopathies

Transmissible spongiform encephalopathies (TSEs) are a group of neurodegenerative disorders that are thought to be caused by the misfolded prion protein. These disorders affect humans, sheep, goats, cattle, mink, deer, elk, felines both domestic and wild, and wild ruminant species.

TSEs were originally thought to be caused by a slow virus until recent evidence which has shown that this is not the case. Despite extensive work, the disease agent could not be classified as a nucleic acid nor have attempts to isolate the infectious particle been fruitful. Evidence supporting the hypothesis that the causative agent was a protein (Griffith, 1967) was provided by the discovery that the scrapie agent persisted despite treatment to inactivate nucleic acids (Alper *et al.*, 1966, 1967; Haig and Clarke, 1968; Latarjet *et al.*, 1970). Further work done by Bolton *et al.* identified a major component of the scrapie agent to be a sialoglycoprotein (Bolton *et al.*, 1982), which in turn led to the more specific characterization that the agent responsible for inducing disease state was a proteinaceous infection particle labeled "prion" (Prusiner, 1982). This so called "prion theory" suggests that an abnormal conformation of the prion protein is responsible for transmission and propagation of TSEs. This theory is now widely, although not universally, accepted (Manuelidis, 2007) and has changed scientific interpretation of certain neurodegenerative diseases, including Parkinson's disease and Huntington's disease, as essentially protein conformation disorders.

Human prion diseases can arise through inherited mutations, acquired (iatrogenic) means, or sporadically. Human diseases include Creutzfeldt - Jakob disease (CJD), variant Creutzfeldt-Jakob Disease (vCJD), kuru, Gerstmann-Sträussler-Scheinker disease (GSS), and fatal familial insomnia (FFI). CJD was first described by Creutzfeldt and Jakob in 1920 (Spielmeyer, 1922). CJD occurs throughout the world and the majority of these occurrences are sporadic in origin, although 10-15% of all cases are thought to be inherited. GSS and FFI arise from autosomal dominantly inherited mutations of the prion protein, with the most commonly seen mutation a proline to leucine substitution at amino acid 102 in GSS and substitution of asparagine for aspartic acid at position 178 in FFI. There are over 20 described mutations of PrP

which lead to prion diseases (Collinge, 2001). Transmissible causes of CJD have been attributed to iatrogenic means such as insufficiently decontaminated surgical instruments, dura matter grafts, cadaver derived human growth hormone, and blood transfusions (Brown, 2005; Llewellyn *et al.*, 2004). A newly described variant version of CJD (vCJD) is thought to arise from consumption of BSE-contaminated meat products (Will *et al.*, 1996; Hill *et al.*, 2000). Kuru, a disease which affected the South Fore people of New Guinea, is thought to have been spread through their practice of ritualistic cannibalism (Gajdusek, 1957).

The clinical signs of human prion diseases differ depending on disease type, but overall symptoms include depression, insomnia, behavioural changes, progressive cerebellar ataxia, and cognitive decline (dementia). Pathology includes widespread spongiform change, gliosis, and neuronal loss. Additionally in kuru and GSS abundant amyloid plaques are present. Inherited prion diseases have long incubation periods. In the case of sporadic CJD, age of onset is generally in the 5^{th} or 6^{th} decade of life, and 70% of patients die within 6 months. In contrast, vCJD has an altered pathology with a mean age of onset of 27 years of age (range 12-72 years), and length of incubation period anywhere from 4-30 years. Clinical disease duration of vCJD ranges from 9 to 35 months. GSS has longer mean disease duration of 5 years, but an earlier age of onset (in the 3^{rd} to 4^{th} decade). Kuru disease progresses anywhere from 3 months to 3 years, with a mean duration of 12 months, and age of onset is anywhere between 5 to 60 years. Disease progression occurs more quickly in children (Collinge, 2001; Collins *et al.*, 2001).

While the incidence of prion disease in humans is generally low, the emergence of vCJD in the 1990s brought prion diseases into the mainstream. Data from the UK national CJD surveillance unit indicate that while the known total deaths from vCJD are estimated at 164, the number of vCJD annual deaths has decreased since peaking in 2000. Worldwide figures show a total of 217 cases of vCJD, including 6 patients who are still alive. While vCJD is very rare, a common risk factor was living in the UK between the years 1980-1996.

The worldwide average occurrence of CJD, the most common human prion disease, is an incidence of 1 case per million, with an average annual mortality rate of 1.31 deaths per million (data from the EUROCJD project). In the UK, in the past five years, the average number of deaths from prion diseases including sporadic, iatrogenic, and

familial CJD, GSS and vCJD is 83 (NCJDSU, 2009). Despite the rarity of these diseases, the transmissible and nucleic-acid free nature of infectious agent, along with similarities to other neurodegenerative diseases highlight the need for further study.

Besides humans, several mammalian species are also known to contract TSEs. Scrapie, a TSE which affects sheep and goats, has been known to be in existence for several hundred years (McGowan, 1918). Scrapie was shown to be transmissible to goats in the early 20th century (Cuille and Chelle, 1936). Prion diseases affecting other animals were subsequently described, including bovine spongiform encephalopathy (BSE) which affects cattle (Wells, 1987); chronic wasting disease (CWD) which affects deer and elk (Williams and Young, 1980); and transmissible mink encephalopathy (TME) which affects wild and farmed mink (Marsh and Hadlow, 1992). Wild and domestic felines are affected by feline spongiform encephalopathy (Wyatt *et al*, 1991; Willoughby *et al.*, 1992) and wild and zoo ungulates can also contract a spongiform encephalopathy (Jeffrey and Wells, 1988; Kirkwood *et al.*, 1990).

1.2 The cellular prion protein, PrP^C

The cellular prion protein, PrP^C, is encoded from a single gene, *Prnp* (Oesch *et al.*, 1985). The *Prnp* gene is located on chromosome 20 in humans and on chromosome 2 in mice. I Murine *Prnp* consists of three exons, with the entire coding sequence found in the third exon as shown in Figure 1.1A(Hsiao *et al.*, 1987; Basler *et al.*, 1988). PrP expression is controlled by the *Prnp* promoter (Goldman *et al.*, 1993) and PrP mRNA is expressed throughout the body, although the highest expression levels are found in the central nervous system (CNS) and in particular neurones (Chesebro *et al.*, 1985; Oesch *et al.*, 1985; Kretzschmar *et al.*, 1986). PrP^C concentrations range from 40 to 700 µg per gram of total protein in the CNS (Bendheum *et al.*,, 1988; Pan *et al.*,, 1992).

Murine PrP^C is 254 amino acids long and consists of two signal sequences that are cleaved during cellular processing (see Figure 1.1B). After synthesis, the protein is directed to the endoplasmic reticulum (ER), where residues 1-23 of the N terminus form a signal sequence which interacts with the Sec61 translocon (Chakrabarti and Hegde, 2009). Within the ER, PrP^C is post-translationally modified by the addition of two asparagine-linked oligosaccharides, addition of a glycosylphosphatidylinositol (GPI) moiety at the C-terminus around amino acid residue 230, and correctly folded (Haraguchi *et al.*, 1989; Endo *et al.*, 1989; Stahl *et al.*, 1990; Yost *et al.*, 1990; Chakrabarti and Hegde, 2009). The protein is then trafficked to the Golgi apparatus,

where glycan and GPI anchor modification takes place. PrP^C is attached to the membrane via the GPI anchor at the cell surface. The synthesis process takes about 30 minutes. Once the mature PrP^C is at the cell surface, the protein is internalised, possibly via clathrin-coated pits, membrane rafts, or caveoli (Taylor *et al.*, 2007; Sunyach *et al.*, 2003; Shyng *et al.*, 1994; Galvon *et al.*, 2005). The protein is then either recycled to the cell surface or sent to lysosomal/endosomal compartments for degradation. Total cycling times are estimated between 3-6 hours (Borchelt *et al.*, 1990; Shyng *et al.*, 1993).

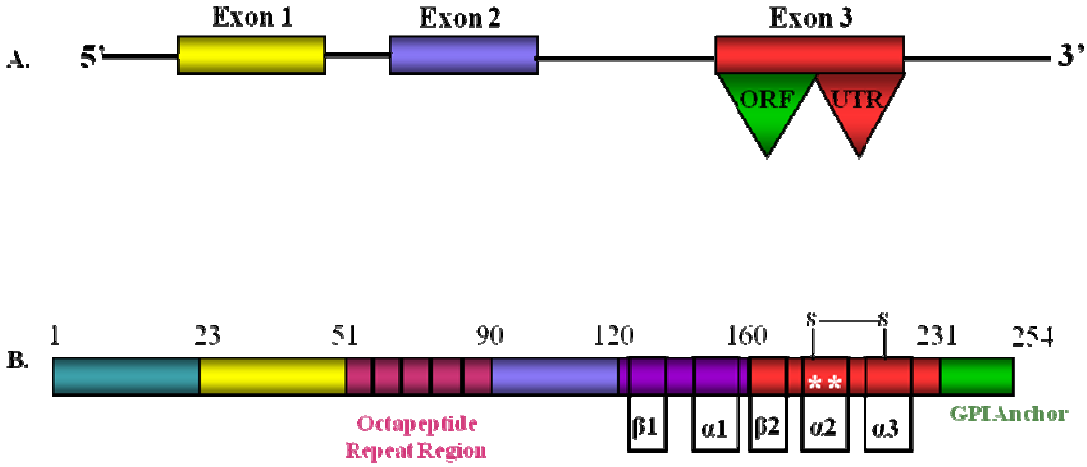

Figure 1.1. Schematic representations of murine *Prnp* gene and murine PrP^C. A) Murine *Prnp* consists of three exons, with the entire open reading frame (ORF) residing in exon 3 along with an untranslated region (UTR). B) Murine PrP^C is 254 amino acids long with a N-terminal signal sequence of 22 amino acids that is cleaved during proteolytic processing. Structural elements within the C-terminal domain include 2 β-sheets (β1 128-131 and β2, 161-164) and three α-helices (α1, 144-154; α2, 179-193; α3, 200-217). A disulfide cysteine bridge links residues 179 and 214 and there are two asparagine linked glycosylation sites located at residues 180 and 196, represented by asterisks,

PrP^C has a highly conserved nucleic acid sequence of the N-terminal tail between mammalian species (Rivera-Millar *et al.*, 2006). Structural studies using Fourier-transform infrared spectroscopy (FITR), circular dichromism (CD) spectroscopy and nuclear magnetic resonance (NMR) spectroscopy and have shown that PrP^C consists of flexible N-terminal region spanning residues 23-125, containing five copies of the octameric repeat PHGGGWGQ in the N-terminus. The C-terminus consists of 2 short β-sheets and 3 α-helices with a disulfide bridge linking cysteine residues 179 and 214, and in the murine protein there are two asparagine linked oligosaccharides at residues 180 and 196 (Riek *et al.*, 1996, 1997; Donne *et al.*, 1997; Zahn *et al.*, 2000).

1.3 Functions of PrP^C

The precise function of PrP^C has not yet been agreed although many hypotheses exist regarding the normal function.

The development of transgenic $PrP^{-/-}$ animals highlighted potential functions for PrP. $PrP^{-/-}$ animals have altered synaptic function (Collinge *et al.*, 1994), circadian rhythms (Tobler *et al.*, 1996), motor function (Katamine *et al.*, 1998; Nazor *et al.*, 2007), memory (Büeler *et al.*, 1992), copper metabolism (Brown *et al.*, 1997) and impaired response to oxidative stress (Brown *et al.*, 1997; Klamt *et al.*, 2001; Wong *et al.*, 2001a,c). These altered phenotypes have led to several hypotheses regarding the normal function of PrP^C.

1.3.1 PrP^C functions in cellular signalling, processing, and survival

A role for PrP^C in cellular signalling arose from evidence suggesting the PrP^C was capable of binding to several proteins which have a role in cell signalling pathways. Grb2 and casein kinase 2 have both been shown to interact with PrP^C and these proteins have been shown to play a role in cell signal transduction (Spielhaupter and Schatzl, 2001). In addition, the signalling molecule stress-inducible protein 1 (STI1) has been shown to bind PrP^C, and upon endocytosis mediate signal transduction via protein kinase A (PKA) and ERK 1/2 pathways (Zanata *et al.*, 2002; Lopes *et al.*, 2005; Americo *et al.*, 2007; Caetano *et al.*, 2008). It has also been shown that PrP^C-mediated signalling by P59Fyn kinase can modulate cellular survival although current data does suggest the involvement of another intermediate component (Mouillet-Richard *et al.*, 2000; Santuccione *et al.*, 2005). While the precise mechanism is unknown, PrP^C has been shown to modulate the cAMP/PKA pathway (Martins *et al.*, 1997; Chiarina *et al.*, 2002). Other potential signalling pathways that PrP^C may play a role in involve tyrosine kinases, protein kinase C, as well as the PI3 kinase/Akt pathway (Schnieder, *et al.*, 2003; Stuermer *et al.*, 2004; Botto *et al.*, 2004; Santuccione *et al.*, 2005; Kanaani *et al.*, 2005, Vassallo *et al.*, 2005; Weise *et al.*, 2006; Krebs *et al.*, 2006).

Hypotheses that PrP^C may function in cellular processing including cellular adhesion arose from studies which show PrP binds to neuronal cell adhesion molecules, or NCAMs (Manson *et al.*, 1992; Schmitt-Ulms *et al.*, 2001; Santuccione *et al.*, 2005). Additionally PrP^C may have a role in neuronal and non-neuronal cell proliferation (Cashman *et al.*, 1990; Mabbott *et al.*, 1997; Mazzoni *et al.*, 2005), neuronal cell differentiation (Mobley *et al.*, 1988; Graner *et al.*, 2000 a,b; Chen *et al.*, 2003;

Santuccione *et al.*, 2005; Kanaani *et al.*, 2005), and cell cycle regulation (Satoh *et al.*, 2000; Liang *et al.*, 2007).

A potential role for PrP^C in cellular survival and/or protection has also been suggested following evidence that PrP^C interacts with Bcl-2, an anti-apoptotic molecule as well as inhibiting Bax-mediated death (Kurshner and Morgan, 1995; Roucou *et al.*, 2003; Chen *et al.*, 2003; Kanaani *et al.*, 2005). Conversely, however, it has been shown the PrP^C may increase sensitivity of cells to staurosprine-induced death with increased caspase 3 activity (Paitel *et al.*, 2002). However, PrP^C also seems to play a protective role in other cellular stress situations, including hypoxic ischaemia as PrP^C expression is up-regulated following an ischaemic insult (McLennon *et al.*, 2004; Weise *et al.*, 2004, 2006; Sakurai-Yamashita *et al.*, 2005; Shyu *et al.*, 2005), as well as after other stress conditions such as heat shock and hypoglycaemia (Shyu *et al.*, 2000, 2004). Further protective roles have been suggested including the theory that PrP^C can act as an antioxidant as studies have shown that PrP^C is able to detoxify superoxides (Brown, 1999; Brown *et al.*, 2001; Cui *et al.*, 2003; Treiber *et al.*, 2007; Stanczak *et al.*, 2007) and that altering levels of PrP^C induces changes to superoxide dismutase levels and vice versa (Brown and Besinger, 1998; Kralovicova *et al.*, 2009).

1.3.2 PrP^C and metals

A link between metals and prion diseases was proposed when Pattinson and Jebbett identified a similarity in brain lesion profiles of mice treated with the Cu^{2+} chelator cuprizone to those of scrapie infected mice (Pattison and Jebbett, 1971a,b). Since then several studies have shown PrP is capable of metal binding and there is evidence that copper, manganese, zinc, and iron have a further role in prion biology (Hornshaw 1995 a, b; Brown *et al.*, 1997, 2000; Whittal *et al.*, 2000; Jackson *et al.*, 2001; Thompsett *et al.*, 2005; Leach *et al.*, 2006; Pushie *et al.*, 2007; Davies *et al.*, 2009). Furthermore it has been demonstrated that the levels of some metals are altered during disease progression (Wong *et al.*, 2001b; Thackray *et al.*, 2002b), and that metals, in particular copper and zinc, are involved in PrP endocytosis (Pauly and Harris *et al.*, 1998; Brown and Harris, 2003).

1.3.2.1 Copper

PrP^C isolated from brains has copper bound (Brown *et al.*, 2001), and in the absence of PrP^C, synaptosomal preparations have decreased copper levels when compared with wild type controls (Herms *et al.*, 1999; Brown, 2003). Exposure to copper has been

shown to increase and modulate the expression of PrP in cells (Brown *et al.*, 1997; Hijazi *et al.*, 2003; Varella-Nallar *et al.*; 2006; Toni *et al.*, 2005) and in cells lacking PrP^C copper uptake is decreased (Brown, 1999, 2004). Further evidence shows that dietary copper can affect PrP^C expression (Mitteregger *et al.*, 2009; Kralovicova *et al.*, 2009), and other proteins involved in copper metabolism are differentially expressed in mice during prion disease progression depending on PrP expression levels (Kralovicova *et al.*, 2009).

The N-terminus (residues 23-125) of PrP binds copper ions within the octameric repeat region (residues 51-90 mouse sequence) and at an additional site within the N-terminus (Hornshaw, 1995 a, b; Brown *et al.*, 1997, 2000; Viles *et al.*, 1999; Aronoff-Spencer *et al.*, 2000; Jones *et al.*, 2004; Thompsett *et al.*, 2005). Copper binding to PrP has been demonstrated by a variety of methods and binding affinities vary largely from femtomolar to micromolar although recent evidence suggests binding is likely within the nanomolar range at pH 7.4 (Nadal *et al.*, 2009). PrP-copper binding involves copper-histidine interactions, as identified by Raman spectroscopy (Mihauser *et al.*, 1999), and PrP binds five or possibly six copper ions within the N-terminal region of PrP. It is thought that there are 4 binding sites within the octameric repeat region and another binding site centred around His95, His110 (His96/His111 in human PrP) (Klewpatinoid *et al.*, 2008; Davies *et al.*, 2009). There are reports of copper binding elsewhere on PrP, including within the C-terminus at two sites involving His187 and potentially aspartic or glutamic acid residues (Cereghetti *et al.*, 2001). There are also reports of non-specific binding during high copper concentrations at acidic pH (Davies and Brown, 2008). Furthermore it has been suggested that copper may bind via methionine residues within the central domain, at residues Met109, Met112 (Shearer *et al.*, 2008).

PrP-copper binding is thought to involve cooperativity, although the exact binding coordination is unknown. There are many models of copper binding cooperativity: three-nitrogen and one oxygen (3N1O) coordination involving three nitrogens (one imidazole and two glycines) and an oxygen from carbonyl of the last glycine, or four nitrogen (4N) coordination (Chattopadhyay *et al.*, 2005; Davies and Brown, 2008). Binding coordination is dependent on copper occupancy and pH. Within the octameric repeats, the maximum copper occupancy (one copper ion per PHGGGWGQ repeat) occurs at pH 7.4 and is thought to have 3 nitrogen-1 oxygen (3N1O) coordination (del Pino *et al.*, 2007; Davies *et al.*, 2009).

Copper binding to PrP may play an important role in the normal function of PrP, and there is much evidence that points to copper involvement in prion biology. Additionally, copper binding in the octameric repeat region induces endocytosis of the prion protein in response to physiological concentrations of copper (Pauly and Harris, 1998; Perera and Hooper, 2001; Brown and Harris, 2003; Haigh *et al.*, 2005). Deletion of the octameric repeat region ablates copper-induced endocytosis and alterations of the numbers of octameric repeat sequence differentially regulates the copper-induced endocytosis effect (Pauly and Harris, 1998; Perera and Hooper, 2001; Haigh *et al.*, 2005). Expanded octapeptide repeat regions, similar to those seen with GSS, do not result in copper-mediated endocytosis (Krasemann *et al.*, 1995). Endocytosed PrP is delivered to early endosomes and Golgi (Brown and Harris, 2003) and copper mediated endocytosis occurs via a clathrin-mediated mechanism (Madore *et al.*, 1999; Sunyach *et al.*, 2003; Taylor *et al.*, 2005).

Disease associated forms of PrP have an inability to be retained in copper-loaded resin (Sakaguchi *et al.*, 1996; Thackray *et al.*, 2002b; Hijazi *et al.*, 2003) and purified PrP from prion-infected brains have decreased levels of bound copper. Analysis of blood, CNS, and other tissues from prion-infected animals show a decrease in copper levels by as much as 50% (Wong *et al.*, 2001b; Thackray *et al.*, 2002b; Hesketh *et al.*, 2007, 2008). Further, high concentrations of copper can reduce PrP^{Sc} accumulation in cells (Hijazi *et al.*, 2003). In support of this, it has been shown that high doses of copper can delay disease onset in prion-infected hamsters (although at highly toxic concentrations) and that copper chelators can alter the onset of disease (Hijazi *et al.*, 2003; Sigurdsson *et al.*, 2003). This evidence suggests a definite role for copper in prion biology.

PrP has also been shown to bind manganese, zinc, nickel, iron, cobalt, and other metals with much lower affinity than copper (Brown et al., 2000; Whittal et al., 2000; Jackson et al., 2001; Leach et al., 2006; Pushie et al., 2007; Kenward et al., 2007; Walter et al., 2007; Davies et al., 2009). Although some studies have shown that PrP is capable of binding copper and manganese concurrently (Brown et al., 2000), copper has been shown to be the preferential metal binding partner within the octameric repeat region (Stockel et al., 1998; Pushie et al., 2007).

1.3.2.2 Manganese

Several studies have shown levels of manganese are altered in both animals and humans infected with prion diseases (Wong *et al.*, 2001b; Thackray *et al.*, 2002b;

Hesketh *et al.*, 2007, 2008; Mitteregger *et al.*, 2009). Brains from sCJD patients showed a ten-fold increase in manganese levels, and PrP purified from these brains had manganese bound (Wong *et al.*, 2001b). Furthermore, in blood and the CNS of prion-affected animals (cattle, sheep, and mice) manganese levels were increased (Thackray *et al.*, 2002b; Hesketh *et al.*, 2007, 2008). These studies have led to the suggestion that increased manganese levels could potentially be used as a marker for prion disease (Wong *et al.*, 2001b; Hesketh *et al.*, 2008).

PrP binds manganese at two sites within the N-terminus of the protein: a high affinity site centred on His95 (murine numbering) and a low affinity site in the octameric repeat region (Brazier *et al.*, 2008). The binding affinities of PrP to manganese are similar to other manganese-binding proteins, such as DMT-1, a known manganese transporting protein (Brown, 2009).

1.3.2.3 Zinc

PrP has been shown to bind zinc, although with lower affinity than copper (Whittal *et al.*, 2000; Brown *et al.*, 2000; Jackson *et al.*, 2001; Qin *et al.*, 2002; Walter *et al.*, 2007; Kenward *et al.*, 2007; Davies *et al.*, 2009). Zinc binds at two sites within the octameric repeat region, one site with micromolar affinity and one site with millimolar affinity. PrP may additionally bind zinc within the His95/His110 region in the absence of the octameric repeat region (Davies *et al.*, 2009). Zinc binding is only possible at low copper concentrations, as PrP preferentially binds copper (Walter *et al.*, 2007). Zinc binding has been shown to promote PrP-PrP interaction (Kenward *et al.*, 2007).

As with copper, zinc can induce endocytosis of PrP (Watt *et al.*, 2003; Brown and Harris, 2003). Recently it was shown that PrP can protect against zinc-mediated toxicity by modifying metallothionien and intracellular zinc levels (Rachidi *et al.*, 2009).

1.3.2.4 Nickel, iron and other metals

Studies suggest that PrP is able to bind other metals including nickel, iron, cobalt, palladium, and platinum although the reported affinities for these metals is very low and binding would inevitably be outcompeted by copper binding (Jackson *et al.*, 2001; Pushie *et al.*, 2007; Davies *et al.*, 2009). Nickel binding occurs within the octameric repeatregion at pH 7 and possibly at His95/His110 in the absence of the octameric repeat region (Jackson *et al.*, 2001; Davies *et al.*, 2009).

Iron binds optimally around the His95/His111 site at acidic pH levels and at two sites within the N terminus at neutral pH (Davies *et al.*, 2009). Of the other metals, only iron has a demonstrated physiological link. PrP^{C} has been shown to modulate cellular iron uptake and intracellular iron content, as over-expression of PrP^{C} increases the intracellular iron pool as well as the amount of iron stored in ferritin (Singh *et al.*, 2009a). PrP knockout mice have altered iron metabolism and are iron deficient in the brain and other major organs (Singh *et al.*, 2009c). The altered iron metabolism is restored upon expression of PrP^{C}. Iron homeostasis may also play a role in the disease state. Levels of iron and iron regulatory proteins are altered in brains of prion infected mice, hamsters, and humans during disease progression (Singh *et al.*, 2009b) and ferritin, an iron storage protein, is found within aggregated PrP27-30 (Giorgi *et al.*, 2009). Iron imbalance is also seen in scrapie infected neuroblastoma cells, rendering the cells more susceptible to iron-induced oxidative stress (Kim *et al.*, 2000; Fernaeus *et al.*, 2005 a, b).

This overwhelming amount of evidence suggesting metals play a role in either the normal function of PrP^{C} or pathogenesis of prion disease. Despite - the numerous - suggested functions for PrP there is no consensus to date regarding the precise role of PrP *in vivo*. It is clear that expression of PrP^{C} is required for disease pathogenesis. $Prnp^{0/0}$ transgenic mice are phenotypically normal and deletion of the *Prnp* gene is non lethal. However, transgenic $Prnp^{0/0}$ mice and cattle do not develop prion disease when innoculated with infectious scrapie, BSE, or TME isolates (Büeler *et al.*, 1993; Prusiner *et al.*, 1993; Weissmann *et al.*, 1994a,b; Sakaguchi *et al.*, 1995; Richt *et al.*, 2007). Prion disease susceptibility is restored upon expression of even a single allele of *Prnp*, and incubation times appear inversely proportional to PrP^{C} expression levels (Büeler *et al.*, 1994; Fischer *et al.*, 1996).

1.4 PrP^{Sc}

The disease associated isoform of PrP^{C} is referred to as PrP^{Sc} (Sc for scrapie). PrP^{C} and PrP^{Sc} are encoded by the same gene and have the same primary amino acid sequence but their tertiary structure differs greatly (Basler *et al.*, 1986). One of the most striking differences is a complete structural rearrangement of the globular C-terminal region from a mainly α-helical structure to a predominantly β-sheet structure. PrP^{C} has about 40% α-helical content with low β-sheet content. In contrast, PrP^{Sc} has 45% β-sheet content and 30% α-helical content, suggesting PrP^{Sc} undergoes a major rearrangement of the C-terminus (Pan *et al.*, 1993; Safar *et al.*, 1993). There are additional

distinguishing factors such as protease sensitivity and solubility. PrP^{Sc} is partially protease resistant and when digested with proteinase K (PK), the protein is cleaved in the N-terminus to produce a truncated core which is often referred to as PrP27-30 (McKinley *et al.*, 1983; Harrison *et al.*, 1997). PK resistance is the most commonly used method to indicate whether the disease form is present, although several studies have shown that PK-resistant PrP^{Sc} levels are not directly correlated to the infectious transmissibility of the disease agent (Collinge *et al.*, 1995; Wille *et al.*, 1996; Lasmezas *et al.*, 1997). However, PK-resistant PrP remains the standard for identification of TSEs.

Furthermore, in afflicted individuals, PrP^{Sc} has been shown to accumulate in aggregates whereas PrP^{C} does not (Prusiner *et al.*, 1983). These accumulations can form amyloid plaques, which occur in 10-15% of sporadic CJD (sCJD) patients and are also found in kuru and GSS patients (Sikorska *et al.*, 2009). These plaques differ depending on type of prion disease but can either be florid (dense and unicentric, surrounded by spongiform vacuoles) or multi-centric (a merged network of unicentric plaques). Plaques and other accumulations of PrP^{Sc} contain high amounts of PrP as well as other proteins such as ubiquitin, ferritin, tubulin, and apolipoprotein E, and molecules such as proteoglycans (Snow and Wright, 1989; Snow *et al.*, 1990; Giorgi *et al.*, 2009).

It has been demonstrated that PrP^{Sc} is formed after PrP^{C} reaches the cell surface (Caughey, 1991; Tarabolous *et al.*, 1992; Gilch *et al.*, 2001) as cleaving PrP^{C} from the cell surfaces prevents PrP^{Sc} formation (Campana *et al.*, 2005). However, the precise site of conversion of PrP^{C} to PrP^{Sc} remains unclear. While a small percentage of PrP^{Sc} can be seen at the cell surface (Vey *et al.*, 1996), the majority of PrP^{Sc} is located intracellularly (Tarabolous *et al.*, 1992; Caughey, 1991; McKinley *et al.*, 1991; Marijanovic *et al.*, 2009). Therefore the proposed cellular location of prion protein conversion is either at the cell surface or within the endocytic pathway (Caughey *et al.*, 1991b; Caughey and Raymond, 1991; Borchelt *et al.*, 1992; Taraboulos *et al.*, 1992). Recently, the endocytic recycling compartment, part of the endocytic pathway, was identified as a likely site for conversion (Marijanovic *et al.*, 2009). However, despite further narrowing down of the likely site of conversion, the actual mechanism and causes of conversion remain unclear.

1.5 Conversion of the prion protein to the disease-associated form

The underlying mechanism behind the conversion of the normal PrP^{C} to a disease-associated form has been extensively studied but is not well understood. It is generally accepted that the normal cellular PrP^{C} molecule undergoes a conformational conversion to the disease-associated form PrP^{Sc}, which is then able to aggregate and accumulate in the brain.

1.5.1 Kinetic theories of prion conversion

Conversion of PrP has been modelled using three kinetic theories, which include template assisted-aggregation (Cohen *et al.*, 1994), nucleation-elongation polymerisation (Harper and Lansbury, 1997), and branched-chain polymerisation (Baskakov, 2007). Each of these theories employs the idea that a smaller unit of PrP is responsible for further catalysing protein aggregation. Initial studies led to the hypothesis that prion conversion followed a template assisted aggregation pathway wherein PrP^{Sc} acts as a template and upon binding to PrP^{C}, recruits the normally folded molecule to refold into a PrP^{Sc} conformation (Cohen *et al.*, 1994; Aguzzi, 2004). Branched-chain polymerisation means the rate of the formation of end products is dependent on the number and polymerisation of active centres, as well as the volume of the reaction. Once the end product is formed, the "lag time" of the multiplication of active centres is reduced and the reaction proceeds until a plateau is reached (Baskakov, 2007). In nucleation-dependant polymerisation where monomeric protein is the predominant species until a critical concentration is achieved, then polymerisation to fibril precursors (nuclei) occurs. The length of time required for the fibril precursor nuclei to form is referred to as lag time (Harper and Lansbury, 1997). As yet there is no conclusive evidence that any of these kinetic theories is the correct model.

1.5.2 Prion aggregation models

Several mechanisms for prion protein aggregation have been proposed. For example, β-oligomer structure can arise from a non-amyloid pathway, wherein the protein forms amorphous, β–structure rich aggregates which then arrange into spherical β-oligomers. Another model postulates that the pathway to amyloid fibrils involves a pre-amyloid intermediary which is a reversible mainly α-helical in structure and may exist in equilibrium with the native monomer (El Moustaine *et al.*, 2008). This intermediate state then proceeds to a dimer stage. Dimerisation has been shown to be a crucial if not

an initiatory step in fibrillisation (Priola *et al.*, 1995; Luhrs *et al.*, 2006; Goggin *et al.*, 2007; Stohr *et al.*, 2008). From the dimer formation, acquisition of β-sheet content leads to growth of proto-filaments to proto-fibrils, and finally to mature fibrils. The progression from proto-filaments to mature fibrils seems to be common to all amyloid-forming proteins. The common structure of amyloid fibrils consists of a cross β spine containing a double sheet of stacked, parallel β-rich segments. These segments stack in a head to tail structure, and are bound to their neighbour via side chains which act like a zipper, using hydrogen binding and interactions between the backbones to form the structure (Makin *et al.*, 2002; Torok *et al.*, 2002; Margittai *et al.*, 2004; Nelson *et al.*, 2005; Shewmaker *et al.*, 2006; Chen *et al.*, 2007). In mammalian prions, the cross β-core correlates to amino acids 127-230 (Cobb, *et al.* 2007; Lu *et al.*, 2007; Sun *et al.*, 2008) and the N-terminal tail, including the hydrophobic region of PrP, has been shown to be at the surface of fibrils as determined by antibody mapping (Novitskaya *et al.*, 2006b).

1.5.3 Structural changes of conversion

The C-terminal domain of the prion protein undergoes structural rearrangement during conversion of the disease-related isoform, and many suggestions have been proposed concerning the extent of structural rearrangement. At present, data are conflicting. It has been proposed that the C-terminal domain of PrP undergoes major structural rearrangement during conversion to an amyloid form, resulting in complete abolition of alpha helical structure (Lu *et al.*, 2007). Alternatively, the C-terminal region retains α-helical conformation, while either four regions spanning residues 116-119, 119-132, 135-140, and 160-164 assemble into a β-sheet (DeMarco *et al.*, 2004) or residues 89-175 assemble into three left handed β-helices (Govaerts *et al.*, 2004).

It is thought that α-helix 1 of PrP may be important for aggregation (Dima and Thirumalai, 2002; Watzlawik *et al.*, 2006; Yu *et al.*, 2007; Bujdoso *et al.*, 2005), although its role is unclear as it may not convert fully to a β-sheet form (Watzlawik *et al.*, 2006) and it is stable over a range of pH values and solvent conditions (Liu *et al.*, 1999; Speare *et al.*, 2003; Ziegler *et al.*, 2003; Norstrom and Mastrianni, 2006). It has been theorised that the formation of asparagine-arginine salt bridges in α-helix 1 stabilise PrP and form intermolecular bonds with other PrP molecules which could lead to aggregation (Morrissey *et al.*, 1999). However the bridges appear to stabilise PrP^C *in vitro* (Speare *et al.*, 2003). It has therefore been suggested that the specific orientation of charged residues within α-helix 1, particularly the C-terminal end of α-helix 1, is

essential for conversion. This data corroborates the observation that interactions between glutamic acid 196, aspartic acid 202 and glycine 90 may be important for dimer formation (Kaimann *et al.*, 2008). Further evidence that the C-terminus of the prion protein is rearranged during conversion was demonstrated by Fiztmaurice, *et al* who showed the ease of unwinding of α-helix 2 was correlated with modulation of the stability and aggregation of ovine PrP (Fiztmaurice *et al.*, 2008).

Additionally, the N-terminal region is capable of modifying PrP aggregation (Frankenfield *et al.*, 2005), but is not strictly necessary for aggregation to occur as numerous studies use an N-terminally truncated PrP.

1.5.4 Mutations to PrP and conversion

Mutations of the prion protein are likely to affect PrP conversion. There are more than 20 mutations of the *Prnp* gene, to human prion diseases has been attributed (Mead, 2006). The most prevalent mutations are E200K, D178N, P102L and octapeptide repeat insertionsHuman PrP exists in two allelic forms with a polymorphism at amino acid position 129. This polymorphism has been linked to disease susceptibility in kuru, vCJD and iatrogenic CJD (Collinge *et al.*, 1991; Collinge *et al.*, 1996; Zeidler *et al.*, 1997; Hill *et al.*, 1999; Collinge, 2001; Lee *et al.*, 2001; Mead, 2006). Investigation of the different alleles on both the structure of PrP^C and on aggregation indicate that the polymorphism at 129 of human PrP^C has no effect on the globular structure or stability (Hosszu *et al.*, 2004), or the ability of the protein to convert into a β-sheet rich form (Wong *et al.*, 2000a; Lewis *et al.*, 2006). However, it has been demonstrated that the initial folding state of the protein defines the kinetics of the conversion reaction (Tahiri-Alaoui *et al.*, 2004, 2005, 2006; Baskakov and Bocharova, 2005). While there are no differences between the allelic forms in conversion of α-monomeric human PrP to amyloid under non-denaturing conditions, (Liemann *et al.*, 1999; Hosszu *et al.*, 2004; Tahiri-Alaoui and James, 2005), under denaturing conditions there are differences. PrP with a methionine at 129 has a more exposed α-helix 1 and is more prone to form β-rich oligomers and to aggregate (Tahiri-Alaoui *et al.*, 2004; Pham *et al.*, 2008). Aggregation of PrP with a valine at 129 gains β-sheet structure more rapidly than methionine at 129 and has a shorter lag period, although the rates of amyloid growth do not differ between the two (Baskakov and Bocharova, 2005).

In addition, there are many other pathogenically-associated mutations whose effects on aggregation and amyloid formation have been described. Aggregation and disease

manifestation of the commonly found human PrP mutation D178N has been shown to be modulated by the allelic form of PrP at codon 129 (Apetri *et al.*, 2005). Recombinant protein with another disease-associated mutation, F198S, also has a higher propensity for aggregation than wild type protein (Vanik *et al.*, 2002). Furthermore, these pathological mutations appear to increase the propensity of monomeric folding intermediates and these folding intermediates again may be important in the pathway to amyloid formation. Finally, the polymorphism at 129 was also shown to affect the structure but not the aggregation of C-terminally truncated PrP containing N-terminal pathological mutations (Apetri and Surewicz, 2002; Apetri *et al.*, 2004).

Another common pathological mutation associated with prion disease is the insertion of extra octapeptide repeats within the N-terminal region. PrP with these insertion mutations has an increased propensity to aggregate proportional to the number of insertions (Singh *et al.*, 1997; Moore *et al.*, 2007; Tank *et al.*, 2007; Yu *et al.*, 2007), A yeast model comparing similar insertions found the resulting fibrils are less stable (Kalastavadi and True, 2008). In cell culture, extra octapeptide repeats leads to increased aggregation and increased protease resistance (Priola *et al.*, 1998).

In addition to variations in human PrP aggregation, variations in conformation and aggregation of different sheep alleles of PrP have been shown (Bossers *et al.*, 1997, 2000; Rezaei *et al.*, 2002; Thackray *et al.*, 2004b; Bujdoso *et al.*, 2005; Yang *et al.*, 2008). Cell-free conversion of different allelic forms of ovine PrP mimicked scrapie susceptibility *in vivo*. The most susceptible allelic form, $V_{136}R_{154}Q_{177}$, had the highest rate of conversion to a protease resistant form of PrP, where the allelic form associated with scrapie resistance had a limited ability to form protease resistant PrP in the study (Bossers *et al.*, 1997, 2000). Scrapie-resistant ovine PrP alleles have decreased β-sheet content in aggregation intermediates when compared to scrapie-susceptible allele (Rezaei *et al.*, 2002; Yang *et al.*, 2008). Furthermore copper-induced structural changes appear to be modulated by the ovine polymorphism M/T112, as M112 $A_{136}R_{154}Q_{177}$, a scrapie susceptible allele appears to be more thermostable but has a higher β-sheet content than T122 $A_{136}R_{154}Q_{177}$ (Yang *et al.*, 2008). Thus, studies of the structural characteristics induced by polymorphisms and pathological mutations provide insight not only into the mechanism of prion aggregation, but potentially explain the differences in pathogenicity seen between various diseases (Collinge and Clarke, 2007) as well as the susceptibility of specific polymorphisms to these diseases.

1.5.5 Additional factors affecting conversion

Additional factors that have been theorised to affect prion protein conversion include metals, polyanionic compounds, glycosaminoglycans, and dendrimers.

1.5.5.1 Metals

Copper binding to PrP induces conformational change, as copper binding imposes structure on the unstructured N-terminal region (Stockel *et al.*, 1998). This has been shown to increase β-sheet content of the protein as well as confer protease resistance, although the protease resistance is distinct from PrP^{Sc} protease resistance (McKenzie *et al.*, 1998; Stockel *et al.*, 1998; Wadsworth *et al.*, 1999; Brown *et al.*, 2000; Qin *et al.*, 2000; Quaglio *et al.*, 2001; Wong *et al.*, 2000b; Jones *et al.*, 2004; Nishida *et al.*, 2004; Liu *et al.*, 2007). Polymorphisms can influence the degree to which copper can induce β-sheet structure, for instance, the scrapie-susceptible ovine allele $V_{136}R_{154}Q_{177}$ has a greater increase in β-sheet structure when compared to the scrapie-resistant $A_{136}R_{154}R_{177}$ allele (Rezaei *et al.*, 2002; Wong *et al.*, 2004). This copper-induced conformational change is mediated by the presence of the N-terminal region of PrP (Wong *et al.*, 2004) and is thought to be due to the differences in α-helix 1 and residue 171 (Thackray *et al.*, 2004b).

The actual effect of copper on prion protein aggregation is contradictory, as the addition of copper (II) ions has been shown to inhibit aggregation (Giese *et al.*, 2004; Bocharova *et al.*, 2005b; Ricchelli *et al.*, 2006; Liu *et al.*, 2008) and cell-free conversion (Orem *et al.*, 2006) but can also initiate aggregation of recombinant protein (Requena *et al.*, 2001; Rezaei *et al.*, 2002, 2005; Shiraishi *et al.*, 2005, 2006; Tsiroulnikov *et al.*, 2006; Redecke *et al.*, 2007; Fitzmaurice *et al.*, 2008), suggesting a differential effect dependent on experimental conditions.

In addition to copper, PrP is able to bind manganese as described in section 1.3.2.2. Upon binding to PrP, manganese induces conformation change and increased protease resistance (Brown *et al.*, 2000; Abdelraheim *et al.*, 2006; Kim *et al.*, 2005; Treiber *et al.*, 2006). Manganese-loaded PrP has been shown to initiate aggregation of PrP (Brown *et al.*, 2000; Giese *et al.*, 2004; Lekishvili *et al.*, 2004; Kim *et al.*, 2005). This initiation of aggregation is due to the structural change manganese confers on PrP once bound (Brown *et al.*, 2000), similar to the manner that copper causes a conformational change.

1.5.5.2 Other factors effecting conversion

RNA, polyanions and glycosaminoglycans (GAGs) stimulate cell-free conversion of synthetic peptides, recombinant and brain-derived PrP into a protease resistant form of PrP (Wong *et al.*, 2001d; Gonzalez-Iglesias *et al.*, 2002; Deleault *et al.*, 2005; Boshuizen *et al.*, 2007; Yin *et al.*, 2007). This may be particularly relevant to disease pathogenesis, as it has been shown that GAGs can bind recombinant PrP (Pan *et al.*, 2002; Warner *et al.*, 2002), and they are essential for prion replication (Hijazi *et al.*, 2005; Horonchik *et al.*, 2005). The polyanion Congo Red (CR) has been shown to inhibit conversion of PrP *in vitro* at high molecular ratios by inducing PrP to adopt a more denatured state (Caughey *et al.*, 1992, 1993; Caspi *et al.*, 1998; Frid *et al.*, 2007) and at low molecular ratios to promote aggregation (Rudyk *et al.*, 2000). This differential effect is may be because CR does not act upon pre-existing PK-resistant PrP molecules (Caughey and Raymond, 1993). Finally, branched polymers called dendrimers have been shown to modulate aggregation of PrP peptides by inhibiting or slowing aggregation, modulating the amount of fibrils produced and rendering the resulting aggregations more protease-sensitive (Supattapone *et al.*, 1999; Klajnert *et al.*, 2006, 2007).

1.6 Transmissibility, neuroinvasion, and neurodegeneration

As yet there is no definitive cause for the conversion of the prion protein, nor do we know why the conversion and subsequent accumulation of the prion protein leads to the disease state. It has been theorised that conversion of the protein leads to the accumulation of misfolded protein, possibly in oligomeric structures which then leads to neuronal loss and eventually patient death. One theory is that small oligomers are in fact the culprit in prion disease as it has been postulated that the infectious form of PrP was around 50-150 kDa in size (Alper *et al.*, 1966; Gabizon *et al.*, 1987; Bellinger-Kawahara *et al.*, 1988; Caughey *et al.*, 2003) and later suggestions that a minimal infectious unit corresponded to a PrP molecule around 600 kDa in size (Tzaban *et al.*, 2002). As monomeric PrP is around 25-30 kDa, this suggests the infectious culprit would be an aggregated form of PrP. When PrP^{Sc} aggregates were dissociated, it was found that that the most infectious PrP aggregates were round spherical oligomers, 17-27 nm in length and 300-600 kDa in size, corresponding to 14-28 PrP molecule units (Silveira *et al.*, 2005). Further analysis of a PrP aggregation pathway, which produces well-ordered β-oligomers of PrP, has shown that oligomers consist of 25 monomeric equivalents of PrP. This evidence supports the idea of the oligomer as the minimal

infectious unit (Redecke *et al.*, 2007). Recently it has been shown that small PrP oligomers are present in pre-clinical stages of prion disease and these oligomers increase in concentration as the disease progresses (Sasaki *et al.*, 2009). Accordingly, these and other data indicate that prion protein oligomers are toxic to the cells and are responsible for disease development (Novitskoya *et al.*, 2006a, 2007; Simoneau *et al.*, 2007; Dear *et al.*, 2007).

Considering the uncertainty surrounding the exact structure of infectious PrP, it is unsurprising that the mechanism of transmission is as yet unknown. In addition to the CNS, prion infectivity has been identified in several tissues of the body including blood, spleen, tonsil, fat, skin and muscle (Pattison and Millson, 1962; Hadlow *et al.*, 1982; Bosque *et al.*, 2002; Thomzig *et al.*, 2004, 2006, 2007; Castilla *et al.*, 2005; Angers *et al.*, 2006; Race *et al.*, 2008, 2009; Cardone *et al.*, 2009; Terry *et al.*, 2009). Also, prion infectivity is found in bodily secretions including milk, saliva, urine, and faeces (Miller *et al.*, 2004; Mathiason *et al.*, 2006, 2009; Vascellari *et al.*, 2007; Gregori *et al.*, 2008; Safar *et al.*, 2008; Krüger *et al.*, 2009). Transmissibility to humans has been shown to occur via blood transfusions and dura matter grafts (Hunter *et al.*, 2000; Llewelyn *et al.*, 2004; Peden *et al.*, 2004; Hunter, 2003; Mathiason *et al.*, 2009) as well as via consumption of prion-affected material as with kuru and vCJD (Gajdusek, 1977; Scott *et al.*, 1999). Ovine and mouse-adapted scrapie as well as CWD has been shown to be transmitted via environmental exposure (such as housing uninfected animals in the same cages which previously held infected animals), Thus, while it can be argued that these diseases are contagious, it is not precisely clear how this transmission occurs (Pattison *et al.*, 1971c; Miller *et al.*, 2004; Ryder *et al.*, 2004; Georgsson *et al.*, 2006).

Experimentally, prion diseases are traditionally transmitted via intracranial and intraperitoneal inoculation for the most consistent results. However, oral entry seems the most likely route of transmission for naturally acquired (not inherited) prion diseases such as scrapie, BSE, CWD and possibly kuru and vCJD (Pattison *et al.*, 1974; Hadlow, *et al.,* 1982; Andreoletti *et al.*, 2000; van Keulen *et al.*, 2000; Marsh and Bessen, 1993; Sigurdson, *et al.,* 2001; Williams and Miller, 2003; Gajdusek, 1977; Cervenakova *et al.*, 1998). Transmission via oral entry has been shown to result in subclinical disease even after a low dose of infectious innoculum and this subclinical presentation resulted in high levels of infectivity despite the lack of clinical signs (Thackray *et al.*, 2002a, 2003a). This subclinical yet highly infectious disease resulting

from oral exposure to prions may represent a mechanism of environmental transmission, particularly as it has been recently shown that asymptomatic deer infected with CWD excrete infectious prions in faeces (Tamguney *et al.*, 2009).

The spread of prion infection throughout the body is not completely understood, but evidence suggests that upon oral entry, prion infectivity generally spreads from the alimentary canal to the lymphoid system, and from the lymphoid system to the peripheral nervous system and then to the CNS (Beekes and McBride, 2007; Kovacs and Budka, 2009). From the CNS prion infectivity may then spread back through the body to muscles via spinal or cranial motor neurons (Andrelotti *et al.*, 2004; Thomzig *et al.*, 2004).

In experiments with animals fed infectious material, the first signs of prion infectivity are seen in the ileum and caudal jejunum (Krüger *et al.*, 2009). From the gut, infection spreads to the gut-associated lymphoid tissues (GALT) including Peyer's patches, tonsils, and GALT-draining lymph nodes (Maignien *et al.*, 1999; Beekes and McBride, 2000; van Keulen *et al.*, 2000, 2002; Bruce *et al.*, 2001; Wadsworth *et al.*, 2001). From the GALT, infection spreads to other lymphatic tissue including the spleen (Kimberlin and Walker, 1989a,b; Beekes *et al.*, 1996) except in BSE, where lymphatic involvement is restricted to GALT only (Terry *et al.*, 2003; Epinosa *et al.*, 2007; Hoffmann *et al.*, 2007). The spread of prion infectivity in the lymphoid system could be due to several different types of cells that have been shown to harbour disease-related PrP including follicular dendrite cells (FDC), follicle associated epithelial cells, dome and tangible macrophages, microfold cells, and dendritic cells (DCs) (Beekes and McBride, 2000; Huang *et al.*, 2002; Koperek *et al.*, 2002). It has been shown that interfering with FDC maturation delays TSE neuroinvasion (Muramoto *et al.*, 1992; Klein *et al.*, 1998; Mabbott *et al.*, 2000 a, b) and ablating specific B cell receptors accelerates TSE neuroinvasion by altering the FDC network (van Poser-Klein *et al*, 2008). This suggests that mature FDCs with specific intact B-cell signalling are required to spread prion infection.

From the lymphatic tissue, prion neuroinvasion occurs via the peripheral nervous system involving the splanchnic and vagus nerves (which innervate the lymphatic tissue and gastrointestinal tract respectively) as well as the enteric nervous system (Goelher *et al.*, 1999; McBride and Beekes, 1999). It is likely that neuroinvasion is facilitated by FDC and DC transportation of prion infectivity (Beekes and McBride,

2007). Once neuroinvasion occurs, prion infectivity spreads along enteric and cervical ganglia and is transported to the brain and spinal cord (Williams and Miller, 2003; Schultz-Schaeffer *et al.*, 2000; Haik *et al.*, 2003). The mechanism of prion propagation through the brain and spinal cord is unknown and may involve axonal transportation, spread through the neural interspaces, sequential infection of Schwann cells or even serial conversion via PrP-PrP contact along cell membranes (Kimberlin *et al.*, 1983, 1989a; Glatzel and Aguzzi, 2000; Follet *et al.*, 2002; Kunzi *et al.*, 2005; Kovacs *et al.*, 2005).

Once the disease has entered the CNS (either by acquired or inherited modes) it is unclear how neuronal damage, loss and eventual patient death actually occurs; whether it is loss-of-function of PrP, whatever the function may be, or gain of toxic function (toxic aggregates or abnormal cellular forms) by PrP (Kovacs and Budka, 2009; Chakrabarti and Hegde, 2009). Several mechanisms have been proposed to explain how prion infection leads to neuronal loss, including apoptosis, endosomal or lysosomal dysfunction, endoplasmic reticulum stress, oxidative stress, and ubiquitin-proteasome dysfunction (Forloni *et al.*, 1996; Bence *et al.*, 2001; Clarke *et al.*, 2001; Guentchev *et al.*, 2002; Wojcik, 2002; Hetz *et al.*, 2003; Kovacs *et al.*, 2004, 2007; Brown *et al.*, 2005; Unterberger *et al.*, 2005; Voigtländer *et al.*, 2006; Kristiansen *et al.*, 2007). It is possible that more than one mechanism contributes to the overall neurodegeneration seen in prion disease.

A great deal of uncertainty plagues the field of prion disease research, despite intensive efforts by those working in the field. The normal function of PrP^{C} is still debated, as is the mechanism behind the conversion to the disease state. Furthermore, there is no agreement as to what extent other molecules play in prion disease. There are several lines of evidence supporting a role for metals in prion disease, including the metal-binding capabilities of PrP, altered metal levels associated with the disease, and the influence of metals on the structure of PrP.

1.7 Aims

The aim of this work is to further identify the role metals and glycosaminoglycans play in prion diseases, and in particular the conversion from the normal PrP^C to a disease related isoform.

- **Metals**.
    - Firstly, a method for cellular prion infection will be developed using either infectious brain homogenate or chronically infected neuronal cells as an infectious source for uninfected neuronal cell. Whether the role of metals is either promotional or inhibitory in regards to the transfer of cellular prion infection will be assessed.
    - To determine whether the effect is due to metal-PrP interactions, a new method will be developed to study the conversion of PrP in an *in vitro* system using bacterially expressed recombinant protein. Experiments done using this system will assess whether metals have a stimulatory effect PrP aggregation under neutral pH and non-denaturing conditions. There is no precedent for this experimental approach, as most aggregation studies used extreme pH, temperature, or denaturants to study metal-PrP aggregation effects. Using a neutral system will provide us with information which may be more physiologically relevant and further our understanding of the role of metals in prion conversion.

- Glycosaminoglycans.
    - To address the nature of the PrP-GAG interactions, ITC will be used as a novel technique to study PrP-GAG binding.
    - Subsequently, the role of heparin in PrP conversion, whether promotional or inhibitory, will be assessed by using the aforementioned cellular prion infection model.
    - Finally, to determine whether this affect is specific to a PrP-GAG interaction, the effect of heparin on the PrP aggregation system will be studied. If the effect is due to a PrP-GAG interaction, a similar (promotional or inhibitory) result will be obtained from these conversion methods.

In summary, this work aims to assess whether there is a promotional or inhibitory role of metals and glycosaminoglycans in conversion of the prion protein from a normal, cellular form to the disease-associated prion molecule, using recombinant protein aggregation and binding assays as well as a cellular prion infectivity culture model.

2. Materials and Methods

2.1 Materials

All reagents were purchased from Sigma (Poole, UK) unless otherwise noted.

2.2 Molecular Biology Techniques

Mammalian expression constructs pcDNA3.1+-mPrP(1-254), pcDNA3.1+-mPrP(1-254 Δ67-90), and pcDNA3.1+-mPrP(1-254 Δ51-89) were created by Kate Edwards (University of Cambridge, Cambridge, UK). Constructs p3XFLAG-mCTR1, p3XFLAG-mCTR2, p3XFLAG-mCCS, and p3XFLAG-mATOX1 were created by Silvia Kralovicova (University of Bath, Bath, UK) (Table 1). Schematic representation of pcDNA3.1+-mPrP(1-254) is illustrated in Figure 2.1.

Full Construct Name	Denotation	Created By
pcDNA3.1+-mPrP(1-254)	pcDNA3.1+-mPrP	Kate Edwards, Cambridge University, UK
pcDNA3.1+-mPrP(1-254Δ51-89)	pcDNA3.1+-mPrP(Δ51-89)	Kate Edwards, Cambridge University, UK
pcDNA3.1+-mPrP(1-254Δ67-90)	pcDNA3.1+-mPrP(Δ67-90)	Kate Edwards, Cambridge University, UK
p3XFLAG-mCTR1	p3XFLAG-CTR1	Silvia Kralovicova, University of Bath, UK
p3XFLAG-mCTR2	p3XFLAG-CTR2	Silvia Kralovicova, University of Bath, UK
p3XFLAG-mCCS	p3XFLAG-CCS	Silvia Kralovicova, University of Bath, UK
p3XFLAG-mATOX1	p3XFLAG-ATOX1	Silvia Kralovicova, University of Bath, UK

Table 2.1 Mammalian protein expression constructs. All constructs were murine.

Figure 2.1 Schematic representation of pcDNA3.1+-mPrP(1-254).

Bacterial expression constructs pET3a-mPrP(89-231), and pET3a-mPrP(23-231 Δ106-126) were created by Jo Wright (University of Bath, Bath, UK). pET23a-mPrP(23-231) was created by Salama R. Abdelraheim (University of Bath, Bath, UK). pET23a-mPrP(23-231 H95A+H110A) were created by Andrew Thompsett (University of Bath, Bath, UK). Constructs pET23a-mPrP(23-231 H95A), pET23a-mPrP(23-231 H110A pET23a-mPrP(23-231H60A,H68A,H76A,H84A,H95A,H110A), and pET23a-mPrP(23-231 H60A,H68A,H76A,H84A),were created by Paul Davies (University of Bath, Bath, UK) (Table 2). All proteins used in this thesis were expressed and purified personally. Schematic representation of mPrP mutations used for bacterial expression is shown in Figure 2.2.

Full Construct Name	Denotation	Created by
pET3a-mPrP(23-231)	pET3a-mPrP(23-231)	Sarah Fontaine, University of Bath, UK
pET3a-mPrP(23-231 Δ51-89)	pET3a-mPrP(Δ51-89)	Sarah Fontaine, University of Bath, UK
pET3a-mPrP(23-231 Δ67-90)	pET3a-mPrP(Δ67-90)	Sarah Fontaine, University of Bath, UK
pET3a-mPrP (89-231)	pET3a-mPrP (89-231)	Jo Wright, University of Bath, UK
pET3a-mPrP(23-231 Δ106-126)	pET3a-mPrP(Δ106-126)	Jo Wright, University of Bath, UK
pET23a-mPrP(23-231)	pET23a-mPrP(23-231)	Salama Abdelraheim University of Bath, UK
pET23a-mPrP(23-231 H95A)	pET23a-mPrP(H95A)	Paul Davies, University of Bath, UK
pET23a-mPrP(23-231 H110A)	pET23a-mPrP(H110A)	Paul Davies, University of Bath, UK
pET23a-mPrP(23-231 H95A+H110A)	pET23a-mPrP(H95A+H110A)	Andrew Thompsett, University of Bath, UK
pET23a-mPrP(23-231 H60A,H68A,H76A,H84A)	pET23a-mPrP(H95+H110A)	Paul Davies, University of Bath, UK
pET23a-mPrP(23-231 H60A,H68A,H76A,H84A,H95A,H110A)	pET23a-mPrP(Null)	Paul Davies, University of Bath, UK

Table 2.2. Bacterial mPrP constructs.

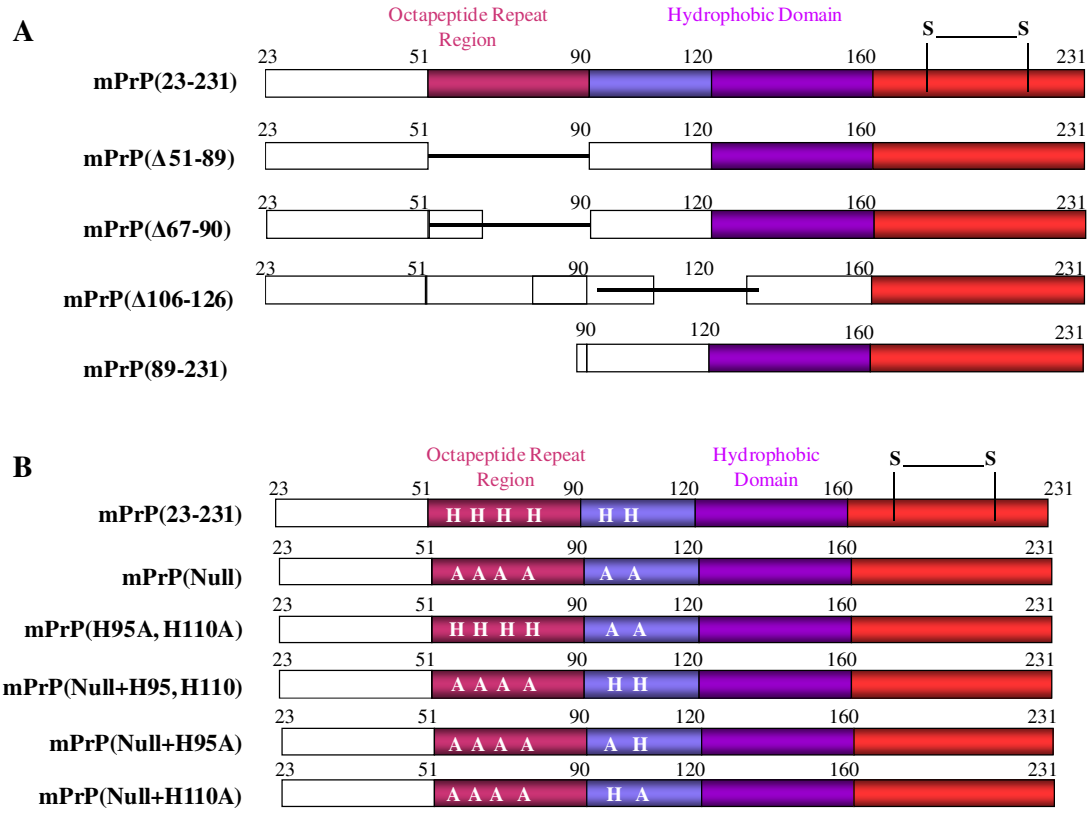

Figure 2.2. Schematic representation of mPrP constructs used for recombinant protein expression. A) Deletion and truncation mutants. B) Mutations of copper-binding histidine residues.

2.2.1 Purification of DNA

2.2.1.1 Additional Materials

Wizard SV Miniprep Kit (Promega)

Luria-Bertani (LB) Broth (Melford, UK)

Carbenicillin sodium salt (Melford, UK)

2.2.1.2 Method

Single colonies were inoculated into 5 mL LB with 50 µg/mL carbenicillin. Cultures were grown overnight at 37°C with shaking at 200 r.p.m. The next day cultures were centrifuged for 5 min at 4000 r.p.m. to pellet cells. The supernatant was discarded and DNA extracted from cells per manufacturer's instructions.

2.2.2 Polymerase chain reactions

2.2.2.1 Additional Materials

BamHI (Promega, UK)

NdeI (New England Biolabs, UK)

PWO DNA polymerase (Roche, UK)

Deoxyribonucleotides (dNTPs) (New England Biolabs, UK)

Sterile MillQ water, pH 7.4

25 μM primers (MWG, UK)

2.2.2.2 Method

Custom primers were designed with restriction endonuclease sites *NdeI* and *BamHI*. The PCR reaction mixture consisted of 1 μg DNA (as extracted previously), 25 μM primers, sterile MilliQ water, 10x PWO Buffer with MgSO4, 25 μM dNTPs and 2.5 Units PWO DNA polymerase per 50 μL reaction. PCR reaction conditions are as follows:

95 °C: 1 min

95 °C: 20 s
61 °C: 20 s
72 °C: 1 min
} 40 cycles

72 °C: 4 min

mPrP 23-231 was amplified from pCDNA3.1+-mPrP(1-254). mPrP(Δ51-89) was amplified from pcDNA3.1+-mPrP(1-254Δ51-89), and mPrP(Δ67-90) was amplified from pcDNA3.1+-mPrP(1-254Δ67-90) using forward primer

5’ GCGCATATGAAAAAGCGGCCAAAGCCT 3’ and reverse primer

5’ TATGGATCCTTACTAGCTGGATCTTCTCCC 3’.

2.2.3 Agarose Gel Electrophoresis

2.2.3.1 Additional Materials

Agarose (Melford, Ipswich, UK)

Tris-acetate (TAE) buffer (40 mM Tris acetate, 1 mM EDTA, pH 8.0)

GeneRuler 1 kb DNA ladder (Fermentas, UK)

2.2.3.1 Methods

Agarose gels were prepared by dissolving agarose in TAE buffer to a final concentration of 1%. Typically, 1 g agarose was added to 100 mL TAE buffer and dissolved by heating in a 800 watt microwave at high power for 3 min. 10 µL 10 mg/mL ethidium bromide was then added so DNA samples could be visualised with UV light. The agarose was poured into moulds (BioRad) and allowed to set. Once gel had solidified, it was transferred to the electrophoresis apparatus (BioRad) and DNA samples were mixed with 5X DNA loading dye before loading into wells. A 1 kb DNA ladder was run alongside samples to determine size.

2.2.4 Gel Purification

2.2.4.1 Additional Materials

QIAquick Gel Extraction Kit (Qiagen, UK)

2.2.4.2 Method

DNA samples to be purified were run on a 1.5% agarose gel containing ethidium bromide for 1h at 100 volts. The gel was briefly exposed to UV light and correctly sized fragments were excised using razor blades and transferred to a sterile 1.5 mL eppendorf. Gel slices were then purified according to manufacturer's directions using a QIAquick Gel Extraction kit. DNA was eluted from the column with the addition of 30 µL nuclease free water and incubation for 60 s at room temperature. The columns were transferred to a sterile 1.5 mL eppendorf tube, and centrifuged for 60 s to elute the bound DNA.

2.2.5 Restriction Enzyme Digests

2.2.5.1 Additional materials

NdeI (New England Biolabs UK)

BamHI (Promega, UK)

Buffer 3 (New England Biolabs UK)

10 mg/mL Bovine Serum Albumen (BSA) (Promega, UK)

MilliQ sterile

2.2.5.2 Method

Restriction enzyme digests were typically performed on 1-10 µg DNA using restriction endonucleases at 10-20 Units. Double digests were performed utilising a suitable buffer for both enzymes (as determined from the manufacturer's instructions). Digestions only included 0.25 µg/µL BSA if required by a specific enzyme. Digests were incubated at 37°C typically for 2 hours, or if the enzymes did not exhibit star activity (wherein the enzyme begins to bind within your DNA of interest to sequences similar to the recognition site) digests were allowed to incubate overnight.

2.2.6 Vector preparation

2.2.6.1 Additional Materials

Shrimp Alkaline Phosphatase (SAP) (Promega, UK)

pET3a (Novagen, UK)

Buffer 3 (New England Biolabs, UK)

10 mg/mL BSA (Promega, UK)

2.2.6.2 Method

5 µg pET3a DNA was digested for 4h with *NdeI* and *BamHI* in Buffer 3 with BSA as in 2.2.6. Digested vectors were then gel-purified and eluted in 40 µL of nuclease-free water. 5 µL 10X SAP buffer and 5 µL SAP (1 Unit/µL) were added to the eluted DNA and incubated at 37°C for 15 min. The SAP was then inactivated by incubation at 70°C for 15 min

2.2.7 Phosphorylation of PCR products

2.2.7.1 Additional materials

T4 Polynucleotide Kinase (Promega, UK)

10x Ligation buffer from T4 ligase (Promega, UK)

2.2.7.2 Method

PCR products that had been gel-purified were phosphorylated for blunt-ended ligations. 8 µl each PCR product was mixed with 1 µl 10X T4 ligation buffer and 1 µl T4 polynucleotide kinase. The reaction was incubated at 37°C for 30 min and then the T4 polynucleotide kinase was inactivated by incubating at 70°C for 10 min. PCR products were then ligated into an intermediate vector.

2.2.8 Preparation of intermediate vector for blunt-ended ligations

2.2.8.1 Additional materials

10 mg/mL Bovine Serum Albumen (BSA) (Promega, UK)

EcoRV (Promega, UK)

2.2.8.2 Method

pcDNA3.1+ was used as an intermediate vector. 5 µg pcDNA3.1+ was digested with 2.5 µL *EcoRV* with 0.5 µg BSA at 37°C overnight. The digested pcDNA3.1+ was then gel purified (2.2.5) and eluted in 40 µL nuclease free water, then SAP treated (2.2.7) and stored at -20°C until use.

2.2.9 Ligation Reactions

2.2.9.1 Additional materials

T4 DNA ligase (Promega, UK)

Sterile MilliQ water

2.2.9.2 Method

Ligation reactions containing 100 ng vector DNA were typically performed in 20 μL volumes. A 3:1 ratio of insert DNA: vector DNA was typically used, following the manufacturer's protocol. 1 μL T4 DNA ligase and 2 μL 10X T4 DNA ligase buffer was added to the DNA and sterile MilliQ water was used to bring the volume to 20 μL. Ligations were incubated overnight at 16°C and stored at -20°C until transformed into competent cells.

2.2.10 Preparation of calcium competent cells

2.2.10.1 Additional Materials

0.1 $MgCl_2$

0.1 M $CaCl_2$

0.1 M $CaCl_2$ + 15% glycerol

JM109 cells (Promega, UK)

BL21-DE3 cells (Novagen, UK)

2.2.10.2 Method

Cells were streaked onto an LB plate and incubated overnight at 37°C. A single colony was inoculated into LB and incubated with shaking at 150 r.p.m. overnight at 37°C. The following day 10 mL of overnight culture was inoculated into 200 mL LB and grown at 37°C with shaking at 200 r.p.m. until the $O.D._{600}$ = 0.6. Cells were then pelleted by centrifuging for 10 min at 4000 r.p.m. at 4°C, and then resuspended by gently pipetting up and down in 200 mL ice cold 0.1 M MgCl2. Cells were pelleted by centrifuging for 10 min at 4000 r.p.m. at 4°C. Cells were gently resuspended in 200 mL ice cold 0.1 M $CaCl_2$ and incubated on ice for 20 min. The centrifugation and resuspension was repeated for final time in 10 mL ice cold 0.1 M $CaCl_2$ + 15% glycerol. Cells were aliquotted quickly into pre-chilled sterile eppendorfs and stored immediately at -80°C.

2.2.11 Transformation of DNA into *Escherichia coli* JM109 or BL21-DE3 cells

2.2.11.1 Additional materials

SOC buffer (10 mM sodium chloride, 2.5 mM potassium chloride, 10 mM magnesium sulphate, 10 mM magnesium chloride, yeast extract, tryptone, 0.4% glucose)

2.2.11.2 Method

Calcium-competent JM109 or BL21-DE3 cells in 10% glycerol (v/v) were thawed on ice. 3 µL of the DNA to be transformed was added to a 1.5 mL sterile eppendorf tube and kept on ice whilst an aliquot of cells thawed. Once completely thawed, 100 µL of the competent cell suspension was transferred aseptically into the pre-chilled eppendorf tubes containing the DNA. This mixture was allowed to incubate on ice for 30 min.

After the incubation, a heat shock was performed at 42°C for exactly 45 s. Reactions were immediately placed back on ice for 2 min before 400 µL SOC buffer was added to each tube. Reactions were incubated at 37°C with shaking for no more than 1 h. Suspensions were then gently centrifuged to pellet the cells which were then resuspended in approximately 150 µL SOC and plated directly onto LB-agar plates containing 50 µg/mL carbenicillin. The plates were then incubated at 37°C overnight to allow successfully transformed colonies to grow.

2.3 Cell Culture Methods

All tissue culture and prion infection work was performed under biosafety level 2 standards. Prion contaminated material was thoroughly decontaminanted in 2 M NaOH as described by standard protocols for prion work by D.R.Brown.

2.3.1 General cell culture: routine maintenance of cell lines

2.3.1.1 Additional Materials

Dulbecco's Modified Eagle Medium (DMEM) with 4.5 g/L glucose, without L-glutamine (Lonza, UK)

Eagle's Minimum Essential Medium (EMEM) (Lonza, UK)

Medium 199 (Lonza, UK)

Trypsin-EDTA (Gibco, UK)

Newborn Calf Serum (NCS), heat-inactivated, USA origin

Foetal Bovine Serum (FBS), heat-inactivated, origin (Lonza, UK)

L-gluatmine (Gibco, UK)

Non-essential amino acids (NEAA) 100X solution (Lonza, UK)

Penicillin-streptomycin

2.3.1.2 Method

All cells were maintained at 37°C and 5% CO_2 in a humidified incubator.

2.3.1.2.1 N2a Cells

Neuro2a (N2a) cells originate from a spontaneous tumour of an albino mouse (Klebe and Ruddle, 1969). N2a cells were maintained in EMEM supplemented with 10% FBS, 2.5 mM L-gluatmine, 1 X NEAA, and 1% penicillin-streptomycin. Cells were passaged at 1:10-1:15 for maintenance once confluent.

2.3.1.2.2 SMB and SMB-PS Cells

Scrapie mouse brain (SMB) cells originate from brains of mice infected with the Chandler strain of scrapie (Clarke and Haig, 1970). SMB-PS cells are SMB cells that were treated with pentosan sulphate to clear prion infection, as shown by the lack of detectable PK-resistant PrP in these cells. Cells were maintained in Medium 199

supplemented with 10% FBS, 5% NCS and 1% penicillin-streptomycin. SMB cells were passaged at 1:3 when 90% confluent and SMB-PS were passaged at 1:4-1:6 when confluent.

2.3.1.2.3 Zpl and Zwl cells

Zpl and Zwl cells are derived from Zurich mice (Kim *et al.*, 2005) and were a kind gift from Professor Yong-Sun Kim, the New York State Institute for Basic Research in Developmental Disabilities. Cells were maintained in DMEM supplemented with 10% FBS and 1% penicillin-streptomycin and passaged 1:20 when confluent.

2.3.2 Cryopreservation of cell lines

2.3.2.1 Additional Materials

Freezing medium (90% (v/v) FBS, 10% (v/v) DMSO 99.7% pure)

2.3.2.2 Method

Cells were grown to 70-90% confluency before dissociating with trypsin and re-suspending in fresh medium. Cells were pelleted by centrifugation for 5 min at 1000 g. The medium was aspirated carefully away and cells were resuspended with 1-2mL freezing medium per 75 cm^2 flask. Cell suspensions were immediately placed in a plastic freezing vessel filled with isopropanol and placed in the -80˚C freezer for 4h to overnight. Cells were stored long-term in liquid nitrogen.

Cells were thawed by warming each vial in a 37˚C water bath until fully thawed. Then cells were diluted in pre-warmed complete culture medium. Cells were pelleted by centrifugation for 5 min at 1000 g. The medium was aspirated carefully away and cells resuspended with 6 mL of complete culture medium, then transferred to a 25 cm^2 flask. Cells were placed in the incubator and allowed to adhere overnight.

2.3.3 Transfection

2.3.3.1 Additional Materials

Fugene HD (Roche, UK)

DNA purified from QIAprep Spin Miniprep Kits (Qiagen, UK)

EMEM, DMEM, M199 serum free (Lonza, UK)

G418 Sulphate (PAA, UK)

2.3.3.2 Method

2.3.3.2.1 Creation of stably transfected cell lines

Cells were plated into 6 well plates at a density of $1x10^5$ cells per well and allowed to adhere overnight. In a sterile 1.5 mL eppendorf, 2 μg DNA was diluted in 100 μL serum free media. To this mixture 3 μL Fugene HD was added and the reaction was allowed to incubate at room temperature for 15 mins. The entire reaction was then added to each well, dropwise, and the cells were returned to the incubator for 48 h. Cells expressing the protein of interest were then selected for by adding the appropriate amount of G418 sulphate (PAA) to each well. G418 concentrations were determined by performing kill curves on each cell line wherein untransfected cells were treated with G418 and assessed twice a day to determine rate of death. The concentration which took one week to kill all the cells was chosen for use in the stable transfections. After one week all control cells were dead, and transfected cells were analysed by Western blot for successful expression of desired proteins. Cells were then maintained in normal culture media with G418 added. G418 concentrations for each cell line are listed in Table 2.3.

2.3.3.2.2 Creation of transiently transfect cell lines

Cells were plated into 6 or 12 well plates at a density of $1.09x10^4$ cells per cm^2 surface area and allowed to adhere overnight. In a sterile 1.5 mL eppendorf, 2 μg DNA was diluted in 100 μL serum free media. To this mixture 3 μL Fugene HD was added and the reaction was allowed to incubate at room temperature for 15 min. The entire reaction was added to each well, dropwise, and the cells were returned to the incubator for 48 h and protein expression levels were analysed by Western blot.

Cell line	G418 concentraion (µg/mL culture media)
N2a	700
SMB-PS	150
Zwl/Zpl	600

Table 2.3 G418 concentrations required for stably transfected cell lines. Concentrations were determined by performing kill curves and assessing cells after one week of treatment with various G418 concentrations.

2.3.4 MTT Assay for cell viability

2.3.4.1 Additional Materials

3-(4,5-Dimethylthiazol-2-yl)-2,5-diphenyltetrazolium bromide (MTT)

Isopropanol (Fisher, UK)

2.3.4.2 Method

Cells were plated in a 96 well plate and treated accordingly. At the end of treatment, the media was removed and 50 µL 2.5mg/mL MTT in complete culture media was added to each well. Cells were then incubated at 37°C, 5% CO_2 for 30 min. The MTT solution was removed and 100 µL isopropanol was added to each well. The plate was then incubated for a further 30 min at 37°C, 5% CO_2. The reaction was pipetted up and down in the well to ensure an even reading and read at 562 nm on a FluroStar Omega reader (BMG). Data was analysed by comparing optical density (O.D.) values at 562 as a percentage of the control as follows:

(optical density of sample)/(mean optical density of control) x 100%

2.3.5 MTS Assay for cell viability

2.3.5.1 Additional materials

3-(4,5-dimethylthiazol-2-yl)-5-(3-carboxymethoxyphenyl)-2-(4-sulfophenyl)-2H-tetrazolium) (MTS) (Promega UK)

Complete culture media (as in 2.3.1)

Dulbecco's PBS (Lonza UK)

Phenazine methosulfate

2.3.5.2 Method

Cells were plated in 96 well plates typically 1 x 10^4 cell per well and treated as required. At the end of the treatment period, 2 mL prepared MTS solution (50 mg/mL in PBS, sterile filtered) was combined with 100 µL 0.92 mg/mL phenazine methosulfate solution and 20 µL of this solution was added per well. Plates were returned to the incubator for 1-4 h and read at 495 nm. Results were calculated as in 2.3.4.2 using 495 nm values.

2.3.6 Preparation of Chelex Treated Media

2.3.6.1 Additional Materials

Media preparations as described in 2.3.1

Chelex-100 resin

$MgSO_4$

$CaCl_2$

2.3.6.2 Method

2.5 g Chelex-100 resin was added to 50 mL complete media and incubated typically overnight at 4°C with rocking, or for 1 h at room temperature with rocking. The media was then sterile-filtered using a 0.22 µm syringe filter (Millipore) and $CaCl_2$ and $MgSO_4$ was added back to basal levels (as published by the manufacturer). The media was allowed to equilibrate at 37°C, 5% CO_2 before use.

2.3.7 Infectious inoculate preparation

2.3.7.1 Additional materials

Sterile PBS

2.3.7.2 Method

2.3.7.2.1 Preparation of brain homogenates

Brains from mice infected with prion strains 79A and Me7 were suspended in 9 volumes of PBS homogenised by serial passages through needles to create a 10% (w/v) homogenate. Presence of PK-resistant PrP was checked by digesting with PK as described in 2.3.10. Homogenates were stored at -80°C until use.

2.3.7.2.2 Preparation of infected cell homogenates

SMB or infected N2a cells over expressing mPrP were grown to confluence in 75 cm^2 or 175 cm^2 flasks (Grenier BioOne) and trypsinised. Cells were counted, centrifuged, re-suspended in sterile PBS and subjected to five rapid freeze-thaw cycles. Rapid freezing and thawing was accomplished by immersing cells into liquid nitrogen until fully frozen and then transferring to a 37°C water bath.

After freeze-thawing, cells were homogenised by repeatedly passing through a 30 G needle (at least 20 times per homogenate preparation). 20 µL of this homogenate was then plated in complete culture medium and observed for 48 h to ensure homogenate did not contain viable cells. Homogenates were stored at -80°C until use.

2.3.8 Cell Infection

2.3.8.1 Additional materials

Complete culture media (as in 2.3.1)

G418 sulphate (PAA, UK)

Sterile PBS (135 mM NaCl, 26.5 mM KCl, 15 mM KH_2PO_4, 8 mM Na_2HPO_4)

2.3.8.2 Method

For infection experiments, ratios for cell infections were determined by continually plating and assessing confluency of N2a cells by eye over time periods corresponding to the infection experiments. The ideal densities would allow for the healthiest cell growth without cells becoming too over confident and allow enough cells that even if some cells succumbed (due to natural handling or any potential toxic effects of the

infectious innoculum) there would still be enough cells to take up and replicate prions. Cell density ratios were determined by seeding different ratios of target cells and choosing the ratio were cells were still viable but not over-confluent for the duration of the experiment. Ideal plating was determined to be 5.3 x 10^4 cells per cm^2 of growth area. Growth area is determined from the culture vessel manufacturer's specifications. Cell ratios of higher than this density resulted in over confluence and loss of cells. Lesser densities did not reliably show transfer of prion infectivity. Seeding densities for different culture vessels are listed in Table 2.4.

Culture Vessel	**Growth area (cm^2)**	**Seeding Density**
24 well plate	1.9	1.01 x 10^5 cells per well
12 well plate	3.8	2.02 x 10^5 cells per well
6 well plate	9.4	4.98 x 10^5 cells per well

Table 2.4 Starting seeding densities for infection assay experiments.

2.3.8.2.1 Infection using scrapie brain homogenates

Cells were plated in cell-culture treated 12 or 24 well plates (Nunc) as described in Table 2.3 and allowed to adhere in the incubator at least 6 h or preferably overnight. Once cells had adhered and determined to be of appropriate density (by eye), the media was aspirated and infectious homogenate was added to each well (no more than 10% total volume) and cells were incubated for 2 h, after which complete culture media was then added and cells incubated for a further 70 h. After this incubation, the media was removed by aspirating and cells were washed three times in sterile PBS before removal to a fresh plate. Cells were split after 4 days and passaged every 3-4 days thereafter at 1:5-1:10. After 4 passages, cells were plated onto 13mm glass cover slips, grown to 100% confluency and analysed as in Section 2.3.9..

2.3.8.2.2 Infection using infected cell homogenates

Cells were plated and allowed to adhere as in 2.3.8.2.1. Homogenates were prepared to the required concentrations and diluted in 1 mL complete culture media. The media was aspirated from each well and replaced with the homogenate suspension as appropriate, and the plate was returned to the incubator for the desired length of time.

After incubation for the appropriate time course, inoculate was aspirated and cells were washed twice with sterile PBS and then cultured in complete media until cells were

confluent. Once confluent, cells were trypsinised and plated onto cover slips for a cell blot, in a 24 well plate for Western blot analysis, and into a 12 well plate for continued culture.

2.3.8.2.3 Infection by co-culturing with SMB cells

This method is adapted from a published method (Kanu, 2002). Target cells were uninfected cells stably transfected to over-express mPrP. Both target and SMB cells (the infectious source) were trypsinised and counted. Cells were then combined at varying target: infected cell ratios and co-cultured in complete Medium 199, with no selection for 5 days. After 5 days, the medium was changed to favour the target cells and G418 was added to select for the target cells only. Cells were then cultured in G418 selection until all SMB cells were dead. Cells were then passaged and presence of PK resistant PrP confirmed by cell or Western blot.

2.3.9 Cell Blot Assay for detection of proteinase K resistant PrP

2.3.9.1 Additional materials

13 mm glass cover slips (Best, Fisher, UK)

24 well plate (Grenier BioOne, UK)

Immobilon-P Polyvinylidene Fluoride (PVDF) membrane (Millipore, UK)

Cell blot lysis buffer (50 mM Tris, 150 mM NaCl, 0.5% sodium deoxycholate (w/v), 0.5% Triton-100 (v/v), pH 7.4)

Guanidine thiocyanate (Acros Organics, UK)

Proteinase K (PK)

2.3.9.2 Method

The method is adapted from Victoria Lewis, University of Melbourne and based on a previously published method (Bosque and Pruisner, 2000). Sterile 13 mm glass cover slips were coated with poly-L-lysine for 5 min, and then rinsed with sterile PBS. Cover slips were then placed inside wells of a 24-well plate using forceps. Cells to be analysed were plated onto the cover slips then grown to 100% confluency. Cells were then washed twice with PBS with the last wash being left on the cells so there is no surface tension between the cover slip and the bottom of the plate. An appropriately sized piece of PVDF membrane was then soaked in 100% methanol for 5 min. The

membrane was then washed in MilliQ water briefly and transferred to cell blot lysis buffer. An appropriately sized piece of cellulose blotting paper was soaked in lysis buffer and placed on top of a glass plate and using a 21G 1 ½" needle and tweezers, the cover slips were removed from the wells and placed face up on the blotting paper. Then the membrane was placed carefully on top of the coverslips and a dry piece of blotting paper placed on top. The sandwich was completed by another glass plate. Using the palms of both hands, pressure was then exerted on the sandwich for 2 min. Afterwards, the membrane was carefully removed, transferred to a dry container and dried for 1h at 37°C in a dry incubator. At this stage membranes were sometimes wrapped in cling film and frozen at -20°C. Frozen membranes were allowed to thaw for a few min before PK digesting. To PK digest, the dry membrane was first soaked in lysis buffer for 5 min at room temperature before incubation in a solution of lysis buffer containing 8 μg/mL PK at 37°C for 90 min. After the incubation, the PK solution was poured off and washed three times in MilliQ water. To inactivate any infectious material, the membrane was incubated 3M guanidine thiocyanate with 10 mM Tris pH 7.4 for 10 min at room temperature. The blot was then washed three times with MilliQ water and then blocked and blotted as for Western blotting.

2.3.10 Preparation of samples for SDS-PAGE analysis

2.3.10.1 Additional Materials

Lysis buffer (sterile PBS with 1% Igepal and 1% Triton X-100)

4X loading dye (20% B-mercaptoethanol, 40% glycerol, 240 mM Tris-HCl pH 6.8, 8% SDS, 0.2% bromophenol blue)

Sterile PBS (as 2.3.8)

Proteinase K (PK)

2.3.10.2 Method

Samples were prepared for Western blot analysis by removing culture media cells and rinsingtwice with PBS. 150 μL lysis buffer was added per well in a 12 well plate, 74 μL lysis buffer was added per well in a 24 well plate, and 20 μL lysis buffer was added per well in a 96-well plate. Cells were incubated with lysis buffer for 20 min at 37°C, then scraped and removed to appropriately labelled sterile eppendorfs. Protein concentration was determined using Bio-Rad assay (see 2.3.7) and all samples were normalised for protein concentration. PK digestion, when required, was performed at

this stage using 1 μg/μL PK at a PK to total protein ratio of 1:20. Samples were digested for 1 h at 37°C. 4X loading dye was added to each sample to a final concentration of 1X and either stored frozen or used immediately for a gel. Prior to loading on gel, all samples were boiled at 100°C for 5 min.

2.3.11 Bio-Rad method for protein concentration determination

2.3.11.1 Additional Materials

BSA standards (0, 1, 2, 3, 4, 5 mg/mL)

BioRad dye reagent concentrate (BioRad, UK)

MilliQ water

2.3.11.2 Method

Samples and standards were all done in triplicate. 1 μl of each sample or standard was pipetted per well in a 96 well plate. A working reagent of the dye was prepared by combining 1 part dye reagent to 4 parts MilliQ and filtering through a 0.22 μm syringe to remove particles. 200 μL of the working reagent was added per well and mixed by pipetting up and down. The plate was incubated at room temperature for 5 min before being read on a plate reader at 595 nm. A standard curve was calculated and protein concentration was determined using the standard curve.

2.3.12 Sodium dodecyl sulphate polyacrylamide gel electrophoresis (SDS-PAGE)

2.3.12.1 Additional Materials

MilliQ water

1 M Tris pH 8.8

1 M Tris pH 6.8

Amonium persulphate (20% w/v)

Sodium dodecyl sulphate (SDS) (10% w/v)

N,N,N',N'-Tetramethylethylenediamine (TEMED)

Isopropanol (Fisher, UK)

Gel apparatus (ATTO Corporation, Japan)

Running buffer (25 mM Tris, 200 mM glycine, 0.1% SDS)

Prestained Protein Marker, 175-6 kDa (New England Biolabs, UK)

Unstained Protein Marker, 212-6 kDa (New England Biolabs, UK)

2.3.12.2 Method

2.3.12.2.1 Separating gels

Atto gel cassettes were assembled per manufacturer's instructions. Briefly, a rubber grommet was laid around the grooves in the glass gel plate, which was then sandwiched between another glass plate. This was held in place with securing clips. For 15% separating gels, 4 Ml 30% acrylamide, 2.6 mL 1 M Tris pH 8.8, 1.3 mL MilliQ water, 80 µL 10% SDS, 12 µL 20% APS and 10 µL TEMED were combined and poured into the glass plate cast. 1 mL isopropanol was then added on top of the gel mixture to ensure oxygen did not interfere with the polymerisation reaction and to ensure the resulting gel was level. Once the gel had set, the isoproanol was poured off and the gel rinsed with MilliQ water. Then the 5% stacking gel containing 625 µL 30% acyrlamide, 625 µL 1 M Tris pH 6.8, 3.6 mL MilliQ water, 50 µL 10% SDS, 20 µL 20% ammonium persulphate and 10 µL TEMED was mixed and poured on top of the separating gel. A comb was carefully inserted to avoid air bubbles and this gel was allowed to set until firm.

Once the gels had been set, the grommits, combs, and securing clips were removed and the gel cassettes were secured into the electrophoresis apparatus and the apparatus was filled with running buffer per manufacturer's instructions. Samples were denatured by heating at 100°C in 4X loading dye before loading onto gel. Gels were electrophoresed at 260 volts, 35 milliamps per gel, 100 watts for 45 min or until the dye front had reached the bottom of the gel. Gels were then disassembled from cassettes and either stained with Coomassie blue stain or transferred as for Western Blot.

2.3.12.2.2 Gradient gels

Atto gel cassettes were assembled per manufacturer's instructions. Briefly, a rubber grommet was laid around the grooves in the glass gel plate, which was then sandwiched between another glass plate. This was held in place with securing clips. 20% and 5% acrylamide mixtures were prepared as follows: for each 20% gel, 3.3 mL 30%

acrylamide, 1.625 mL 1 M Tris pH 8.8, 50 µL 10% SDS, and 8.75 µL 20% APS were mixed. For each 5% gel 833 µL 30% acrylamide, 1.625 mL 1 M Tris pH 8.8, 25 mL MilliQ water, 50 µL 10% SDS, and 8.75 µL 20% APS was mixed. 5 mL of each reaction was aliquoted into two separate falcon tubes, then 5 µL TEMED was added to each tube, rapidly mixed by inverting and immediately poured into gradient gel mixer. This reaction was allowed to fill a prepared gel cassette. A comb was carefully inserted to avoid air bubbles and the gel was allowed to set until firm.

Once the gels had been set, the grommets, combs, and securing clips were removed and the gel cassettes were secured into the electrophoresis apparatus. Samples were denatured by heating at 100°C in 4X loading dye before loading onto gel. Gels were electrophoresed and further processed as described in 2.3.12.2.1

2.3.13 Western blot

2.3.13.1 Additional Materials

Methanol

Transfer Buffer (12.5 mM Tris, 100 mM glycine, 0.5% SDS (w/v), 20% methanol (v/v))

Cellulose blotting paper extra thick

Immobilon-P PVDF membrane (Millipore, UK)

Ponceau S stain (0.2% w/v Ponceau S, 1% (v/v) acetic acid)

Marvel no fat milk powder (Sainsbury's, Bath, UK)

BSA, cold ethanol precipitated fraction V (Fisher UK)

Tris buffered saline with 0.1% (v/v) Tween-20 (TBS-T) (40mM Tris, 150mM NaCl pH 7.8)

Immobilon horseradish peroxidise (HRP) Substrate (Millipore, UK)

Antibodies:

ICSM-18 anti PrP antibody (D-Gen, UK)

8B4 anti PrP antibody (Alicon, Switzerland)

Monoclonal Anti-α tubulin (Sigma, Poole, UK)

Anti-FLAG (Sigma, Poole, UK)

Goat anti-mouse immunoglobulins (Dako, Ely, UK)

	Primary dilution	Secondary dilution
ICSM-18	1:15,000	1:20,000
8B4	1:20,000	1:30,000
Anti α-tubulin	1:30,000	1:30,000

Table 2.5 Antibody dilutions used in Western blotting.

2.3.13.2 Method

SDS-PAGE gels were run as described. Immobilon-P membrane was cut to fit the gel and soaked in methanol for 5 min, before soaking in transfer buffer. Gels were soaked in transfer buffer for 15 min. Two appropriately sized pieces of cellulose blotting paper were wetted in transfer buffer before placing in a Trans-Blot semidry transfer cell (BioRad). Using forceps, the membrane was placed on top of the blotting paper and carefully smoothed to ensure no air bubbles would interfere with the transfer. The gel was then placed carefully on top of membrane before completing the sandwich with another two pieces of transfer buffer-soaked blotting paper. Transfers were done either at 100 watts, 20 volts, 100 milliamps per 6 x 9 cm membrane, for 2 h or 100 watts 6 volts, 16 milliamps per 6 x 9 cm membrane, overnight.

Once transfers were completed, the membrane was stained in Ponceau S, a reversible stain, for 2 min. After successful transfers were confirmed, membranes were rinsed in MilliQ water until all stain had been removed and then blocked in 5% BSA or 5% non fat milk powder in TBS-T for 1h at room temperature. Membranes were then incubated with primary antibody dilutions as indicated in Table 2.5,with rocking either for 2 h at room temperature or overnight at 4°C. After primary antibody incubation, membranes were rinsed twice in TBS-T then washed for three 5 min washes in TBS-T with rocking. Membranes were then incubated with secondary antibodies conjugated with horseradish peroxidase, in dilutions as indicated Table 2.5, for 1-2 h at room temperature with rocking before washing exactly as for the primary antibody. After the

last wash, membranes were laid face up on cling film and Immobulin HRP Western Reagent as applied evenly to the membrane. Membranes were incubated for five min, then the reagent was removed and membranes were wrapped in cling film and developed in a dark room by exposing Fujifilm X ray film to the membranes and developed.

2.3.14 Coomassie Blue staining

2.3.14.1 Additional Materials

Coomassie stain (0.25 g Coomassie, 45% methanol (v/v), 10% glacial acetic acid (v/v))

Destaining buffer (7% glacial acetic acid (v/v), 8% methanol (v/v))

2.3.14.2 Method

Gels were removed from the glass plate apparatus and carefully placed in a square plastic Petri dish filled with Coomassie stain. Gels were incubated in stain either overnight at room temperature with rocking or microwaved on high for 15 s then rocked at room temperature for 5 min. Stain was carefully poured away and gels were rinsed once with destain buffer to remove excess stain before incubating overnight in fresh destaining buffer.

2.3.15 Densitometry analysis of Western blots

2.3.15.1 Additional materials

Computer scanner

ImageJ software version 1.43n (http://rsbweb.nih.gov/ij/index.html)

2.3.15.2 Method

Western blot images to be quantified were scanned and analysis performed using ImageJ software. Relevant bands were measured using the same measuring area for each separate blot. Background values were subtracted from each sample and all samples normalised to their α-tubulin values to control for protein loading. Data are presented as normalised to the untreated control.

2.4 Recombinant Protein Techniques

2.4.1 Expression of recombinant mPrP constructs

2.4.1.1 Additional Materials

LB (Melford, UK)

Carbenicillin sodium salt (Melford, UK)

Isopropyl β-D-1-thiogalactopyranoside (Apollo Scientific, UK)

2.4.1.2 Method

A single colony of the desired PrP construct, transformed into BL21 cells as above was inoculated into 100 mL LB containing 50 μg/mL carbenicillin and incubated with shaking at 160 r.p.m., overnight at 37°C. The next day, 15 mL of overnight culture was inoculated into each 1 L of LB media containing 50 μg /mL carbenicillin and incubated at 37°C with shaking at 200 r.p.m.. The optical density of the cells was monitored at 600 nm and once the density reached 0.6, expression of the protein constructs was induced by the addition of 1 mM IPTG. Protein expression was carried out for a further five hours at 37°C with shaking at 200 r.p.m.. Cells were then pelleted by centrifugation at 4000 r.p.m. for 5 min. These pellets were stored at -20°C until lysis.

2.4.2 Bacterial Cell Lysis

2.4.2.1 Additional materials

Bacterial lysis buffer (0.2 M NaCl, 0.5 M Tris, 1 mM EDTA pH 7.6)

Lysozyme

Deoxyribonuclease I

Phenylmethanesulphonylfluoride

Ribonuclease I

2.4.2.2 Method

Bacterial cells were re-suspended in 2 mL lysis buffer per gram of pellet. 15 mg lysozyme was added per 30 mL of solution to lyse the bacterial cells and 0.8 mM phenylmethanesulphonylfluoride was added to prevent degradation of recombinant protein. This reaction was incubated at 37°C for 30-45 min, and then 50 mg sodium

deoxycholate was added to solubilise membrane components and incubated for a further 45 min. Next, 1 mg each of deoxyribonuclease I and ribonuclease I was added to the 30 mL lysis solution and incubated for 1 hour to ensure all DNA and RNA had been degraded. The lysed solution was then centrifuged for 25 min at 12,500 r.p.m. and the supernatant was discarded. This pellet was then stored at -20°C or immediately processed for purification.

2.4.3 Purification of recombinant PrP

The preparation of PrP has been described previously (Thompsett *et al.*, 2005).

2.4.3.1 Additional Materials

Bacterial lysis buffer (0.2 M NaCl, 0.5 M Tris, 1 mM EDTA pH 7.6)

8 M urea buffer (8 M urea, 200 mM NaCl, 50 mM Tris pH 7.6)

His-tag wash buffer (8 M urea buffer, 20 mM imidazole, pH 7.6)

0.3 M $CuSO_4$

0.2 M EDTA

1 M sodium hydroxide (NaOH)

1 M sodium chloride (NaCl)

Elution buffer (8 M urea, 200 mM NaCl, 50 mM Tris, 300 mM imidazole, pH 7.6)

20% ethanol (EtOH)

Metal chelating sepharose, fast flow (GE Healthcare, UK)

2.4.3.2 Method

2.4.3.2.1 Purification by immobilised metal affinity chromatography

Immobilised metal affinity chromatography (IMAC) was used to purify PrP with copper binding regions intact. As PrP has a high affinity for copper, untagged recombinant proteins can be purified using copper-charged metal chelating sepharose. His-tagged proteins were purified using nickel-charged metal chelating sepharose.

The pellet from the bacterial cell lysis was re-suspended by sonication at minimum power in 25 mL wash buffer A (bacterial lysis buffer, 1% Triton X-100, 0.5% Igepal) and centrifuged for 5 min at 12,500 r.p.m. and 4°C. The supernatant was discarded and

the wash step repeated once. Then the pellet was re-suspended by sonication at minimum power in 25 mL wash buffer B (lysis buffer, 1% Igepal) and centrifuged for five min at 12500 r.p.m., 4°C. The supernatant was discarded and the step repeated. The sonication/re-suspension/centrifugation step was then performed using lysis buffer only to clear any detergents from the preparation and the pellet retained. The pellet was solubilised in 8M urea buffer by sonicating at 75% maximum power 3 times in 30 s bursts. This re-suspended solution was then centrifuged for 25 min at 12500 r.p.m., 4°C. The supernatant was then filtered through a 0.45 μm syringe filter and this protein solution used for IMAC purification.

The IMAC column was prepared by packing an appropriate column with chelating sepharose and washing through with sterile MilliQ water. 6 column volumes (CVs) of 0.2 M EDTA was then washed through, followed by MilliQ water, a further 6 CVs of 1 M sodium hydroxide, then MilliQ water. Once an appropriate volume of MilliQ water had been washed through, the column was charged by pumping 6 CVs of 0.3 M $CuSO_4$ (non-tagged PrP) or 0.3 M $NiSO_4$ (his-tagged PrP) through the column, followed by a MilliQ wash and 8 M urea buffer to prepare the column. The protein solution was then applied to the column and the column was washed with 8 M urea buffer without imidazole for non-tagged PrP or with his-tag wash buffer for his-tagged PrP. The flow through was monitored by UV absorbance readings at A_{280} until there was no protein in the flow through. The PrP was eluted from the column using elution buffer with the eluate collected in 3 mL fractions. These fractions were analysed by SDS-PAGE for purity and protein identity. The IMAC column was then regenerated by washing with 0.2 M EDTA, 1 M NaCl, then 1 M NaOH, with each followed by MilliQ water. The column was stored in 20% EtOH at 4˚C when not in use.

2.4.3.2.2 Purification using the wash method

For PrP with reduced or without copper binding sites, a purification protocol using a wash method was developed.

The pellet from the bacterial cell lysis was re-suspended by sonication at minimum power in 25 mL wash buffer A (bacterial lysis buffer, 1% Triton X-100, 0.5% Igepal) and centrifuged for 5 min at 12500 r.p.m., 4°C. The supernatant was discarded and the sonication /re-suspension/centrifugation step repeated for a total of six times. The pellet was then re-suspended by sonication at minimum power in 25 mL wash buffer B (lysis buffer, 1% Igepal) and centrifuged for five min at 12500 r.p.m. at 4°C. The

supernatant was discarded and the step repeated six times. The sonication/re-suspension/centrifugation step was then performed four times using lysis buffer only to clear any detergents from the preparation and the pellet retained. The pellet was then solubilised in 8 M urea buffer by sonicating at 75% maximum power 3 times in 30 s bursts. This re-suspended solution was centrifuged for 25 min at 12500 r.p.m., 4°C. The supernatant was then filtered through a 0.45 μm syringe filter and analysed by SDS-PAGE.

2.4.4 Refolding

2.4.4.1 Additional Materials

Glutathione (reduced form)

Glutathione (oxidised form)

Sodium phosphate buffer pH 5.8

Sodium phosphate buffer pH 7.4

2.4.4.2 Method

2.4.4.2.1 Standard refolding

PrP solubilised in 8 M urea is completely denatured. Re-naturation took place at room temperature. To re-nature the protein, the urea must be slowly diluted and dialysed so the protein folds into its native conformation. For use in Thioflavin T assays, glutathione in both oxidised and reduced forms was added to PrP in urea buffer at a final concentration of 6 mM each. This solution was then aliquoted into sets of three 1 mL fractions. To the first 1 mL fraction, 10 mL sterile 10 mM sodium phosphate buffer, pH 5.5 was added very slowly with mixing. If any precipitate formed, it is assumed to be mis-folded (non-native) PrP and thus the solution was then centrifuged at 4000 r.p.m. until the solution cleared and misfolded protein was pelleted. This supernatant was then added very slowly to the second 1 mL fraction with stirring. The protein solution was again centrifuged until clear, and this supernatant was added slowly to the third 1 mL fraction with mixing. This solution was centrifuged until clear and transferred to fresh tube until dialysis. For ITC assays, PrP was refolded in sterile MilliQ water, pH 5.5.

2.4.4.2.2 Copper loaded refolding

Re-naturation took place at room temperature. To load the PrP with $CuS0_4$, urea was sequentially diluted in 5 mM $CuSO_4$, concentrating the solution between dilutions using a VivaSpin 10,000 MW cut-off concentrator. All solutions were centrifuged to remove precipitation before dialysis as in 2.4.4.2.1.

mPrP construct	Purification	Pre-refolding (mg/L culture)	Post-refolding (mg/L culture)
mPrP(23-231)	Cu-IMAC	10-15	6-8
mPrP(23-231)	Wash method	20-35	2-5
mPrP(89-231)	Wash method	15-20	2-4
mPrP(Δ51-90)	Wash method	15-20	2-4
mPrP(Δ67-90)	Wash method	15-20	2-4
mPrP(Δ06-126)	Wash method	15-20	2-4
mPrP(Null)	Wash method	20-25	2-5
mPrP(H95A+H110A)	Cu-IMAC	8-13	5-8
mPrP(H95A+H110A)	Wash method	20-35	2-5
mPrP(Null +H95, H110)	Wash method	20-25	2-5
mPrP(Null + H95)	Wash method	20-25	2-5
mPrP(Null +H110)	Wash method	20-25	2-5

Table 2.6 Yeilds of mPrP protein preparations. All yields are calculated in mg per L of culture.

2.4.5 Dialysis

2.4.5.1 Additional Materials

12-14000 Dalton cut off tubing (Medicell, UK)

7000 Dalton cut off tubing (Medicell, UK)

MilliQ water

Sodium phosphate pH 5.8 and pH 7.4

Dialysis tubing preparation buffer (2% (w/v) sodium bicarbonate, 1 mM EDTA)

2.4.5.2 Method

Dialysis tubing was prepared by cutting appropriate sized lengths of tubing then rinsing with MilliQ water. The rinsed tubing was then immersed into dialysis tubing preparation buffer and heated to 80°C for 30 min. The tubing was then rinsed repeatedly in MilliQ and stored in 20% ethanol until use.

Dialysis tubing was prepared for dialysis by rinsing tubing repeatedly in MilliQ water to remove all traces of ethanol. After double knotting the end of the dialysis tubing, protein was added to the tubing, sealed by double knotting and dialysed at 4°C against MilliQ water (GAG studies) or 10 mM sodium phosphate (ThT studies). Dialysis typically took place at pH 5.8 until the final round when the pH was adjusted to 7.4. The protein solution was dialysed at least 10^6 fold to ensure sufficient dilution of urea.

Dialysed proteins were either stored at -80°C in aliquots until use to prevent freeze-thawing or at 4°C for use within a week.

2.4.6 Concentration Determination

2.4.6.1 Additional materials

Quartz cuvettes (CaryBio)

2.4.6.2 Method

Recombinant protein concentration was determined by measuring the absorption of 1 mL of protein solution at 280 nm in quartz cuvettes in a CaryBio UV-Vis spectrophotometer. Concentrations were calculated using an extinction coefficient obtained by entering the primary sequence into the ProtParam tool on the ExPASy database (Gasteiger *et al.,* 2003). Extinction coefficients used are summarised in Table 2.4.

PrP Construct	M-1 cm-1	A_{280} (mg/mL)	MW	pI	length (aa)
pET3a-mPrP(23-231)	63495	2.743	23150.5	9.56	210
pET3a-mPrP(89-231)	27515	1.682	16360.2	8.84	143
pET3a-mPrP(Δ51-89)	35995	1.868	19268.4	9.56	171
pET3a-mPrP(Δ67-90)	46996	2.264	20760	9.56	186
pET3a-mPrP(Δ106-126)	63495	2.97	21377.4	9.49	189
pET23a-mPrP(H95A)	63495	2.761	22997.3	9.56	210
pET23a-mPrP(H110A)	63495	2.761	22997.3	9.56	210
pET23a-mPrP(H95A+H110A)	63495	2.769	22931.3	9.56	210
pET23a-mPrP(Null)	63495	2.801	22535.8	9.56	210
pET23a-mPrP (Null + H95, H110)	63495	2.785	22799.1	9.56	210

Table 2.7 Recombinant PrP parameters calculated using primary amino acid sequences

2.4.7 Preparation of recombinant samples for SDS-PAGE analysis

2.4.7.1 Additional Materials

4X loading dye (20% B-mercaptoethanol, 40% glycerol, 240 mM Tris-HCl pH 6.8, 8% SDS, 0.2% bromophenol blue)

2.4.7.2 Method

Protein concentration was calculated as in 2.4.6. All samples were normalised for protein concentration and sample volume. 4X loading dye was added to each sample to a final concentration of 1X and samples were either stored at -20°C if not used immediately for a gel. Prior to loading on gel, all samples were boiled at 100°C for 5 min.

2.4.8 Aggregation Assays

2.4.8.1 Additional Materials

Sodium Phosphate Buffer pH 7.4

$CuS0_4$ (Fisher, UK)

$MnS0_4$ (Fisher, UK)

$ZnCl_2$ (Fisher, UK)

Thioflavin T (ThT)

3 mm glass beads

2.4.8.2 Method

2.4.8.2.1 Aggregation reactions

Recombinant protein was refolded as described in 2.4.4 and dialysed against 10 mM sodium phosphate buffer. The final dialysis was performed in 10 mM sodium phosphate, pH 7.4 and protein concentrated to a final concentration of 20 μM. 100 μL of the protein was added to each well of a black 96-well plate and metals or heparin added as appropriate. 10 μL ThT dissolved in 10 mM sodium phosphate, pH 7.4 was added to each well for a final concentration of 10 μM and one sterile glass bead added per well. The plate was covered with a film, placed on a GrantBio plate shaker and incubated at 37°C whilst shaking at 600 r.p.m.. Measurements were taken at various

time intervals on a Fluoroskan (Thermofisher) using excitation wavelength 444 nm and emission wavelength 482 nm or on a FLUOstar Omega (BMG) using 445-5nm excitation and 480-10nm emission filters.

2.4.8.2.2 Kinetic calculations.

Rate calculations were done on normalised data on the linear increase of the aggregation curve. Any obvious outliers were excluded from calculations. All rate values were compared to an untreated control for comparative results. Rate is defined as in Equation 1:

$$rate = \frac{\Delta fluorescence\ intensity}{\Delta time}$$

Equation 1

Maximum fluorescence values were calculated by determining the highest fluorescence intensity reached during the reaction and comparing the value back to the untreated control.

2.4.9 Transmission Electron Microscopy

2.4.9.1 Additional materials

Uranyl acetate

2.4.9.2 Method

Aggregation products were imaged using transmission electron microscopy (TEM) by Ms Ursula Potter of the Centre for Electron Optical Studies, University of Bath. mPrP aggregation reaction end products were coated onto copper grids, washed twice with MilliQ water and then negatively stained with 0.2% uranyl acetate. Microscopy imaging was performed on 80 kV Jeol-1200EX electron microscope and samples viewed at 100,000x magnification.

2.4.10 Isothermal Titration Calorimetry

2.4.10.1 Additional materials

Heparin sodium sulphate, 3000 MW

MilliQ water

Recombinant mPrP as prepared in sections 2.4.1-2.4.5

2.4.10.2 Method

2.4.10.2.1 ITC method

Recombinant mPrP was refolded as described previously and dialysed against MilliQ water. During the final round of dialysis, the pH was adjusted to 7.4. Heparin sodium sulphate was then prepared in sterile MilliQ water pH 7.4. Measurements were performed using a VP-ITC (MicroCal). The heparin was loaded into the cell of the ITC machine and the temperature reference chamber was filled with MillQ water. mPrP was loaded into the syringe. Once assembled, the correct concentrations were entered into the VP-ITC control software and the injection parameters were 30x 4 μL injections with 120 s equilibration between injections, with constant stirring at 300 r.p.m.. Once the machine had equilibrated to 25°C, the reaction began. In between runs, the chamber and syringes were cleaned 10 times using MilliQ water.

2.4.10.2.2 Data analysis of ITC data

Data was analysed using Origin 5.0 software (MicroCal). It was determined by trial and error that sequential binding models best fit the data produced in these experiments, as determined by the χ^2 value (the lowest value is a judgement for the validity of the binding model fit). For sequential binding, the binding constants K1, K2, ...Kn must be defined relative to the progress of saturation, so that

$$K_1 = \frac{[LM]}{[L][M]} \quad K_2 = \frac{[LM_2]}{[LM][M]} \quad K_3 = \frac{[LM_3]}{[LM_2][M]} \quad K_n = \frac{[LM_n]}{[LM_{n-1}][M]} \qquad (1)$$

In the sequential model only the total number of sites that are saturated are assessed. If the sites are identical, a statistical degeneracy associated with the sequential saturation since the first ligand to bind has more empty sites of the same kind to choose from than does the second ligand. For identical interacting sites the phenomenological binding constants Ki (defined by equation (1)) and the intrinsic binding constants *Kio* can be distinguished where the effect of degeneracies has been removed. The relationship between the two binding constants is given by the following equation:

$$Ki = \frac{n-i+1}{i} K_i^0 \qquad (2)$$

All calculations given below, as well as parameters reported from curve-fitting, are in terms of Ki values but these can be manually converted to *Kio* values, if desired, using equation (2) (this is done within the program). As all concentrations of bound species [LM_n] can be defined relative to unbound species [L] then the various fractions of L with n bound M can be defined by F_n in equations (3)

$$F_0 = \frac{1}{X} \quad F_1 = \frac{K_1[\mathrm{M}]}{X} \quad F_2 \frac{K_1 K_2[\mathrm{M}]^2}{X} \quad F_n = \frac{K_1 K_2 \ldots . K_n[\mathrm{M}]^n}{X} \qquad (3)$$

Where

$$X = 1 + K_1[\mathrm{M}] + K_1 K_2[\mathrm{M}]^2 + \ldots\ldots + K_1 K_2 \ldots K_n[\mathrm{M}]^n \qquad (4)$$

$$Xt = [X] + Mt \sum_{i-1}^{n} iF_i \qquad (5)$$

The parameter n and K can now be assigned through trial and error, allowing equations 3, 4 and 5 to be solved by the Bisection method. The total fractions can then be determined and related to the heat content Q after each titration of ligand by equation 6.

$$Q = LtVo(F_1\Delta H_1 + F_2[\Delta H_1 + \Delta H_2] + \ldots\ldots + F_n[\Delta H_1 + \Delta H_2 + \ldots\ldots + \Delta H_n) \qquad (6)$$

Using the same definitions as before. The effect of each injection i, allowing for a correction for the displaced volume after i is then defined by 7

$$\Delta Q(i) = Q(i) + \frac{dV_i}{V_o}\left[\frac{Q(i) + Q(i-1)}{2}\right] - Q(i-1) \quad (7)$$

Which is then submitted to the Levenburg-Marquardt minimization routine. This analysis is done through the Origin 5.0, where all these equations are built in and parameters are easily manipulated.

2.4.11 Computational peptide analysis

2.4.11.1 Additional materials

TANGO (http://tango.crg.es/)

WALTZ (http://switpc7.vub.ac.be/cgi-bin/submit.cgi)

Mobyle (http://mobyle.pasteur.fr/cgi-bin/MobylePortal/portal.py?form=charge)

2.4.11.2 Method

2.4.11.2.1 TANGO

Analysis of mouse PrP (NM_0011170) protein aggregation propensity was done using the on-line program TANGO ((http://tango.crg.es/), developed by L.Serrano, European Molecular Biology Laboratory. Analytical conditions were set at 310.15 K, pH 7.4, 0.01M ionic strength, default stability (-10) and TFE concentration (0%).

2.4.11.2.2 WALTZ

Analysis of amyloidgenic regions in murine PrP (NM_0011170) was done using the on-line program WALTZ (http://switpc7.vub.ac.be/cgi-bin/submit.cgi), developed by the Switch Laboratory, Vrije Universiteit Brussel, Belgium. Analyses were performed using primary amino acid sequences of murine PrP. Analytical conditions were set at high specificity and at pH 7.0.

2.4.11.2.3 Mobyle

Analysis of protein charge distribution of PrP (NM_0011170) was performed using the Mobyle program (http://mobyle.pasteur.fr/cgibin/MobylePortal/portal.py?form=charge), developed by

The European Molecular Biology Open Software Suite (EMBOSS). Analyses were performed using primary amino acid sequences of murine PrP.

2.5 Statistical Analyses

Paired Student's T-tests were performed on samples using Microsoft Excel Data Analysis Pak (2007) to determine significance at 95% confidence levels or above.

3. Metals and cellular prion infection

3.1 Introduction

Transmissible spongiform encephalopathies are often considered to be infectious diseases as studies have shown they are transmissible from animal to animal (Cuille and Cheille, 1936). The exact mechanism of transmission is unknown, as there is still very little insight into how the infection occurs.

The infectious particle is generally thought to either consist solely of or include an abnormal version of the prion protein, called variously PrP^{Sc}, PrP^{res}, or PrP^{TSE} all of which refer to the disease-associated prion molecule. Standard identification of infectious material is identified by resistance to proteinase K and transmissibility *in vitro* cell culture or animal bio assays. TSE's were first transmitted to laboratory animal models in the 1960's and 1970's (Chandler *et al.*, 1961; Chandler and Turfry, 1972; Zlotnik and Stamp, 1965). These rodent-adapted prion strains have been characterised in mouse and hamster models, and more recently in bank voles (Cartoni *et al.*, 2005). The generation of transgenic mice expressing other mammalian PrP including hamster, bovine, ovine, cervid, and human PrP has allowed for characterisation of naturally occurring prion diseases such as scrapie, BSE and CWD (Hsiao *et al.*, 1990; Browning *et al.*, 2004; Buschmann *et al.*, 2000; Telling, 2004; Kupfer *et al.*, 2007). Study of prion disease in laboratory animal models is advantageous as they have a shorter incubation period than the host animal and laboratory animals are easier to maintain. However, while disease incubation periods are relatively reduced in laboratory animals, the experiments still take many months, and as with all animal experiments there is always a cost factor.

Cell culture models of prion infectivity are an alternative to expensive animal bioassays. The advantages of cell culture models of prion infection are that the experiments are usually conducted in a much shorter length of time and are less expensive than maintaining animals for bioassay. Cell culture models are a useful method of obtaining more information regarding prion infectivity, although proof of principle is usually expected from animal bioassays. Only a handful of cell lines are permissive to prion infection, and both neuronal and non-neuronal cells have been shown to support prion infection. The first cell model of prion disease was the SMB

cell line, which was derived from the brain of a scrapie-infected mouse (Clarke and Haig, 1970). Further work identified neuronal cell types which support prion infection including neuroblastoma, hypothalamic, hippocampal, pheochromocytoma, septal neural cells and neural stem cells (Race *et al.*, 1987; Schatzl *et al.*, 1997; Rubenstein *et al.*, 1984; Baron *et al.*, 2006; Milhavet *et al.*, 2006; Maas *et al.*, 2007). In addition, primary neuronal cultures have also been shown to support prion infection (Cronier *et al.*, 2004). As symptoms of prion disease are largely neuronal, neuronal cell cultures are widely used to investigate prion disease *in vitro*. However a number of non-neuronal cells have been demonstrated to support prion infection, including epithelial cells, muscle cells, fibroblasts, and microglial cells (Vilette *et al.*, 2001; Vorberg *et al.*, 2004; Dlakic *et al.*, 2007; Iwamaru *et al.*, 2007). Understanding prion infection in these cell models may provide more information regarding transmission of disease.

Prion infection in cell culture models can be accomplished in several ways. The most common method is to expose uninfected cells to homogenates of brains from infected animals, or to use homogenised infectious cell preparations (Race *et al.*, 1987; Butler *et al.*, 1988; Bosque and Prusiner, 2000; Enari *et al.*, 2001). Additionally infection can be accomplished by co-culturing infected and uninfected cells, or by applying partially purified prion preparations (e.g., prion rods) to cells (McKinley *et al.*, 1991; Kanu *et al.*, 2002; Hijazi *et al.*, 2003). Once cells are exposed to the infectious material, they are analysed for the presence of PK-resistant PrP as a marker for infection.

It has been well documented that PrP is capable of metal binding, as described in 1.3.2. The evidence suggests that metals may play a role not only in the normal function of the protein but potentially in disease pathogenesis as well. However, the precise role metals play in prion disease progression is unclear.

Cell culture models have been used to identify PrP^C interactions, anti-prion therapies, cellular changes in response to infection, PrP trafficking pathways, as well as identification of cellular components that may be involved in of the transfer of infectivity (Solassol *et al.*, 2003; Hornchik *et al.*, 2005; Morel *et al.*, 2005; Vilette, 2008). Despite this, relatively few studies have focused on the role of metals in prion infection in cell culture. This study aims to identify the role of metals, in particular copper, manganese, and zinc, in the transfer of prion infectivity (that is, conversion from PrP^C to PK-resistant PrP associated with prion disease) using a cell culture model of prion infection.

Further to this investigation, there are many proteins which have specific functions controlling the movement and concentration of metal ions within the cell, including the copper associated proteins CTR1, CTR2, CCS and ATOX1. These proteins play an important role in copper movement through the cell. CTR1 is a copper transporter involved in regulating copper entry into the cell and CTR2, another transporter, is involved in mobilisation of copper from organelles to the aqueous cytoplasm (Prohaska and Gybina, 2004; Guo *et al.*, 2004; van de Berghe *et al.*, 2007). ATOX1 and CCS are copper chaperones. ATOX1 ferries copper to the trans-Golgi network, and CCS is responsible for distributing copper to copper/zinc superoxide dismutase (Prohaska and Gybina, 2004). The effect of these copper transporters on PrP expression and transfer of prion infectivity will be studied to determine if these proteins influence prion infection.

3.2 Method Development

To assess whether or not metals could influence the transfer of prion infectivity in cell culture, a model first had to be developed.

3.2.1 Infected brain homogenates as infectious source

Initial infection experiments were performed using homogenised infectious mouse brains. The mice were infected with the 79A or Me7 strain of mouse-adapted scrapie and inoculates prepared as described in 2.3.7.2.1.Only very limited quantities of the brains were available.

Brain homogenates were assessed for PK-resistant PrP by Western blot (Figure 3.1). All cell blot and Western blot analysis throughout this chapter were performed using anti-PrP antibody ICSM-18. Western blot results show no PK-resistant PrP in the control (uninfected) homongenate samples, as expected. Samples of both Me7 and 79A brain homogenate contained detectable PK-resistant PrP.

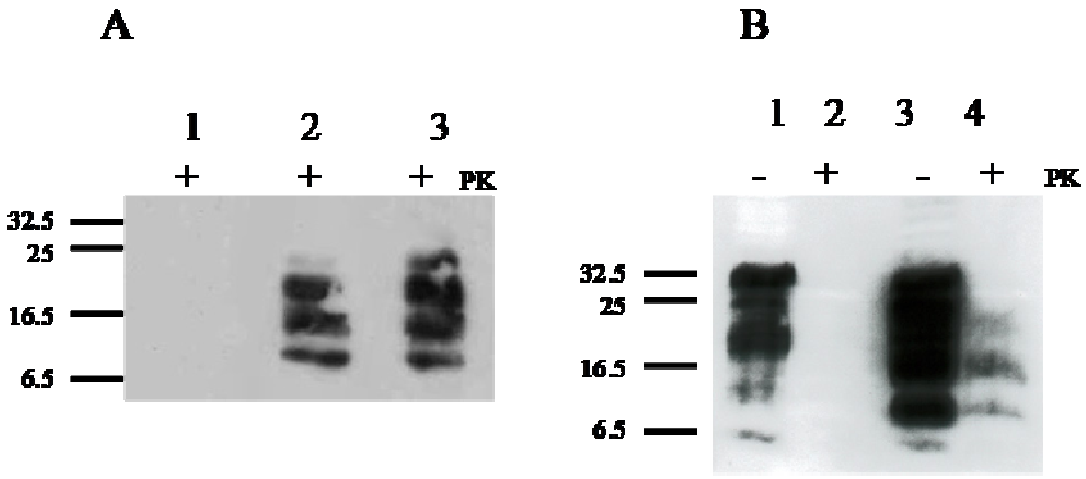

Figure 3.1 Western blot of Proteinase K resistant PrP in infected brain homogenates. A) PK digested samples only of brain homogenates. Lane 1 is control brain homogenate and does not have any PK-resistant PrP present. Lane 2, brain homogenated from a mouse infected with the Me7 prion strain. Lane 3, brain homogenate from a mouse infected with the 79A prionstrain. Multiple bands can be seen in both the Me7 and 79A prion strain samples, representing differently glycoyslated forms of PrP after PK digestion. All samples are 20 µg of 1% whole brain homogenate digested with 1 µg PK for 1 h at 37°C. B) Brain homogenates treated and not treated with PK to show PrP glycoprofiles.Lane 1 and 2 control, Lane 3 and 4 79A strain. Samples are 20 µg of 10% brain homogenate with and without PK digestion (1 µg PK for 1 h at 37°C).

The target cells for the infection experiment with brain homogenate were N2a cells, which are a well characterised murine neuroblastoma cell line derived from a spontaneous tumour in albino mice (Klebe and Ruddle, 1969). N2a cells are routinely used for prion studies as they are susceptible to prion infection (Race *et al.*, 1987). As over-expression of PrP in N2a cells increases susceptibility to prion infection (Nishida *et al.*, 2000), all N2a cell used throughout this study were stably transfected to over express pcDNA3.1+mPrP(1-254) and denoted N2a(mPrP). PrP expression levels of in N2a and N2a(mPrP) cells are shown in Figure 3.2. Classic PrP banding patterns show di-, mono-, and unglycosylated forms of PrP at bands corresponding to approximately 35, 24, and 18 kDa.

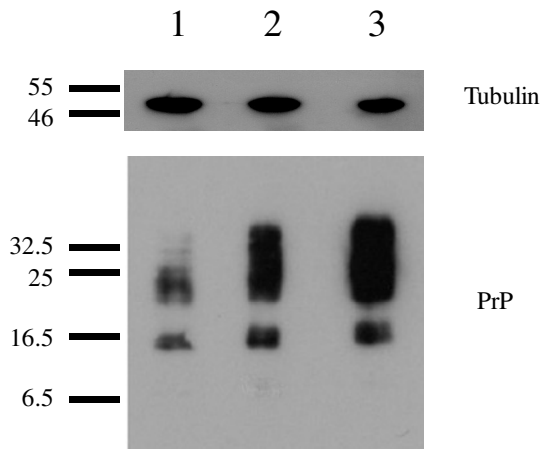

Figure 3.2 Western blot of PrP^C expression in N2a cells. Lane 1, untransfected N2a cells. Lanes 2 and 3, N2a(mPrP). Lanes 2 and 3 represent two polyclonal stably over-expressing populations of N2a(mPrP) cells which were created at different times. Both populations express higher levels of PrP than un-transfected N2a cells. Markers are in kDa and the pattern of bands is characteristic of PrP blots and correspond to di-, mono- and unglycosylated forms of PrP.

Target N2a(mPrP) cells were plated as described in in Section 2.3.8. Cells were allowed to adhere overnight, and then the media was removed and fresh media containing 0.1% or 1% infectious brain homogenate was added to each well. Uninfected brain homogenate was used as a control. Cells were then analysed for PrP^{Sc} 4 passages post infection to detect *de novo* prion infectivity.

Prion infection of the brain homogenate infectivity assays is detected by cell blot. To ensure only prion infectivity (that is, PK-resisant PrP) and not residual cellular PrP signal was detected, the activity of PK was tested before each analysis to determine the appropriate concentration of PK to use. Tests were performed on SMB (scrapie mouse brain) cells, a chronically infected cell line (Clarke and Haig, 1970) and uninfected N2a(mPrP). The appropriate level of PK was judged to be where signal was present in SMB samples but no signal was detected in the N2a(mPrP) sample (Figure 3.3A). Figure 3.3B highlights that despite the high level of PrP^C expression in N2a(mPrP) (lanes 1-2), only SMB cells express PK-resistant PrP (lanes 3 and 4), as shown by Western blot.

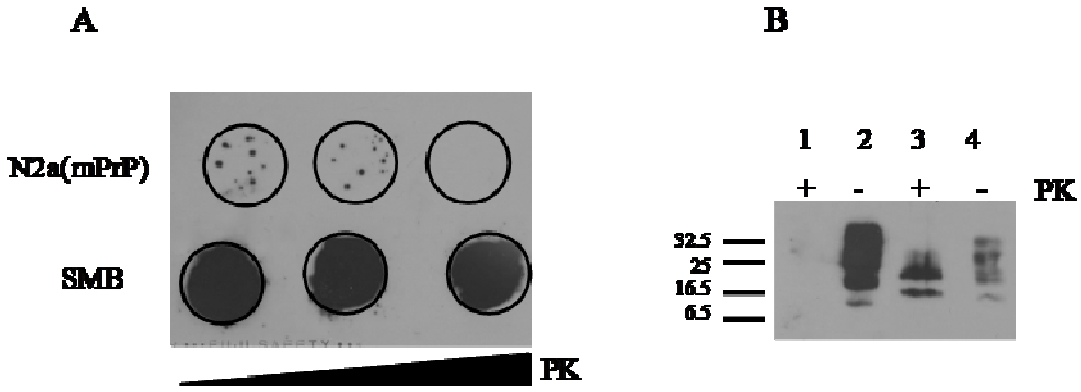

Figure 3.3 PK-resistant PrP in N2a(mPrP) and SMB cells. A) Cell blot showing example of PK digestion trial. Uninfected N2a(mPrP) and SMB cells were subjected to cell blot analysis with to increasing concentrations of PK (from left to right). B) Western blot of N2a(mPrP) and SMB. Lane 1 and 2, uninfected N2a(mPrP); Lane 3 and 4, SMB cells. PK-digested samples were subjected to 1 µg PK per 20 µg total protein and digested for 1 h at 37°C. Markers are in kDa.

Results of infectivity assays using infected brain homogenates as the infectious source indicated PK-resistant PrP in target cells that were infected with 1% and 0.1% 79A homogenate but not with Me7 homogenate (Figure 3.4). These data support previously published observations asN2a cells are known to replicate Chandler, Fukokura, and RML prion strains, but do not replicate Me7 prions (Bosque *et al.*, 2000; Klohn *et al.*, 2003). Further access to prion-infected brains was not possible, so an alternative infectivity assay was devised.

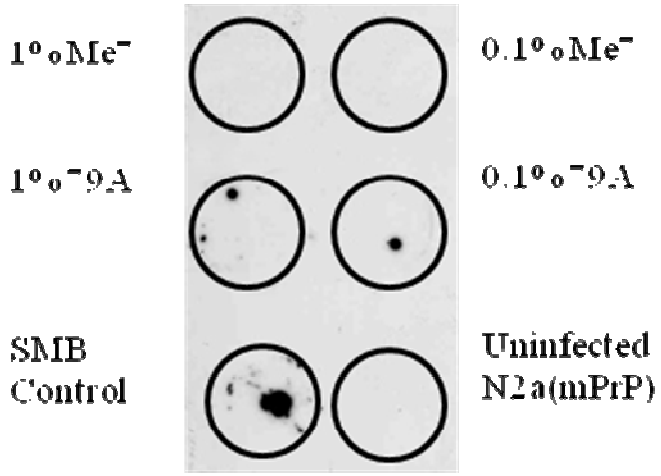

Figure 3.4 Cell blot from brain homogenate infectivity assay, analysed 4 passages post infection. 1% and 0.1% (w/v) brain homogenates were from Me7 and 79A infected mice, n=2.

3.2.2 Infection by live cell co-culture

Infection protocols were developed utilizing the co-culturing method described by Kanu *et al* (Kanu *et al.*, 2002) and was first used by previous lab members who had adapted it from the original published results.

3.2.2.1 SMB-PS as target cell line

SMB (scrapie mouse brain cells) were used as the infectious source, SMB cells are a line derived from the brain of a mouse clinically ill with scrapie (Clarke *et al.*, 1970). These cells contain PK-resistant PrP as described in 3.2.1 and shown in Figure 3.3B. Target cells were stably transfected SMB-PS cells over-expressing mPrP (SMB-PS(mPrP)). SMB-PS cells are SMB cells which have been treated with pentosan sulphate (PS) and no longer express detectable PK-resistant PrP^{Sc} (Birkett *et al.*, 2001).

For the infection assay, cells were cultured in the same flask at various ratios based on cell number (1:10, 1:50, 1:100 (SMB-PS(mPrP):SMB) for 5-7 days, and then G418 sulphate was added to kill the susceptible SMB cells. The stably transfected SMB-PS(mPrP) cells are resistant to G418 sulphate and therefore survive. Cells were then propagated for four passages and assessed for infection by detecting PK-resistant PrP by Western blotting. Results from the SMB-PS(mPrP) cells showed no PK-resistant PrP at any infectious dose tested despite expressing higher levels of PrP^{C} than SMB cells(Figure 3.5).

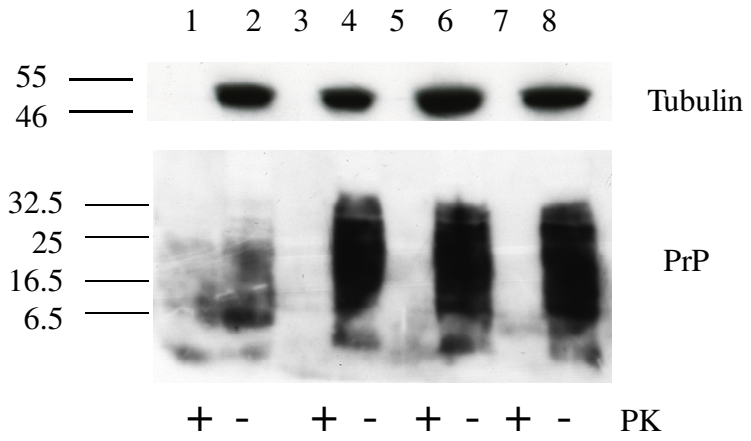

Figure 3.5 Western blot of co-culturing assays with SMB-PS(mPrP) cells. Lanes 1 and 2, SMB control; Lanes 3 and 4, 1:10 (SMB-PS(mPrP):SMB) co-culture; Lanes 5 and 6, 1:50 (SMB-PS(mPrP):SMB) co-culture; Lanes 7 and 8 1:100 (SMB-PS(mPrP):SMB) co-culture. Cells were co-cultured for one week before G418 selection. Markers are kDa.

To kill the SMB cells, a high concentration of G418 sulphate is used initially followed by dropping the concentration to a maintenance level. This may also have killed any SMB-PS cells that were infected, as infected cells have been shown to have increased susceptibility to stress (Milhavet *et al.*, 2000) and apoptiotic or necrotic death signalling could have adversely affected the robustness of the remaining cells. While no PK-resistant PrP can be detected with SMB-PS cells, the mechanism by which PS clears the infection in this cell line is unknown, and additional effects of PS on the cell

are not well understood. Therefore it was decided to use previously uninfected target cells, rather than the SMB-PS(mPrP) cell line.

3.2.2.2 N2a(mPrP) as target cell line

The next step was to use SMB cells as an infectious source but use N2a(mPrP) cells as the target. SMB medium, complete Medium 199 was used, as N2a(mPrP) cells tolerated the medium change much better than SMB cells tolerated N2a medium. No cell death, gross changes in morphology or cellular division rates were seen in N2a(mPrP) cells during the co-culture period. The protocol was altered during the killing stage. N2a(mPrP) cells have a higher LD_{90} for G418 than the SMB cells, and therefore only levels of G418 sulphate to maintain stably transfected cells (see 2.3.3.2.1) were used. This meant that the N2a cells were not subjected to higher doses of G418, which may adversely affect the initially infected N2a(mPrP) cells. The SMB cells were still killed at an appropriate rate using this concentration of G418 sulphate. Additionally, the co-culture period was decreased from a week with the SMB-PS cells to days with the N2a(mPrP) cells. Once all SMB cells were dead, N2a(mPrP) cells were then passaged four times before analysis to ensure *de novo* prion detection.

N2a(mPrP) cells were incubated SMB cells at either a 1:1, 1:100 or 1:1000 ratio of N2a(mPrP):SMB. Cell blot results show that transfer of infectivity in all ratios tested after 72 h (Figure 3.6A). Western blot analysis of infectivity assay cell lysates also showed PK-resistant PrP in 1:1, 1:100 or 1:1000 (N2a(mPrP):SMB) ratio (Figure 3.6B).

A range of incubation periods was tested with the co-culturing infectivity assay. N2a(mPrP) cells were incubated SMB cells at either a 10:1, 1:1 or 1:100 (N2a(mPrP):SMB) ratio. PK-resistant PrP was present in 1:1 and 1:100 ratios in all incubation periods tested (Figure 3.6C).

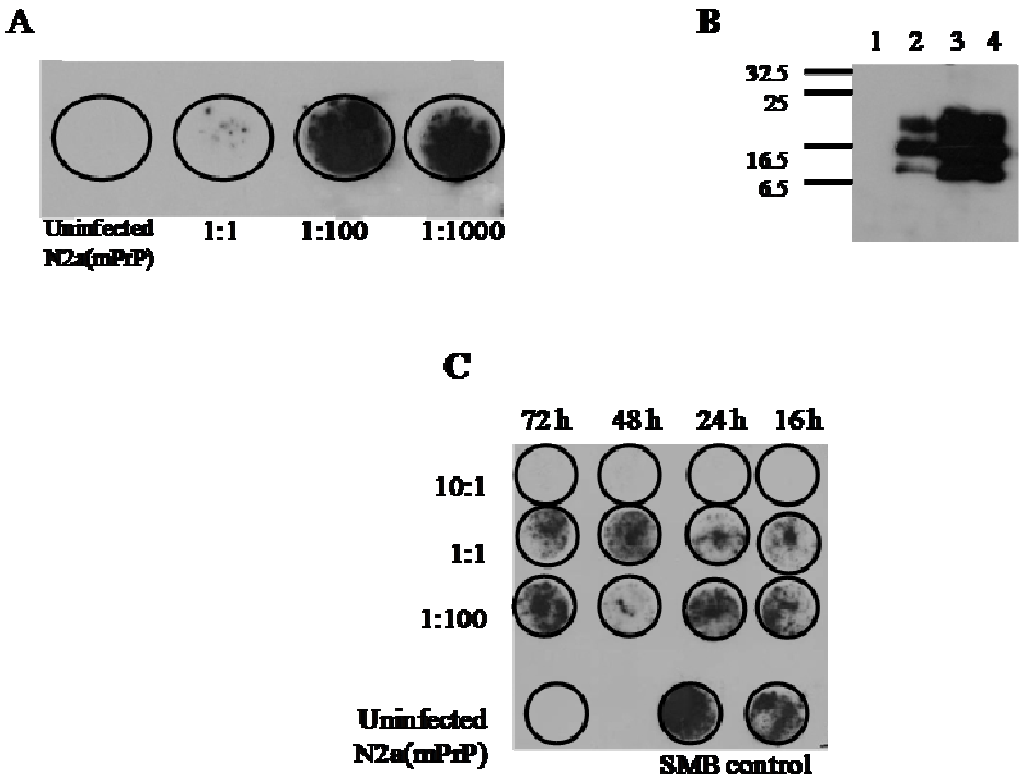

Figure 3.6 Live cell co-culture infectivity assays. A) Cell blot analysis of N2a(mPrP) cells co-cultured with SMB cells for 72 h. PK-resistant PrP is present in 1:1 and 1:100 N2a(mPrP):SMB ratios. B) Western blot of PK-digested N2a(mPrP) cells co-cultured with SMB cells for 72 h. No PK-resistant PrP is detected in Lane 1 which are uninfected N2a(mPrP). Lane 2 N2a(mPrP):SMB 1:1, Lane 3 N2a(mPrP):SMB 1:100, Lane 4 N2a(mPrP):SMB 1:1000 all show PK resistant PrP bands. C) Cell blot analysis of N2a(mPrP) cells co-cultured with SMB cells for 16, 24, 48 or 72 h. PK-resistant PrP is present in 1:1 and 1:100 N2a(mPrP):SMB ratios in all time points examined. All experiments were repeated at least three times.

3.2.3 Infection by infected cell homogenates

The difficulty in growing large amounts of SMB cells to use in experiments prompted development of the a cell homogenate method, based on the method described by Bosque and Prusiner wherein infectious cell cultures are homogenised by serial passage through needles and used as the infectious source (Bosque and Prusiner, 2000). This method allows for a reduction in the amount of infected cells required and the aim was to use ScN2a(mPrP) as sole infectious source in further experiments on these cells. To determine if the cell homogenate method would work in this system, SMB homogenates were tested. All experiments were repeated a minimum of three times.

3.2.3.1 SMB homogenates

SMB cells were harvested in PBS and rapidly frozen and thawed five times. Suspensions were then homogenised in PBS by serial passage from large to small gauged needles. Fifty µL of this homogenate was plated in complete media, returned to

the incubator and observed for 48 h but no cells survived. This homogenate was stored at -80°C until use and an as infectious sources for N2a(mPrP) target cells.

Infectivity assays were performed by incubating target N2a cells with 1:100 and 1:10 ratio (N2a:SMB, ratio based on cell number) of SMB homogenate for 48h. Both N2a(mPrP) and N2a(pcDNA3.1+) stably transfected cell lines were tested. Infectious homogenate was then removed and cells were washed three times in sterile PBS, and then propagated for four passages before analysis. Cell blot and Western blot results show transfer of prion infectivity to N2a(mPrP) cells in both 1:10 and 1:100 ratios as demonstrated by the presence of PK-resistant PrP in these samples. N2a(pcDNA3.1+) cells, which are transfected with the empty vector only, were also subjected to the infectivity assay to determine whether transfection alone was able to increase susceptibility to prion infection. No infection was seen in N2a(pcDNA3.1+) cells, confirming that over-expression of mPrP governs susceptibility to infection for N2a cells (Figure 3.7A).

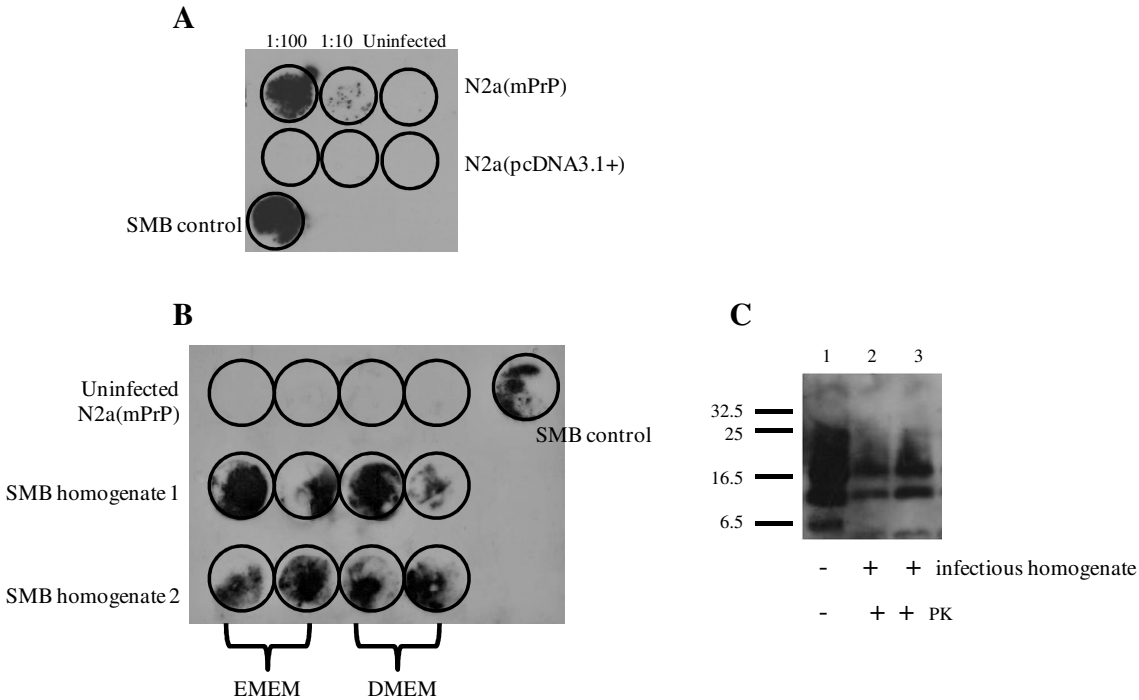

Figure 3.7 Infection by SMB homogenate. A) Cell blot of N2a(mPrP) and N2a(pcDNA3.1+) cells incubated with 1:10 or 1:100 (N2a:SMB) dose of homogenate for 48 h. PK-resistant PrP was seen only in N2a(mPrP) cells at both the 1:10 and 1:100 ratio. No PK-resistant PrP was seen in the N2a(pcDNA3.1+) cells at either infectious dose. B) Cell blot of N2a(mPrP) cells infected by 1:100 dose of SMB homogenate. N2a(mPrP) cells were incubated in either complete EMEM or DMEM during the infection period. The transfer of infectivity was not affected by culture media differences as PK resistant PrP was detected in all samples tested. C) Western blot of N2a(mPrP) cells infected by 1:100 (N2a(mPrP):SMB. N2a(mPrP) cells were incubated in either complete EMEM or DMEM during the infection period. Lane 1, uninfected N2a(mPrP) control; Lane 2, cell incubated win EMEM; Lane 3 cells incubated in DMEM. No differences in PK-resistant PrP were detected.

Some studies suggest there is an effect of media on prion infectivity assays (Bosque and Prusiner, 2000). Therefore to identify whether media made a difference in these assays, N2a(mPrP) cells were infected by 1:100 (N2a(mPrP):SMB, cell number ratio) and incubated in either complete Eagle's Minimum Essential Medium (EMEM, N2a normal medium) or high glucose Dulbecco's Modified Eagle Medium (DMEM) during the infection period. PK-resistant PrP was detected in all N2a(mPrP) cells infected at this ratio, and both cell blot and Western blot show no detectable difference in transfer of infectivity with either medium (Figure 3.7B, C). Therefore all infectivity assays were performed in the normal medium for N2a cells, complete EMEM medium.

3.2.3.2 ScN2a(mPrP) homogenates

As the SMB homogenates successfully transferred prion infectivity to N2a(mPrP), the next step was to determine if homogenised infected N2a(mPrP) cells, referred to as ScN2a(mPrP), were also capable of transferring prion infectivity.

ScN2a(mPrP) cells were homogenised as described in 2.3.7.2.2 and used as an infectious source for N2a(mPrP) target cells.

Infectivity assays were initially performed by incubating target N2a(mPrP) with 1:100 ratio (N2a(mPrP):ScN2a(mPrP)) of ScN2a(mPrP) homogenate for 48 h. Infectious homogenate was removed and cells were washed three times in sterile PBS, and then propagated for four passages before analysis. Cell blot results show transfer of prion infectivity occurred as demonstrated by the presence of PK-resistant PrP in target N2a(mPrP) cells (Figure 3.8A).

Infectious ScN2a(mPrP) homogenates were then pooled to increase reproducibility in further experiments. To determine what infectious doses could transfer prion infectivity, assays were performed by incubating target N2a(mPrP) with 1:100, 1:50, 1:25, 1:10, and 1:1 (N2a(mPrP):ScN2a(mPrP)) doses of ScN2a(mPrP) homogenate for 48 h. Infectious homogenate was removed and cells were washed three times in sterile PBS, and then propagated for four passages before analysis. Cell blot results show

transfer of prion infectivity as demonstrated by the presence of PK-resistant PrP in the 1:10, 1:25, 1:50, and 1:100 samples. No PK-resistant PrP was seen in the 1:1 or uninfected control samples (Figure 3.8B).

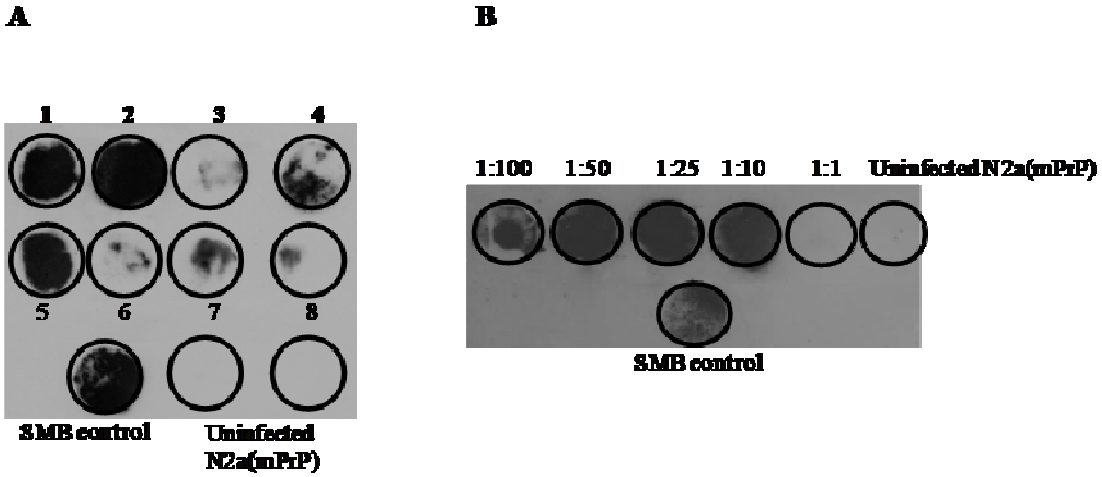

Figure 3.8 Cell blot analysis of ScN2a(mPrP) infectivity assay. A) N2a(mPrP) incubated with 1:100 (N2a(mPrP):ScN2a(mPrP)) dose of ScN2a(mPrP) homogenates for 48 h. Circles 1-5 are ScN2a(mPrP) cells originally infected by live cell co-culture and circles 6-8 are ScN2a(mPrP) cells originally infected by SMB homogenates. PK-resistant PrP is seen in all circle except the uninfected N2a(mPrP) negative control. B) N2a(mPrP) incubated with 1:100, 1:50, 1:25, 1:10, 1:1 (N2a(mPrP):ScN2a(mPrP)) doses of ScN2a(mPrP) homogenates for 48 h. PK-resistant PrP is detected in 1:10, 1:25, 1:50 and 1:100 N2a(mPrP):SMB samples but not in 1:1 or uninfected samples.

Despite the success of ScN2a(mPrP) as an infectious source for N2a(mPrP), ScN2a(mPrP) homogenate was unable to infect N2a cells at any infectious dose tested from 1:77 to 1:300 (N2a:ScN2a(mPrP) (Figure 3.9). This confirms observations from other studies that over-expression of mPrP increases sensitivity of N2a cells to prion infection (Nishida *et al.*, 2000).

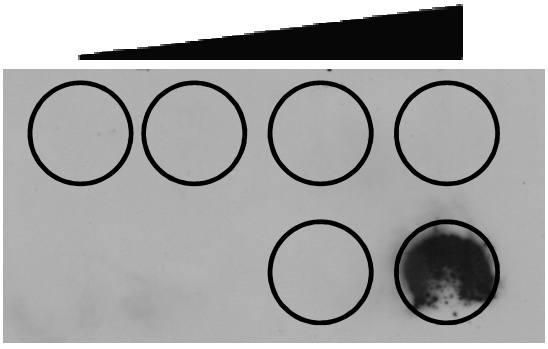

Figure 3.9 Cell blot of infectivity assay with un-transfected N2a cells as target cells and ScN2a(mPrP) homogenate. No infection was observed in any infectious dose.

3.2.4 PrP null cell line expressing mPrP

Ideally, to study the effects of certain PrP domains on prion infectivity, a PrP-null cell line would be transfected with different PrP constructs and infectivity assays performed. This would eliminate endogenous PrP as a factor in the infectivity assay. However, not many PrP null cell lines exist, and those that do have poor susceptibility to prion infection (Solassol *et al.*, 2003).

To develop a system where PrP null cells could be used in a cellular prion infection system to study the different domains of the protein, the Zpl cell line was used which is derived from transgenic Zurich mice lacking *Prnp* (Kim *et al.*, 2005). Figure 3.10A shows Zpl cells do not express PrP^C whereas Zwl and N2a cells both express PrP^C.

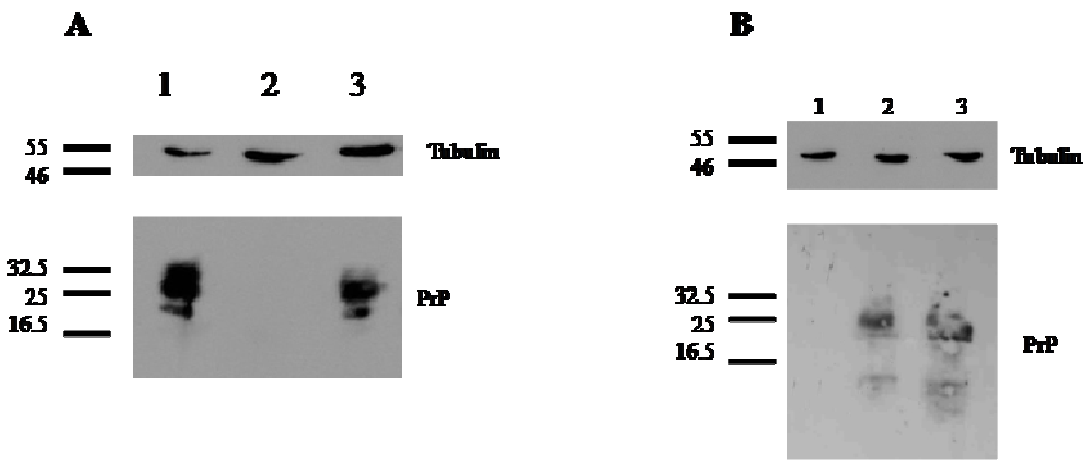

Figure 3.10 Western blot of PrP^C expression. A) PrP^C expression in Zwl, Zpl and N2a cells. Lane 1, Zwl cells which express PrP^C; Lane 2, Zpl cells which do not express PrP; Lane 3, N2a cells showing PrP expression. Tubulin blots confirm the absence of PrP in Lane 2. B) PrP^C expression in Zpl cells and Zpl(mPrP) cells. Lane 1, untransfected Zpl cells which do not have detectable PrP^C; Lanes 2 and 3, Zpl(mPrP) which show PrP^C expression. Markers are in kDa..

In order to determine whether these cells were susceptible to prion infection, Zpl cells were first stably transfected to over-express mPrP(1-254), as shown by the Western blot in Figure 3.10B.

Zpl(mPrP) cells were then used as the target line in infectivity assays. Infectivity assays were performed with SMB homogenate and ScN2a(mPrP) homogenate as the infectious source and Zpl(mPrP) as the target cells. Assays were performed as described in section 3.2.3, with target cells being incubated for 48 h with infectious homogenate. Results were assessed by cell blot (Figures 3.11A and B) and indicated

that Zpl(mPrP) cells were not able to be infected, determined by the lack of detectable PK-resistant PrP. Co-culturing infectivity assays were performed with Zpl(mPrP) and Zwl cells as target cells. No PK-resistant PrP was seen with either cell line (Figure 3.11 B, C).

This suggests the Zpl line is not susceptible to prion infection, even when transfected to over-expressing PrP. The parallel cell line Zwl, which does express PrP, was also not successful at propagating prion infection. This is not completely unexpected as many cell lines are unable to propagate prions (Solassol *et al.*, 2003; Bedecs, 2008). An additional cause could be related to the fact both the Zpl and Zwl cell lines have a higher cellular division rate than N2a cells, and it has been suggested that cell division and prion propagation are related (Ghaemmaghami *et al.*, 2007). Therefore Zwl and Zpl cell lines have no susceptibility for prion infection, and are not suitable for infectivity assays.

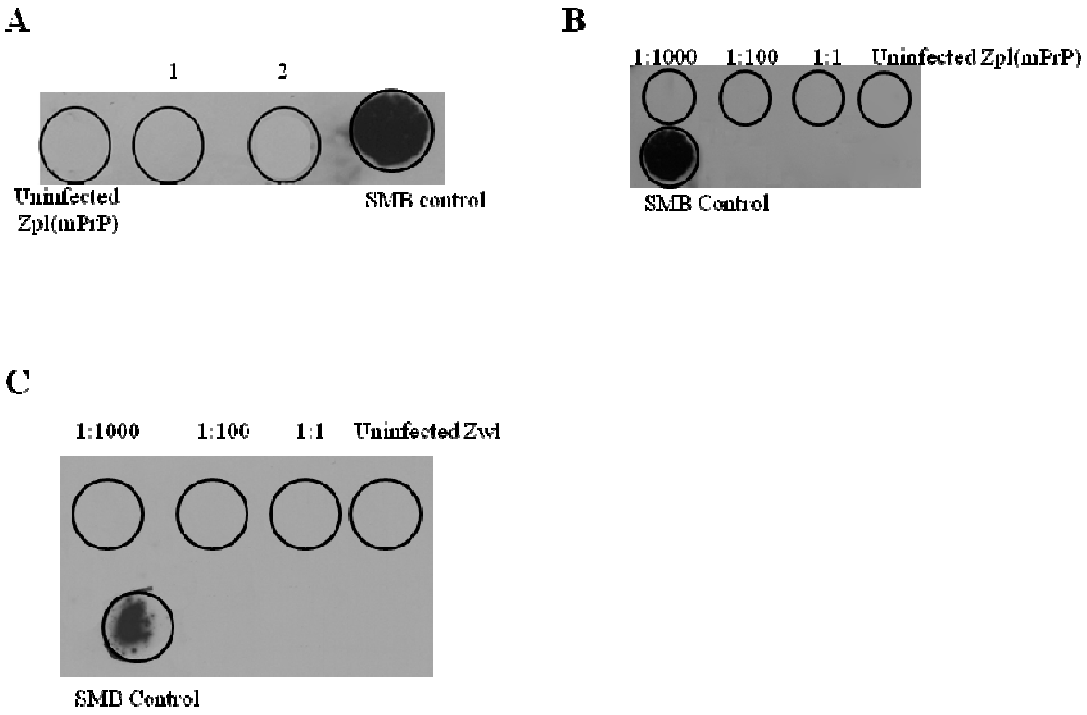

Figure 3.11 Cell blots of Zpl(mPrP) and Zwl infectivity assays. A) Cell blot of Zpl(mPrP) incubated for 48 h with cell homogenates. Circle 1, 1:100 (Zpl(mPrP):ScN2a(mPrP). Circle 2 1:100 (Zpl(mPrP):SMB). Neither infectious source could transfer prion infectivity to the Zpl(mPrP) cells. B) Cell blot of Zpl(mPrP) co-cultured with SMB cells for 48h. No PK-resistant PrP was seen in any sample. C) Cell blot of Zwl cells co-cultured with SMB cells for 48 h.

3.3 Role of metals in transfer of prion infectivity in cell culture

The role of metals in prion infectivity is poorly understood. While it is understood that metal levels alter during prion disease progression (Wong *et al.*, 2001; Thackray *et al.*, 2002; Hesketh *et al.*, 2007, 2008) the precise role metals play in prion disease is unclear. To assess the effect of metals in the transfer of prion infectivity, infectivity assays were performed in Chelex-treated media. Chelex-100 is commonly used to deplete metal ion concentrations in media (Rayner and Suzuki, 1995; White and Cappai, 2004; Du *et al.*, 2008). Chelex treatment is described in 2.3.6. Copper, manganese and zinc were then added to the Chelex-treated medium to determine whether the metals affected transfer of prion infectivity.

3.3.1 Viability of cells in Chelex media

To confirm that the experimental conditions would not result in widespread cell death, viability assays were performed on N2a(mPrP) cells (the target cells used in the infectivity assay). Cells were treated in Chelex-treated media (with basal calcium and magnesium levels added back) for 48 h and viability was assessed using an MTS assay. Results indicate there is no statistically significant difference in cell viability in cells grown in Chelex-treated media compared to non treated control (Figure 3.12).

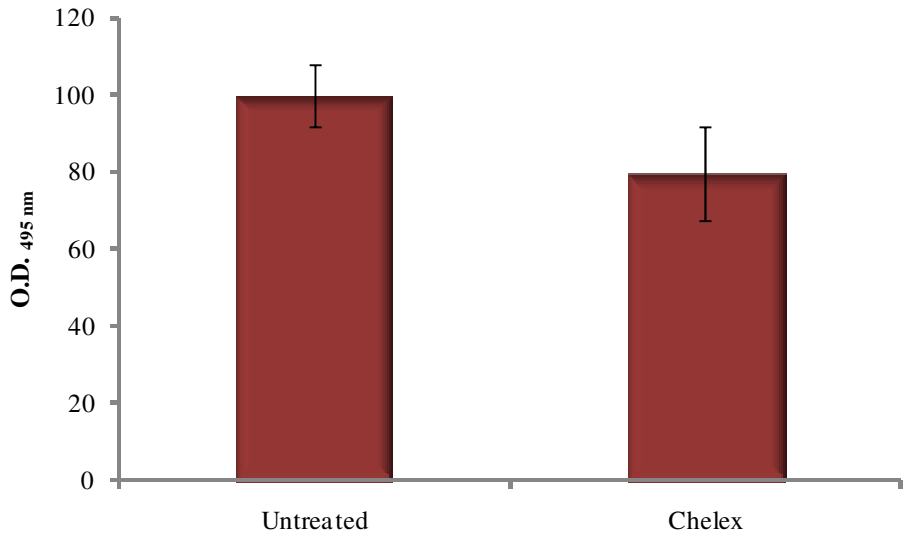

Figure 3.12. Viability of N2a(mPrP) cells in Chelex-treated media determined by MTS assay. Cells were grown for 48 h in Chelex-treated media and viability was assessed. No significant effect on viability was seen in cells grown in Chelex-treated media compared to untreated cells. Error bars ± SEM, n=5.

Next, the effect of metals on cell viability was tested. N2a(mPrP) cells were treated for 48 h in Chelex-treated media with 100 µM $CuSO_4$, $MnSO_4$ or $ZnCl_2$ added. Viability

was assessed using MTT assay. Results indicate there is no statistically significant loss of viability in cells treated with copper, manganese or zinc treated compared to no metal control but there is trend of decreasing viaibility seen across all experiments. (Figure 3.13).

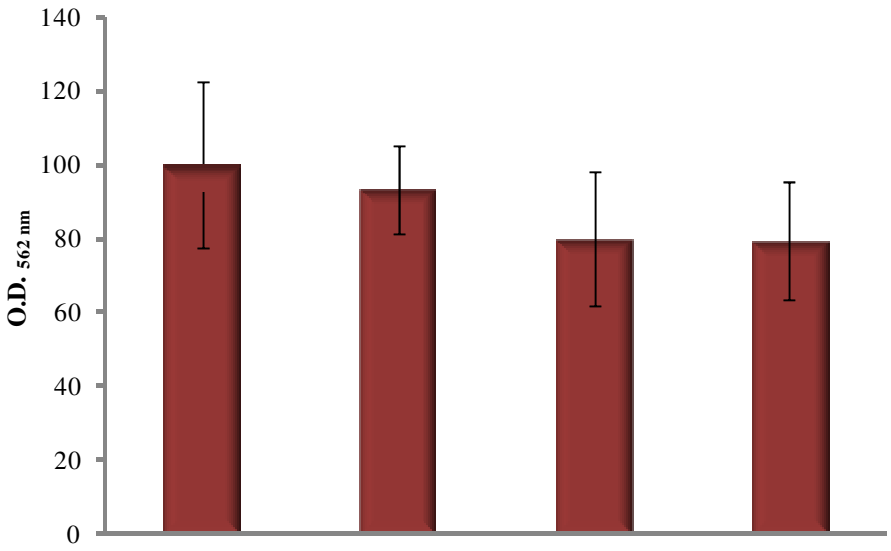

Figure 3.13. Viability of N2a(mPrP) cells in Chelex-treated media with 100 µM $CuSO_4$, $MnSO_4$ or $ZnCl_2$ added determined by MTT assay. Cells were grown for 48 h in Chelex-treated media with basal calcium and magnesium concentrations added back and viability was assessed. Error bars ± SEM, n=3.

3.3.2 Cellular infectivity assay and metals

3.3.2.1 Infectivity assays in Chelex-treated medium

The effect of metals in prion infectivity was assessed by performing infectivity assays in Chelex-treated medium. In these experiments, the effect of metals on the infectivity assays cannot be due to a regulatory effect of metals on PrP expression, as the over-expression of PrP^C in the N2a(mPrP) cells is driven by the cytomegalovirus promoter and not the *Prnp* promoter.

A minimum of four independent infectivity assays were performed. N2a(mPrP) cells were incubated with 1:100, 1:50, 1:25, 1:10 and 1:1 (N2a(mPrP):ScN2a(mPrP)) doses of ScN2a(mPrP) homogenate for 48 h. Cells were propagated four passages post infection and analysed by cell blot.

Cell blot results show PK-resistant PrP was seen in 1:100, 1:50, and 1:25 (N2a(mPrP):ScN2a(mPrP)) infectious doses in cells infected in Chelex-treated medium. In contrast, infectivity assays performed in the normal medium showed PK-resistant PrP in the 1:10 infectious dose (Figure 3.14).

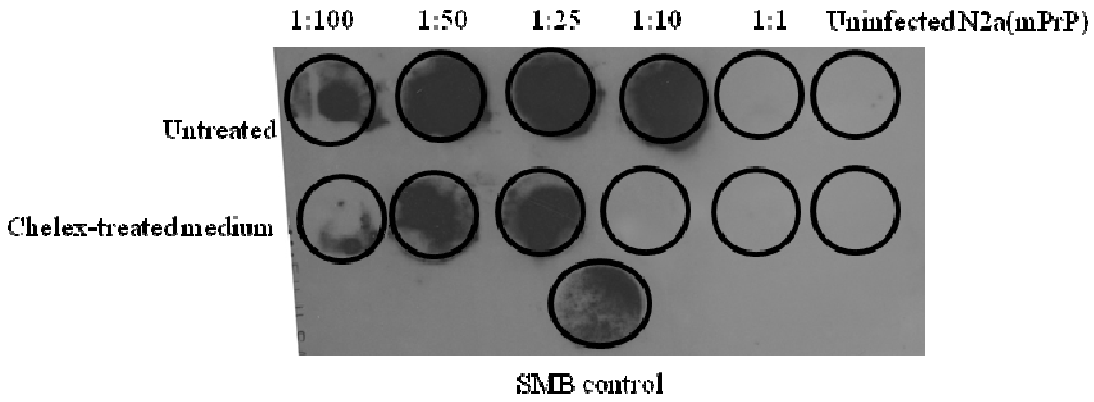

Figure 3.14 Effect of Chelex-treated media on transfer of prion infectivity. Representative cell blot of infectivity assay. N2a(mPrP) cells were incubated with 1:100, 1:50, 1:25, 1:10 and 1:1 (N2a(mPrP):ScN2a(mPrP)) doses of ScN2a(mPrP) homogenate for 48 h in Chelex-treated medium and compared with cells incubated in normal medium. PK-resistant PrP was not seen at the 1:1 or 1:10 dose in cells cultured in Chelex-treated medium, in contrast to cells cultured in normal medium where PK resistant PrP was seen at the 1:10 dose.

To assess the effect of metals on the transfer of prion infectivity, infectivity assays were performed in Chelex-treated medium and either 100 µM $CuSO_4$, $MnSO_4$, or $ZnCl_2$ was added to the medium. A minimum of four independent infectivity assays were performed. N2a(mPrP) cells were incubated with 1:100, 1:50, 1:25, 1:10 and 1:1 (N2a(mPrP):ScN2a(mPrP)) doses of ScN2a(mPrP) homogenate for 48 h. Cells were propagated four passages post infection and analysed by cell blot.

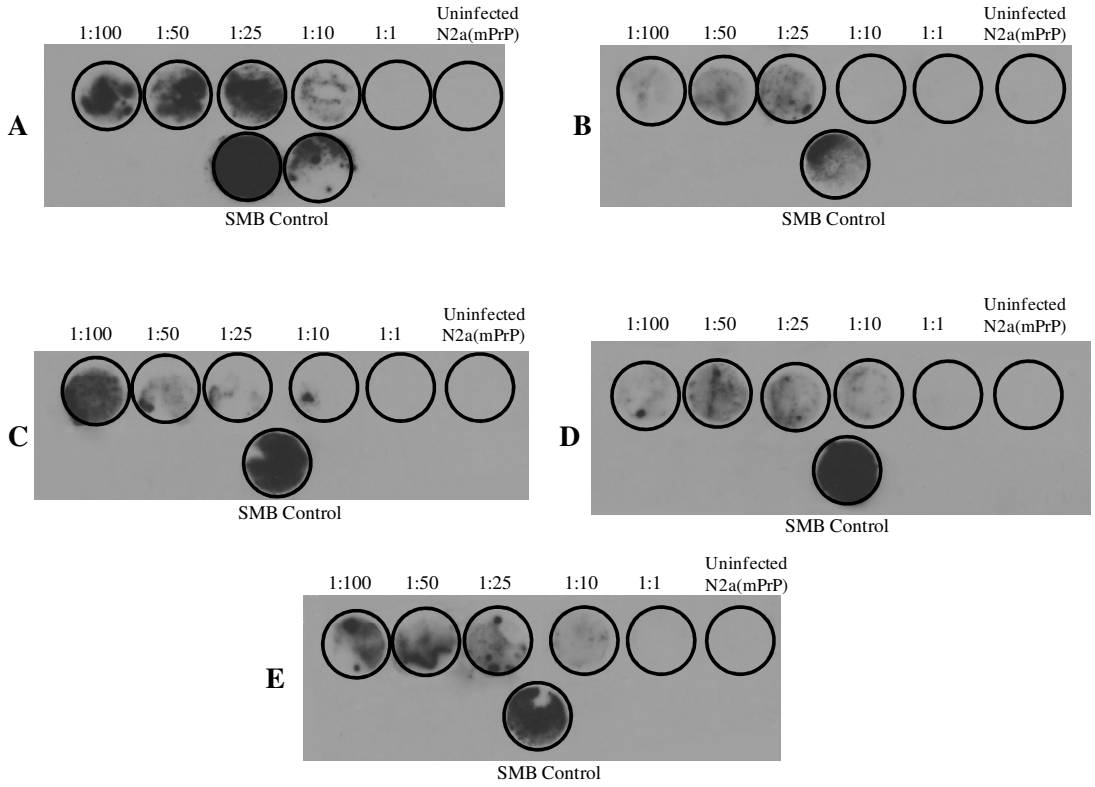

Figure 3.15 Representative cell blots of infectivity assays with metals. N2a(mPrP) cells were incubated for 48 h with 1:100, 1:50, 1:25, 1:10 and 1:1 (N2a(mPrP):ScN2a(mPrP)) doses of ScN2a(mPrP) homogenate. A) Control (no metal and normal medium). PK-resistant PrP is seen in the cell samples treated with 1:10, 1:25, 1:50, and 1:100 infective doses. B) Chelex treated medium. PK-resistant PrP is seen in the 1:25, 1:50, and 1:100 infectious doses. C) Chelex-treated medium with 100 µM $CuSO_4$. PK-resistant PrP is seen in the 1:10, 1:25, 1:50, and 1:100 infective doses. D) Chelex-treated medium with 100 µM $MnSO_4$. D) PK-resistant PrP is seen in cells treated with the 1:10, 1:25, 1:50, and 1:100 infective doses. Chelex-treated medium with 100 µM $ZnCl_2$. PK-resistant PrP is seen cells treated with all infectious doses save 1:1 infective doses.

As with Figure 3.14, results show infection with Chelex treated medium is only detected in 1:25 infectious dose that compared to the control (no metal and normal media) where PK-resistant PrP is present at the 1:10 infectious dose (Figure 3.15 A and B).

Addition of 100 µM $CuSO_4$, $MnSO_4$, or $ZnCl_2$ to Chelex-treated media resulted in PK-resistant PrP detected in the 1:10, 1:25, 1:50 and 1:100 infectious doses, similar to the no-metal, no-Chelex control (Figure 3.15C-E). These results indicate that depletion of metal ions from the media lowers susceptibility of N2a(mPrP) cells to infection – as indicated by a higher infectious dose (1:25) required in order to detect PK-resistant PrP. The addition of copper, manganese, and zinc all restored the susceptibility of N2a(mPrP) cells to infection to control levels

3.4 Metal transporter proteins in prion disease

As PrP^{C} expression levels cannot be responsible for the metal-mediated effects seen in the infectivity assays, the next step was to determine whether altered metal transporter expression had any effect on transfer of prion infection.

Plasmid constructs of copper transporting proteins were transfected into SMB and SMB-PS cells to determine whether these copper-transporting proteins affect PrP expression. PrP expression was analysed by Western blots quantified by densitometry. The results proved variable so data are treated as preliminary. Over-expression of ATOX1, CCS, CTR1 or CTR2 did not significantly affect the expression of PrP^{C} in uninfected SMB-PS cells (Figure 3.16A) or N2a cells (Figure 3.16B). PrP^{Sc} expression in the infected SMB cells was also not significantly altered when ATOX1, CCS, CTR1 or CTR2 was over-expressed (Figure 3.16A).

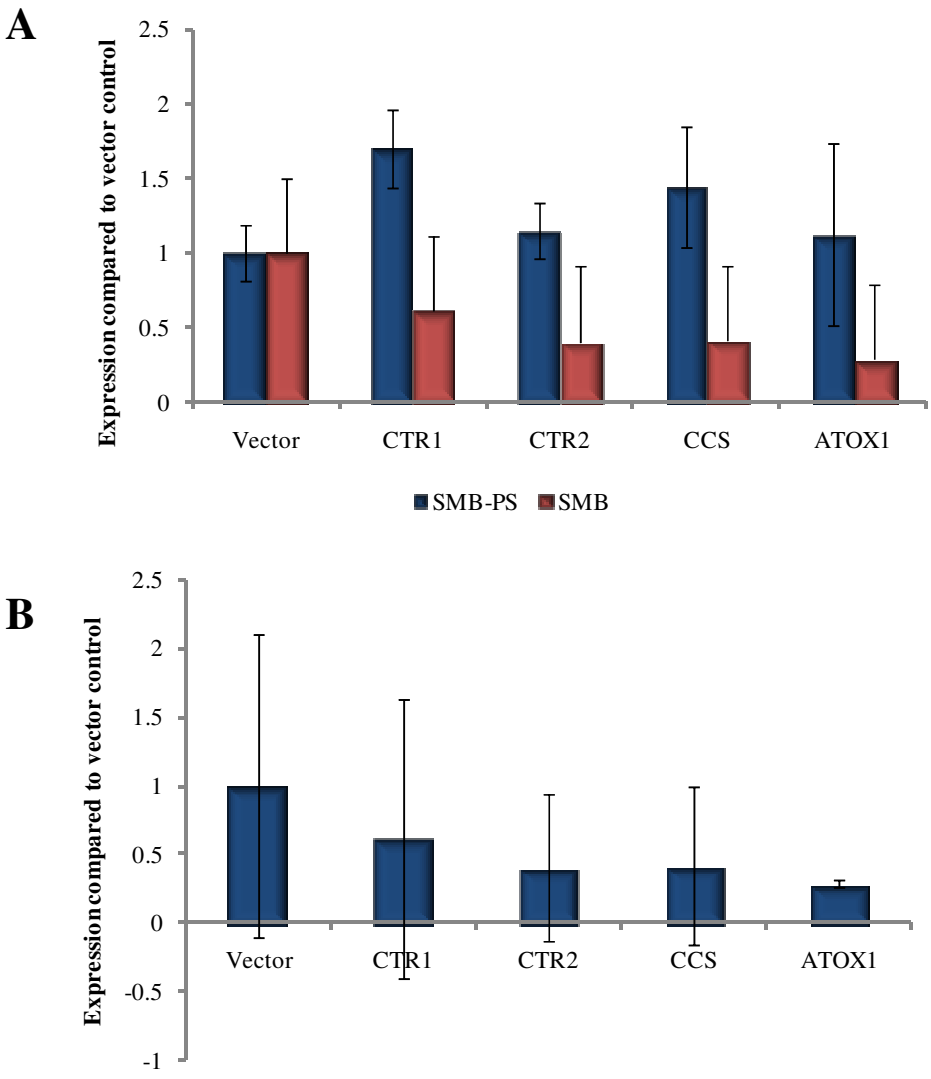

Figure 3.16 PrP expression is unaffected by over expression of copper transporting proteins. A) Over-expression of copper transporting proteins did not affect PrP^{C} (SMB-PS) or PrP^{Sc} (SMB) expression levels. n=3. B) PrP^{C} expression in N2a cells over-expressing copper transporters. n=3.

To determine if increased copper transporter expression would increase the susceptibility of N2a cells to prion infection, infectivity assays were performed using N2a cells over expressing ATOX1, CCS, CTR1 or CTR2. Cells were incubated with 1:1, 1:100, 1:1000 (target:ScN2a(mPrP) for 48h and cells were propagated four passages post infection and analysed by cell blot. No infection was seen in any of the N2a cells over expressing copper transporting proteins with either ScN2a(mPrP) homogenate (Figure 3.17) or SMB homogenate (not shown). These data are consistent with previous findings that N2a cells are not susceptible to infection without over-expression of PrP (Section 3.2.3.2). Therefore over expression of copper transporters did not render N2a cells more susceptible to infection.

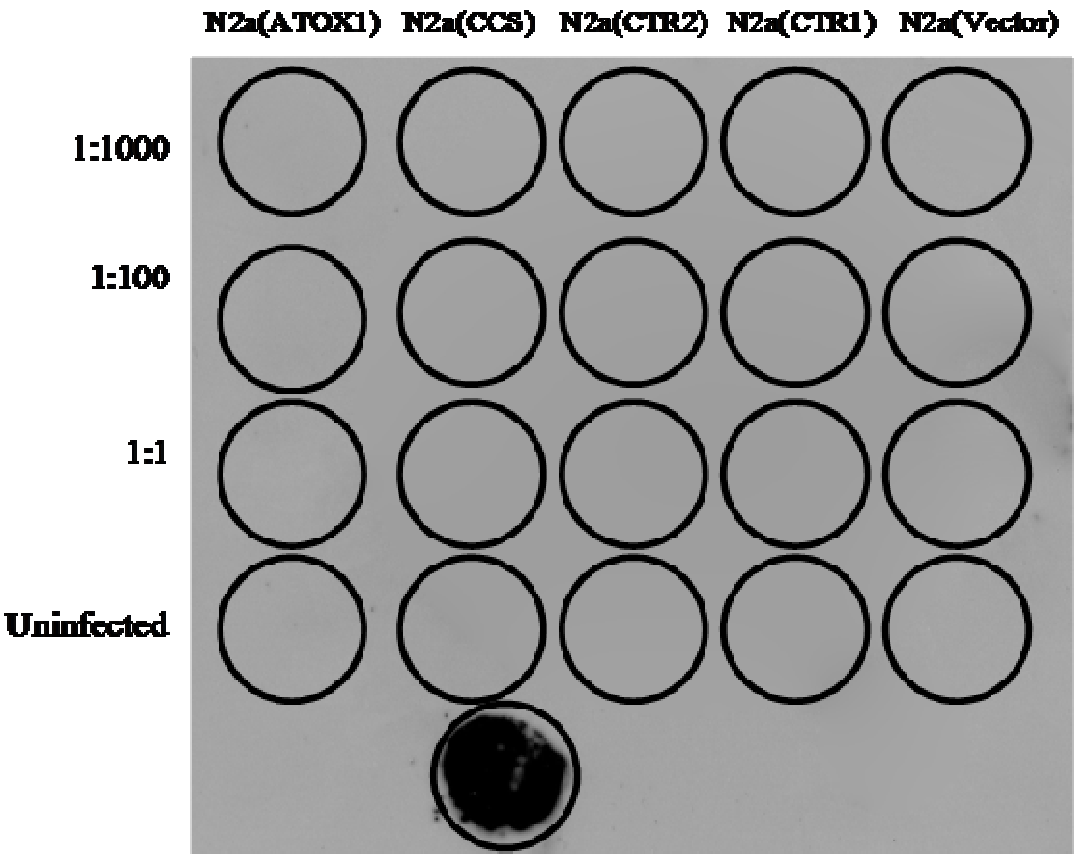

Figure 3.17 Cell blot of infectivity assay of N2a cells over-expressing ATOX1, CCS, CTR1, and CTR2 in a FLAG-tagged vector. No PK-resistant PrP was detected at any infectious dose tested.

3.5 Discussion

Cell culture is comparatively a less expensive and time-consuming method than animal bioassay, and is used to study several aspects of prion biology including prion infection. This study used cell culture infectivity assays to assess the role of metals in the transfer of prion infectivity to previously uninfected cells.

3.5.1 Development of prion infectivity assays

The basic protocol to establish prion infection protocol in cell culture requiresincubation ofthe target cells with an infectious source and then propagation of the target cells for a number of passages to detect *de-novo* prion infection. Prion infection in cell culture can be accomplished using different sources of infectious material, albeit with varying success rates. Infectious sources used in the development of a suitable method for this study included infectious brain homogenate, live cells, and cell homogenates.

The infectivity assays performed with brain homogenate yielded successful transfer of prion infection to the N2a(mPrP) cells, although this was strain-dependent, as the Me7

strain homogenate did not infect N2a(mPrP). Prion strains are classified *in vivo* by incubation period and neuropathological effects which are faithfully propagated. These strain characteristics are reproduced after secondary propagation in a different species. Biochemically, prion strains exhibit different glycosylation profiles, protease resistance, and electrophoretic mobility. Some prion strains in mice include RML, 22L, Chandler, Fukurora, Me7, and 79A (Morales *et al.*, 2007). The results of this study showed that infectious brain homogenate from the 79A strain, but not the Me7 strain was able to infect N2a(mPrP) cells. These data are in agreement with previously published studies (Bosque and Prusiner, 2000; Klohn *et al.*, 2003).

The limited availability of infectious brain homogenate required development of an alternative infection assay, namely live cell co-culturing using a chronically infected cell line and infectious cell homogenates. These techniques were adapted from published methods for use in our laboratory (Bosque and Prusiner, 2000; Kanu *et al.*, 2002) and required SMB cells as the infectious source.

The two cell lines utilised as target cells for live cell co-culturing were SMB-PS cells and N2a cells. It was necessary that both cell lines over-express mPrP, as selection of infected target cells is based on antibiotic resistance conferred by the mammalian expression plasmid pcDNA3.1+. In contrast to work published by Kanu *et al*, SMB-PS(mPrP) cells were not able to be infected by live cell co-culture in this study perhaps on account of the pentosan sulphate used to clear the cell of detectable prion infection (Birkett *et al.*, 2001). The exact mechanism by which pentosan sulphate clears prion infection is unknown as are any other effects pentosan may have on cellular processes. This and subtle differences in culture conditions could explain why some SMB-PS(mPrP) cells were not susceptible to infection by co-culture. Further, the use of an antibiotic to select the SMB-PS(mPrP) cells after live cell co-culture may have affected cell survival. As prion infection is known to decrease the cellular response to oxidative stress (Brown and Bessinger *et al.*, 1998), the increased stress on the cells from both antibiotic selection and SMB cell death may have been too strenuous for the newly infected SMB-PS(mPrP) cells. Finally, infected SMB-PS(mPrP) cells could have ejected the pcDNA3.1+-mPrP plasmid after the co-culture period as they were without constant selective pressure, thus rendering them susceptible to the antibiotic once they were added back. All things considered, further experiments were done using N2a(mPrP) cells.

In contrast to SMB(mPrP) cells, live cell co-culturing was very successful with N2a(mPrP) cells. This success could be attributed to fact that the shorter incubation period allowed cells to be with continuous antibiotic selection for a greater time period. Additionally SMB cells suffer death more quickly than N2a(mPrP) cells which require a higher dose of G418 selection. Finally, these data show that N2a(mPrP) cells were more susceptible to infection from SMB cells than infectious brain homogenate.

Since it was impractical to use live cell co-culture as the sole method for infection, homogenates of infectious cells were used. This method was the most reproducible and economical method of infection for N2a(mPrP) cells, but did not successfully infect untransfected N2a cells or Zpl(mPrP) and Zwl(mPrP) cells. The lack of infection in the Zpl/Zwl cell lines is most likely due to an inability to support prion infection. The inability of several cell lines, including neuronal lines, to support prion infection has been previously documented but is poorly understood (Vilette, 2008). Qualitative estimates indicated this inability to support prion infection was not due to loss of viability or alteration to cell division or morphology. These results show Zpl(mPrP) and Zwl(mPrP) cells are not suitable for a model for prion infection.

Once the infectious cell homogenate method stably produced results, the role of metals in transfer of infectivity was examined.

3.5.2 Metals and prion infectivity

The results here show that depleting the medium of metals results in a decreased susceptibility to lower prion doses; this suggests that metals may play a promotional role in infection. This decreased susceptibility was not due to a decreased viability, as shown by cell viability assays in 3.3.1. Adding copper, manganese, or zinc back restores susceptibility of the N2a(mPrP) cells back to those of the control, suggesting that adding metals to Chelex-treated media promotes prion infection. These results do not provide any insight as to how this occurs, but as these cells were over-expressing PrP under the control of the cytomegalovirus promoter it is unlikely this effect was due to an influence on protein expression.

The restorative effect of metals on a Chelex-depleted background could be due to metal interactions with PrP^{C} or with PrP^{Sc} which could induce conformational changes that in turn promote acquisition of infection. It has been well described that metal binding to PrP results in increased β-sheet content of the protein (McKenzie *et al.*, 1998; Stockel

et al., 1998; Wadsworth *et al.*, 1999; Brown *et al.*, 2000; Qin *et al.*, 2000; Quaglio *et al.*, 2001; Wong *et al.*, 2000b; Jones *et al.*, 2004; Nishida *et al.*, 2004; Liu *et al.*, 2007). Manganese is also able to induce a conformation change in PrP (Brown *et al.*, 2000; Abdelraheim *et al.*, 2006; Kim *et al.*, 2005; Treiber *et al.*, 2006). Zinc and copper has also been shown to promote PrP-PrP interactions (Kenward *et al.*, 2007). These metal-induced conformation changes and increased PrP self-interaction could promote and/or permit conversion to occur and thereby infection to occur more readily.

Another possibility for the restoration effect seen with manganese could be due to the requirement for manganese in glycosylation. It has been shown that specific unglycosylated PrP mutants are still able to convert to a protease resistant form, although altered PrP glycosylation has been shown to modulate response to different prion strains (Korth *et al.*, 2000; Tuzi *et al.*, 2008). Depletion of manganese in the cells leads to inhibition of N- and O-linked glycosylation (Suigiura *et al.*, 1982; Elhammer and Kornfeld, 1986; Kaufman, *et al.*, 1994) and this may be due to inactivation of SPCA1, the mammalian analogue of the yeast protein Pmr1 (Kaufman *et al.*, 1994). This calcium(II)/manganese(II) transporter is responsible for supplying calcium and manganese to glycosylation, ER, and protein degradation pathways (Hu *et al.*, 2000; Van Baelen *et al.*, 2001). Therefore loss of manganese could alter N-linked glycosylation of the prion protein and result in a decreased response to prion infection, as seen in the Chelex-treated medium infectivity assays. This response would be ameliorated by resupplying manganese to the system, as was seen in section 3.3.

On a broader level, while overall cell viability was not affected by the treatments in the experiments, it is probable that alterations in metal homeostasis occurred possibly including leaching of metal stores to ensure essential enzymes function properly in the case of reduced metal media treatments, or increase in metal transport, storage, and export. As the relationship between PrP and metals has yet to be fully defined, it is possible that alteration in the metal metabolism of the cell contributed to the increased susceptibility of these cells to infection. Indeed it has been shown that there are significant alterations to metal metabolism during disease pathogenesis, including altered metal levels in tissue and altered metal transporter expression levels (Wong *et al.*, 2001b; Thackray *et al.*, 2002b; Hesketh *et al.*, 2007, 2008; Kralovicova *et al.*, 2009; Mitteregger *et al.*, 2009).

Proteins involved in copper homeostasis were examined in 3.4 by over-expressing copper transporters and chaperones in SMB, SMB-PS and N2a lines. There was no significant effect on prion protein expression. In particular the results of ATOX1 are in contrast to those by Wright *et al.*, who showed that ATOX1 over expression resulted in increased PrP^C expression (Wright *et al.*, 2009a) and that ATOX1 was able to up-regulate *Prnp* promoter activity. However, the mammalian expression vector used to express ATOX1 in the Wright *et al.* study was pCDNA3.1+ as opposed to the p3xFLAG vector used here. The FLAG tag was found to interfere with the DNA-binding region of ATOX1 (J.A. Wright, personal communication) and therefore would not be able to affect the *Prnp* promoter and PrP^C expression in the N2a cells. Given the results of Wright *et al.*, and those showing that ATOX1 has copper-mediated transcriptional response (Itoh *et al.*, 2008), it would be interesting to determine if (using an appropriate expression vector) ATOX1 over-expression in a copper-enriched environment was able to increase susceptibility of cells to prion infection by regulating *Prnp* expression. Increased *Prnp* promoter activity in response to metals could represent a mechanism by which increased metals promote transfer of prion infection.

In summary, a successful cell culture model was established to study transfer of prion infectivity in culture. Successful transfer of prion infectivity was achieved using either co-culture with chronically infected cells as well as with infected cell homogenates. This method was used to determine whether metals affected the transfer of prion infectivity and results showed that depletion of environmental metals lowered susceptibility of N2a(mPrP) cells to infectivity transfer. This effect was ameliorated when copper, zinc, or manganese was added back to the system. The next step therefore is to identify how the metal-PrP interaction could influence conversion of the protein into a disease related form using a simplified *in vitro* aggregation system.

4. Metals and PrP Aggregation

4.1 Introduction

Evidence suggests that an aggregated form of PrP^{Sc} is in fact the key component in the disease (Prusiner *et al.*, 1983; Pan *et al.*, 1993; Nguyen *et al.*, 1995) but the precise character of the infectious aggregates is unclear. *In vivo*, PrP^{Sc} exists in intracellular aggregate depositions (Prusiner *et al.*, 1998). In humans, a proportion of these depositions are amyloid-like plaques, and these plaques differ in morphology between different types of prion disease (reviewed in Liberski and Ironside, 2004). It has been demonstrated that *in vitro* conversion ability is related to infectivity (Caughey *et al.*, 1997; Raymond *et al.*, 1997). The study of *in vitro* aggregation of recombinant PrP is instrumental in providing insight into the mechanisms behind conversion from PrP^{C} to PrP^{Sc} and aggregate accumulation. In addition it provides a means with which to study the conformation and species that is likely responsible for prion pathogenesis.

Analysis of aggregated PrP is done using several methods. These include turbidometry, Fourier transform infrared spectroscopy (FTIR), circular dichromism spectroscopy (CD), electron microscopy, atomic force microscopy, and by the use of amyloid-binding dyes such as Congo red, 8-anilino-1-naphthalenesulfonic acid (ANS), Thioflavin T (ThT), and Thioflavin S (LeVine III, 1993; Ban *et al.,* 2003). These dyes provide a useful method for monitoring the formation of amyloid structures as these dyes bind only to common β-sheet structures, allowing for distinction between β-sheet and non-β-sheet material. ThT in particular binds exclusively to β-rich 8-9Å diameter cavities which run along the length of the fibril axis (Groenning *et al.*, 2007a,b). The emission wavelength of ThT upon binding to fibril-like structures (excitation 440 nm, emission 482 nm), is markedly different from that of the dye itself (excitation 350 nm, emission 438 nm) and also to the fluorescence pattern in water (excitation 440 nm, emission 493 nm) (Naikai *et al.*, 1989; Maskevich *et al.*, 2007). This makes the use of ThT a valuable method to study the conversion of α-helical PrP to β-sheet PrP, as the dye fluorescence pattern will increase as the β-sheet PrP proportion increases. PrP^{C} has been shown to bind copper as well as other metals such as manganese, nickel, and zinc, both within the N-terminal octapeptide repeat region and within the hydrophobic region (Hornshaw *et al.*, 1995a,b; Katamine *et al.*, 1998; Viles *et al.*, 1999; Brown *et al.*,

2000; Collinge and Clarke *et al.*, 2007; Yang *et al.*, 2008). In addition, these metals are able to impart structural changes to PrP and it has been theorised that PrP may have a function in metal homeostasis as discussed in 1.3.2, which has led many investigators to look into the role of metals in PrP aggregation.

It is important to understand the role metals play in PrP aggregation, it has been suggested that metals, in particular copper, play a role in the normal function of the prion protein (Brown *et al.*, 1997). The interaction with metals, in particular manganese, in the aggregation process could be instrumental in understanding the disease pathogenesis. Previous studies on prion protein aggregation were performed under conditions such as low pH and/or denaturing reagents such as urea or guanidine hydrochloride (Jackson *et al.*, 1999; Baskakov *et al.*, 2001; Bocharova *et al.*, 2005a,b). The site of PrP^{C}-PrP^{Sc} conversion is unknown and two potential sites for conversion could be within lysosomes where the pH is low or on the cell surface, where the protein would be in a more pH neutral environment (Caughey *et al.*, 1991; Caughey and Raymond 1991; Borchelt *et al.*, 1992). As many groups have published work on PrP aggregation under low pH conditions, the aim of this work is assess the effect metals have on recombinant mPrP aggregation using neutral pH and buffer conditions the protein is more likely be exposed to either inside the cell (cytosol) or on the cell surface (extracellular space).

4.2 Results of cloning, expression, and purification of PrP constructs

The choice was made to clone several murine prion protein constructs, to produce constructs without a tag. Murine PrP pET3a-mPrP(23-231), pET3a-mPrP(Δ51-89), and pET3a-mPrp(Δ67-90) constructs were sub-cloned by PCR amplification of pcDNA3.1+ mPrP(1-254), a mammalian expression construct using primers with *NdeI* and *BamHI* restriction enzyme sites. The PCR amplified constructs were then ligated into an untagged bacterial expression vector, pET3a. Ligation into the appropriate vector was accomplished by either sticky- or blunt-ended ligation methods. All constructs were sequenced before use to confirm the gene product was correct.Once the mPrP constructs had been cloned and sequences were confirmed, constructs were transformed into competent *Escherichia coli* BL21-DE3 cells and expression trials were carried out to confirm the production of the correct protein. Figure 4.1 shows expression of

mPrP(23-231), mPrP(Δ51-89), and mPrP(Δ67-90). All mPrP constructs were tested for expression before use.

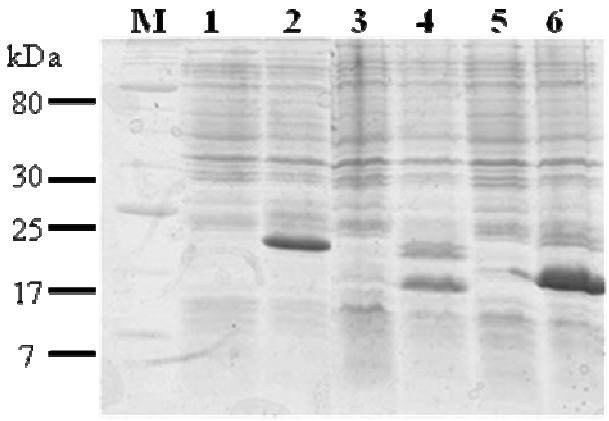

Figure 4.1Expression trial showing induction of mPrP expression in BL21 *E.coli*. BL21 *E.coli* were transformed with pET3a-mPrP constructs and mini cultures were grown as in Section 2.4.1. Pre-and post-induction samples were analyse to determine whether mPrP over-expression was present. Lanes 1, 3 and 5 are pre-induction samples and lanes 2, 4, and 6 are 3h post induction samples. Lanes 1 & 2 are mPrP(23-231), lanes 3 & 4 are mPrP(Δ51-89) and lanes 5&6 are mPrP(Δ67-90).

Purification of these mPrP proteins was either carried out using copper-IMAC or the wash purification method. Figure 4.2A and B show mPrP(23-231) purification and refolding. All mPrP mutants were compared to full length mPrP(23-231) purified by the same method as the mutant. Once purified, the proteins were refolded under oxidative methods as described in Section 2.4.4. Previous work has shown protein refolded using this method is mainly α-helical, similar to the structure of cellular PrP (Wong *et al.*, 2000). Coomassie stained SDS-PAGE gels (performed as described in section 2.3.12 and 2.3.14) were analysed of each preparation to determine purity. Examples of refolded PrP proteins are shown in Figure 4.3. The main band of each lane corresponds to the predicted size of each constructs (see Table 2.4 for molecular weights).

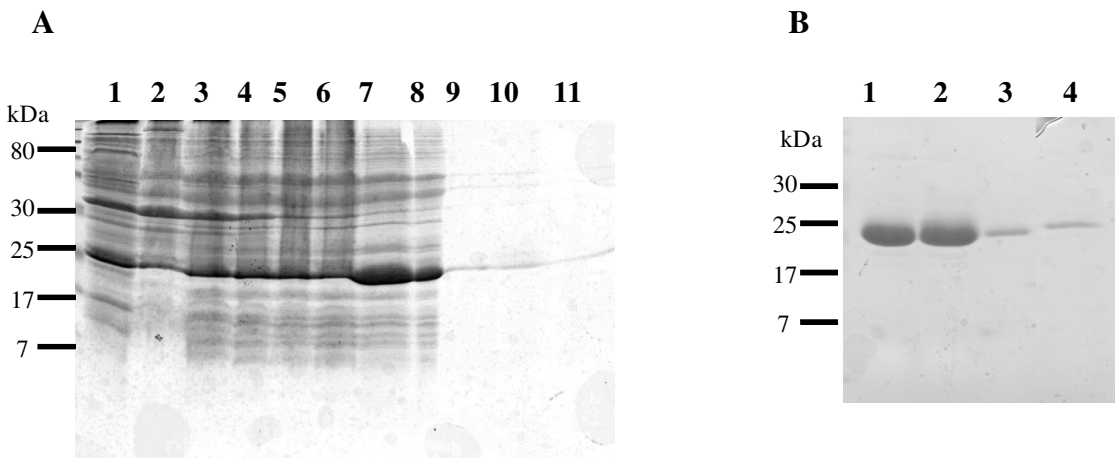

Figure 4.2 Examples of mPrP(23-231) purification and refolding. A) SDS-PAGE gels stained with Coomassie of wash purification method. All samples taken from re-suspended pellets. Lane 1 is sample after initial cell lysis. Lanes 2-8 show successive samples after every 2nd wash cycle. Lanes 9-10 show successive samples during final, no detergent washes. Lane 11 is the final purified product in 8M urea buffer. B) SDS-PAGE gels stained with Coomassie of Cu-IMAC purification. Lanes 1&2 are samples from Cu-IMAC elution fractions. Lane 3 is re-natured protein before dialysis and lane 4 is re-natured protein after dialysis.

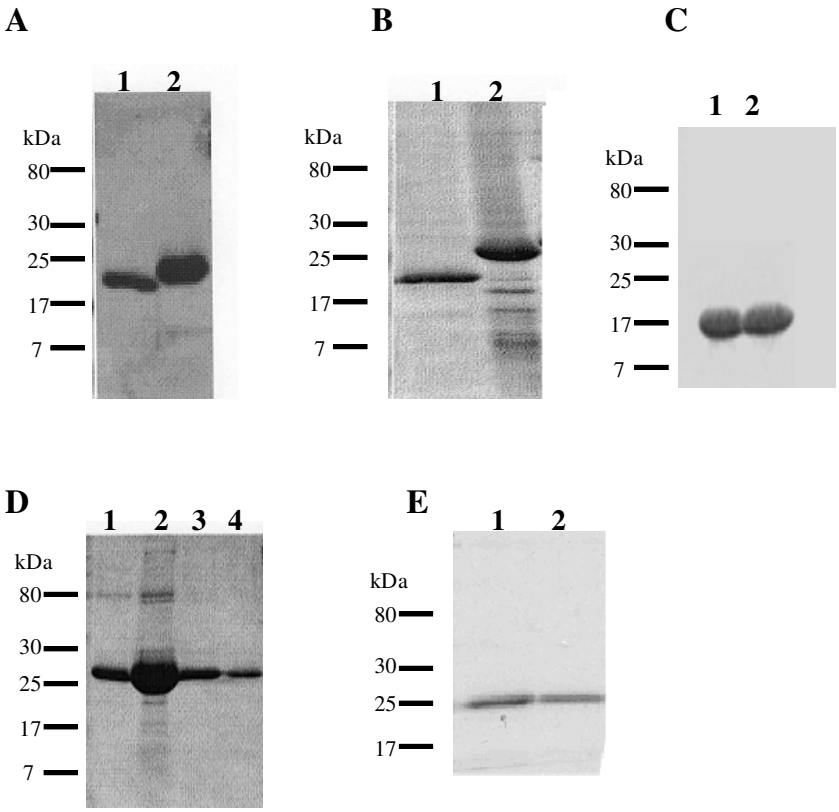

Figure 4.3 Coomassie staining of SDS-PAGE analysis of refolded mutant mPrP proteins. SDS-PAGE gels and staining was performed as indicated in Section 2.3.12 and 2.3.14. A) Lane 1 is mPrP(Δ67-90). Lane 2 is mPrP(Δ106-126). B) Lane 1 is mPrP(Δ51-90) and lane 2 is mPrP(23-231) from a different purification than Figure 4.2. C) Lanes 1 and 2 are two samples from the same mPrP(89-231) purification. E) Lane 1 is mPrP(Null +H95, H110), lane 2 is mPrP(Null), lanes 3 and 4 are mPrP(H95A+H110A) from the same wash purification. E) Lane 1 is mPrP(Null +H95) and lane 2 is mPrP(Null+H110). All markers are in kDa.

To further confirm the identity of the protein preparations, Western blot analysis (section 2.3.13) of the purified and refolded proteins was performed using the monoclonal ICSM-18 antibody on all constructs except for mPrP(Null), mPrP(Null+H95), mPrP(Null+H110), mPrP (H95A+H110A) and mPrP(Null + H95, H110). These constructs were blotted using the anti-PrP 8B4 antibody (Figure 4.4). These results show mPrP at the predicted sizes, although for the mPrP(Δ51-90) and mPrP(Δ67-90) the bands were rather blobby which could be due to protein overload of the gel.

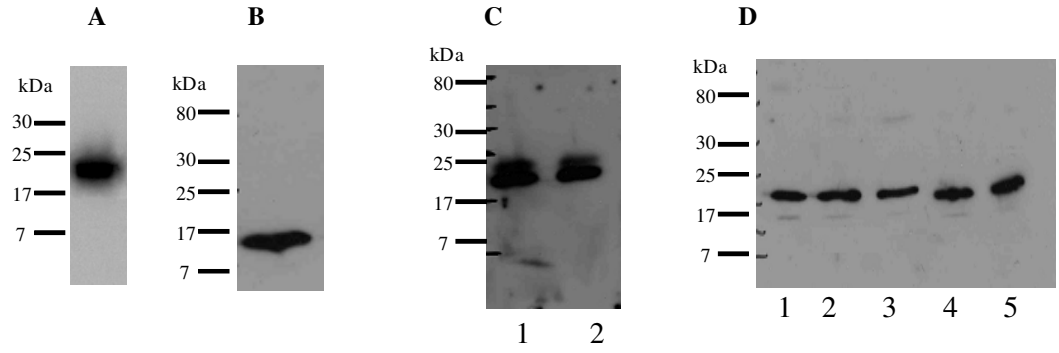

Figure 4.4 Western blot analysis of post-refolded mPrP proteins. A) Western blot of mPrP(23-231) detected with anti-PrP antibody ICSM18.

4.3 Method Development

For the aggregation reactions, recombinant protein was prepared as described in 2.4.1-2.4.6 and aliquoted into triplicate separate wells of a 96 well plate. Aggregation reaction method is described in 2.4.8 but the basic method is briefly reiterated here to illustrate how the buffer development occurred. Thioflavin T (ThT) dissolved in sterile pH 7.4 deionised water was prepared freshly every time. The reactions were incubated at 37°C, and agitated at 600 rpm as described by Bocharova *et al* (Bocharova *et al.*, 2005). Fluorescence measurements were taken at various time points using a BMG FLUOstar Omega multi-plate reader using filter sets 445-5 nm (excitation wavelength) and 480-10 nm (emission wavelength). Background fluorescence was subtracted from each sample before plotting the data versus time. In this system, aggregation is described as an increase in fluorescence intensity over time above that of the initial reading, as the ThT signal emitted at 482 nm will only increase if the amount of β-sheet increases in the reaction.

First, a range of solvent conditions were tested (Figure 4.5). All conditions were tested on mPrP(23-231) prepared exactly the same way, and all were agitated at the same time, with the same solution and concentration of ThT added to monitor the reaction. All reactions were incubated at 37°C and agitated at 600 r.p.m. Buffer conditions initially tested were from published studies (Bochorova *et al.*, 2005; Baskakov and Bocharova, 2005) and were assessed both with and without denaturing components. As seen in Figure 4.5A, the aggregation reaction results were quite different under these solvent conditions compared to the published results. In many cases including using the 1M GdnHCl, 3M Urea, 50 mM HEPES, pH 6.0 buffer specified by Bocharova *et al*, and the buffer specified in Baskakov and Bocharova (1 M GdnHCl, 2.4M urea, 20 mM sodium acetate at pH 5.0), very little aggregation was seen compared to reactions without denaturants (Bocharova *et al.*, 2005; Baskakov and Bocharova, 2005). Other buffers tested included 1M GdnHCl, 3M Urea, 50 mM HEPES pH 6.0 (Bocharova *et al.*, 2005); 1 M GdnHCl, 2,4M urea, 20 mM sodium acetate pH 5.0 (Baskakov and Bocharova, 2005); 10 mM PBS pH 7.3; 50 mM HEPES pH 6.8; 50 mM HEPES pH 7.2. Of these only reactions using PBS showed any aggregation (Figure 4.5B).

The differences in the results of experiments presented here compared with previously published works may be due to the differences in protein preparation in this study compared to in previous studies. However, 3M urea or 1.5M guanidine are relatively high concentrations of denaturants and not likely to be encountered *in vivo*, and as this study is to assess PrP conversion under more physiological conditions a sodium phosphate buffer system was tested. 10 mM sodium phosphate buffers at pH 5.5, 6.8 and 7.4 were tested (Figure 4.3C) with the pH 7.4 buffer producing the best aggregation reaction.

After testing it was decided that 20 μM protein was an appropriate concentration to use, as it would allow for the greatest number of experiments to be done per preparation of protein and was a high enough concentration so the reaction was visible. Therefore all aggregation experiments described were performed at 37°C with agitation at 600 rpm. Each 100 μL reaction contained 20 μM protein and 10 μM ThT in 10 mM sodium phosphate, pH 7.4, with a sterile 3mm glass bead. At least two protein preparations were analysed for each PrP construct, with a minimum of three independent experiments performed (with each protein purified and refolded independently).

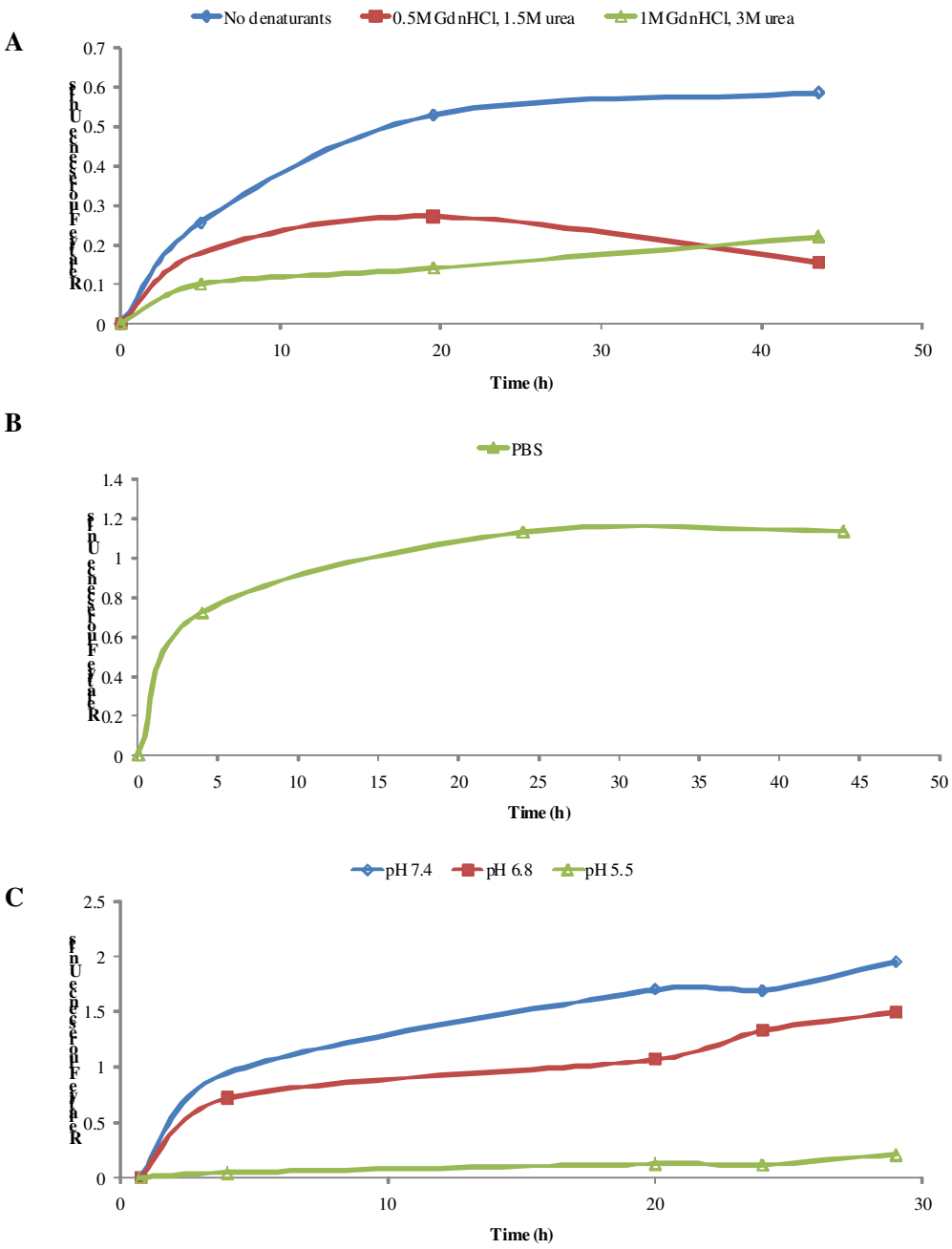

Figure 4.5 Optimisation of mPrP aggregation as assessed by ThT fluorescence. A) Aggregation reactions in same base buffer with increasing levels of denaturants. The addition of denaturants had a decreased response in this assay. B) Aggregation reaction with PBS. C) Aggregation of mPrP is dependent of pH. Aggregation reactions in 10 mM sodium phosphate at either pH 5.5, 6.8, or 7.4 using 50 µM protein were monitored by ThT fluorescnce. All experiments were performed a minimum of two times for preliminary studies.

The drawback of this method was the variability seen in the maximal fluorescence calculations – that is, the extent of the reaction although the kinetic traces seen were similar. Figure 4.6 shows the maximum fluorescence values from mPrP(23-231) aggregation reactions. The variability made for more difficult statistical analysis so data were normalised to the no metal control to help account for this variability.

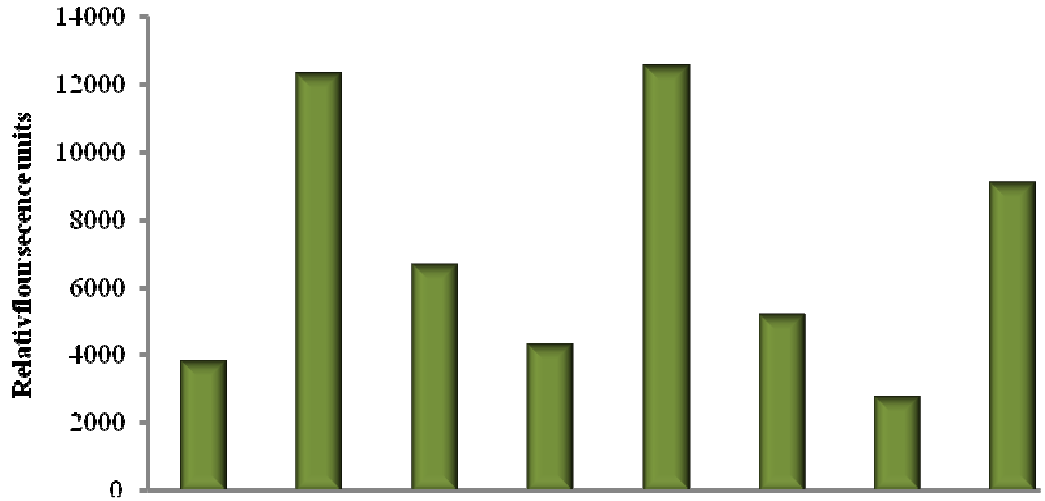

Figure 4.6 Variability in mPrP(23-231) maximum fluorescence values. Variety in protein preparation is evident from the variability seen in these values. While the kinetic curves are similar, the maxima are quite different. Each bar corresponds to an independently refolded aggregation reaction, and at least four separate protein purifications are represented.

4.4 Aggregation of mPrP(23-231)

The first step was to analyse the aggregation of full-length, recombinant mPrP(23-231), determine whether those aggregation products were capable of self-propagation, and finally investigate the effect the metals $CuSO_4$, $MnSO_4$ and $ZnCl_2$ had on the aggregation.

To assess the aggregation of recombinant mPrP(23-231), aggregation reactions were performed as described in section 2.4.8. Aggregation is described by a rate, which describes how quickly aggregation occurs, and overall maximum fluorescence intensity, calculated from the greatest fluorescence intensity measured to describe the amount of β-sheet content in the reaction.

In other studies using mPrP(23-231), aggregation rates can be fitted to a sigmoidal curve (Baskakov and Bocharova, 2005); however this was not seen in this study. Aggregation increased in a linear fashion before reaching a plateau, after which no further aggregation was seen even in experiments continued past 24 h (Figure 4.7). Therefore only the linear rate was analysed by determining the linear increase for each reaction (from time zero to the start of the plateau). In this study, mPrP(23-231) aggregation had an average linear rate of 1273.8± 321.7, n=11.

A distinct maximal fluorescence value was calculated from each aggregation experiment. The average maximal fluorescence for mPrP(23-231) was 6282.7 ± 1270.9, n=11 relative fluorescence units.

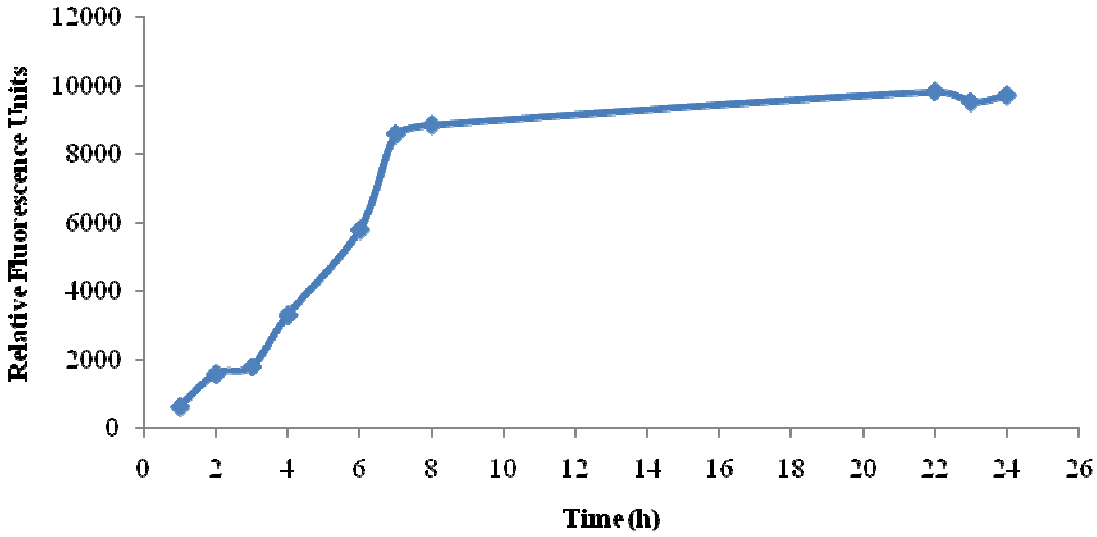

Figure 4.7 Representative graph of recombinant mPrP(23-231) aggregation. The aggregation was monitored using ThT fluorescence and values are relative fluorescence units (excitation 445 nm, emission 482 nm) plotted over time.

To assess what type of aggregates were formed by mPrP(23-231) aggregation, aggregate end products were subjected to transmission electron microscopy (TEM). Samples were negatively stained with uranyl acetate before imaging at 100,000 times magnification. TEM images showed that under these aggregation conditions aggregate end products were amorphous structures (see Figure 4.8). No discrete fibril or pre-fibrillar products were observed. These results indicate that in neutral pH conditions, amorphous non-fibril aggregates are formed.

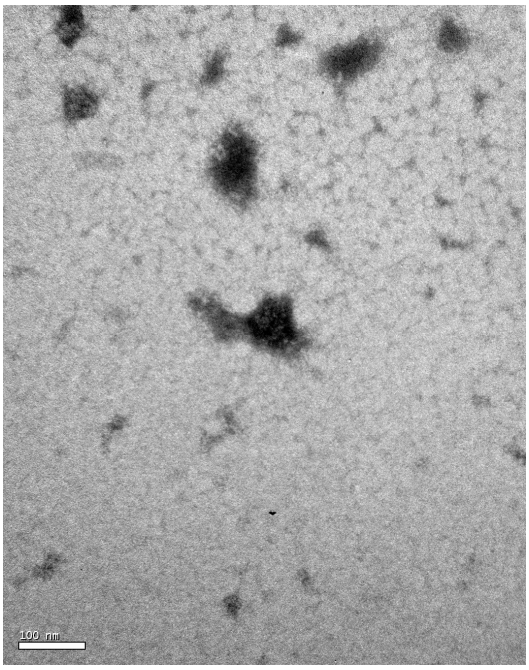

Figure 4.8 Negatively stained TEM image of mPrP(23-231) aggregate end products from aggregation reactions. The predominant structures are amorphous aggregates. No fibril structures were seen.

4.4.1 Self-seeding capabilities of mPrP(23-231)

A property of prion diseases is the capability to induce conformation change in natively folded PrP molecules. To test whether aggregates formed under these conditions were able to induce a conformation change or seed a reaction, mPrP(23-231) aggregation reactions were run for 6, 50, or 126h and then 20 µL of the end product was added to 100 µl of 20 µM recombinant mPrP(23-231) containing 10 µM ThT.

There was no significant effect on the rate of the reaction or on the maximum fluorescence achieved with the addition of any of the pre-formed seeds (Fig 4.9). Several other conditions including different concentrations of seed were tested and none were able to cause any significant increase in the rate or maximum fluorescence of any reaction (not shown). As the pre-formed material did not cause any significant seeding effect, these experiments were not pursued further.

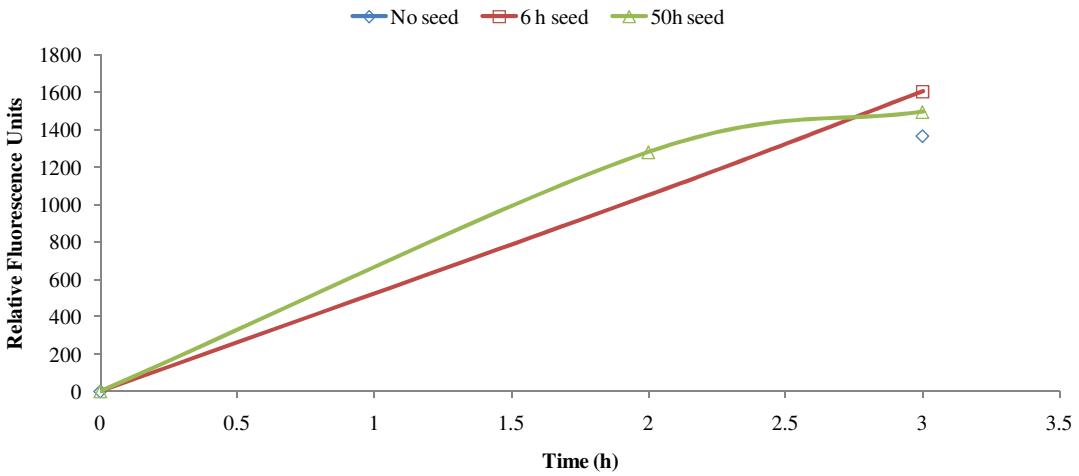

Figure 4.9 Aggregation of seeded mPrP(23-231) reactions. Aggreation reactions were run for 6 or 50h before adding 20 µL of the end product to the start of a fresh aggregation reaction. A representative graph is shown comparing seeded(6h and 50h preformed product)reactions versus no seed control, n=3

4.4.2 Effect of metals on mPrP(23-231) aggregation

The effect of metals was then assessed by the addition of metals to the aggregation reaction. $CuSO_4$, $MnSO_4$ and $ZnCl_2$ buffered in 10 mM sodium phosphate, pH 7.4 were added to 20 µM recombinant mPrP for a final metal concentration of 100 µM. Aggregation reactions were then performed as described in 2.4.8. As in the no metal experiments, after the linear increase in aggregation the reaction reached a plateau, and while the experiment was allowed to proceed for more than 20h, no further increases in aggregation were. Therefore the linear rate was determined for each reaction as well as maximum fluorescence.

Results show mPrP(23-231) aggregation reactions with the addition of metals (Figure 4.10A). Copper, manganese, and zinc addition did not affect the maximal fluorescence achieved in a statistically significant manner (Figure 10.8B). Linear rate calculations of aggregation also indicate a trend for metals to decrease the rate of the reaction when compared to the no metal control, although again this was not statistically significant (Figure 4.10C).

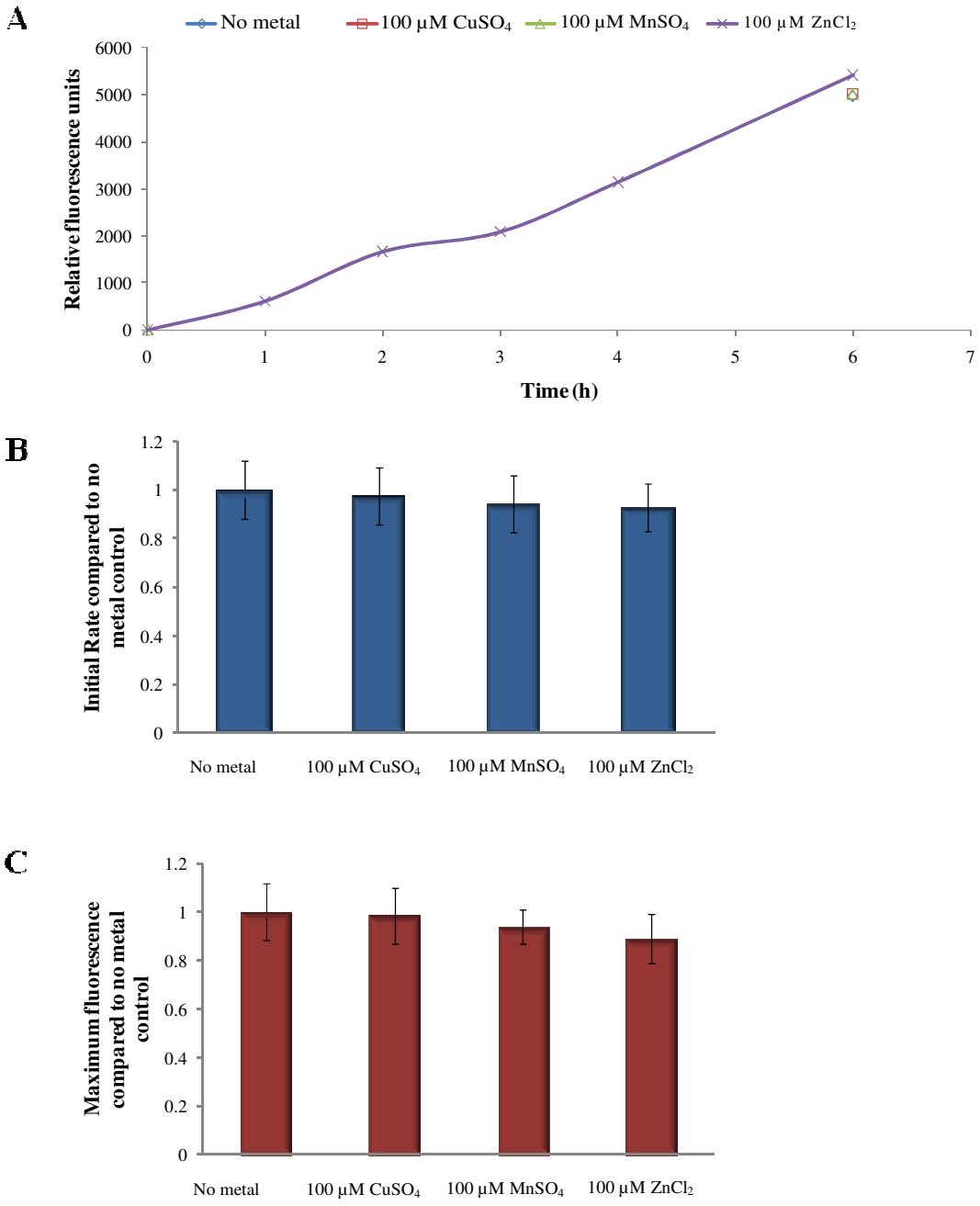

Figure 4.10 Aggregation of mPrP(23-231) with 100 µM metals as monitored by ThT fluorescence. A) Representative graph of linear aggregation with 100 µM metals. B) Average linear rate of aggregation with metals compared to no metal control. C) Average maximal fluorescence of each reaction with metals compared to no metal control. Error bars are n=8, ± SEM.

Next, end products of aggregation reactions were run on 5-20% gradient SDS-PAGE gels and assessed by Western blot (as in section 2.3.12 and 2.3.13) to determine whether there was any difference in the end product between metal added reactions (Figure 4.11). No high molecular weight aggregates were seen in the Western blots, and there was no difference between the control and metal added reactions. Smaller PrP fragments were seen around 10-12 kDa, and even smaller fragments were present

at 6.5 kDa. Additionally, fragments were seen at around 16kDa, a size corresponding to N-terminal truncated PrP. To further determine what these smaller fragments were, the antibody 8B4 was used which recognises an epitope in the N-terminus only (residues 35-45). The results show the disappearance of some fragments, and a strong band at 6.5 kDa suggesting the fragments not were truncated up to residue 45. Smaller fragments were present which could correspond to cleaved N-terminal products. It is possible the bands present which are larger than the monomer (23kDa) could be aggregated fragments of the N-terminus. To further determine whether this may be true, imaging studies would need to be performed.

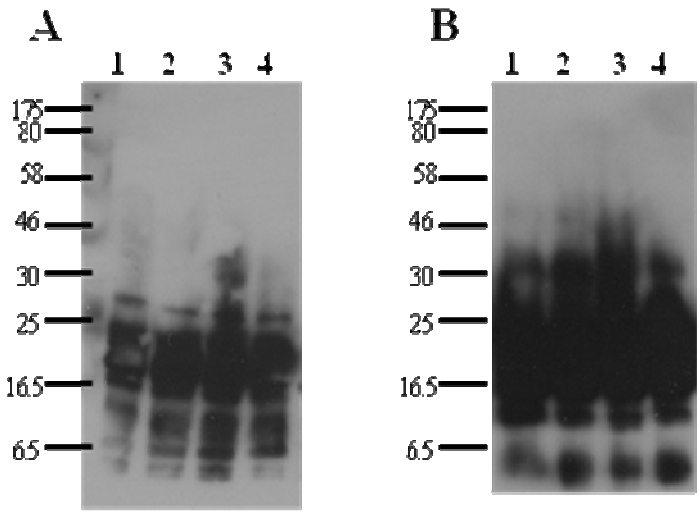

Figure 4.11 Western blots of aggregate end products of mPrP(23-231). A) Western blot with anti-PrP antibody ICSM18. B) Western blot with anti-PrP antibody 8B4. In both blots, lane 1 is aggregate with no metal, lane 2 is with 100 µM $CuS0_4$, lane 3 is with 100 µM $MnSO_4$, and lane 4 is with 100 µM $ZnCl_2$. Markers are in kDa.

4.5 Aggregation of truncated and deletion mutant mPrP

The next set of mutant PrP used to examine which aspects of metal binding domains were responsible for metal-induced effects on aggregation were N-terminal truncation mutations and octapeptide repeat region deletion mutations (see Figure 2.2A).. A N-terminally truncated mutation was used to determine whether in these conditions the N-terminally truncated protein aggregation was affected by the presence of metals, as any effect seen would be solely due to the 5th site.

The octameric repeat region is accepted as an important metal binding region of PrP. Therefore two deletion mutants were used to examine the effects of the octapeptide region on aggregation. PrP(Δ51-89) does not have any octapeptide repeats whereas mPrP(Δ67-90) has one repeat. mPrP(Δ106-126) was studied for several reasons: this

region has been thought to contain a sequence necessary for amyloid formation and has been found to cause neonatal lethality in mice (Li *et al.*, 2007). In addition, this region has been shown to have neurotoxic properties as a peptide (Forloni *et al.*, 1993; Brown *et al.*, 1996). Previous peptide analysis has shown this region conformation can be influenced by metals (Jobling *et al.*, 2001).

4.5.1 Computational analysis of mPrP aggregation propensity

Having determined that metals did not significantly affect the rate or amount of aggregation of mPrP(23-231), computer analysis was performed using WALTZ and TANGO online programs to help reason why this might be. Mutant PrP was also used to predict whether the N-terminal mutations used in this study would behave differently. WALTZ is a program which calculates the likely amyloidgenic regions of a protein sequence. Using this program, the primary amino acid sequences for all mutant PrP were inputted. Results indicate the main amyloidgenic regions of mPrP are situated within the C-terminus at residues 137-142; 149-154; 156-163; 204-210 (see Figure 4.12). As metal binding occurs at the N-terminus of the protein, the amyloidgenic sequences should not be directly affected by metal interactions. However this does not preclude metals from causing an effect on the aggregation by indirect means.

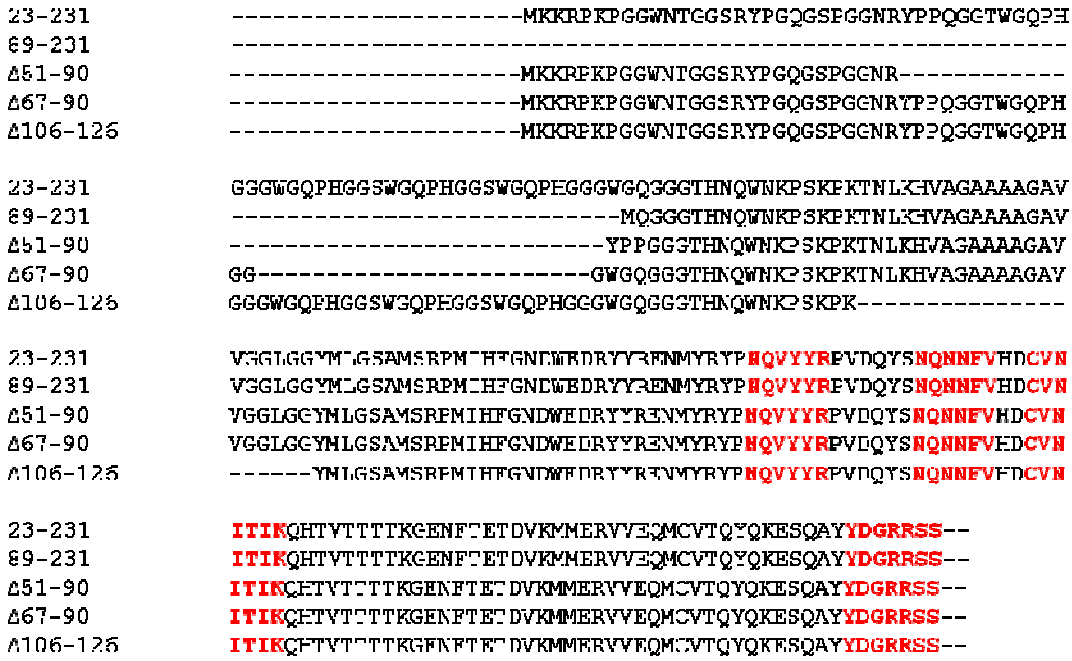

Figure 4.12 WALTZ-predicted amyloidgenic regions in mPrP. Predicted amyloidgenic regions encompassing residues 137-142, 149-154, 156-163, and 204-210 are highlighted in bold red.

Next, the PrP mutants were analysed by TANGO, an on-line program which predicts the aggregation propensity of a peptide sequence. Analysis showed that mPrP(89-231) has a higher AGG value, which indicates an increased propensity to aggregate into β-sheet structures, compared to mPrP(23-231) (Figure 4.13). In contrast, mPrP(Δ106-126) had a lower AGG value, which indicated a decreased tendency to aggregate compared to mPrP(23-231). All mutants had a similar HELIX (a probability determinant for a-helix content) and HELAGG (a measure of helix-mediated aggregation) values when compared to mPrP(23-231), but all TURN values (which predict β-turn propensity) were decreased.

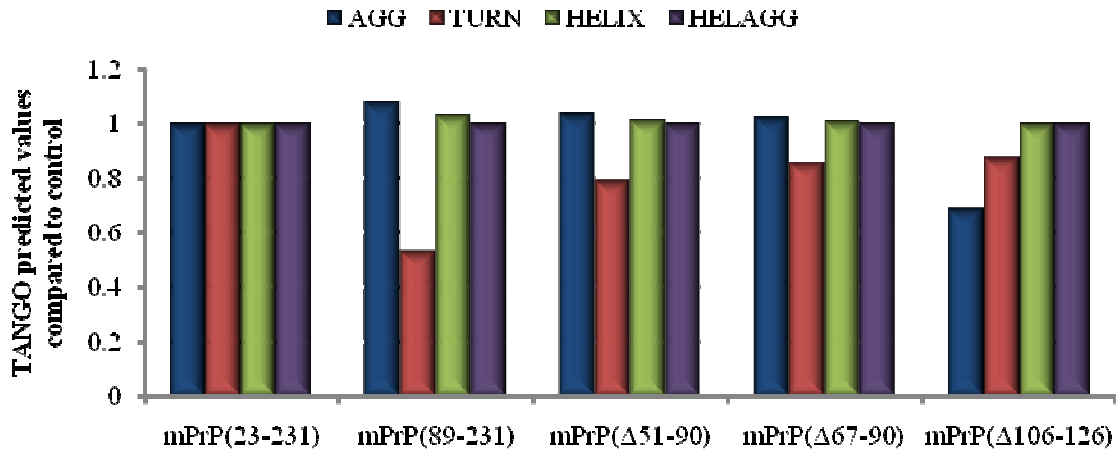

Figure 4.13 TANGO-predicted values for mPrP deletion and truncation mutant aggregation. All values are compared to the full length control.

4.5.2 Aggregation of mPrP(23-231) versus truncated and deletion mutant mPrP

The initial rate of aggregation of the mutant PrP compared to wild type (mPrP(23-231)) was assessed (Figure 4.14). As with mPrP(23-231), all mutant PrP showed initial linear increase in aggregation, and after 20h no further increases in aggregation were seen. Results indicated that deletion and truncation mutant mPrP had a higher linear rate than full length mPrP(23-231), although this was not statistically significant (Figure 4.14). Analysis of the maximum fluorescence showed mPrP(89-231) and mPrP(Δ67-90) were decreased in comparison to mPrP(23-231), although this was not statistically significant. Maximum fluorescence was increased very slightly with mPrP(Δ106-126) and mPrP(Δ51-89), although this was not significant.

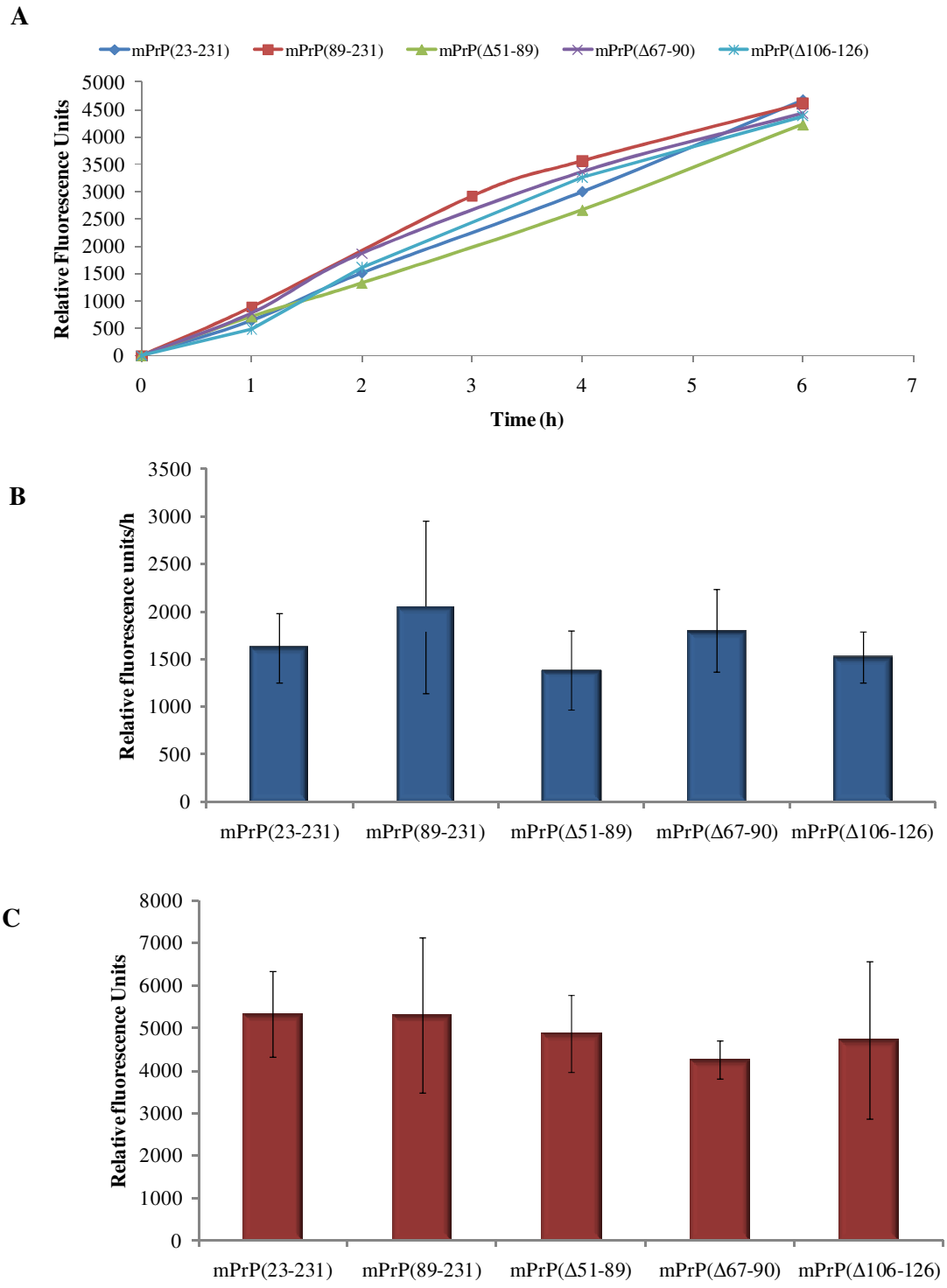

Figure 4.14 Initial rate and maximum fluorescence of no-metal mPrP aggregation. A) Representative graph of initial aggregation of full length, deletion and truncation mutant mPrP. B) Linear rate of aggregation of truncation and deletion mutants compared to full length mPrP. Error bars are ± SEM, n=8 mPrP(23-231), n=3 mPrP(89-231), n=4 mPrP(Δ51-89), n=4 mPrP(Δ67-90), and n= 5 mPrP(Δ106-126). C) Maximum fluorescence of aggregation of truncation and deletion mutants compared to full length mPrP. Error bars are ± SEM, n=11 mPrP(23-231), n=3 mPrP(89-231), n=4 mPrP(Δ51-89), n=4 mPrP(Δ67-90), and n= 5 mPrP(Δ106-126).

4.5.3 Aggregation of truncated mPrP(89-231) with metals

First the effect of metals on an N-terminally truncated mPrP was assessed. mPrP(89-231) lacks the octapeptide repeat region, which is important for metal binding. Therefore any effect seen would be due to the metals interacting with the so-called 5th site at His95 and His110. Aggregation reactions with mPrP(89-231) were performed as in 4.4.2 and linear rate of aggregation and maximum fluorescence was determined.

mPrP(89-231) aggregation reactions with 100 µM $CuSO_4$ and $ZnCl_2$ showed addition of metals did not affect to the linear rate or the maximum fluorescence of the reaction compared to the no metal control (Figure 4.15 B, C). However, addition of 100 µM $MnSO_4$ caused a significant ($p<0.05$) increase to the initial rate and maximum fluorescence compared to the no metal control (Figure 4.1 5B,C). This increase of the rate of the reaction may be due to the interaction of the manganese around the 5th site (His95, H110) which is the available metal binding region in this protein, and this stands to reason as this region has a higher affinity for manganese than the octameric repeat (Brazier *et al.*, 2008).

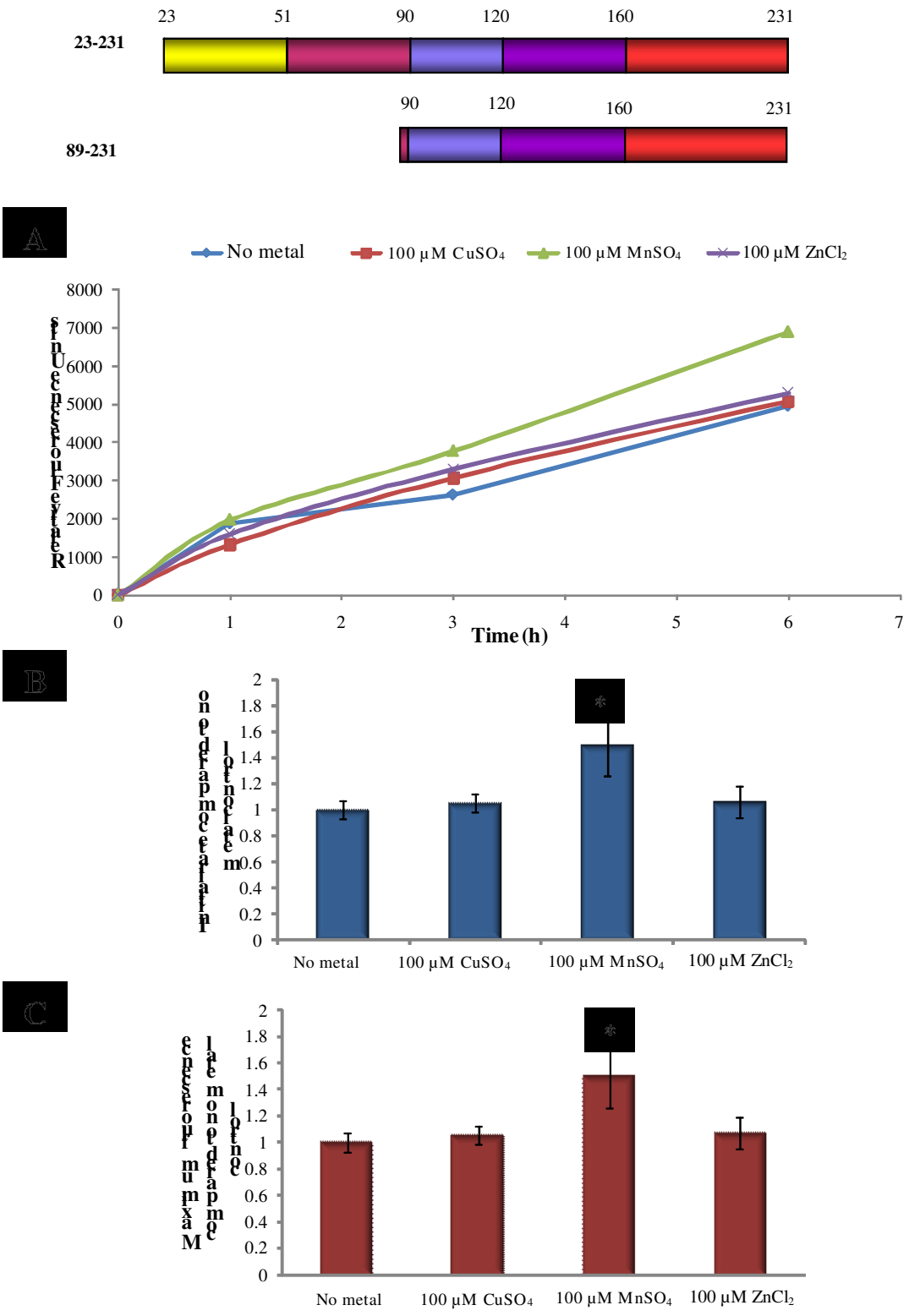

Figure 4.15 Aggregation of mPrP(89-231) with 100 µM metals as monitored by ThT fluorescence. The schematic shows mPrP(89-231) compared to the to full length mPrP(23-231). A) Representative graph of aggregation of mPrP(89-231). B) Rate of aggregation with copper and zinc compared to no metal control shows no significant differences, whereas addition of manganese to the reaction caused a significant increase in rate. C) Maximum fluorescence of aggregation with copper and zinc compared to no metal control shows no significant differences. A significant increase in maximum fluorescence is seen with manganese addition. Error bars are SEM, n=3. * p<0.05

Next, end products of aggregation reactions were analysed by Western blots. Some bands were seen in the ICSM-18 blot (Figure 4.16A), particularly in the no metal control aggregation that are indicative of dimers (~32kDa). The banding pattern also suggests small oligomers were formed. There was no significant difference between the end products of the reactions with metals, although fewer bands were present in the metal-added reactions. These results supports the idea that these reaction conditions caused β-sheet formation which does not lead to large aggregates but rather smaller, amorphous β-sheet-rich structures.

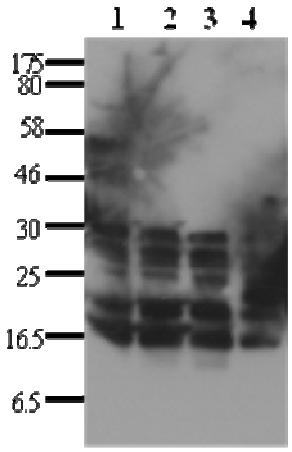

Figure 4.16 Representative Western blot of aggregate end products of mPrP(89-231) aggregation with and without metal. Western blots were performed with anti-PrP antibody ICSM18 and at least one blot per aggregation experiment was performed (n=3). Lane 1 is aggregate with no metal, lane 2 is with 100 µM $CuS0_4$, lane 3 is with 100 µM $MnSO_4$, and lane 4 is with 100 µM $ZnCl_2$. Markers are in kDa.

4.5.4 Aggregation of deletion mutants of PrP with metals

4.5.4.1 Octameric repeat region deletion mutants

To further assess the role of the octapeptide repeat region in metals an aggregation, aggregation assays were performed using two mutant constructs either lacking the octapeptide repeat region only (mPrP(Δ 51-89)) or with one repeat present (mPrP(Δ67-90)).

4.5.4.1.1 Aggregation of mPrP(Δ51-89)

Aggregation reactions with metals were performed as in 4.4.2 and the rate of aggregation and maximum fluorescence of each reaction was determined. Linear aggregation of mPrP(Δ51-89) with the addition of 100 µM metals is shown in Figure 4.17A. mPrP(Δ51-89), like mPrP(89-231) lacks the octameric repeat domain, so any effect of metals may be due to interactions with the 5th site at residues His95 and His110. Aggregation reactions with the addition of copper, manganese, or zinc all

showed a slight but statistically insignificant decrease in the initial rate of reaction when compared to no metal controls (Figure 4.17B). Addition of manganese, copper or zinc decreased the maximum fluorescence achieved compared to the no metal control but this was not statistically significant (Figure 4.17C).

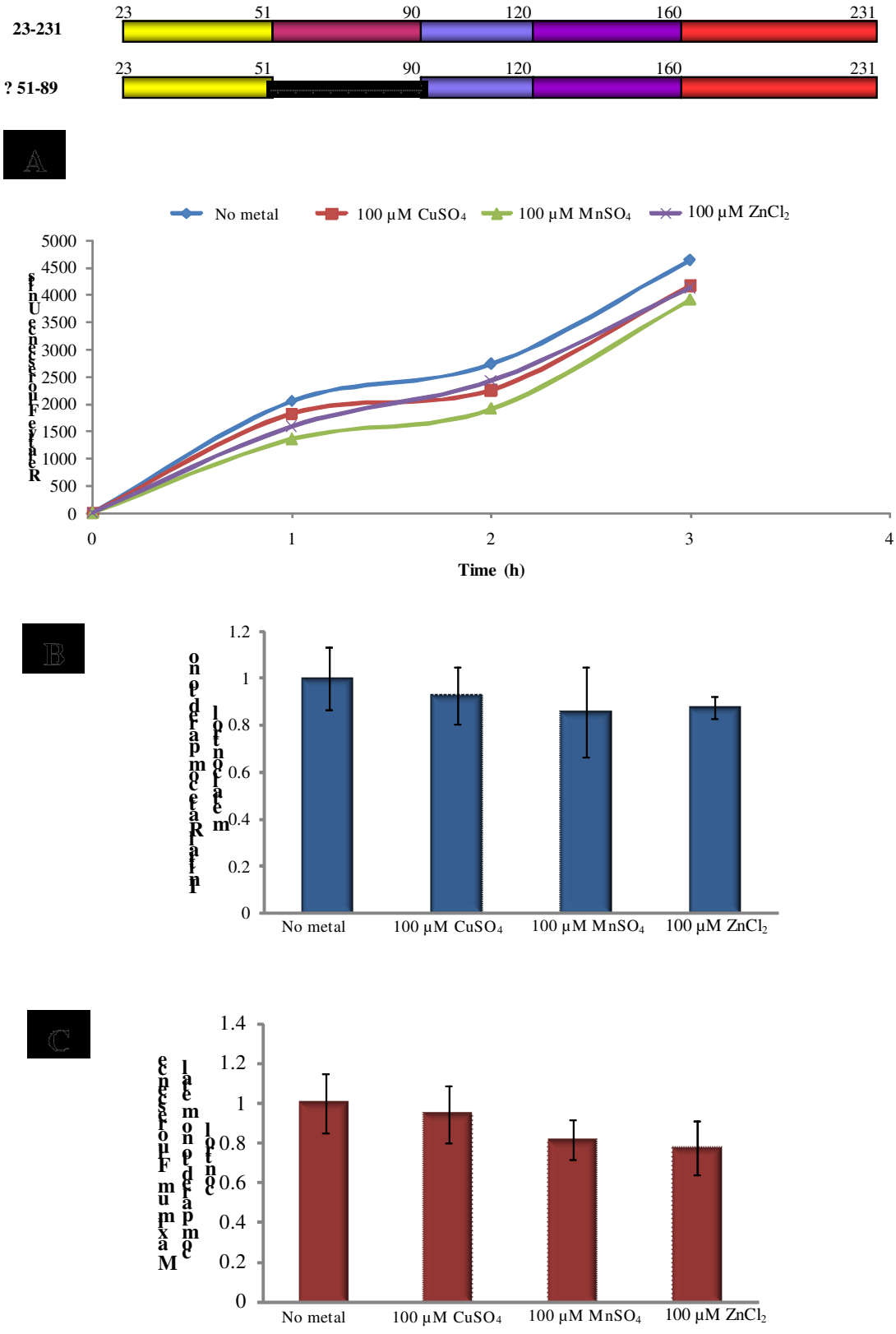

Figure 4.17 Aggregation of mPrP(Δ51-89) aggregation with 100 µM metals as monitored by ThT fluorescence. Schematic shows mPrP(Δ51-89) mutation in relation to full length mPrP(23-231). A) Representative graph of mPrP(Δ51-89) aggregation with metals. B) Comparison of the rate of aggregation with metals to the no metal control show no significant differences. C) Maximal fluorescence reached during aggregation with metals compared to no metal control shows no significant differences. Error bars are SEM, n=4.

End products of aggregation reactions analysed by Western blot with two different anti-PrP antibodies, ICSM-18 and 8B4 as described in 2.3.13 (Figure 4.18). No high molecular weight bands are present which would indicate large oligomeric structures. Bands corresponding to a dimer (~38kDa) could be seen in several samples. Overall, there was no significant difference between the metal added aggregate products and the no metal control. However, smaller PrP fragments were present at 10-12 kDa, as well at much smaller sized bands. These fragments may correspond to cleavage products of the protein which occurred during aggregation. Furthermore, bands which are larger than the monomer (19 kDa) yet smaller than the dimer (38 kDa) were present which could be aggregated N-terminal fragments.

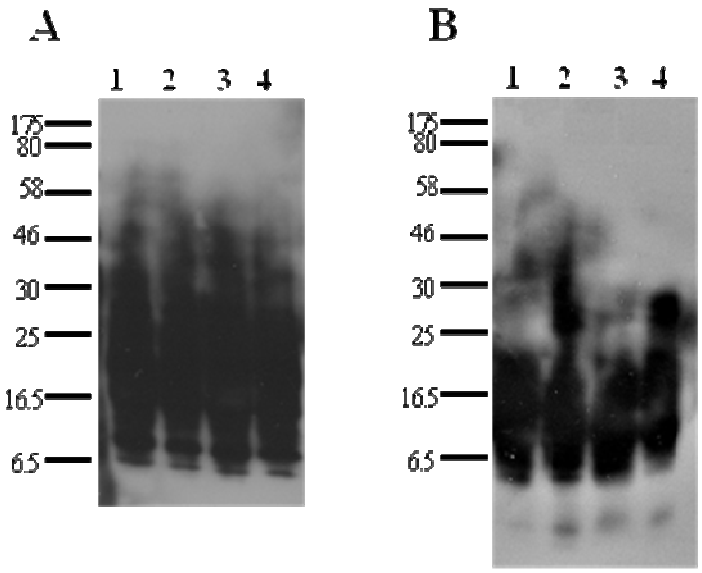

Figure 4.18 Western blots of aggregate end products of mPrP(Δ51-89). A) Western blot with anti-PrP antibody ICSM18. B) Western blot with anti-PrP antibody 8B4. Aggregates were analysed after each experiment (n=4). In both blots, lane 1 is aggregate with no metal, lane 2 is with 100 µM $CuS0_4$, lane 3 is with 100 µM $MnSO_4$, and lane 4 is with 100 µM $ZnCl_2$. Markers are in kDa.

4.5.4.1.2 Aggregation of mPrP(Δ67-90)

mPrP(Δ67-90) aggregation reactions were performed with metals as described in 4.4.2.

Linear aggregation of mPrP(Δ67-90) with the addition of 100 µM metals is shown in Figure 4.19A. Aggregation reactions with the addition of zinc produced data which was not able to be analysed and therefore were excluded. Addition of 100 µM copper significantly increased the initial rate and maximum fluorescence of the reaction ($p<0.05$). Addition manganese to mPrP(Δ67-90) aggregation reactions caused an

insignificant decrease in the initial rate and maximum fluorescence reached by the reaction compared to no metal control (Figure 4.19B and C).

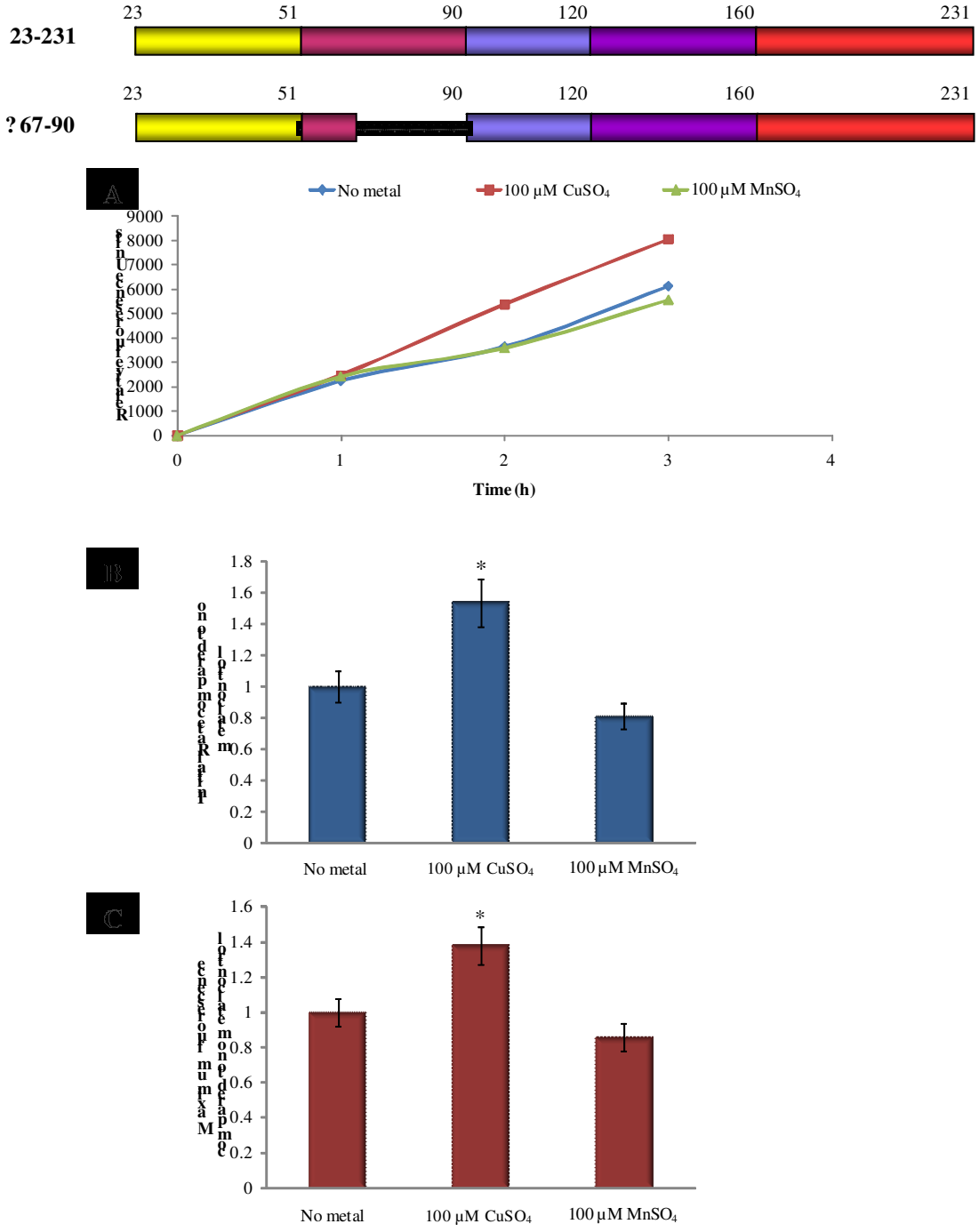

Figure 4.19 Aggregation of mPrP (Δ67-90) aggregation with 100 µM metals as monitored by ThT fluorescence. Schematic shows mPrP(Δ67-90) mutation in relation to full length mPrP(23-231). A) Representative graph of mPrP(Δ67-90) aggregation with metals. B) Rate of aggregation with metals compared to no metal control. Only the addition of copper caused a significant increase in the rate. C) Maximal fluorescence reached during aggregation with metals compared to no metal control. Addition of copper but not manganese caused a significant increase in the maximum fluorescence achieved. Error bars are SEM, n=4. *p<0.05

Finally, Western blots with two different anti-PrP antibodies were performed as described in 2.3.13 to determine whether there was any difference in the end product

between metal added mPrP(Δ67-90) reactions (Figure 4.20). No significant difference was seen between the metal and no metal reactions. As with previous blots of mPrP aggregates formed with this method, no high molecular weight aggregates were present but the blots show smaller PrP fragments. These fragments may correspond to cleavage products of the protein which occurred during aggregation. Furthermore, bands which are larger than the monomer (20 kDa) yet smaller than dimer (40 kDa) were present. These bands may correspond to aggregated N-terminal fragments.

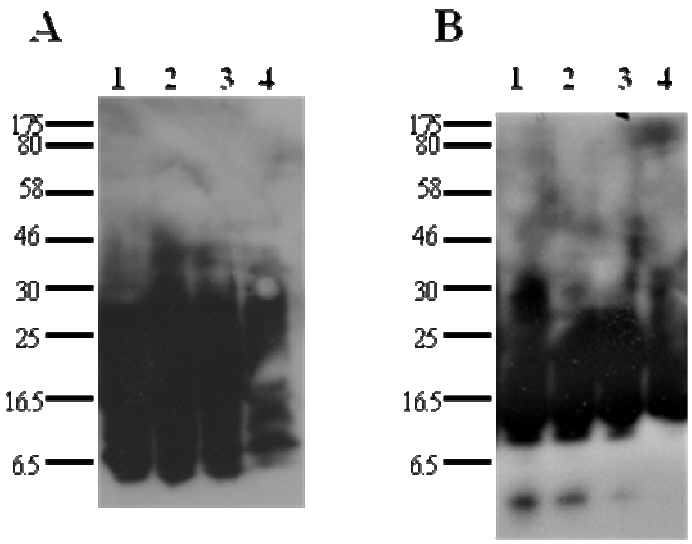

Figure 4.20 Western blots of aggregate end products of mPrP(Δ67-90). A) Western blot with anti-PrP antibody ICSM18. B) Western blot with anti-PrP antibody 8B4. Aggregates were analysed after each aggregation experiment (n=4). In both A and B, lane 1 is aggregate with no metal, lane 2 is with 100 µM $CuS0_4$, lane 3 is with 100 µM $MnSO_4$, and lane 4 is with 100 µM $ZnCl_2$. Markers are in kDa.

4.5.4.2 Aggregation of mPrP(Δ106-126) with metals

Aggregation of mPrP(Δ106-126) reactions with metals were performed as previously described in 4.4.2.

Linear aggregation of mPrP(Δ106-126) with the addition of 100 µM metals is shown in Figure 4.21A. Aggregation reactions with the addition of $CuSO_4$, $MnSO_4$ and $ZnCl_2$ tended to increase the initial linear rate compared to the no metal added control (Figure 4.21B). Although this was statistically insignificant, this trend was seen in every experiment. The statistics may not have stacked up as reactions this mPrP construct were highly variable in terms of maximum fluorescence. Addition of copper, manganese and zinc all caused an increase in the maximum fluorescence reached by the aggregation reaction, compared to no metal control, although this trend was not statistically significant (Figure 4.21C).

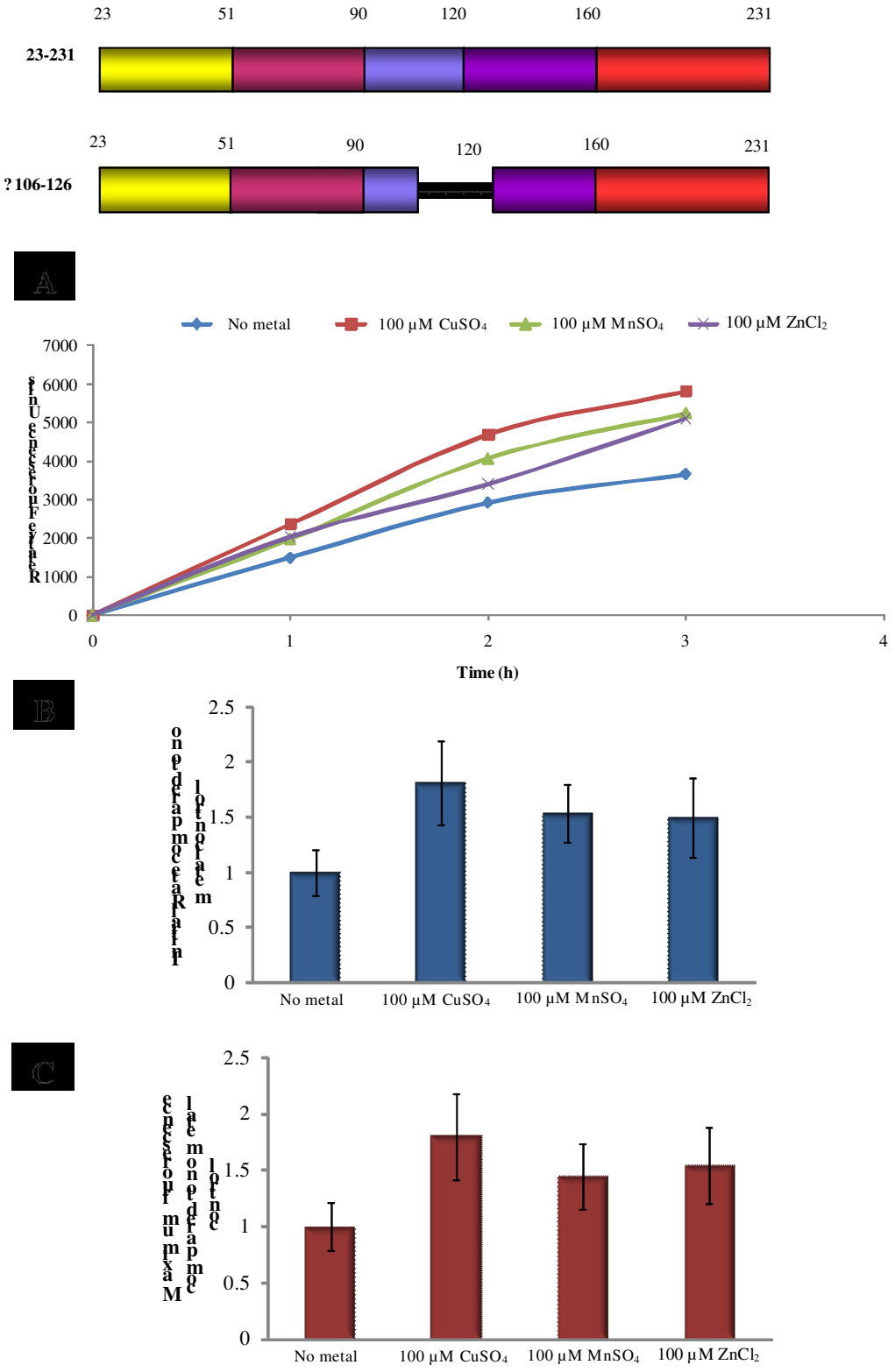

Figure 4.21 Aggregation of mPrP(Δ106-126) with the addition of 100 µM metals as monitored by ThT fluorescence. The schematic representation of the mutation compared to full length mPrP(23-231) is illustrated above. A) Representative graph of aggregation of mPrP(Δ106-126) with the addition of metals. Kinetic data: B) Rate of aggregation with metals compared to no metal control shows no significant difference. C) Maximal fluorescence reached during aggregation with metals compared to no metal control. No significant difference is seen. Error bars are SEM, n=5.

Next, end products of aggregation reactions were assessed by Western blots with two different anti-PrP antibodies (Figure 4.22). No high molecular weight aggregates were present, and there was no difference between the metal added aggregate products and the no metal control. The Westerns show PrP fragments at 10-12 kDa, as well as some 6.5 kDa fragments. These fragments may correspond to cleavage products of the protein which occur as the protein is agitated during aggregation. Bands were present that correspond to a size that is larger than the monomer (21 kDa) yet smaller than a dimer. These could be aggregated N-terminal fragments (Figure 4.223A). This is supported by the Westerns with the N-terminal specific antibody, as those bands are not present (Figure 4.22B).

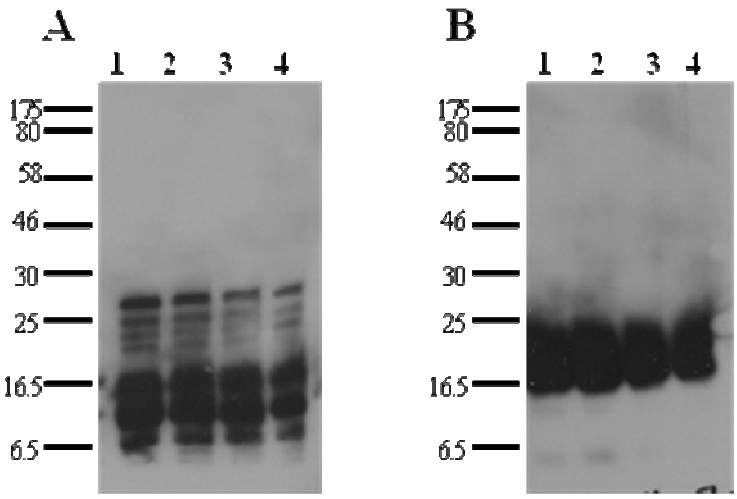

Figure 4.22 Western blots of aggregate end products of mPrP(Δ106-126). A) Western blot with anti-PrP antibody ICSM18. B) Western blot with anti-PrP antibody 8B4. In both blots, lane 1 is aggregate with no metal, lane 2 is with 100 µM $CuS0_4$, lane 3 is with 100 µM $MnSO_4$, and lane 4 is with 100 µM $ZnCl_2$. Markers are in kDa.

4.6 Aggregation of metal binding point mutations of mPrP

In order to dissect which domain of the protein was responsible for the effect of the metals on PrP aggregation several point mutation forms of PrP were used. PrP has been shown to bind metals such as copper, manganese, zinc, and nickel, as described in 1.3.2, and it is through histidine coordination this binding occurs. Therefore site-directed mutagenesis was used to develop PrP mutant with histidine→alanine mutations (Figure 2.2 B). These mutations could therefore be used to determine whether the histidines within the octapeptide repeat region or the so-called 5th site

region were responsible for the effects seen with metals. Aggregation of each mutant mPrP was monitored by ThT fluorescence as described in 2.4.8.

4.6.1 Computational analysis of metal-binding point mutations

As determined in section 4.5.1, the WALTZ-predicted amyloidogenic sequences are located within the C-terminus of the protein. Next, the PrP mutants were analysed by TANGO, an on-line program which predicts the aggregation propensity of a peptide sequence. TANGO values predicted the TURN (β-turn propensity) values for mPrP(Null) and mPrP(Null+H95, H110) were decreased compared to other PrP (Figure 4.23). However, there was no difference in the AGG (propensity to aggregate), HELIX and HELAGG (helical aggregation propensity). This suggests there should be no difference in the propensity of these metal-binding point mutant mPrP aggregation reactions.

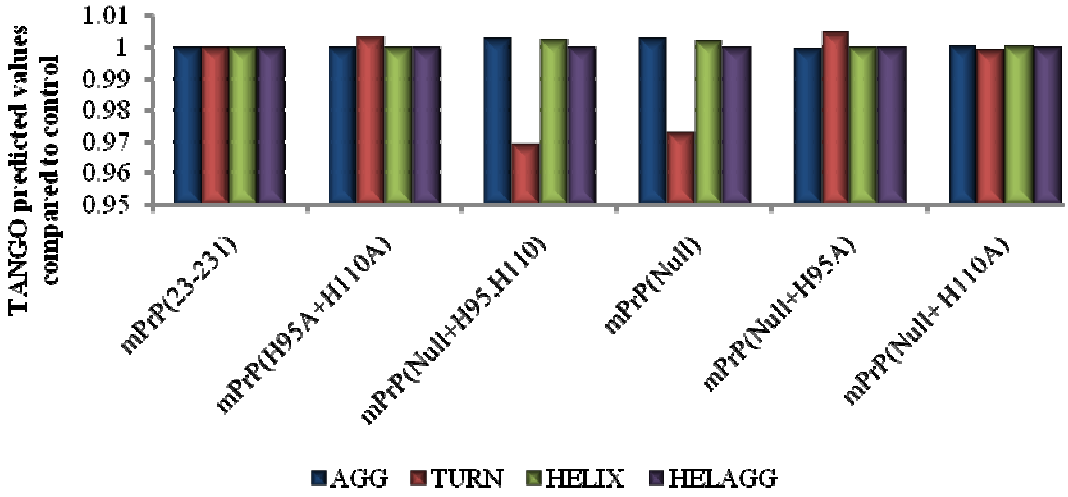

Figure 4.23 TANGO-predicted values for metal-binding point mutation mPrP aggregation, compared to wild type mPrP(23-231).

4.6.2 Aggregation of mPrP(Null+H95), mPrP(Null+H110), mPrP(Null+H95, H110) and mPrP(Null)

In order to determine whether the histidine residues involved in metal binding are essential for metal-mediated effects on aggregation, the mutant mPrP(Null), which has all histidine within the octameric repeat region and the 5th site binding region mutated to alanines, was used. In mPrP(Null), mPrP(Null+H110A), mPrP(Null+H95A) and mPrP(Null+H95, H110) reactions, no fluorescence signal was detected beyond that of the blank which indicates this protein did not aggregate in any reaction, Raw

fluorescence data for mPrP(Null) aggregation reaction is shown in Figure 4.24 and no signal above the blank is detected.

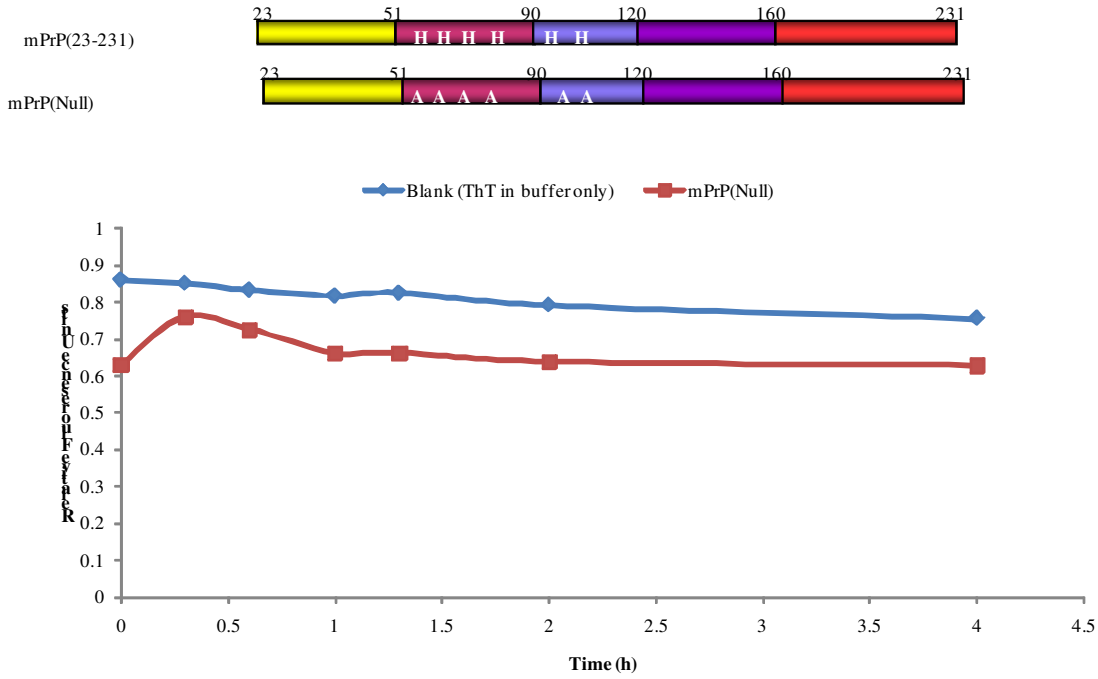

Figure 4.24 Representative aggregation reaction of mPrP(Null) monitored by ThT fluoresescence. The schematic shows the point mutations relative to wild type mPrP(23-231). No fluorescence is dectected at levels above that of the dye alone blank.

4.6.3 Aggregation of mPrP(H95A+H110)

Next, the aggregation of the metal-binding mutant mPrP(H95A+H110A) was examined to determine whether this mutant protein could aggregate and whether absence of the 5th site produced any metal-induced effect on aggregation of mPrP. Aggregation reactions were performed as described in 2.4.8. First, the linear rate of aggregation and maximum fluorescence achieved was determined without metals added, and compared to the full length mPrP (Figure 4.25A). Both the initial rate and maximum fluorescence were decreased compared to full length mPrP although this was not statistically significant (Figure 4.25 B,C). Data from mPrP(H95A+H110A) reactions was very variable and difficult to analyse. This protein is more difficult to prepare and has a tendency to precipitate during purification.

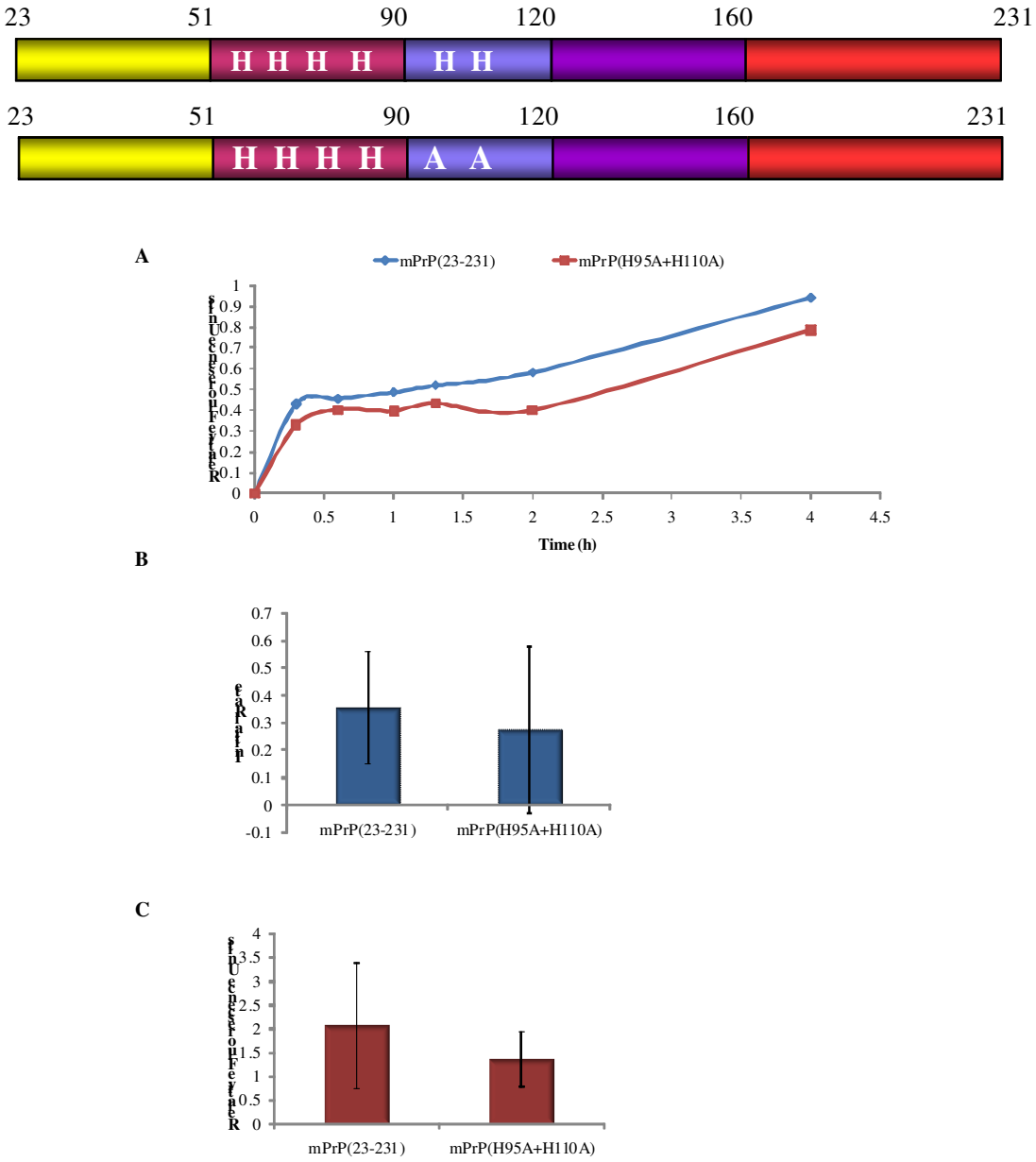

Figure 4.25 Rate and maximum fluorescence of no-metal mPrP(H95A+H110A) aggregation as monitored by ThT fluorescence. A) Rate of aggregation of point mutation mPrP(H95A+H110A) compared to full length mPrP(23-231) shows no significant differences. B) Maximum fluorescence of point mutation mPrP(H95A+H110A) compared to full length mPrP(23-231) is not significantly different. Error bars are ± SEM, n=4.

Next, to assess the effect of metals on mPrP(H95A+H110A) aggregation, $CuSO_4$ and $MnSO_4$ buffered in 10 mM sodium phosphate at pH 7.4 were added for a final metal concentration of 50 µM. Aggregation reactions were performed as described in 2.4.8. Results from aggregation reactions with 50 µM metals were highly variable and were not able to be analysed and are not included.

End products of mPrP(23-231) and mPrP(H95A+H110) aggregation reactions were analysed by Western blot as in 2.3.13 to determine whether there was any difference in the end product between mutants (Figure 4.25). Neither aggregation reaction showed high molecular weight aggregates which would indicate fibrils and/or amorphous aggregates, although 10-12 kDa PrP fragments were present. This suggests that aggregation of these mutants under these reaction conditions form β-sheet-rich PrP structures which do not lead to large ordered aggregates.

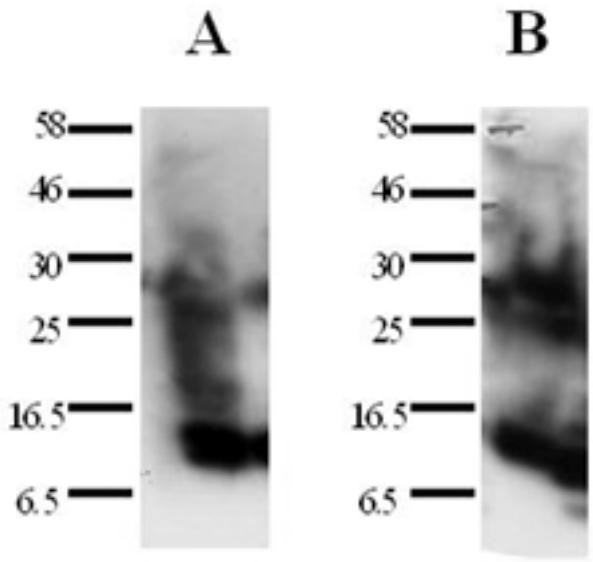

Figure 4.26 Western blot analysis of aggregation end products without metals. All blots were probed with anti-PrP antibody ICSM18. A) mPrP(23-231) and B) mPrP(H95A+H110A).

4.7 Conclusion and Discussion

In this study a method was developed to assess the aggregation of mPrP under conditions more representative of physiological conditions than previously published aggregation studies (Baskakov *et al.*, 2001, Baskakov and Bocharova, 2005; Bocharova *et al.*, 2005a,b) and determine whether the addition of copper, manganese, or zinc played any role in the aggregation.

Aggregation of mPrP mutant protein showed no significant differences when compared to full length mPrP under the conditions developed for this assay. Specifically, shorter mPrP constructs did not differ in rate of aggregation or the extent of β-sheet content compared to full length mPrP. These results do not completely align with the predicted aggregation propensity obtained from the online program TANGO as mPrP(Δ106-126)

was predicted to have a decreased aggregation propensity compared to full length mPrP(23-231).

Aggregation of mPrP with metal binding point mutations, in contrast to full length mPrP control, yeilded unexpected results. The online program WALTZ predicted amyloidogenic sequences of PrP were all C-terminal, suggesting that there would be no direct effect with N-terminal alterations. Additionally, the TANGO-predicted aggregation propensity was the same between wild type and point mutation mPrP. However under the conditions used here, mPrP(Null), mPrP(Null+H95A), mPrP(Null+H110A) and mPrP(Null+H95, H110) did not aggregate. Disagreement between predicted and observed aggregation propensities may be explained by the fact that online computations consider only amino acid sequence, and therefore any structural instability of the folded protein would not be taken into account. Furthermore, online prediction programs assume 100% protein purity which is difficult to achieve when working with a highly insoluble protein like PrP. mPrP(Null), in particular, was found to be quite unstable and degraded quickly. Additionally mPrP(H95A+H110A) is very difficult to purify and solubilise and tends to precipitate quickly. Data obtained from this mPrP was highly variable. These factors could have contributed to the differences between predicted and experimental results.

Under neutral aggregation conditions, the addition of metals to full length mPrP and various mutants did not show any significant alterations to how quickly the aggregation occurred (linear rate), or to the accumulation of β-sheet content (maximum fluorescence, a parameter to measure extent of aggregation) during the reaction compared to a no metal control. No significant effect of metals was seen with the mutant lacking the octameric repeat region, mPrP(Δ51-89) and while the trend of metals increasing mPrP(Δ106-126) aggregation was seen in all experiments, it was not statistically significant.

However addition of manganese to mPrP(89-231) caused a statistically significant increase in the initial rate and maximum fluorescence achieved by the reaction. No significant effect was seen with either copper or zinc. According to recently published data, mPrP(89-231) has only one high affinity binding site for manganese, residue His95 (Brazier *et al.*, 2008). Metal binding sites are influenced by fragment length (Klewpatinond and Viles, 2007) and it may be that manganese interacts with this binding differently to the full length protein. This would also explain the differences

seen between the full length protein and with the mutant mPrP(Δ51-89), which also lacks any octameric repeat binding regions for manganese. It is possible that the additional residues 23-50 influence the manner in which manganese would interact with the high affinity binding site centred on residue His95.

Copper addition to mPrP(Δ67-90) significantly increased the initial rate of aggregation as well as the maximum fluorescence achieved by the reaction relative to the no metal control. No effect was seen with manganese addition. mPrP(Δ67-90) lacks all but one of the octameric repeats and in theory would be able to bind 2-3 coppers – one within the octameric repeat and 1-2 copper ions within the "5th site" region involving histidines 95 and 110. This protein alone showed a promotional effect with copper. These data may suggest that a different metal-protein interaction will be observed when the 5th site region is alone (as in mPrP(Δ51-90)) and when it is present with the full complement of octameric repeats. It may be that the 5th site acts in concert with the octameric repeats to maintain normal interactions with respect to metals (as with wild type protein) but alterations to the 5th site –octameric repeat partnership result in variable metal-induced effects. Also, it may be that a completely different binding geometry and therefore N-terminal structure is generated upon copper interacting with mPrP(Δ67-90) and is responsible for the promotional effect seen on aggregation.

Several factors may have contributed to the differences in results for metals and PrP aggregation observed here and in comparison to those seen in previously published work. Many methods used to study PrP aggregation require low pH and denaturing materials (Jackson *et al.*, 1999a,b; Baskakov *et al.*, 2001; Martins *et al.*, 2006). Low pH conditions mimic those of the lysosome/early endosome, which are proposed sites for prion conversion (Caughey, 1991). The concentration of the denaturant guanidine hydrochloride, which is a common reagent in recombinant PrP aggregation assays, influences not only the kinetics of PrP aggregation but also has profound effects on the structure of PrP both in solution and as aggregated products (Polano *et al.*, 2009). It is known from PrP trafficking studies that the protein it is naturally exposed to neutral pH as well. Not only is it unlikely denaturing reagents would be present at those concentrations *in vivo*, it is important to consider the interaction between metals and denatured PrP is very different from the interaction of metals and re-natured PrP in a native-like state at neutral pH. It has not been demonstrated how PrP associates with metals under conditions presented by Baskakov *et al.*, whereas the association between metals and PrP at neutral conditions has been well described (Jackson *et al.*, 2001;

Davies *et al.*, 2009). The discrepancy between the results presented here to those seen in previously published work can be attributed to differences in protein preparation , purification, and different reaction conditions.It is thought ThT binds within cavities between β-sheets (Groenning *et al.*, 2007a, b), however there is no evidence indicating whether it only binds to fibril structures and not amorphous β-sheet-rich oligomers. The results in this chapter suggest the aggregates formed under these conditions contain β-sheet structures but are not fibrils. This is evidenced by the TEM data for mPrP(23-231) which did not show any fibril structures and the Western blot analysis which does not show any high molecular weight aggregates. Recently it has been shown that decreasing concentrations of denaturant cause more globular aggregate structures to form, in contrast to the mature amyloid fibrils formed with high (2M) concentrations of denaturant (Polano *et al.*, 2009). Therefore these aggregates produced in the absence of denaturants may be predisposed to form amorphous structures.

PrP is thought to have self-catalytic properties and it has previously been demonstrated that aggregates formed *in vitro* are capable of conferring conformational change onto monomeric proteins, or "seeding" (Colby *et al.*, 2007; Baskakov, 2004; Bocharova *et al* 2005a). In this study since the end products of aggregation reactions were unable to influence initial rate of aggregation, it suggests that the products formed under these specific conditions have very little, if any, self-propagation propensity.

In all mPrP constructs Western blot analysis did not show significant amounts of higher molecular weight aggregates, although some dimers were seen in the N-terminally truncated mutant mPrP(89-231) and in the deletion mutants mPrP(Δ51-90) and mPrP(Δ67-90). Bands which were larger than the monomer yet smaller than the predicted dimer size were seen in Westerns using a C-terminal antibody. With both this antibody and an N-terminal specific antibody, smaller fragments were seen which likely correspond to cleaved N-terminal products. Cleavage of the prion protein has been shown to occur *in vivo* (Pan *et al.*, 1992; Shyng *et al.*, 1993; Jimenez-Huete *et al.*, 1998; Nieznanski *et al.*, 2005). The results therefore suggest one of two possibilities. The first is that PrP forms β-sheet-rich structures which are smaller, possibly amorphous structures which may not be stable and do not survive SDS-PAGE analysis. The second possibility is that these results show the products of a PrP cleavage event acquire β-sheet structure over time but do not necessarily aggregate. TEM images of mPrP(23-231) in this work confirmed the absence of large fibril structures that have

been reported by other groups (Baskakov and Bocharova, 2005; Bocharova *et al.*, 2005a).

To fully determine the role of metals in PrP aggregation, further experiments are necessary. As previously mentioned, differences and variability seen in this assay could be attributed to protein purification. PrP is highly insoluble and difficult to further purify. It does not respond well to futher purification treatments such as FPLC. Alternatively, circular dichromism could be utilised to determine the starting structure for each batch of protein used, which would provide insight into which starting conformations form more highly β-sheet end products. Attempts to further optimise the system by using different controls could lead to the generation of more consistent data. For example, performing the experiments with a known pro-aggregation peptide such as PrP106-126 as well as a proper negative control (e.g., a protein similar in size to PrP) could have helped to optimise the system more fully. Furthermore, overloading the system (using much higher concentration of protein and/or metals) could have more substantially confirmed the effects seen. Separation of the fragments via size exclusion techniques would allow for imaging studies (TEM, FTIR) to be performed on each fragment to determine the structure and the effect metals may have on this aggregation.

Another alternative is that the main influence on PrP conversion is not metals but glycosaminoglycans. To determine whether this is the case, the next step would require investigating the role of GAGs in cellular prion infection (as in Chapter 3) and the aggregation method developed in this chapter.

5. Glycosaminoglycans in PrP aggregation and cellular infection

5.1 Introduction

Glycosaminoglycans (GAGs) are a group of compounds which are produced by most cells and include heparan sulphates, keratin sulphates, dextran sulphates, and chondroitin sulphates. The structure of these compounds consists of long chains of repeating disaccharide units, and they are divided into classes based on these disaccharide chain units and degree of sulphation. The molecules can vary significantly in size, charge distribution, and fine structure (Lander, 1994). Heparin, a highly sulphated version of heparan sulphate, is a well known protein binding partner which has been shown to bind to a variety of proteins that participate in anticoagulation, cell adhesion, and cell proliferation. In addition, heparin and heparan sulphate binding have been implicated in disease-associated processes, including aiding viral entry into cells and amyloid P plaque assembly (Capila and Linhardt, 2002).

There is evidence that GAGs play a role in prion disease, as detailed in 1.5.5.2. Furthermore, it has been shown that recombinant, brain-derived, and mammalian cell-derived PrP^{C} have each been shown to bind to GAGs, particularly heparin and heparan sulphate (Brimacombe *et al.*, 1999; Pan *et al.*, 2002; Warner *et al.*, 2002; Gonzalez-Iglesias *et al.*, 2002). The biological relevance for PrP binding heparin is unclear. It has been demonstrated that endogenous GAG expression is required for disease progression (Horonchik *et al.*, 2005) and GAGs can stimulate the conversion of PrP to a resistant form of PrP (Wong *et al.*, 2001; Deleault *et al.*, 2005; Kajnert *et al.*, 2006); in contrast, however, it has also been shown that the addition of exogenous GAGs can delay onset of disease in animal models and clear PrP^{Sc} from cell culture models (Caughey and Raymond, 1993; Gabizon *et al.*, 1993; Ehlers and Diringer, 1984; Kimberlin and Walker, 1986). The most potent of these compounds are chemically modified high molecular weight dextran sulphate or heparin mimetics. In cells, these anti-prion compounds prevented uptake of infectivity and limited endocytosis of PrP^{C} (Schonberger *et al.*, 2003; Horonchik *et al.*, 2005).

Heparin binding studies with recombinant hamster, human and bovine PrP all indicate the main binding regions are located in the N-terminal region of the protein. This region of the protein is flexible and lacks definitive structure, and has a number of basic residues. Previously studies using molecular modelling have shown the motif XBBBXXBX (where X denotes a non-basic residues and B a basic residue) on the face of α-helix and a second motif XBBXBX on β-strand were common motifs in heparin binding (Cardin and Weintraub, 1989). Specific spatial orientation of basic residues is required for heparin binding, with high affinity binding occurring when basic residues are 20 Å apart from opposite faces of a β-strand and a α-helix (Margalit *et al.*, 1993). Further study of the spacing of basic residues in relation to binding affinity in known heparin-binding proteins showed the most common spacing pattern found included a single non-basic residue between clusters of basic residues (BXB/BXB), and a second pattern of two non-basic residues between each basic residue cluster (BXXB). Clusters containing up to three residues is common, and spacing patterns of up to five but no more than seven non-basic residues between basic residues has been seen (Fromm *et al.*, 1997). Previous studies examining the binding of GAGs to PrP have used primarily biosensor or ELISA techniques to measure the binding to either peptides or his-tagged protein.

Previous heparin-PrP binding studies have been done using ELISA, biosensor, and fluorescent polarisation techniques and using either histidine tagged recombinant protein or peptides. As heparin binding is known to involve basic residues, the use of histidine tagged protein is not ideal. Furthermore, binding effects seen with short peptides may not occur with full length protein. Therefore heparin binding to mPrP was studied using isothermal titration calorimetry (ITC), a method which measures the changes in enthalpy caused by the interaction of two molecules in solution. This work will study the effects of heparin and mPrP binding, aggregation, and cellular infection to determine whether heparin is a promotional or inhibitory molecule in prion pathogenesis.

5.2 Heparin binding to mPrP

Binding studies were performed on deletion and truncation mutant PrP to determine which parts of N-terminal domain of PrP is essential to heparin binding. mPrP(Δ51-89) and mPrP(89-231) were used to determine what difference in binding the presence of a single heparin binding motif in the N-terminal region, at residues 23-27 (KKRPK). The full length mPrP(23-231) construct was used as a control. Figure 5.1 illustrates

previously published heparin binding regions on PrP overlaid on the mPrP constructs used in this work.

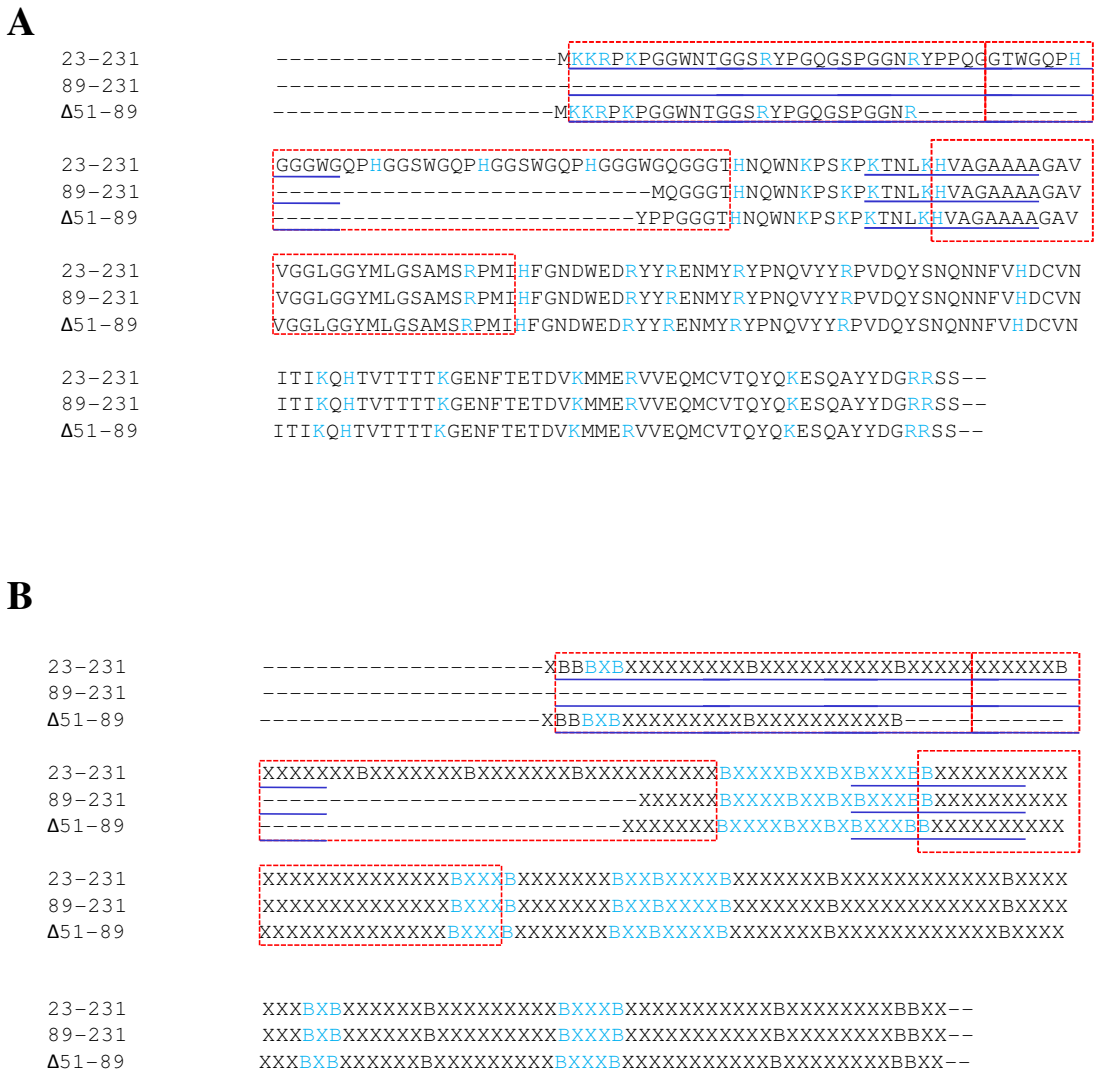

Figure 5.1 Heparin binding of mPrP deletion and truncation mutations overlaid with previously published heparin binding regions. Red box = binding sites from Warner *et al* 2002, blue underline= binding sites from Pan *et al* 2002. A) Basic residues are highlighted in light blue. B) All residues are labelled basic (B) or non-basic (X). Heparin binding motifs are highlighted in light blue.

5.2.1 ITC binding results for mPrP(23-231)

Experiments were performed in at least triplicate with a MicroCal VP-ITC as described in 2.4.10. Briefly, as the protein molecules bound heparin molecules, energy of binding is measured as a temperature change relative to reference cell. The energy change is then plotted against the concentration of the system (calculated from the initial input into the program) and a binding isotherm is produced. Each experiment is

repeated with a minimum of three independently refolded protein preparations. By experimentally fitting binding models to the isotherm within the MicroCal Origin 5.0 software, the number of binding sites and relative binding affinities can be calculated. Trial and error (judging best fit as the lowest χ^2 value) determined that a sequential binding model was the best fit. Details of the binding model are found in 2.4.10.2.2. Briefly, in the sequential model, there is no distinction as to *which* sites are saturated, but only the total number of sites that are saturated. If the sites are identical in terms of affinity, then there is a statistical degeneracy associated with the sequential saturation since the first ligand to bind has more empty sites of the same kind to choose from than does the second ligand and the second ligand has more sites to choose from than does the third, and so forth. For identical interacting sites then, the phenomenological binding constants K_i and the intrinsic binding constants K_{io} can be distinguished where the effect of the statistical degeneracy has been removed. The data is then presented (in the program) as molar stability constants (log K_a) and useful information extrapolated.

Therefore each isotherm obtained was fitted to a sequential binding model, and the model which had the lowest χ^2 value was taken as the best fit. Isotherms obtained from mPrP(23-231) binding heparin over a 1:20 molar ratio best fit a four-site sequential binding model. The percentage difference χ^2 value in binding models was 17% and 39% between a three- and five-site binding model and the four-site model. A representative binding isotherm is shown in Figure 5.2. All binding isotherms are representations of the energy change of the system, where the top graph represents the energy change as a function of time and the bottom graph plots the energy change relative to the molarity of the system.

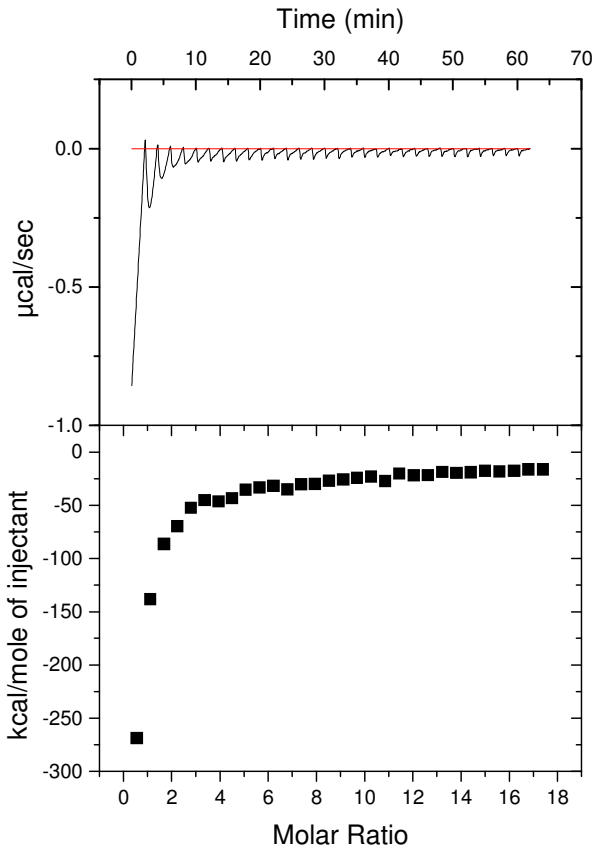

Figure 5.2 Representative ITC binding isotherm for mPrP(23-231) and heparin. mPrP(23-231) was injected into the cell containing a molar excess amount of heparin. All experiments (n=8) were performed at pH 7.4 and 25°C, and data are presented as blank subtracted and fit to a four-site binding model. The top graph represents energy change as a function of time, and the bottom graph represents energy change as a function of molarity.

The log K_a for each site was calculated and the log K_a values for each site from each independent experiment were averaged. All stability constants (K values) were within 8% of the mean, and are summarised in Table 5.1. Affinity values are calculated from the log K_a values by inversion (e.g. 1/log K_a = M). For the first three binding sites range from 10 to 100 nanomolar, with the fourth site is lower affinity and has a range of 1-10 micromolar. The only previously published heparin binding affinity for PrP was also in the 10-100 nanomolar range, which is in agreement with these data (Andrievskaia *et al.*, 2007

	Log K_1 M^{-1}	Log K_2 M^{-1}	Log K_3 M^{-1}	Log K_4 M^{-1}	% Error between K values
mPrP(23-231)	7.48	7.43	7.01	5.90	8
mPrP(Δ51-89)	11.7	6.53	6.03	N/A	1
mPrP(89-231)	6.89	6.97	N/A	N/A	24
mPrP(Null)	6.25	5.78	4.28	2.07	7
Cu-loaded mPrP(23-231)	4.85	4.91	5.02	5.01	21

Table 5.1 Log K_a and number of binding sites for mPrP binding to heparin. All values are averaged from each independent experiment and are in M^{-1}. Wild type (mPrP(23-231)) data are averaged across all experiments performed and used for comparative purposes.

5.2.2 ITC binding results for mPrP(Δ51-89).

Experiments were performed and analysed as in 5.2.1. Heparin binding isotherms obtained from mPrP(Δ51-89) did not fit a four site sequential binding model. The best fit was obtained with a three-site model and a representative isotherm is shown in Figure 5.3. The percentage difference between the three site model and either a two- or four-site sequential binding models was 69% and 2% respectively. However, the three site binding model had a lower relative error within the data and therefore was chosen as the best fit. The reduced binding capacity is further demonstrated by the different shape of the curve of the binding isotherm compared to the isotherm produced with mPrP(23-231) (Figure 5.5). The log K_a was calculated for each of the three binding sites and the values averaged (n=4). All K values were within 1% of the mean and are listed in Table 5.1.

In addition to have one less binding site than mPrP(23-231), the affinity values for heparin binding to mPrP(Δ51-89) were altered, with one high (1-10 femtomolar range) affinity site, and the second and third site having affinity values in the 100 nanomolar and 1-10 micromolar range respectively. These data suggests that without the octameric repeat, the number and nature of heparin binding sites are altered.

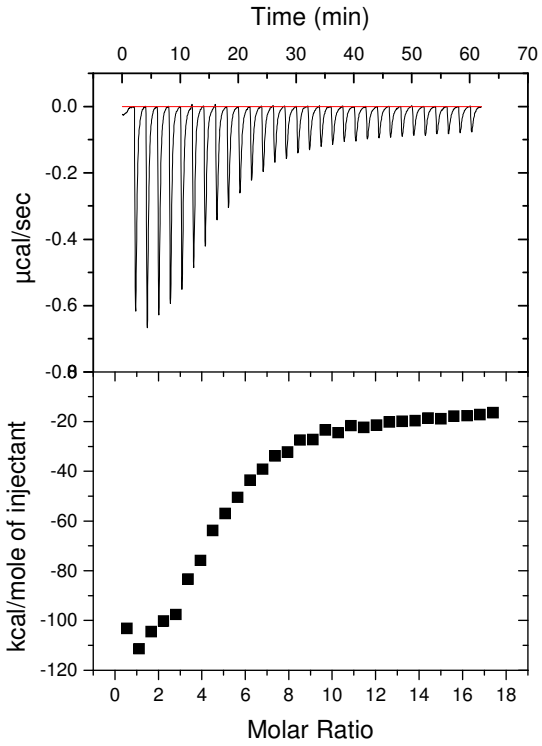

Figure 5.3 Representative ITC binding isotherm for heparin binding to mPrP(Δ51-89). Recombinant mPrP(Δ51-89) was injected into the cell containing a molar excess amount of heparin. All experiments (n=4) were performed at pH 7.4 and 25°C, and data are presented as an energy value. Data presented as blank subtracted and fitted to a three site binding model. The top graph represents energy change as a function of time, and the bottom graph represents energy change as a function of molarity.

5.2.3 ITC binding results for mPrP(89-231)

ITC binding experiments were performed and analysed as in 5.2.1. In contrast to mPrP(23-231) and mPrP(Δ51-89), heparin binding isotherms obtained from mPrP(89-231) did not fit a four site sequential binding model, nor did it fit a three site model. The best fit was obtained with a two-site sequential binding model, shown in Figure 5.4. The percentage difference between two- or four-site sequential binding models was 30% and 8% respectively.

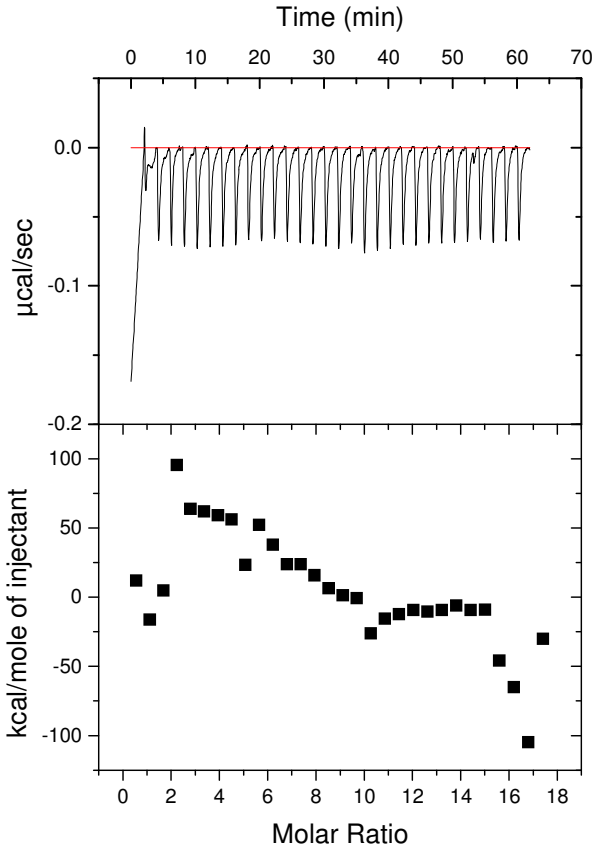

Figure 5.4 Representative heparin binding isotherm for mPrP(89-231). Data are shown as blank subtracted and fit to the appropriate binding model. As with the previous isotherms, the data are presented as energy values as a function of time (top graph) or as a function of molarity of the system (bottom graph). Experiments were performed at pH 7.4 and 25°C, n=3.

The log K_a was calculated for each site (error between K values did not exceed 24%) and averaged from three independent experiments. Values are summarised in Table 5.1. Truncation of the N-terminal region to residue 90 results in reduced heparin binding, as binding affinities for each site were within the 100 nanomolar and 1-10 micromolar range respectively. Reduced binding is further evidenced by the very different shape of the isotherm produced with mPrP(89-231) binding heparin. The curve was very different to those produced from both mPrP(23-231) and mPrP(Δ51-89). A comparison of each of the binding curves produced from these proteins is shown in Figure 5.5.

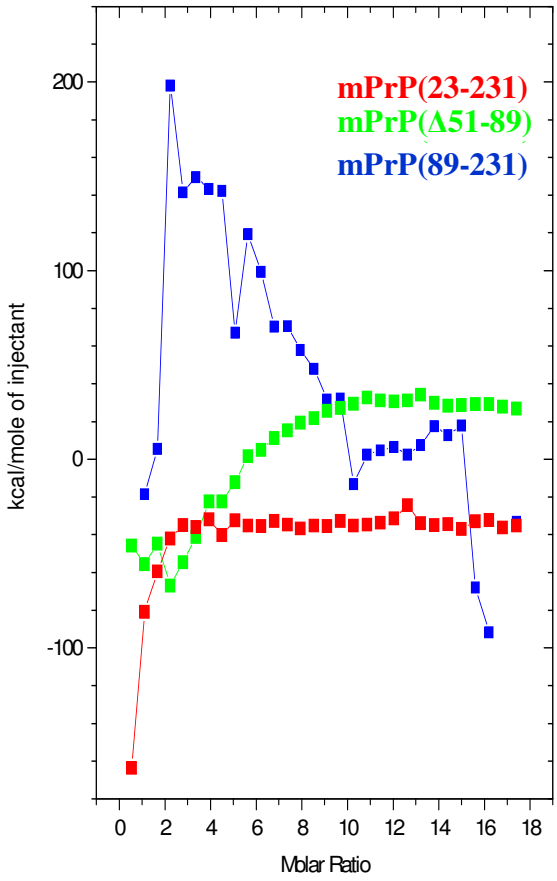

Figure 5.5 Comparison of binding isotherms of mPrP(23-231), mPrP(Δ51-89) and mPrP(89-231). Red = mPrP(23-231), green = mPrP(Δ51-89) and blue = mPrP(89-231). Each isotherm shows a binding experiment, with the background subtracted, at 1:20 molar ratio mPrP:heparin and is plotted as energy change as a function of the molarity of the system. All experiments were performed at 25C and pH 7.4 and all protein purified using the exact same method.

Taken together, these data suggest that wild type mPrP(23-231) has four heparin binding sites, and the N-terminal region (to residue 89) is responsible for at least two heparin binding regions, one of which is located between residues 23 and 51. This binding region is likely to be centred on the heparin binding motif KKRPK at residues 23-27, as loss of the octameric repeat region resulted in a reduced number of heparin-binding sites but a higher affinity for one of the remaining sites whereas truncation of the N-terminus to residue 89 results in loss of the higher affinity site. In addition the binding models, the isotherms produced by mPrP(Δ51-89) and mPrP(89-231) are

different to mPrP(23-231) even though all constructs were tested under the same PrP: heparin molar ratio (Figure 5.6).

5.2.4 Heparin binding to mPrP(H95A+H110A) and mPrP(Null)

The effect of basic to non-basic single amino acids substitutions in the N-terminus of PrP on binding of heparin to mPrP was studied to determine whether alteration of the histidine residues would affect heparin binding. Experiments were performed with mPrP(H95A+H110A) to assess the role of the "5th site" histidine residues. mPrP(Null) was used to determine whether the loss of histidine residues of the N-terminus has any effect on the binding of heparin to mPrP. All binding experiments were compared to the relative control mPrP(23-231). Figure 5.6 shows previously published heparin binding regions on PrP overlaid on the mPrP constructs used in this work.

Figure 5.6. Heparin binding of mPrP histidine to alanine mutations overlaid with previously published heparin binding regions. Red box = binding sites from Warner *et al* 2002, blue underline = binding sites from Pan *et al* 2002. A) Basic residues are highlighted in light blue. B) All residues are labelled basic (B) or non-basic (X). Heparin binding motifs are highlighted in light blue.

The binding of heparin to mPrP(H95A+H110A) was analysed as in 5.2.1.1. The results showed a very different binding curve when compared to mPrP(23-231). The best binding isotherms were produced with a 1:4 molar ratio of PrP: heparin. These results fitted poorly to single or sequential binding site models, but the lowest chi-squared

value was obtained by fitting a sequential 2-site binding model, which had 17% and 22% difference between one- and three- site sequential binding models respectively. However, the experiments proved more variable than the mPrP(23-231), and despite repeating the experiments several (n=4) times only limited data was produced and can be considered preliminary at best. There was evidence of precipitation of the protein during the experiments, which affected the reproducibility of the data and thermodynamic calculations, and resulted in affinity values which ranged over nine orders of magnitude. An example isotherm is shown in Figure 5.7.

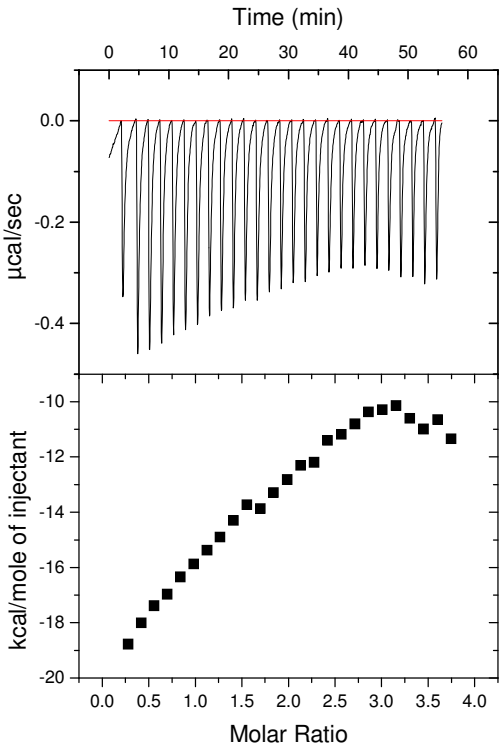

Figure 5.7 ITC isotherm of heparin binding to mPrP(H95A+H110A). All experiments were performed at 25°C and pH 7.4; however limited data was produced due to variability in protein stability and repeated precipitation during the experiments. All values are presented as energy change over time (top) and energy change as a function of molarity (bottom).

Next, the binding of heparin to mPrP(Null) was analysed as in 5.2.1.1. . The results showed a very different binding curve was produced (Figure 5.8) when compared to mPrP(23-231) and mPrP(H95A+H110A). Although this data fit best to a sequential four-site binding model, similar to mPrP(23-231), with a difference of 6.7% and 2.2% between three- and five-binding site models. Error between K values did not exceed 7%, and log K_a data (mean values from n=4) are summarised in Table 5.1.

As with mPrP(23-231), three of the binding sites had affinity values within the 100 nanomolar range, and the fourth site was of a lower 1-10 micromolar range. These values are not significantly different to those of mPrP(23-231) despite the fact mPrP(Null) has six N-terminal histidine residues replaced by alanines.

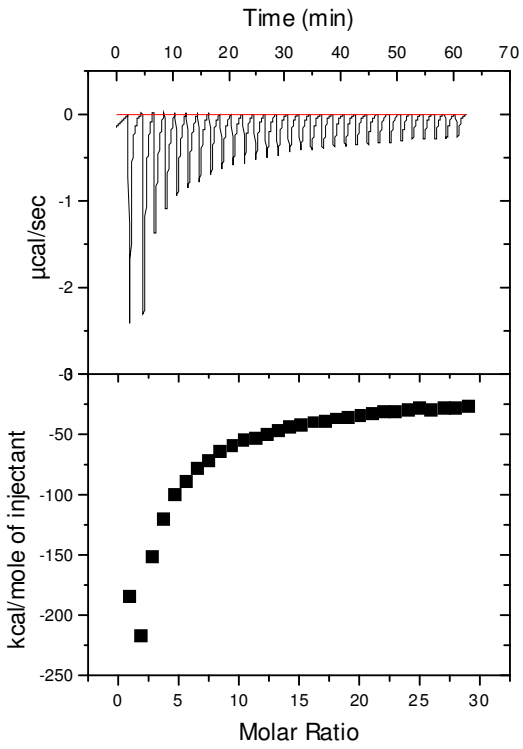

Figure 5.8 Representative ITC isotherm of mPrP(Null) binding to heparin sodium sulphate. Data are blank subtracted and fitted to a four-site sequential binding model. All experiments (n=4) were performed at 25°C and pH 7.4. Data are expressed as energy change as a function of time (top) or molarity of the system (bottom).

Analysis of the charge distribution of these proteins was performed using the online program Mobyle and is shown in Figure 5.9, with areas of interest in the N-terminus circled in red and green. These ITC results therefore show that altering the charge pattern of the N-terminus due to replacement of histidine residues with alanine residues is not sufficient to abolish heparin binding altogether.

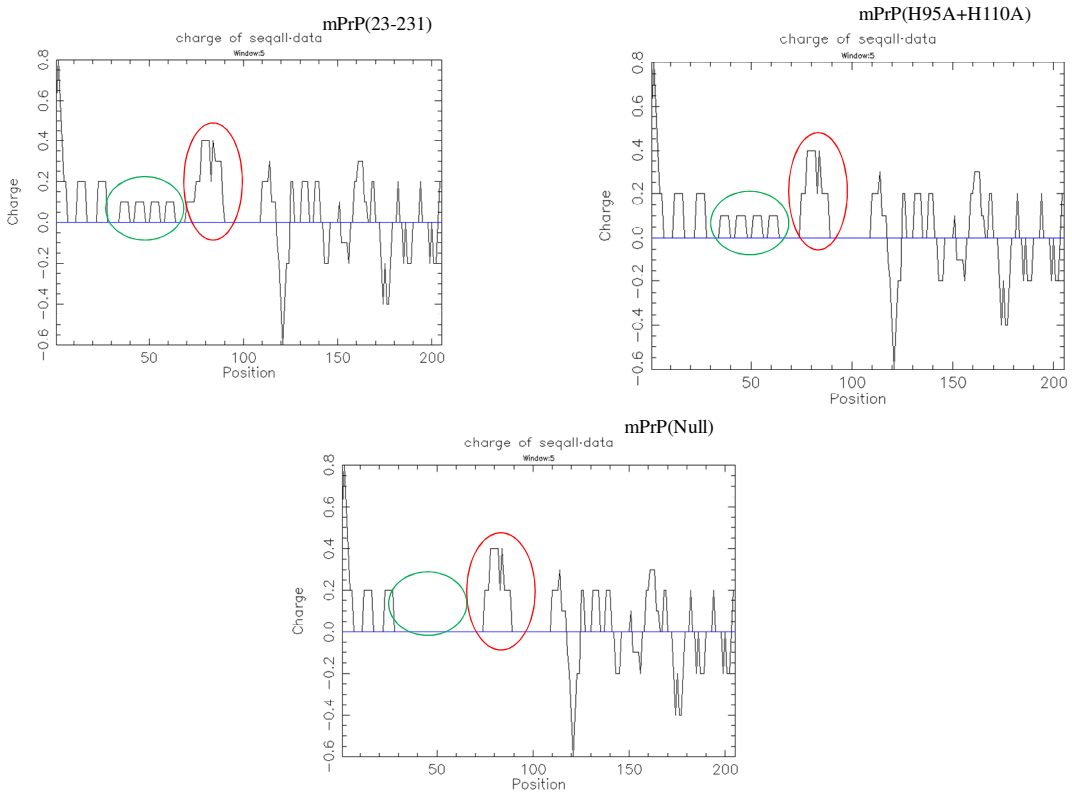

Figure 5.9 Charge distribution of mPrP(23-231), mPrP(H95A+H110A) and mPrP(null). Sequences were analysed by the online program Mobyle and are represented graphically as charge per amino acid residue. Red and green circles show areas where charge distribution is altered compared to the wild type.

5.2.5 Effect of copper on heparin binding to mPrP

Previously published studies indicate metals can modulate or effect the interaction of PrP with GAG, either by formation of stabilising bridges with copper ions, or by directly affecting the nature of binding (Brimacombe *et al.*, 1999; Gonzalez-Iglesias *et al.*, 2002; Pan *et al.*, 2002; Warner *et al.*, 2002). Copper and GAGs bind in the same region of PrP, which suggests metals and GAGs may interact with each other as well as with PrP. Therefore, experiments were performed using protein which had been loaded with copper. Previously published work has shown copper-loaded PrP prepared in this manner has an increased β-sheet content compared to PrP prepared in the absence of metals (Wong *et al.*, 2000).

Experiments were performed and analysed as in 5.2.1.1.copper-loaded mPrP(23-231) showed a similarity in the curve of the isotherm (Figure 5.10), as well as the number of heparin binding sites when compared to the no metal mPrP(23-231). As with the wild type, Copper-loaded mPrP(23-231) data fit best to a sequential four-site binding model, with a difference of 8.9% and 25% between three- and five-binding site models

respectively. All data were within 21% error, with log K_a data for copper-loaded mPrP(23-231) compared to the averaged wild type data are summarised in Table 5.1.

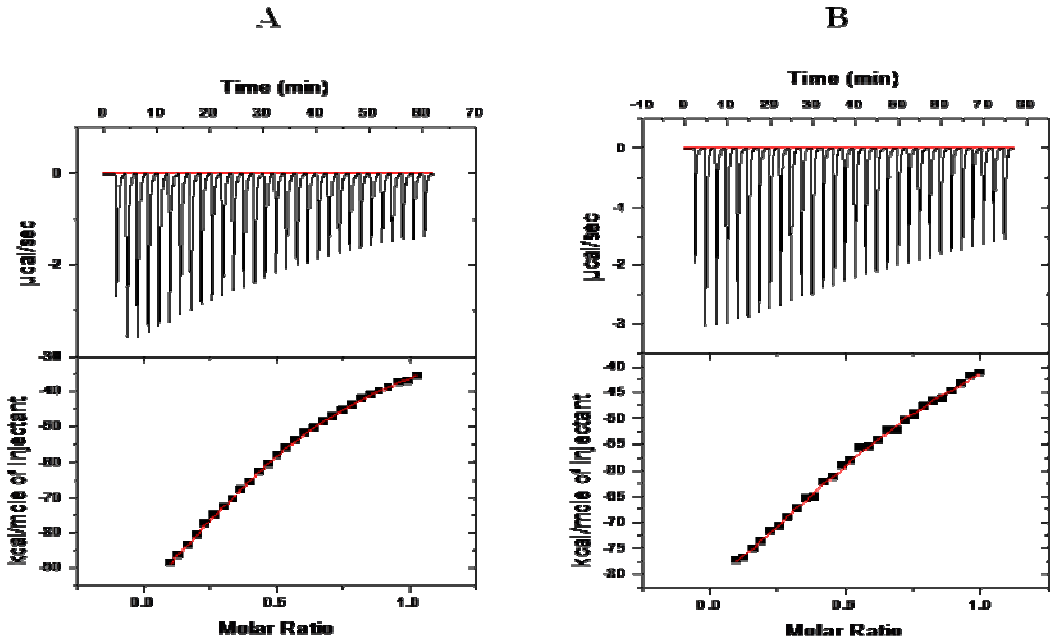

Figure 5.10 Effect of copper on heparin binding to mPrP(23-231). A) mPrP(23-231) without copper (n=8). B) mPrP(23-231) loaded with copper (n=3). All data are presented as blank subtracted energy values plotted against time (top graph) or as a function of the molarity of the system (bottom graph). All experiments were performed at 25°C and pH 7.4.

The affinity values for the first and second binding site in copper-loaded mPrP(23-231) are within the 10-100 micromolar range, and the last site has an affinity in the 1-10 micromolar range. The affinity values are less than those of mPrP(23-231) with no metal bound, which has affinity values within the 10-100 nanomolar range for the higher affinity sites and 1-10 micromolar range for the lower affinity site. These data suggest that when copper is bound to PrP, the protein is still able to interact with GAGs but the interaction is weakened. This is in agreement with previously published studies which show copper does not abolish GAG-PrP binding (Pan *et al.*, 2002; Warner *et al.*, 2002) and with data that indicates copper weakens the heparin-PrP complex (Andreivskaia *et al.*, 2007).

5.2.6 Binding of other glycosaminoglycans to mPrP

PrP has been shown to bind other GAGs as well (Brimacombe *et al.*, 1999; Pan *et al.*, 2002; Warner *et al.*, 2002). Dextran sulphate and in particular high MW dextran sulphate, has been shown to delay the onset of disease symptoms in animals infected with prion disease (Kimberlin and Walker, 1986). It may be that a difference in dextran sulphate and heparin binding to PrP could provide insight as to the contradictory effects of GAGs in prion disease.

ITC binding experiments were performed in at least triplicate as described in 5.2.1.1 except low molecular weight dextran sulphate was used as the ligand.

Unfortunately ITC binding analyses of low-molecular weight dextran sulphate and mPrP(23-231) produced data which proved even more difficult to analyse than that for heparin binding. None of the sequential site binding models would fit the data, so binding models commonly used for pharmaceutical interactions were tested. These more complex models did not fit the data. The same was true with the isotherms from mPrP(H95A+H110A) binding experiments. Representative binding isotherms are shown in Figure 5.13 where, as previously, energy change is plotted as a function of time or system molarity. These data indicate the nature of the interaction of these compounds and mPrP is too complex to be measured by ITC and other methods would need to be used to fully understand these interactions.

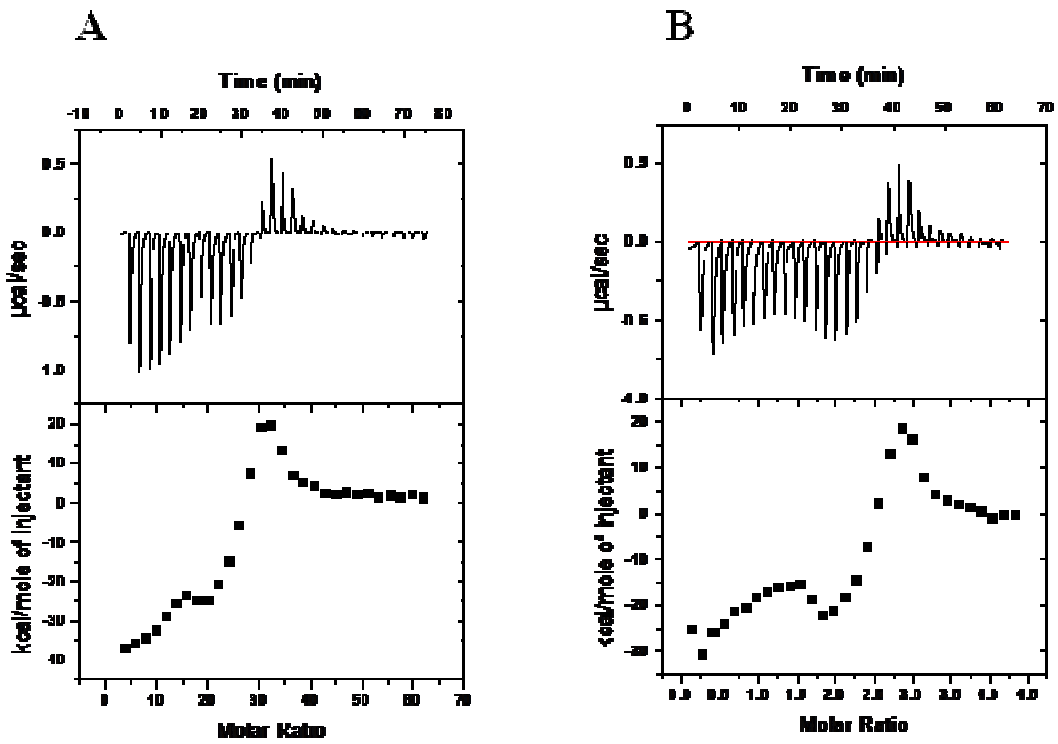

Figure 5.11 Representative ITC isotherms of dextran sulphate binding to mPrP. A) mPrP(23-231). B) mPrP(H95A+H110A). All experiments were performed at 25°C and pH 7.4 and are representative of at least four indepenedent experiments. All data are presented as blank-subtracted energy change as a function of time (top graph) or molarity (bottom graph).

5.3 Heparin and PrP aggregation

Heparin and other GAGs have been shown to stimulate the aggregation of prion proteins (Wong *et al.*, 2001; Deleault *et al.*, 2005; Kajnert *et al.*, 2006; Boshuzien *et al.*, 2007). Therefore the effect heparin had on the aggregation of mPrP constructs with and without specific heparin binding regions was assessed using the aggregation system developed in Chapter 3.

To assess the effect of heparin aggregation of recombinant mPrP(23-231), aggregation reactions were performed as described in 2.4.8 with either 25 µg/mL, 50 µg/mL, 500 µg/mL or 1000 µg/mL heparin sodium sulphate buffered in 10 mM sodium phosphate, pH 7.4. mPrP(23-231) aggregation results show that addition of heparin sulphate to mPrP(23-231) did not significantly affect the linear rate of the aggregation reaction compared to no heparin control (Figure 5.12 B) although there was a trend of increased rate in each experiment. All concentrations of heparin caused an increased trend in the maximum fluorescence achieved during the reaction compared to the no heparin control (Figure 5.12C). Due to variability between the experiments (as discussed

previously in Chapter 4 and probably a result of purification and refolding), statistical analysis was not possible and no significant differences were seen in any reaction with heparin..

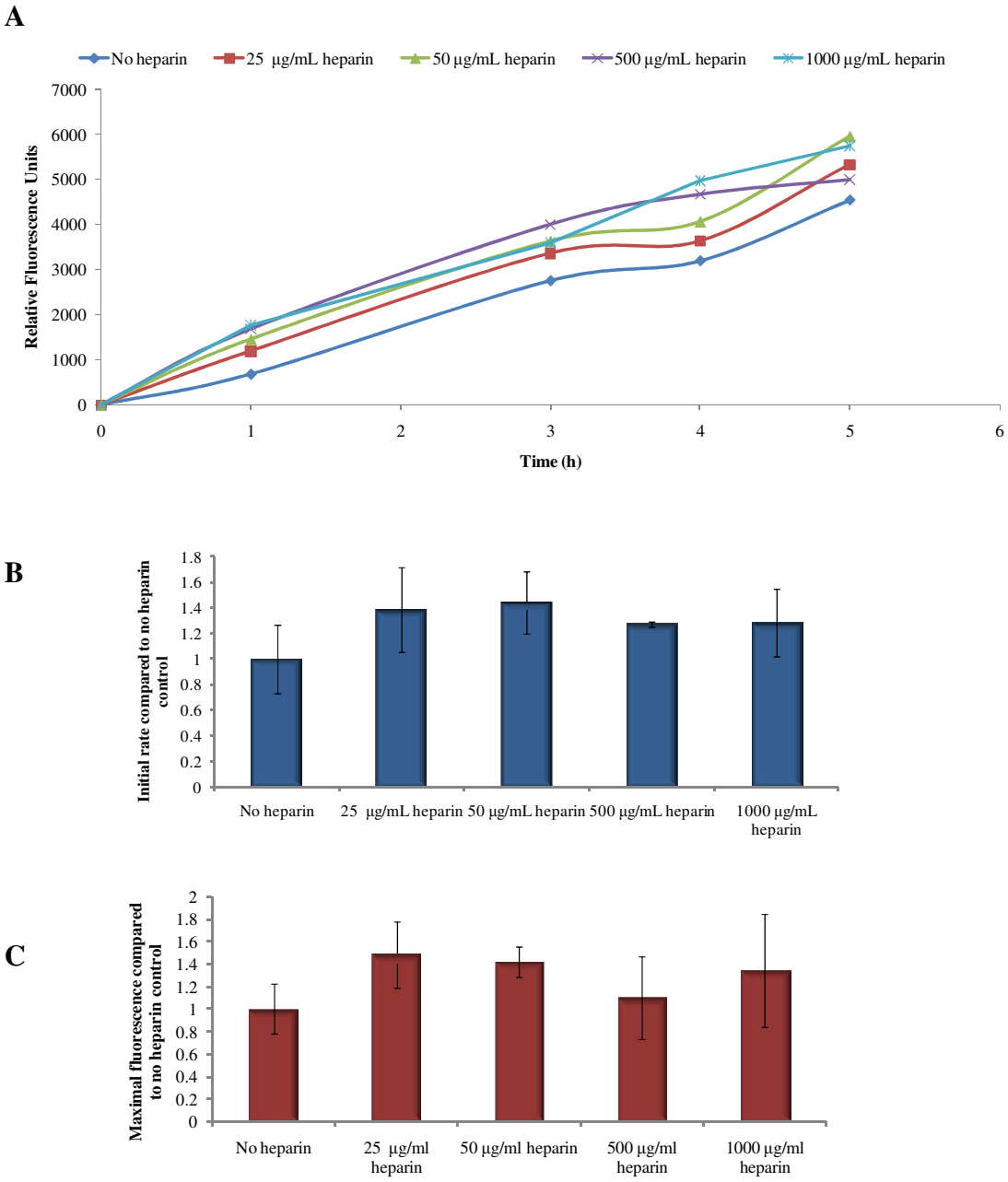

Figure 5.12 Aggregation of mPrP(23-231) with heparin. A) Representative graph showing aggregation of mPrP(23-231) with the addition of various concentrations of heparin. B) Rate of aggregation with heparin compared to no heparin control show no significant differences. C) Maximum fluorescence reached during aggregation reaction with any concentration of heparin is not significant when compared to the no heparin control reactions. Error bars are ±SEM, n=5.

To further assess the effect of heparin on mPrP aggregation, aggregate end products were analysed by Western blots (as in 2.3.13) to determine whether there was any

difference in the end product between heparin added reactions (Figure 5.13). Two anti-PrP antibodies with distinct epitopes (ICSM18, residues 145-154 or 8B4, residues 35-45) were used to help obtain structural information.

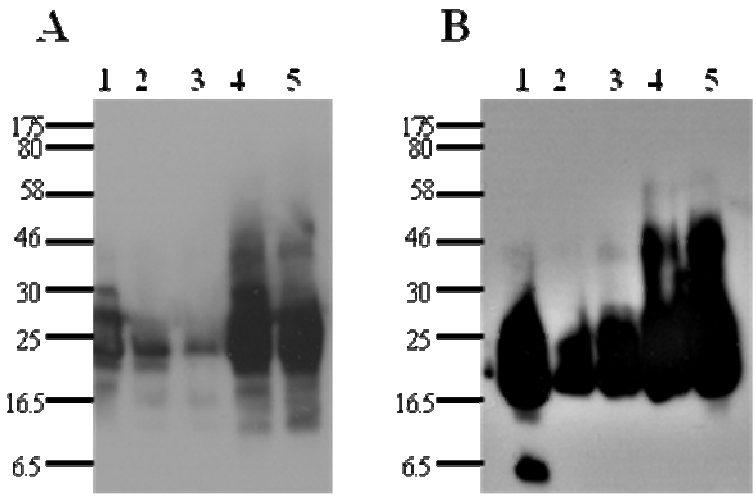

Figure 5.13 Western blots of aggregate end products of mPrP((23-231). A) Western blot with anti-PrP antibody ICSM18. B) Western blot with anti-PrP antibody 8B4. In both blots, lane 1 is aggregate with no heparin added, lane 2 is with 25 µg/mL heparin, lane 3 is with 50 µg/mL heparin, lane 4 is with 500 µg/mL heparin, and lane 5 is with 1000 µg/mL heparin. Markers are in kDa.

Results show there were no very high molecular weight aggregates that would indicate the presence of fibrils. There was no great difference between the heparin and the no heparin control. Some samples with higher concentrations of heparin showed more bands corresponding to higher molecular weight aggregates at ~46kDa, particularly in the Western blots with the C-terminal monoclonal antibody ICSM18. The apparent size makes it likely these fragments correspond to dimers. Smaller PrP fragments (10-12 kDa, as well as, 6.5 kDa) were present.

5.3.1 Deletion and truncation mutations of PrP

Both this work and studies by others shown that heparin binding sites are located within the N-terminus of PrP (Warner *et al.*, 2002; Pan *et al.*, 2002). Therefore the effect of reduced heparin binding sites on mPrP aggregation with heparin was assessed using N-terminal mutations.

As with mPrP(23-231) aggregation, recombinant mPrP(89-231) or mPrP(Δ51-89) was incubated with either 25 µg/mL, 50 µg/mL, 500 µg/mL or 1000 µg/mL heparin sodium sulphate buffered in 10 mM sodium phosphate, pH 7.4. Aggregation reactions were performed and analysed as described in 2.4.8.

Heparin addition did not affect the initial rate of or maximum fluorescence reached of either mPrP(89-231) or mPrP(Δ51-89) aggregation. Unlike mPrP(23-231), no clear trends were seen. mPrP(Δ51-89) rate and maximum fluorescence data is shown as an example (Figure 5.14).

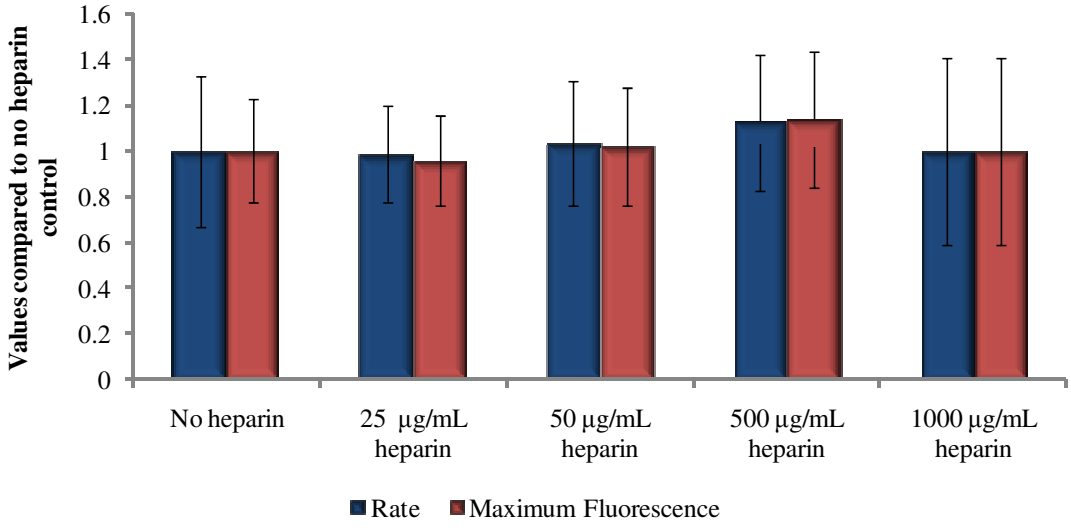

Figure 5.14 Initial rate and maximum fluorescence of mPrP(Δ51-89) aggregation in the presence of varying concentrations of heparin. No significant differences are seen in either protein at any concentration of heparin assessed. All values are compared to the no heparin added control. Error bars are ±SEM, n=3.

5.4 Heparin and cellular prion infection

Experiments have shown endogenous GAGs are required for propagation of prion infection (Horonchik *et al.*, 2005). Experiments wherein cells are treated either with sodium chlorate, an inhibitor of sulphation, or with specific GAG-degrading enzymes fail to become infected when challenged with infection (Horonchik *et al.*, 2005; Ben-Zaken *et al.*, 2003). Reconstitution of infection did not occur when exogenous GAGs were added to these treated cells, indicating the role of GAGs in prion biology is specific to the cells' endogenous population. Additionally, there is evidence that the metabolism of GAGs is in fact disrupted in prion disease (Halimi *et al.*, 2006; Mayer-Sonnenfield *et al.*, 2005) and in cellular infection models ablation of GAG biosynthesis genes reduce the capability of PrP^{Sc} bind to cells (Hijazi *et al.*, 2005). Exogenous heparin sulphate has been shown to enhance infectivity of solubilised PrP27-30, which otherwise showed quite low infectivity (Shaked *et al.*, 2001) further adding evidence to the involvement of GAGs in disease.

The role of heparin sulphate in cellular prion infectivity was examined using the infectivity assay using infectious cell homogenate as devloped in Chapter 3. N2a cells over-expressing pCDNA3.1+-mPrP(1-254), N2a(mPrP), were treated were treated for 24 h with 30 mM sodium chlorate to deplete endogenous GAGs as previously described by Horonchik *et al.* Then, these cells were infected using ScN2aM homogenate at various doses from 1:100, 1:50, 1:25, 1:10 and 1:1 (N2a(mPrP):ScN2a(mPrP)). 25 µg/mL or 100 µg/mL heparin sulphate was added to the cells at the start of the infection incubation periods. Cells were incubated with the exogenous heparin and infectious material for 48 h before being washed three times with PBS. Infection was analysed after 4 passages by cell blot. At least four independent infection experiments were performed.

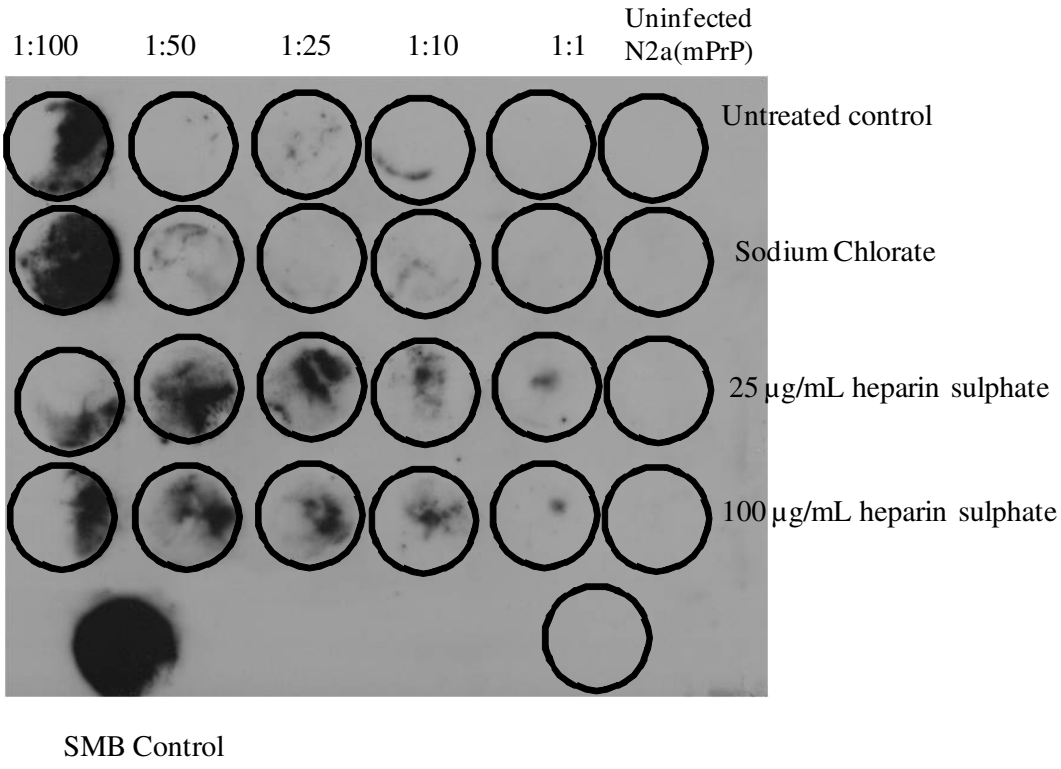

Figure 5.15 Cell blot of infectivity assay of N2a(mPrP) with heparin. Cells were treated with 30 mM sodium chlorate for 24 h to deplete endogenous GAGs and then treated with 25 or 100 µg/mL heparin sulphate for 48 h concurrent with incubation of infectious cell homogenate. The infectious treatment was then removed and cells were washed and propagated for 4 passages before analysis by cell blot.

Results show that sodium chlorate treatment did not inhibit prion infection, as infection was seen at similar infectious doses as the untreated control. However, addition of heparin sulphate increased the susceptibility of N2a(mPrP) to infection by ScN2a(mPrP) cell homogenates, as determined by the presence of PK-resistant material

at a lower infection dose (1:1) than the control (1:10) (Figure 5.15). These results suggest that a low amount of heparin can promote infectivity, in agreement with previously published observations (Shaked *et al.*, 2001).

In order to confirm that the effect on infectivity was not merely due to an effect on heparin on the level of expression in the cells, N2a(mPrP) cells were treated with 30 mM sodium chlorate for 24 h to deplete the endogenous GAGs. Then cells were treated with varying concentrations of heparin sulphate for 48 h and Western blots were performed. PrP^C was quantified by densitometry and normalised to α-tubulin. Results from four independent experiments show there was no significant change in mPrP expression levels in treated cells compared to the non-treated control, although these data are highly variable (Figure 5.16A).

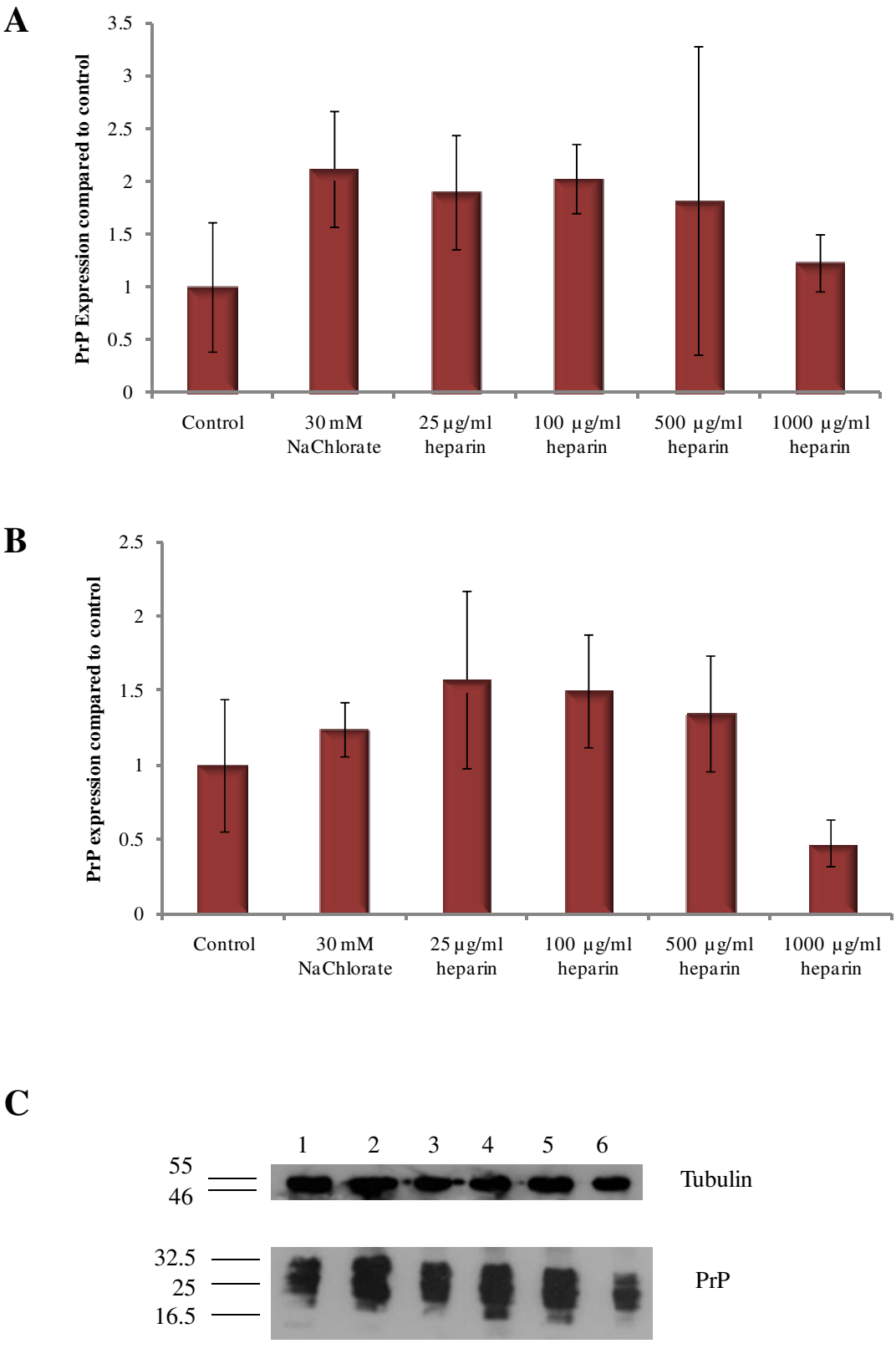

Figure 5.16 Effect of heparin sulphate on PrP^C expression. A) PrP^C expression in N2a(mPrP) cells treated for 24 h with sodium chlorate then 48 h with heparin sulphate. B) N2a cells treated for 24 h with sodium chlorate then 48 h with heparin sulphate. All are ± SEM, n=4. C) Representative Western blots of N2a cells. Lane 1, untreated control; Lane 2, sodium chlorate; Lane 3, 25 µg/mL heparin sulphate; Lane 4, 100 µg/mL heparin sulphate; Lane 5, 500 µg/mL; and Lane 6, 1000 µg/mL heparin sulphate. Markers are in kDa.

These results are in agreement with previously published observations that heparin does not increase PrP^C expression in cells, whereas heparin sulphate (the less sulphated GAG) does (Gabizon *et al.*, 1993). Also, N2a(mPrP) cells over-express PrP^C but the high level PrP expression is under the control of the CMV promoter. The CMV promoter constitutively expresses protein at very high levels in cells, and therefore subtle changes to endogenous PrP^C expression (under the control of the *PRNP* promoter) would not be detected. To confirm PrP^C expression was unchanged by heparin treatment due to the high level of PrP^C expression in N2a(mPrP) cells, expression was also quantified in N2a cells (Figure 5.16 B,C). However, no significant difference was seen.

5.5 Discussion

The presence of GAGs are required for prion infection to occur (Horonchik *et al.*, 2005; Ben-Zaken *et al.*, 2003), thus understanding their role in prion biology is essential.

5.5.1 GAGs and PrP binding

The first way to assess the role of heparin in prion biology is to analyse heparin binding. Heparin binding studies using ITC indicate that mPrP(23-231) binds four heparin molecules. Data from binding studies with mPrP(Δ51-89) and mPrP(89-231) showed three and two binding sites respectively, indicating that at least 2 of those binding sites are located in the N-terminal region encompassing residues 23-90. These data agree with previously published studies indicating the main heparin binding region of PrP is located in the N-terminus of the protein (Warner *et al*., 2002, Pan *et al*, 2002).

Mutation of N-terminal histidines to alanines did not completely abolish heparin binding at pH 7.4. mPrP(Null) heparin binding data best fit a four site model, as with mPrP(23-231), but the results had very different isotherms. This suggests that the ablation of six histidine residues from mPrP affects the nature but not necessarily the number of heparin binding sites. While the overall charge structure has been altered with mPrP(Null), it is probable that other binding regions compensate for the loss of the histidines in the N-terminal region. It has been demonstrated that hydrophobic interactions and hydrogen bonding can also participate in GAG-protein binding.

mPrP(Null) still contains the heparin binding motif KKRPK at residues 23-27, as well as arginine and lysine residues prior to the octameric repeat region which may account for some heparin binding sites. Data from mPrP(Δ51-89) showed that when the

octameric repeats were deleted PrP was still able to bind heparin at three sites, and one of these was a high (1-10 femtomolar range) affinity site. This site is likely to be centred around residues 23-51, which are rich in heparin binding motifs. Truncation of the N-terminus of the protein to residue 89 results in loss of a further heparin binding site, suggesting there are two binding sites located further along the protein. These data indicate that within residues 23-89, the octameric repeat region (residues 51-89) is responsible for one binding site and residues 23-51 comprise the other binding site.

As for the other two binding sites on the protein, they may be located further along the C-terminus(Warner *et al.*, 2002). To determine whether the region around residues 95-110 is involved in heparin binding, experiments were performed with mPrP(H95A+H110A). However this data was problematic and highly variable compared to wild type data. As mentioned in 4.7, this protein proved difficult to purify and also had a high tendency to precipitate prior to and during the experiments. Only limited conclusions can be drawn regarding the data gleaned from these data as the analysis software does not compensate for the thermodynamics of precipitation. Work from this laboratory has shown that mPrP(H95A+H110A) ITC experiments with metals are also highly variable and precipitation is rampant (P. Davies, personal communication and unpublished results). Possibly, different mutants would need to be used to definitely determine where the other heparin binding sites are located on mPrP. Finally, it has been suggested that there is a heparin binding region at residues 185-208 (Klajnert *et al.*, 2006). It is unknown whether this is a major binding site in the wild type protein but it may participate if there is significant alteration to the charge pattern of the N-terminus.

Copper has been reported on different occasions to enhance PrP-GAG binding as well as to weaken it (Gonzalez-Iglesias *et al.*, 2002; Warner *et al.*, 2002; Pan *et al.*, 2002; Andreivskaia *et al.*, 2007). The results obtained with ITC in this chapter demonstrate that PrP with copper already bound has lower binding affinities for heparin than metal-free mPrP. This is in agreement with the results by Andreivskaia *et al.* Copper-loaded mPrP has increased structure within the N-terminal region compared to no metal mPrP (Wong *et al.*, 2000b). This structural difference would affect the nature of the PrP-GAG interaction. There are also possible steric complications due to the presence of copper which could weaken the interaction between mPrP and heparin. To further clarify the relationship between copper and heparin, binding experiments could be performed

where copper is added directly into the binding assay, instead of saturating the copper binding sites as in the ITC experiments.

Overall, the results presented here are a novel method of studying PrP-heparin interactions and the data support previously published data identifying the N-terminal region of the protein as the heparin-binding region (Warner *et al.*, 2002; Pan *et al.*, 2002). These results also confirm the previously published binding affinity for heparin and PrP which is also within the 10-100 nanomolar range (Adreivskaia *et al*, 2007).

5.5.2 GAGs and PrP aggregation

Several studies show that GAGs can stimulate the aggregation of PrP (Gonzalez-Iglesias *et al.*, 2002; Yin *et al.*, 2007; Wong *et al.*, 2001; Bozhuezin *et al.*, 2007; Deleault *et al.*, 2005). The results of this study show that addition of heparin to mPrP aggregation caused a trend of increased initial rate of aggregation and maximum fluorescence compared to the no heparin reaction. Variability, perhaps due to methodology, made statistical analysis difficult. In Chapter 4 it was shown this method produces amorphous β-sheet structures, not fibrils (Figure 5.15). These overall trends suggested by the data also agree with previously published data indicating at neutral pH GAGs stimulate PrP aggregation, although the experiments described were performed with different protein concentrations and at different temperatures (Yu *et al.*, 2008).

The lack of aggregation stimulation by heparin on mPrP(89-231) and mPrP(Δ51-89) could be explained by the reduced number of binding sites available. It is possible that the octameric repeat region is responsible for any stimulatory effect of heparin. This is supported by a study by Yu *et al.*, showing that aggregation of PrP without the octameric repeat region was not stimulated by GAGs, which is in agreement with the data seen in this work.

5.5.3 GAGs and prion infectivity

The interaction between GAGs and prion infectivity is complex. PrP^{Sc} has been shown to bind heparin (Hijazi *et al.*, 2005) and several reports have shown that long-term inhibition of GAG biosynthesis can reduce the amount of PrP^{Sc} in chronically infected cell cultures (Gabizon *et al.*, 1993; Ben-Zaken *et al.*, 2003; Horonchik *et al.*, 2005). It has been shown that heparin sulphate participates in initial PrP^{Sc} binding to cells and a heparinase III-sensitive heparin sulphate compound is required for transfer of prion infectivity (Ben-Zaken *et al.*, 2003; Hijazi *et al.*, 2005; Horonchik *et al.*, 2005). The

infectivity assay results in this study show that sodium chlorate treatment for 24 h does not abolish transfer of prion infectivity. Sodium chlorate is an inhibitor of sulphation and long term treatment has been shown to decrease PrP^{Sc} in infected cells (Gabizon *et al.*, 1993). Despite identical chlorate treatments (30mM for 24 h) the results here are in contrast to observations by Horonchik *et al.,* who saw significant reduction of PrP^{Sc} uptake in chlorate-treated cells (Horonchik *et al.*, 2005). However, there are several methodology differences between the two studies including the cell type, source of prion infection and the length of incubation with the infectious source.

Further results of the infectivity assays showed that addition of exogenous heparin to chlorate-treated cells increases susceptibility of N2a(mPrP) cells to prion infection, and renders cells more susceptible to lower doses of infectivity. Soluble heparan sulphate and chondroitin sulphate (another GAG) have also been shown to increase detectable PrP^{Sc} after chlorate treatment (Ben-Zaken *et al.*, 2003). It has been suggested that cell surface GAGs are required for prion infection to occur, and chlorate treatment inhibits sulphation but does not degrade endogenous GAGs. Therefore there are likely some GAGs still present at the cell surface that act as receptors for PrP^{Sc}. Additionally, heparin can bind PrP^{Sc} which may make the infectious PrP more attractive to internalisation by the cell, as GAGs have also been shown to stimulate internalisation of PrP^{C} (Shyng *et al.*, 1995a; Hijazi *et al.*, 2005).

5.5.4 Future directions

Future work should be undertaken to further identify where heparin binding sites are located on PrP. The precise identification of GAG binding sites on PrP and more profound understanding of their biological relevance may be useful in further development of therapeutics for prion diseases. To fully compare the results presented here, binding experiments with a known heparin-binding protein could be performed to provide a control for these experiments. Many chemically modified GAGs and naturally occurring GAGs are known to decrease PrP^{Sc} and delay disease on set *in vivo* (Ehlers and Diringer, 1984; Kimberlin and Walker, 1986; Ladogana *et al.*, 1992; Gabizon *et al.*, 1993; Caughey and Raymond, 1993; Horonchik *et al.*, 2005; Schonberger *et al.*, 2003; Adjou *et al.*, 2003; Ouidja *et al.*, 2007) and therefore precise binding information and activity of those binding sites in prion infectivity would be instrumental in developing more targeted molecules for possible treatments.

6. Discussion

6.1 Summary of results

In this study the role of metals in scrapie infectivity was assessed by developing a cell culture model using mouse-adapted scrapie as the prion source. The successful model used N2a(mPrP) cells which had been infected by SMB cells (e.g. Sc(N2a(mPrP) cells) as an infectious source and uninfected N2a(mPrP) cells as the target cell line. The role of metals was assessed by using chelated medium to reduce the metal concentrations in the extracellular environment and resulted in cells having a reduced susceptibility to the transfer of prion infectivity. The addition of copper, zinc or manganese to the chelated medium resulted in restoration of infectivity to the control level of prion susceptibility. These results suggest that while metals may play a regulatory role in prion infectivity; the exact role cannot be discerned by these results.

The conversion assay and cell culture infectivity methods were utilised to determine the effect of the glycosaminoglycan heparin in prion protein conversion. First, the nature of PrP and heparin binding was studied using isothermal titration calorimetry, a method which is novel to PrP-heparin interaction study. Results from the ITC experiments confirmed previous reports that PrP binds heparin within the N-terminus of the protein, and that residues 23-90 account for at least two of the binding sites. One of the binding sites comprises residues 23-51 and the other involves the octameric repeat region (resiudes 51-89). Next, the role of heparin in modulating PrP aggregation was studied although the data did showed heparin did not have either a significant inhibitory or promotional effect on mPrP aggregation. In a cellular infection model, addition of exogenous heparin was found to increase the susceptibility of target cells to prion infection.

The results presented in this thesis demonstrate that both metals and GAGs play a role in prion protein conversion. However, further work in this area is needed in order to fully understand how metals and GAGs are involved in aggregation and infection. Possible mechanisms related to aggregated PrP, infection and cell death are discussed in the following sections, along with some suggested future work to help further define the role of metals and GAGs in prion disease.

6.3 PrP aggregates, metals, and glycosaminoglycans

The results of this work show non-fibril aggregates are the products of aggregation assays both with metals and GAG under neutral conditions. Several other groups have studied PrP aggregation under various conditions, and have reported different resulting structures as well as different effects of metal and GAGs on PrP aggregation (Bocharova *et al*., 2005b; Gonzales-Iglesias *et al*., 2002; Wong *et al.*, 2004; Thackray *et al.*, 2004; Giese *et* Qin *et al.*, 2000; Rezaei *et al.*, 2002, 2005; Morrissey and Shakhnovich, 1999; Redecke *et al.*, 2007; Ricchelli *et al.*, 2006). The aggregates shown in this work may represent a normal form of aggregation which under normal cellular circumstances is cleared by protein quality control mechanisms.

Conformational change and oligomerisation of the prion protein have been shown to be produced in response to copper and GAGs (Tsiroulnikov, 2006; Rekecke, 2007; Gonzales-Iglesias *et al*., 2002; Yang *et al.*, 2008; Wong *et al*, 2004). Metals have also been shown to modulate aggregation of and toxic effects of other neurodegenerative disease-related proteins such as tau and α-synuclein (Zhou *et al.*, 2007; Wright *et al.*, 2009). Furthermore, heparin has been shown to bind metals in particular copper and manganese (Parmar *et al.*, 2003) and GAGs are associated with prion plaques (Snow *et al.*, 1989, 1990). Divalent cations have previously been reported to promote GAG-protein complexes (Björk *et al.*, 1989; Renne *et al.*, 2000). Zinc and to a lesser extent copper have been shown to promote heparin binding of amyloid precursor protein (Multhaup *et al.*, 1995; Borza and Morgan, 1998). Possible mechanisms by which metals associate with PrP^{Sc} may include metals binding PrP thereby changing its conformation to a more aggregation-prone structure or heparin binding PrP and similarly affecting aggregation. The metal- or GAG-PrP aggregates could then associate, possibly strengthening the structure, as it has been shown that PrP-GAG complexes are stabilised by the presence of copper (Gonzales-Iglesias *et al.*, 2002). Further work would need to be done in order to determine which scenario is the most likely, and whether the effect metals and/or GAGs have non-fibril aggregates modulates the toxicity or infectious nature of these oligomers.

6.2 Oligomeric PrP, toxicity and infection

The infectious form of PrP has been theorised to be around 50-600 kDa in size (Alper *et al*, 1966; Gabizon *et al*, 1987; Bellinger-Kawahara *et al.*, 1988; Tzaban, 2002; Caughey and Lansbury, 2003). Disassociation of PrP^{Sc} aggregates suggested the most

infectious PrP aggregates were spherical oligomers, 17-27 nm in length and 300-600 kDa in size, corresponding to 14-28 PrP molecule units (Silveira *et al.*, 2005). This has been supported by reports that a pathway producing well-ordered β-oligomers of PrP consist of the equivalent of 25 monomers of PrP (Redecke *et al.*, 2007). Although the size of oligomers can vary depending on the experimental conditions under which they were produced, roughly spherical and globular oligomers are common products of prion misfolding pathways (Lu and Chang, 2002; Rezaei *et al.*, 2005; Vendrely *et al.*, 2005; Redecke *et al.*, 2007). It has been suggested that the formation of smaller oligomeric structures in misfolding pathways are the key components to prion diseases and that these intermediates are in fact the molecule responsible for infection (Morillas *et al.*, 2001; Baskakov *et al.*, 2002; Sokolowski *et al.*, 2003; Govaerts *et al.*, 2004; Weissmann, 1991).

Current research now supports the idea that β-oligomers are not formed on the amyloid fibril pathway but exist in a dynamic state with α-helical monomers (Baskakov *et al.*, 2002; Bocharova *et al.*, 2005a; Teplow *et al.*, 2006; Haass and Selkoe, 2007; El Moustaine *et al.*, 2008; Soto and Estrada, 2008). If this is true, it is important to understand what structures aggregates form under non-denaturing conditions, and how these structures might participate in prion disease. It may be that these aggregates are able to transfer prion infectivity and/or are neurotoxic depending on the stage of the disease.

It has been established that PrP^{Sc} is toxic to cells and that synthetic and recombinant prion protein peptides exhibit neurotoxicity (Forloni *et al.,* 1993; Brown, 2000; Daniels, *et al.*, 2001). More recent evidence indicates that prion oligomers and fibrils, which are both rich in β-sheet content, have been shown to be toxic *in vivo* and *in vitro* (Kazlauskaite *et al.*, 2005; Novitskaya *et al.*, 2006a, 2007; Corsaro *et al.*, 2006; Villa *et al.*, 2006; Chiovitti *et al.*, 2007; Simoneau *et al.*, 2007). The controversy as to whether β-oligomers are more toxic than amyloid fibrils may stem from the fact cells have varied responses to alternative protein conformations. It was shown that β-oligomers induced apoptosis, whereas amyloid fibrils first induce cell aggregation around the fibrils prior to apoptosis (Novitskaya *et al.*, 2006a).

PrP-induced toxicity and prion infection may or may not be mutually exclusive (Chesebro *et al*, 2005; Fioriti *et al.*, 2005). Cells that are persistently prion-infected undergo apoptosis (Schatzl *et al.,* 1997). Evidence suggesting that aggregated PrP

induces apoptosis includes experiements where covalently cross-linked PrP (Solforosi *et al.*, 2004) and β-oligomeric forms of PrP triggered apoptotic cell death (Watzlawik *et al.*, 2006; Demuro *et al.*, 2005). Whether or not aggregated PrP is the sole toxic reagent is unknown. It has been demonstrated that PrP oligomer toxicity may not require PrP^{C} expression, as both ovine and murine PrP β-oligomers cause apoptosis-mediated death even on $PrP^{-/-}$ mice and cell cultures (Simoneau *et al.*, 2007). Additionally, PrP^{C} expression is not required for toxicity of cytosolic PrP, another candidate for the toxic form of PrP (Mironov *et al.*, 2003). In contrast, the use of small interfering RNA for knock-down expression of PrP in cells was shown to reduce the toxicity of both fibrils and oligomers in those cells (Novitskaya *et al.*, 2006). This observation by Novitakaya *et al.* is in agreement with published work that shows endogenous PrP^{C} is necessary for the effect of PrP^{Sc} (Brandner *et al.*, 1996; Blattler *et al.*, 1997). This suggests that oligomer toxicity independent of high levels of PrP^{C} expression could be a mechanism by which widespread neurotoxicity and degeneration occurs, regardless of whether or not PrP oligomers are the transmissible agent.

6.3 Mechanisms of oligomer toxicity and neurodegeneration

Many lines of evidence suggest there is a common toxic mechanism with oligomeric proteins due to shared structural features (Bucciantini *et al*, 2002; Reixach *et al*, 2004). The ability to fold into a β-rich structure is a general property of proteins and is not exclusive to proteins associated with neurodegeneration (Guijarro *et al.*, 1998). Oligomers derived from many different neurodegenerative conditions including Alzheimer's, Parkinson's and Huntington's diseases react to the same oligomer-specific antibody (Hernandez and Avila, 2008; Kayed *et al*., 2003, 2006, 2007; Lafaye, 2009; Moore *et al*., 2009). It has also been shown that oligomers of non-disease related or non-mammalian proteins can cause cell death (Pieri *et al.*, 2006) and even induce neurodegeneration (Vieira *et al.*, 2007). These data suggest that oligomer structure may bestow toxicity that is not in and of itself inherent to the specific protein composition of these oligomers. This commonality regarding oligomer structure and associated toxicity may manifest through similar mechanisms. Several proposed mechanisms are discussed below.

One favoured mechanism suggested for oligomeric mediated toxicity is increased oxidative stress and free radicals within the cell. Oxidative stress may be caused by protein accumulation itself (Behl *et al*., 1994; Hsu *et al*., 2000), and there is evidence

that oxidative damage to RNA occurs at the very early stages of neurodegenerative disease (Nunomura *et al*., 2007; Breusing and Grune, 2008).

Generation of reactive oxygen species can mediate protein folding (Nakomura and Lipton, 2009). Further, gross oxidative stress associated with the presence of oligomers has been demonstrated in several other neurodegenerative disorders and may in fact represent a common pathway of neurodegeneration (Halliwell, 2006; Calabrese *et al*., 2007; Nunomura *et al*., 2009; Petrozzi *et al*., 2007). Oxidative damage has been demonstrated at early stages of Alzheimer's, Parkinson's, and Huntington's disease (Browne and Beal, 2006; Nunomura *et al*., 2001; Wang *et al*., 2006) and it has been shown that oxidative stress increases with ageing (Pratico and Sung, 2004). As many neurodegenerative conditions occur later in life, the corresponding increase in oxidative stress during ageing may be due to increased oligomeric protein load within the cells.

In terms of prion disease, markers of and susceptibility to oxidative stress are increased in prion-afflicted cells and mice (Yun *et al*, 2006; Brazier *et al*., 2006; Freixes *et al*., 2006; Brown and Bessinger, 1998; Milhavet, 2000). In addition, PrP^C and in particular the octameric repeat region can protect against reactive oxygen species-mediated cellular damage (Zeng *et al*., 2003; Watt *et al*, 2007; Malaisé *et al*., 2008; Haigh *et al*., 2009). This suggests that the conformational change which occurs during prion conversion may obliterate the protective effect of PrP^C in regards to oxidative stress in prion disease. Thus, it can be argued that oxidative stress may be a mechanism through which aggregated abnormal forms of PrP enhance cell death.

All things considered, elucidating how metals might contribute to oxidative cell death will provide insight into potential mechanisms of disease progression. Disruptions in brain metal homeostasis, like those observed in prion disease (Wong *et al.*, 2001b; Thackray *et al.*, 2002; Hesketh *et al.*, 2007, 2008) have been shown to increase reactive oxygen species production, possibly through Fenton chemistry-dependent or independent means (Linert, 2006). Aberrant metal homeostasis also may contribute to oxidative damage and toxicity of Aβ oligomers (Maynard *et al*., 2005). It is interesting therefore that aggregates produced from metal-catalysed oxidation have been shown to consist of small stable oligomers (Redecke *et al*., 2007). This suggests that oxidative reactions are permissive to stable oligomer species. Whether high levels of oxidative stress cause the oligomers or oligomers cause oxidative stress has not been proven conclusively. In addition, exposure of recombinant PrP to conditions mimicking those

of oxidative stress resulted in an increase in β-sheet structure, PK resistance, and the ability to act as a seed in aggregation reactions, suggesting oxidative damage could enhance the progression of prion disease (Requena *et al*., 2001, 2004; Dear *et al*., 2008) which would then contribute to activation of apoptosis signalling cascades.

Apart from the well documented phenomenon that the function of the proteasome is impaired during the natural ageing process, an associated hallmark of neurodegenerative disease is proteasome dysfunction due to the presence of aggregated proteins (Carrard *et al.,* 2002; Bennett *et al.,* 2005; Dahlmann 2007) partially due to the fact that the proteasome cannot effectively degrade large amounts of aggregated protein (Verhoef *et al.,* 2002). This suggests that a possible mechanism of oligomer-induced cell death is intracellular accumulation of oligomers saturates the proteasome system thereby initiating apoptosis.

Perhaps the most compelling evidence for the impairment of the ubiquitin-proteasome system as a mechanism of oligomer toxicity comes from the finding that PrP β-oligomers, but not amyloid fibrils, inhibit the activity of the 26S proteasome (Kristiansen *et al.*, 2007). The UPS is involved in turnover of wild type PrP (Yedidia *et al.*, 2001) and it was initially proposed that altered PrP^{C} trafficking impairs the function of the UPS, leading to accumulation of PrP aggregates and apoptosis (Ma and Lindquist, 2001). The function of the UPS is impaired in prion-infected cells, resulting in the accumulation of cytosolic aggresomes containing PrP^{Sc}, ubiquitin, heat shock protein 70, proteasome subunits and other components (Kristiansen *et al.*, 2005). These aggresomes appeared to be neurotoxic and activate caspase 3- and 8-dependent apoptosis (Kristiansen *et al.*, 2005), in agreement with previous demonstrations that caspase 8 is activated in response to aggregates in Huntington's and Alzheimer's diseases (Gervais *et al.*, 2002; Lu *et al.*, 2003). This inhibition was specific only to β-oligomers, as use of oligomer-directed antibodies resulted in an abrogation of the inhibition effect (Kristiansen *et al.*, 2007). Inhibition of UPS activity in response to prion infection was demonstrated using a GFP-reporter system in transgenic mice, thereby demonstrating the impairment of the UPS during prion infection *in vivo* (Kristiansen *et al.*, 2007).

An alternative theory argues that the accumulation of oligomers and aggregates alters endoplasmic reticulum (ER) homeostasis triggering apoptosis by the alteration of ER signalling pathways (Hetz *et al.*, 2007; Hetz and Soto 2006). ER stress has shown to be

caused by changes to structure or function of proteins as well as accumulation of misfolded proteins (Wojda *et al.*, 2008). The resulting aggregation of disease-related proteins can disrupt calcium homeostasis leading to synaptic dysfunction, oxidative stress, and impaired energy metabolism (Marambaud, 2009; Mattson, 2007). ER stress has also been shown to compromise UPS function (Menedez-Benito *et al.*, 2005). Interestingly, oxidative stress has also been shown to cause damage to the 26S proteasome, making it less effective at degrading misfolded or damaged cytosolic protein (Breusing and Grune, 2008). It is very probable that a combination of ER stress, oxidative stress and UPS dysfunction all contribute as mechanisms oligomer-mediated toxicity.

6.4 Future directions and conclusions

Future work could be carried out in order to confirm whether the products from the conversion experiments have any associated toxicity in a cell culture system. Such work should be informed by more detailed structural analysis both for structures formed in the presence and in the absence of metals and heparin. Different structures of oligomers would need to be purified perhaps by size exclusion chromatography or gel filtration. It is likely that conformation of the aggregates formed in the presence of metals is different from those formed in the absence of metals, and the same might be true of heparin. It has been shown that copper binding to the N-terminus of the prion protein can increase the β-sheet content of PrP (Viles *et al.*, 1999; Stockel *et al.*, 1998; Qin *et al.*, 2000). This is also true for manganese binding to PrP (Brown *et al.*, 2000; Abdelraheim *et al.*, 2006; Kim *et al.*, 2005; Brazier *et al.*, 2008). Therefore any effect of metals or heparin seen in PrP aggregation could be due to a binding induced-conformational change within the N-terminus which influences the conformational stability of the C-terminus. This theory is supported by previously published work which has shown that interactions in the N-terminal region of the protein can alter the conformation of the C-terminal region (Thackray *et al.*, 2003; Li, 2000) and that N-terminally PrP aggregation does not undergo as many different pre-amyloid states as full length PrP (Frakenfield *et al.*, 2005). To clarify the role of metals in PrP-GAG interactions, it would be prudent to determine the key region where copper/heparin interaction occurs, whether this is centred around the region 95-110 or whether this interaction occurs within the OR region.

Next, the structure of the sorted oligomers would need to be analysed with EM and potentially more powerful imaging techniques in order to obtain as much information

as possible regarding oligomer structure and toxicity. Once the structure of the aggregates had been thoroughly investigated, the next step would be to expose the products to mammalian cells expressing PrP and also cells which do not express PrP to determine whether the aggregates have any toxic or infectious effect. The toxic effect may or may not be PrP^C dependent, as conflicting studies have shown (Novitskoya *et al.*, 2006; Simoneau *et al.*, 2007; Shiraishi *et al.*, 2009). After determining which structure was responsible for the toxic effect, it would then be interesting to determine whether metals could render the aggregates more toxic, as has been shown in other forms of neurodegenerative disease such as Parkinson's disease (Wright *et al.*, 2009b). It would then follow to determine if heparin or any other GAGs could enhance or ameliorate the toxic effect. This could provide further insight into the normal function of PrP, especially given that both GAG and copper can stimulate internalisation of PrP (Shyng *et al.*, 1995; Pauly and Harris, 1998). Detailed study of the nature of the toxicity elucidating whether it occurs by proteasome dysfunction, increased oxidative stress, increased ER stress, or indeed all three would be necessary to better our understanding neurodegeneration.

Once the structure responsible for toxicity had been identified, further work could be undertaken to determine whether the structures that were toxic also had any transmissibility, i.e. if the structures are able to propagate prion infection. Through the utilization of a cell culture model system, the dependence of prion infection on GAG and metals could be assessed. This could be tested using cells treated with the oligomer structures in assays similar to the one presented in this study, and further confirmed using animal models. This could be extended to include studies looking at the different domains that are required for the effect as well, by using transgenic animals or cells expressing various mutants of mPrP. For clinical applications, it is necessary to understand what part of the protein is required for the potential toxic and/or transmissible effect of oligomeric structures and what role other compounds play in this effect.

Previously published studies showing that metal-bound PrP is able to be extracted from brains of patients with sporadic CJD (Wong *et al.*, 2001b) and that heparan sulphate is found in prion amyloid plaques (Snow *et al*, 1989) dictate the importance of identifying if any similar oligomer species form *in vivo* in diseased brains and whether these species have toxic and or transmissible properties and whether metals or GAGs are associated with those structures. Data from such experiments could potentially resolve

two likely theories – the first stating that oligomers are toxic and thereby contribute to neurodegeneration seen in prion diseases, and the second arguing that oligomers are in fact the transmissible agents. Indeed both scenarios may be true. Whatever the case, the link between PrP oligomers and disease progression needs to be established in order to fully understand how PrP interactions with both metals and GAGs contribute to a disease state.

There are many candidates and arguments for each proposed normal function of the prion protein, elucidation of the normal function of PrP^C is instrumental to understanding prion disease and for any significant contribution that elucidating the role of metals and glycosaminoglycans might have for treatment of the disease. With more detailed understanding of how these compounds interact with and influence the prion protein during its normal cellular activities, we will better be able to understand the mechanisms behind prion pathogenesis and related neurodegenerative disorders. This increased understanding of how these diseases arise and cause neurodegeneration will lead to the development of more effective therapies and treatments, which is all the more pertinent given that greater proportions of the population have been diagnosed with such degenerative conditions. Consequently, the study of prion disease remains a valid field to research in view of its contribution to the understanding of neurodegenerative diseases and effective therapies for their treatment.

This could be done by using further deleted regions such as Δ35-45 and Δ106-126, as well as a further N-terminally truncation mutation such as 113-231 to confirm where binding sites are. This could be done with ITC if an appropriate calculation could be made to allow for any aggregation seen, and confirmed with other binding methods such as 2-dimensional nuclear magnetic resonance, enzyme-linked immunosorbant assay and surface plasmon resonance. Once this has been done it would be interesting to express these mutants in a cell culture infection model, similar to the one in this study but possibly utilising cells with a PrP null background. This could help determine the key heparin binding region responsible for the increased susceptibility to infection seen in section 5.4, and at what minimum heparin concentration is required for the effect. If these experiments were successful it would be very interesting to go on to determine which binding region is responsible for PrP-GAG interaction that clears cells of prion disease/delays onset.

Furthermore as in Chapter 4, it would be interesting to further characterise the aggregates formed in this study with and without heparin, by size-exclusion chromatography and imaging techniques including atomic force microscopy. It would then be interesting to identify whether the non-fibril aggregates produced in the aggregation reactions here had any neurotoxic effects, and if the presence of heparin was able to modulate the toxicity.

To clarify the role of metals in PrP-GAG interactions, it would be prudent to determine the key region where copper/heparin interaction occurs, whether this is centred around the region 95-110 or whether this interaction occurs within the OR region. This could provide further insight into the normal function of PrP, especially given that both GAG and copper can stimulate internalisation of PrP (Shyng *et al.*, 1995; Pauly and Harris, 1998). It would be interesting to potentially discover whether GAG and metals are mutually required for or inhibit each other in prion infection by utilising the appropriate mutants and in a cell culture system background.

References

Abdelraheim, S. R., Kralovicova, S. and Brown, D. R. (2006). Hydrogen peroxide cleavage of the prion protein generates a fragment able to initiate polymerisation of full length prion protein. *International Journal of Biochemistry and Cell Biology*. **38** (1429-1440).

Adjou, K. T., Simoneau, S., Sales, N., Lamoury, F., Dormont, D., Papy-Garcia, D., Barritault, D., Deslys, J. P. and Lasmezas, C. I. (2003). A novel generation of heparan sulfate mimetics for the treatment of prion diseases. *Journal of General Virology*. **84** (2595-2603).

Aguzzi, A. (2004). Understanding the diversity of prions. *Nature Cell Biology.* **6** (290-292).

Alper, T., Cramp, W. A., Haig, D. A. and Clarke, M. C. (1967). Does the agent of scrapie replicate without nucleic acid? *Nature.* **214** (764-766).

Alper, T., Haig, D. A. and Clarke, M. C. (1966). The exceptionally small size of the scrapie agent. *Biochemical and Biophysical Research Communications*. **22** (278-284).

Americo, T. A., Chiarini, L. B. and Linden, R. (2007). Signaling induced by hop/STI-1 depends on endocytosis. *Biochemical and Biophysical Research Communications*. **358** (620-625).

Andreoletti, O., Berthon, P., Marc, D., Sarradin, P., Grosclaude, J., van Keulen, L., Schelcher, F., Elsen, J. M. and Lantier, F. (2000). Early accumulation of PrP(Sc) in gut-associated lymphoid and nervous tissues of susceptible sheep from a Romanov flock with natural scrapie. *Journal of General Virology*. **81** (3115-3126).

Andreoletti, O., Simon, S., Lacroux, C., Morel, N., Tabouret, G., Chabert, A., Lugan, S., Corbiere, F., Ferre, P., Foucras, G., Laude, H., Eychenne, F., Grassi, J. and Schelcher, F. (2004). PrP^{Sc} accumulation in myocytes from sheep incubating natural scrapie. *Nature Medicine.* **10** (591-593).

Andrievskaia, O., Potetinova, Z., Balachandran, A. and Nielsen, K. (2007). Binding of bovine prion protein to heparin: a fluorescence polarization study. *Archives of Biochemistry and Biophysics.* **460** (10-16).

Angers, R. C., Browning, S. R., Seward, T. S., Sigurdson, C. J., Miller, M. W., Hoover, E. A. and Telling, G. C. (2006). Prions in skeletal muscles of deer with chronic wasting disease. *Science*. **311** (1117).

Apetri, A. C. and Surewicz, W. K. (2002). Kinetic intermediate in the folding of human prion protein. *Journal of Biological Chemistry.* **277** (44589-44592).

Apetri, A. C., Surewicz, K. and Surewicz, W. K. (2004). The effect of disease-associated mutations on the folding pathway of human prion protein. *Journal of Biological Chemistry.* **279** (18008-18014).

Apetri, A. C., Vanik, D. L. and Surewicz, W. K. (2005). Polymorphism at residue 129 modulates the conformational conversion of the D178N variant of human prion protein 90-231. *Biochemistry*. **44** (15880-15888).

Archer, F., Bachelin, C., Andreoletti, O., Besnard, N., Perrot, G., Langevin, C., Le Dur, A., Vilette, D., Baron-Van Evercooren, A., Vilotte, J. L. and Laude, H. (2004). Cultured peripheral neuroglial cells are highly permissive to sheep prion infection. *Journal of Virology.* **78** (482-490).

Aronoff-Spencer, E., Burns, C. S., Avdievich, N. I., Gerfen, G. J., Peisach, J., Antholine, W. E., Ball, H. L., Cohen, F. E., Prusiner, S. B. and Millhauser, G. L. (2000). Identification of the Cu2+ binding sites in the N-terminal domain of the prion protein by EPR and CD spectroscopy. *Biochemistry*. **39** (13760-13771).

Ban, T., Hamada, D., Hasegawa, K., Naiki, H. and Goto, Y. (2003). Direct observation of amyloid fibril growth monitored by thioflavin T fluorescence. *Journal of Biological Chemistry.* **278** (16462-16465).

Baron, G. S., Magalhaes, A. C., Prado, M. A. and Caughey, B. (2006). Mouse-adapted scrapie infection of SN56 cells: greater efficiency with microsome-associated versus purified PrP-res. *Journal of Virology.* **80** (2106-2117).

Baskakov, I. V. (2007). Branched chain mechanism of polymerization and ultrastructure of prion protein amyloid fibrils. *FEBS Journal.* **274** (3756-3765).

Baskakov, I. V. and Bocharova, O. V. (2005). *In vitro* conversion of mammalian prion protein into amyloid fibrils displays unusual features. *Biochemistry*. **44** (2339-2348).

Baskakov, I. V., Legname, G., Baldwin, M. A., Prusiner, S. B. and Cohen, F. E. (2002). Pathway complexity of prion protein assembly into amyloid. *Journal of Biological Chemistry.* **277** (21140-21148).

Baskakov, I. V., Legname, G., Prusiner, S. B. and Cohen, F. E. (2001). Folding of prion protein to its native alpha-helical conformation is under kinetic control. *Journal of Biological Chemistry.* **276** (19687-19690).

Basler, K., Oesch, B., Scott, M., Westaway, D., Walchli, M., Groth, D. F., McKinley, M. P., Prusiner, S. B. and Weissmann, C. (1986). Scrapie and cellular PrP isoforms are encoded by the same chromosomal gene. *Cell*. **46** (417-428).

Bedecs, K. (2008). Cell culture models to unravel prion protein function and aberrancies in prion diseases. *Methods in Molecular Biology.* **459** (1-20).

Beekes, M. and McBride, P. A. (2000). Early accumulation of pathological PrP in the enteric nervous system and gut-associated lymphoid tissue of hamsters orally infected with scrapie. *Neuroscience Letters.* **278** (181-184).

Beekes, M. and McBride, P. A. (2007). The spread of prions through the body in naturally acquired transmissible spongiform encephalopathies. *FEBS Journal.* **274** (588-605).

Beekes, M., Baldauf, E. and Diringer, H. (1996). Sequential appearance and accumulation of pathognomonic markers in the central nervous system of hamsters orally infected with scrapie. *Journal of General Virology.* **77** (Pt 8) (1925-1934).

Bellinger-Kawahara, C. G., Kempner, E., Groth, D., Gabizon, R. and Prusiner, S. B. (1988). Scrapie prion liposomes and rods exhibit target sizes of 55,000 Da. *Virology*. **164** (537-541).

Bence, N. F., Sampat, R. M. and Kopito, R. R. (2001). Impairment of the ubiquitin-proteasome system by protein aggregation. *Science*. **292** (1552-1555).

Bennett, E. J., Bence, N. F., Jayakumar, R. and Kopito, R. R. (2005). Global impairment of the ubiquitin-proteasome system by nuclear or cytoplasmic protein aggregates precedes inclusion body formation. *Molecular Cell.* **17** (351-365).

Ben-Zaken, O., Tzaban, S., Tal, Y., Horonchik, L., Esko, J. D., Vlodavsky, I. and Taraboulos, A. (2003). Cellular heparan sulfate participates in the metabolism of prions. *Journal of Biological Chemistry.* **278** (40041-40049).

Birkett, C. R., Hennion, R. M., Bembridge, D. A., Clarke, M. C., Chree, A., Bruce, M. E. and Bostock, C. J. (2001). Scrapie strains maintain biological phenotypes on propagation in a cell line in culture. *EMBO Journal.* **20** (3351-3358).

Bjork, I., Olson, S. T., Sheffer, R. G. and Shore, J. D. (1989). Binding of heparin to human high molecular weight kininogen. *Biochemistry*. **28** (1213-1221).

Blattler, T., Brandner, S., Raeber, A. J., Klein, M. A., Voigtlander, T., Weissmann, C. and Aguzzi, A. (1997). PrP-expressing tissue required for transfer of scrapie infectivity from spleen to brain. **Nature**. *389* (69-73).

Bocharova, O. V., Breydo, L., Parfenov, A. S., Salnikov, V. V. and Baskakov, I. V. (2005a). *In vitro* conversion of full-length mammalian prion protein produces amyloid form with physical properties of PrP(Sc). *Journal of Molecular Biology.* **346** (645-659).

Bocharova, O. V., Breydo, L., Salnikov, V. V. and Baskakov, I. V. (2005b). Copper(II) inhibits *in vitro* conversion of prion protein into amyloid fibrils. *Biochemistry*. **44** (6776-6787).

Bolton, D. C., McKinley, M. P. and Prusiner, S. B. (1982). Identification of a protein that purifies with the scrapie prion. *Science*. **218** (1309-1311).

Borchelt, D. R., Scott, M., Taraboulos, A., Stahl, N. and Prusiner, S. B. (1990). Scrapie and cellular prion proteins differ in their kinetics of synthesis and topology in cultured cells. *Journal of Cell Biology.* **110** (743-752).

Borchelt, D. R., Taraboulos, A. and Prusiner, S. B. (1992). Evidence for synthesis of scrapie prion proteins in the endocytic pathway. *Journal of Biological Chemistry.* **267** (16188-16199).

Borza, D. B. and Morgan, W. T. (1998). Histidine-proline-rich glycoprotein as a plasma pH sensor. Modulation of its interaction with glycosaminoglycans by ph and metals. *Journal of Biological Chemistry.* **273** (5493-5499).

Boshuizen, R. S., Morbin, M., Mazzoleni, G., Tagliavini, F., Meloen, R. H. and Langedijk, J. P. (2007). Polyanion induced fibril growth enables the development of a reproducible assay in solution for the screening of fibril interfering compounds, and the investigation of the prion nucleation site. *Amyloid*. **14** (205-219).

Bosque, P. J. and Prusiner, S. B. (2000). Cultured cell sublines highly susceptible to prion infection. *Journal of Virology.* **74** (4377-4386).

Bosque, P. J., Ryou, C., Telling, G., Peretz, D., Legname, G., DeArmond, S. J. and Prusiner, S. B. (2002). Prions in skeletal muscle. *Proceedings of the National Academy of Sciences of the United States of America.* **99** (3812-3817).

Bossers, A., Belt, P., Raymond, G. J., Caughey, B., de Vries, R. and Smits, M. A. (1997). Scrapie susceptibility-linked polymorphisms modulate the *in vitro* conversion of sheep prion protein to protease-resistant forms. *Proceedings of the National Academy of Sciences of the United States of America.* **94** (4931-4936).

Bossers, A., de Vries, R. and Smits, M. A. (2000). Susceptibility of sheep for scrapie as assessed by *in vitro* conversion of nine naturally occurring variants of PrP. *Journal of Virology.* **74** (1407-1414).

Botto, L., Masserini, M., Cassetti, A. and Palestini, P. (2004). Immunoseparation of Prion protein-enriched domains from other detergent-resistant membrane fractions, isolated from neuronal cells. *FEBS Letters.* **557** (143-147).

Brandner, S., Isenmann, S., Raeber, A., Fischer, M., Sailer, A., Kobayashi, Y., Marino, S., Weissmann, C. and Aguzzi, A. (1996). Normal host prion protein necessary for scrapie-induced neurotoxicity. *Nature*. **379** (339-343).

Brazier, M. W., Davies, P., Player, E., Marken, F., Viles, J. H. and Brown, D. R. (2008). Manganese binding to the prion protein. *Journal of Biological Chemistry.* **283** (12831-12839).

Brazier, M. W., Lewis, V., Ciccotosto, G. D., Klug, G. M., Lawson, V. A., Cappai, R., Ironside, J. W., Masters, C. L., Hill, A. F., White, A. R. and Collins, S. (2006). Correlative studies support lipid peroxidation is linked to PrP(res) propagation as an early primary pathogenic event in prion disease. *Brain Research Bulletin.* **68** (346-354).

Breusing, N. and Grune, T. (2008). Regulation of proteasome-mediated protein degradation during oxidative stress and aging. *Biological Chemistry.* **389** (203-209).

Brimacombe, D. B., Bennett, A. D., Wusteman, F. S., Gill, A. C., Dann, J. C. and Bostock, C. J. (1999). Characterization and polyanion-binding properties of purified recombinant prion protein. *Biochemical Journal.* **342** Pt 3 (605-613).

Brown, D. R. (1999). Prion protein expression aids cellular uptake and veratridine-induced release of copper. *Journal of Neuroscience Research.* **58** (717-725).

Brown, D. R. (2003). Prion protein expression modulates neuronal copper content. *Journal of Neurochemistry.* **87** (377-385).

Brown, D. R. (2004). Role of the prion protein in copper turnover in astrocytes. *Neurobiology of Disease.* **15** (534-543).

Brown, D. R. (2005a). Neurodegeneration and oxidative stress: prion disease results from loss of antioxidant defence. *Folia Neuropathologica.* **43** (229-243).

Brown, D. R. and Besinger, A. (1998). Prion protein expression and superoxide dismutase activity. *Biochemical Journal.* **334** (Pt 2) (423-429).

Brown, D. R., Clive, C. and Haswell, S. J. (2001). Antioxidant activity related to copper binding of native prion protein. *Journal of Neurochemistry.* **76** (69-76).

Brown, D. R., Hafiz, F., Glasssmith, L. L., Wong, B. S., Jones, I. M., Clive, C. and Haswell, S. J. (2000). Consequences of manganese replacement of copper for prion protein function and proteinase resistance. *EMBO Journal.* **19** (1180-1186).

Brown, D. R., Qin, K., Herms, J. W., Madlung, A., Manson, J., Strome, R., Fraser, P. E., Kruck, T., von Bohlen, A., Schulz-Schaeffer, W., Giese, A., Westaway, D. and Kretzschmar, H. (1997). The cellular prion protein binds copper *in vivo*. *Nature*. **390** (684-687).

Brown, D. R., Schmidt, B. and Kretzschmar, H. A. (1996). A neurotoxic prion protein fragment enhances proliferation of microglia but not astrocytes in culture. *Glia*. **18** (59-67).

Brown, D. R., Wong, B. S., Hafiz, F., Clive, C., Haswell, S. J. and Jones, I. M. (1999). Normal prion protein has an activity like that of superoxide dismutase. *Biochemical Journal.* **344** Pt 1 (1-5).

Brown, L. R. and Harris, D. A. (2003). Copper and zinc cause delivery of the prion protein from the plasma membrane to a subset of early endosomes and the Golgi. *Journal of Neurochemistry.* **87** (353-363).

Brown, P. (2005b). Pathogenesis and transfusion risk of transmissible spongiform encephalopathies. *Journal of Developmental Biology.* **120** (27-33).

Browning, S. R., Mason, G. L., Seward, T., Green, M., Eliason, G. A., Mathiason, C., Miller, M. W., Williams, E. S., Hoover, E. and Telling, G. C. (2004). Transmission of prions from mule deer and elk with chronic wasting disease to transgenic mice expressing cervid PrP. *Journal of Virology.* **78** (13345-13350).

Bruce, M. E., McConnell, I., Will, R. G. and Ironside, J. W. (2001). Detection of variant Creutzfeldt-Jakob disease infectivity in extraneural tissues. *Lancet.* **358** (208-209).

Bucciantini, M., Giannoni, E., Chiti, F., Baroni, F., Formigli, L., Zurdo, J., Taddei, N., Ramponi, G., Dobson, C. M. and Stefani, M. (2002). Inherent toxicity of aggregates implies a common mechanism for protein misfolding diseases. *Nature*. **416** (507-511).

Büeler, H., Aguzzi, A., Sailer, A., Greiner, R. A., Autenried, P., Aguet, M. and Weissmann, C. (1993). Mice devoid of PrP are resistant to scrapie. *Cell*. **73** (1339-1347).

Büeler, H., Fischer, M., Lang, Y., Bluethmann, H., Lipp, H. P., DeArmond, S. J., Prusiner, S. B., Aguet, M. and Weissmann, C. (1992). Normal development and behaviour of mice lacking the neuronal cell-surface PrP protein. *Nature*. **356** (577-582).

Büeler, H., Raeber, A., Sailer, A., Fischer, M., Aguzzi, A. and Weissmann, C. (1994). High prion and PrP^{Sc} levels but delayed onset of disease in scrapie-inoculated mice heterozygous for a disrupted PrP gene. *Molecular Medicine.* **1** (19-30).

Bujdoso, R., Burke, D. F. and Thackray, A. M. (2005). Structural differences between allelic variants of the ovine prion protein revealed by molecular dynamics simulations. *Proteins*. **61** (840-849).

Buschmann, A., Pfaff, E., Reifenberg, K., Muller, H. M. and Groschup, M. H. (2000). Detection of cattle-derived BSE prions using transgenic mice overexpressing bovine PrP(C). Archives of Virology, Supplement. **16** (75-86).

Butler, D. A., Scott, M. R., Bockman, J. M., Borchelt, D. R., Taraboulos, A., Hsiao, K. K., Kingsbury, D. T. and Prusiner, S. B. (1988). Scrapie-infected murine neuroblastoma cells produce protease-resistant prion proteins. *Journal of Virology.* **62** (1558-1564).

Calabrese, V., Lodi, R., Tonon, C., D'Agata, V., Sapienza, M., Scapagnini, G., Mangiameli, A., Pennisi, G., Stella, A. M. and Butterfield, D. A. (2005). Oxidative

stress, mitochondrial dysfunction and cellular stress response in Friedreich's ataxia. *Journal of the Neurological Sciences.* **233** (145-162).

Caldwell, E. E., Nadkarni, V. D., Fromm, J. R., Linhardt, R. J. and Weiler, J. M. (1996). Importance of specific amino acids in protein binding sites for heparin and heparan sulfate. *International Journal of Biochemistry and Cell Biology.* **28** (203-216).

Campana, V., Sarnataro, D. and Zurzolo, C. (2005). The highways and byways of prion protein trafficking. *Trends in Cell Biology.* **15** (102-111).

Capila, I. and Linhardt, R. J. (2002). Heparin-protein interactions. *Angewandte Chemie (International Edition English).* **41** (391-412).

Cardin, A. D. and Weintraub, H. J. (1989). Molecular modeling of protein-glycosaminoglycan interactions. *Arteriosclerosis*. **9** (21-32).

Cardone, F., Thomzig, A., Schulz-Schaeffer, W., Valanzano, A., Sbriccoli, M., Abdel-Haq, H., Graziano, S., Pritzkow, S., Puopolo, M., Brown, P., Beekes, M. and Pocchiari, M. (2009). PrPTSE in muscle-associated lymphatic tissue during the preclinical stage of mice infected orally with bovine spongiform encephalopathy. *Journal of General Virology.* **90** (2563-2568).

Carrard, G., Bulteau, A. L., Petropoulos, I. and Friguet, B. (2002). Impairment of proteasome structure and function in aging. *International Journal of Biochemistry and Cell Biology.* **34** (1461-1474).

Cartoni, C., Schinina, M. E., Maras, B., Nonno, R., Vaccari, G., Di Baria, M. A., Conte, M., Liu, Q. G., Lu, M., Cardone, F., Windl, O., Pocchiari, M. and Agrimi, U. (2005). Identification of the pathological prion protein allotypes in scrapie-infected heterozygous bank voles (Clethrionomys glareolus) by high-performance liquid chromatography-mass spectrometry. *Journal of Chromatography A.* **1081** (122-126).

Cashman, N. R., Loertscher, R., Nalbantoglu, J., Shaw, I., Kascsak, R. J., Bolton, D. C. and Bendheim, P. E. (1990). Cellular isoform of the scrapie agent protein participates in lymphocyte activation. *Cell*. **61** (185-192).

Caspi, S., Halimi, M., Yanai, A., Sasson, S. B., Taraboulos, A. and Gabizon, R. (1998). The anti-prion activity of Congo red. Putative mechanism. *Journal of Biological Chemistry.* **273** (3484-3489).

Castilla, J., Saa, P. and Soto, C. (2005). Detection of prions in blood. *Nature Medicine.* **11** (982-985).

Caughey, B. (1991). *In vitro* expression and biosynthesis of prion protein. *Current Topics in Microbiology and Immunology.* **172** (93-107).

Caughey, B. and Lansbury, P. T. (2003). Protofibrils, pores, fibrils, and neurodegeneration: separating the responsible protein aggregates from the innocent bystanders. *Annual Review of Neuroscience.* **26** (267-298).

Caughey, B. and Raymond, G. J. (1991). The scrapie-associated form of PrP is made from a cell surface precursor that is both protease- and phospholipase-sensitive. *Journal of Biological Chemistry.* **266** (18217-18223).

Caughey, B. and Raymond, G. J. (1993). Sulfated polyanion inhibition of scrapie-associated PrP accumulation in cultured cells. *Journal of Virology.* **67** (643-650).

Caughey, B., Ernst, D. and Race, R. E. (1993). Congo red inhibition of scrapie agent replication. *Journal of Virology.* **67** (6270-6272).

Caughey, B., Raymond, G. J., Ernst, D. and Race, R. E. (1991). N-terminal truncation of the scrapie-associated form of PrP by lysosomal protease(s): implications regarding the site of conversion of PrP to the protease-resistant state. *Journal of Virology.* **65** (6597-6603).

Caughey, B., Raymond, G. J., Kocisko, D. A. and Lansbury, P. T., Jr. (1997). Scrapie infectivity correlates with converting activity, protease resistance, and aggregation of scrapie-associated prion protein in guanidine denaturation studies. *Journal of Virology.* **71** (4107-4110).

Cereghetti, G. M., Schweiger, A., Glockshuber, R. and Van Doorslaer, S. (2001). Electron paramagnetic resonance evidence for binding of Cu(2+) to the C-terminal domain of the murine prion protein. *Biophysical Journal.* **81** (516-525).

Cervenakova, L., Goldfarb, L. G., Garruto, R., Lee, H. S., Gajdusek, D. C. and Brown, P. (1998). Phenotype-genotype studies in kuru: implications for new variant Creutzfeldt-Jakob disease. *Proceedings of the National Academy of Sciences of the United States of America.* **95** (13239-13241).

Chakrabarti, O. and Hegde, R. S. (2009). Functional depletion of mahogunin by cytosolically exposed prion protein contributes to neurodegeneration. *Cell*. **137** (1136-1147).

Chakrabarti, O., Ashok, A. and Hegde, R. S. (2009). Prion protein biosynthesis and its emerging role in neurodegeneration. *Trends in Biochemical Sciences.* **34** (287-295).

Chandler, R. L. (1961). Encephalopathy in mice produced by inoculation with scrapie brain material. *Lancet.* **1** (1378-1379).

Chandler, R. L. and Turfrey, B. A. (1972). Inoculation of voles, Chinese hamsters, gerbils and guinea-pigs with scrapie brain material. *Research in Veterinary Science.* **13** (219-224).

Chattopadhyay, M., Walter, E. D., Newell, D. J., Jackson, P. J., Aronoff-Spencer, E., Peisach, J., Gerfen, G. J., Bennett, B., Antholine, W. E. and Millhauser, G. L. (2005). The octarepeat domain of the prion protein binds Cu(II) with three distinct coordination modes at pH 7.4. *Journal of the American Chemical Society.* **127** (12647-12656).

Chen, S., Mange, A., Dong, L., Lehmann, S. and Schachner, M. (2003). Prion protein as trans-interacting partner for neurons is involved in neurite outgrowth and neuronal survival. *Molecular and Cellular Neurosciences.* **22** (227-233).

Chesebro, B., Race, R., Wehrly, K., Nishio, J., Bloom, M., Lechner, D., Bergstrom, S., Robbins, K., Mayer, L., Keith, J. M. and *et al*. (1985). Identification of scrapie prion protein-specific mRNA in scrapie-infected and uninfected brain. *Nature.* **315** (331-333).

Clarke, A. R., Jackson, G. S. and Collinge, J. (2001). The molecular biology of prion propagation. Philosophical Transactions of the Royal Society of London. *Series B: Biological Sciences.* **356** (185-195).

Clarke, M. C. and Haig, D. A. (1970). Evidence for the multiplication of scrapie agent in cell culture. *Nature.* **225** (100-101).

Cobb, N. J., Sonnichsen, F. D., McHaourab, H. and Surewicz, W. K. (2007). Molecular architecture of human prion protein amyloid: a parallel, in-register beta-structure. *Proceedings of the National Academy of Sciences of the United States of America.* **104** (18946-18951).

Cohen, F. E., Pan, K. M., Huang, Z., Baldwin, M., Fletterick, R. J. and Prusiner, S. B. (1994). Structural clues to prion replication. *Science*. **264** (530-531).

Colby, D. W., Zhang, Q., Wang, S., Groth, D., Legname, G., Riesner, D. and Prusiner, S. B. (2007). Prion detection by an amyloid seeding assay. *Proceedings of the National Academy of Sciences of the United States of America.* **104** (20914-20919).

Collinge, J. (2001). Prion diseases of humans and animals: their causes and molecular basis. *Annual Review of Neuroscience.* **24** (519-550).

Collinge, J. and Clarke, A. R. (2007). A general model of prion strains and their pathogenicity. *Science*. **318** (930-936).

Collinge, J. and Palmer, M. S. (1994). Human prion diseases. *Baillieres Clinical Neurology.* **3** (241-247).

Collinge, J., Palmer, M. S. and Dryden, A. J. (1991). Genetic predisposition to iatrogenic Creutzfeldt-Jakob disease. *Lancet*. **337** (1441-1442).

Collinge, J., Palmer, M. S., Sidle, K. C., Gowland, I., Medori, R., Ironside, J. and Lantos, P. (1995). Transmission of fatal familial insomnia to laboratory animals. *Lancet*. **346** (569-570).

Collinge, J., Sidle, K. C., Meads, J., Ironside, J. and Hill, A. F. (1996). Molecular analysis of prion strain variation and the aetiology of 'new variant' CJD. *Nature*. **383** (685-690).

Collins, S., McLean, C. A. and Masters, C. L. (2001). Gerstmann-Straussler-Scheinker syndrome,fatal familial insomnia, and kuru: a review of these less common human transmissible spongiform encephalopathies. *Journal of Clinical Neuroscience.* **8** (387-397).

Corsaro, A., Paludi, D., Villa, V., D'Arrigo, C., Chiovitti, K., Thellung, S., Russo, C., Di Cola, D., Ballerini, P., Patrone, E., Schettini, G., Aceto, A. and Florio, T. (2006). Conformation dependent pro-apoptotic activity of the recombinant human prion protein fragment 90-231. *Int J Immunopathol Pharmacol.* **19** (339-356).

Cronier, S., Laude, H. and Peyrin, J. M. (2004). Prions can infect primary cultured neurons and astrocytes and promote neuronal cell death. *Proceedings of the National Academy of Sciences of the United States of America.* **101** (12271-12276).

Cui, T., Holme, A., Sassoon, J. and Brown, D. R. (2003). Analysis of doppel protein toxicity. *Molecular and Cellular Neurosciences.* **23** (144-155).

Dahlmann, B. (2007). Role of proteasomes in disease. *BMC Biochemistry.* **8** Suppl 1 (S3).

Davies, P. and Brown, D. R. (2008). The chemistry of copper binding to PrP: is there sufficient evidence to elucidate a role for copper in protein function? *Biochemical Journal.* **410** (237-244).

Davies, P., Marken, F., Salter, S. and Brown, D. R. (2009). Thermodynamic and voltammetric characterization of the metal binding to the prion protein: insights into pH dependence and redox chemistry. *Biochemistry.* **48** (2610-2619).

del Pino, P., Weiss, A., Bertsch, U., Renner, C., Mentler, M., Grantner, K., Fiorino, F., Meyer-Klaucke, W., Moroder, L., Kretzschmar, H. A. and Parak, F. G. (2007). The configuration of the Cu2+ binding region in full-length human prion protein. *European Biophysics Journal.* **36** (239-252).

Deleault, N. R., Geoghegan, J. C., Nishina, K., Kascsak, R., Williamson, R. A. and Supattapone, S. (2005). Protease-resistant prion protein amplification reconstituted with partially purified substrates and synthetic polyanions. *Journal of Biological Chemistry.* **280** (26873-26879).

Demuro, A., Mina, E., Kayed, R., Milton, S. C., Parker, I. and Glabe, C. G. (2005). Calcium dysregulation and membrane disruption as a ubiquitous neurotoxic mechanism of soluble amyloid oligomers. *Journal of Biological Chemistry.* **280** (17294-17300).

Dima, R. I. and Thirumalai, D. (2002). Exploring the propensities of helices in PrP(C) to form beta sheet using NMR structures and sequence alignments. *Biophysical Journal.* **83** (1268-1280).

Dima, R. I. and Thirumalai, D. (2004). Probing the instabilities in the dynamics of helical fragments from mouse PrP^{C}. *Proceedings of the National Academy of Sciences of the United States of America.* **101** (15335-15340).

Dlakic, W. M., Grigg, E. and Bessen, R. A. (2007). Prion infection of muscle cells *in vitro*. *Journal of Virology.* **81** (4615-4624).

Donne, D. G., Viles, J. H., Groth, D., Mehlhorn, I., James, T. L., Cohen, F. E., Prusiner, S. B., Wright, P. E. and Dyson, H. J. (1997). Structure of the recombinant full-length hamster prion protein PrP(29-231): the N terminus is highly flexible. *Proceedings of the National Academy of Sciences of the United States of America.* **94** (13452-13457).

Ehlers, B. and Diringer, H. (1984). Dextran sulphate 500 delays and prevents mouse scrapie by impairment of agent replication in spleen. *Journal of General Virology*. **65** (1325-1330).

El Moustaine, D., Perrier, V., Smeller, L., Lange, R. and Torrent, J. (2008). Full-length prion protein aggregates to amyloid fibrils and spherical particles by distinct pathways. *FEBS Journal.* **275** (2021-2031).

Elhammer, A. and Kornfeld, S. (1986). Purification and characterization of UDP-N-acetylgalactosamine: polypeptide N-acetylgalactosaminyltransferase from bovine colostrum and murine lymphoma BW5147 cells. *Journal of Biological Chemistry.* **261** (5249-5255).

Enari, M., Flechsig, E. and Weissmann, C. (2001). Scrapie prion protein accumulation by scrapie-infected neuroblastoma cells abrogated by exposure to a prion protein antibody. *Proceedings of the National Academy of Sciences of the United States of America.* **98** (9295-9299).

Endo, T., Groth, D., Prusiner, S. B. and Kobata, A. (1989). Diversity of oligosaccharide structures linked to asparagines of the scrapie prion protein. *Biochemistry.* **28** (8380-8388).

Espinosa, J. C., Morales, M., Castilla, J., Rogers, M. and Torres, J. M. (2007). Progression of prion infectivity in asymptomatic cattle after oral bovine spongiform encephalopathy challenge. *Journal of General Virology.* **88** (1379-1383).

Fernaeus, S. and Land, T. (2005a). Increased iron-induced oxidative stress and toxicity in scrapie-infected neuroblastoma cells. *Neuroscience Letters.* **382** (217-220).

Fernaeus, S., Halldin, J., Bedecs, K. and Land, T. (2005b). Changed iron regulation in scrapie-infected neuroblastoma cells. *Brain Research. Molecular Brain Research*. **133** (266-273).

Fernandez-Escamilla, A. M., Rousseau, F., Schymkowitz, J. and Serrano, L. (2004). Prediction of sequence-dependent and mutational effects on the aggregation of peptides and proteins. *Nature Biotechnology.* **22** (1302-1306).

Fischer, M., Rulicke, T., Raeber, A., Sailer, A., Moser, M., Oesch, B., Brandner, S., Aguzzi, A. and Weissmann, C. (1996). Prion protein (PrP) with amino-proximal deletions restoring susceptibility of PrP knockout mice to scrapie. *EMBO Journal.* **15** (1255-1264).

Fitzmaurice, T. J., Burke, D. F., Hopkins, L., Yang, S., Yu, S., Sy, M. S., Thackray, A. M. and Bujdoso, R. (2008). The stability and aggregation of ovine prion protein associated with classical and atypical scrapie correlates with the ease of unwinding of helix-2. *Biochemical Journal.* **409** (367-375).

Follet, J., Lemaire-Vieille, C., Blanquet-Grossard, F., Podevin-Dimster, V., Lehmann, S., Chauvin, J. P., Decavel, J. P., Varea, R., Grassi, J., Fontes, M. and Cesbron, J. Y. (2002). PrP expression and replication by Schwann cells: implications in prion spreading. *Journal of Virology.* **76** (2434-2439).

Forloni, G., Angeretti, N., Chiesa, R., Monzani, E., Salmona, M., Bugiani, O. and Tagliavini, F. (1993). Neurotoxicity of a prion protein fragment. *Nature.* **362** (543-546).

Forloni, G., Bugiani, O., Tagliavini, F. and Salmona, M. (1996). Apoptosis-mediated neurotoxicity induced by beta-amyloid and PrP fragments. *Molecular and Chemical Neuropathology.* **28** (163-171).

Frankenfield, K. N., Powers, E. T. and Kelly, J. W. (2005). Influence of the N-terminal domain on the aggregation properties of the prion protein. *Protein Science.* **14** (2154-2166).

Freixes, M., Rodriguez, A., Dalfo, E. and Ferrer, I. (2006). Oxidation, glycoxidation, lipoxidation, nitration, and responses to oxidative stress in the cerebral cortex in Creutzfeldt-Jakob disease. *Neurobiology of Aging.* **27** (1807-1815).

Frid, P., Anisimov, S. V. and Popovic, N. (2007). Congo red and protein aggregation in neurodegenerative diseases. *Brain Research Reviews.* **53** (135-160).

Fromm, J. R., Hileman, R. E., Caldwell, E. E., Weiler, J. M. and Linhardt, R. J. (1997). Pattern and spacing of basic amino acids in heparin binding sites. *Archives of Biochemistry and Biophysics.* **343** (92-100).

Gabizon, R., McKinley, M. P. and Prusiner, S. B. (1987). Purified prion proteins and scrapie infectivity copartition into liposomes. *Proceedings of the National Academy of Sciences of the United States of America.* **84** (4017-4021).

Gabizon, R., Meiner, Z., Halimi, M. and Ben-Sasson, S. A. (1993). Heparin-like molecules bind differentially to prion-proteins and change their intracellular metabolic fate. *Journal of Cellular Physiology.* **157** (319-325).

Gajdusek, D. C. (1977). Unconventional viruses and the origin and disappearance of kuru. *Science.* **197** (943-960).

Gajdusek, D. C. and Zigas, V. (1957). Degenerative disease of the central nervous system in New Guinea; the endemic occurrence of kuru in the native population. *New England Journal of Medicine.* **257** (974-978).

Gasteiger E., Gattiker A., Hoogland C., Ivanyi I., Appel R.D., Bairoch A. (2003) ExPASy: the proteomics server for in-depth protein knowledge and analysis Nucleic Acids Research **31** (3784-3788).

Georgsson, G., Tryggvason, T., Jonasdottir, A. D., Gudmundsson, S. and Thorgeirsdottir, S. (2006). Polymorphism of PRNP codons in the normal Icelandic population. *Acta Neurologica Scandinavica.* **113** (419-425).

Gervais, F. G., Singaraja, R., Xanthoudakis, S., Gutekunst, C. A., Leavitt, B. R., Metzler, M., Hackam, A. S., Tam, J., Vaillancourt, J. P., Houtzager, V., Rasper, D. M., Roy, S., Hayden, M. R. and Nicholson, D. W. (2002). Recruitment and activation of caspase-8 by the Huntingtin-interacting protein Hip-1 and a novel partner Hippi. *Nature Cell Biology.* **4** (95-105).

Ghaemmaghami, S., Phuan, P. W., Perkins, B., Ullman, J., May, B. C., Cohen, F. E. and Prusiner, S. B. (2007). Cell division modulates prion accumulation in cultured cells. *Proceedings of the National Academy of Sciences of the United States of America.* **104** (17971-17976).

Giese, A., Levin, J., Bertsch, U. and Kretzschmar, H. (2004). Effect of metal ions on de novo aggregation of full-length prion protein. *Biochemical and Biophysical Research Communications.* **320** (1240-1246).

Gilch, S., Winklhofer, K. F., Groschup, M. H., Nunziante, M., Lucassen, R., Spielhaupter, C., Muranyi, W., Riesner, D., Tatzelt, J. and Schatzl, H. M. (2001). Intracellular re-routing of prion protein prevents propagation of PrP(Sc) and delays onset of prion disease. *EMBO Journal.* **20** (3957-3966).

Giorgi, A., Di Francesco, L., Principe, S., Mignogna, G., Sennels, L., Mancone, C., Alonzi, T., Sbriccoli, M., De Pascalis, A., Rappsilber, J., Cardone, F., Pocchiari, M., Maras, B. and Schinina, M. E. (2009). Proteomic profiling of PrP27-30-enriched preparations extracted from the brain of hamsters with experimental scrapie. *Proteomics.* **9** (3802-3814).

Glatzel, M. and Aguzzi, A. (2000). Peripheral pathogenesis of prion diseases. *Microbes and Infection.* **2** (613-619).

Goehler, L. E., Gaykema, R. P., Nguyen, K. T., Lee, J. E., Tilders, F. J., Maier, S. F. and Watkins, L. R. (1999). Interleukin-1beta in immune cells of the abdominal vagus nerve: a link between the immune and nervous systems? *Journal of Neuroscience.* **19** (2799-2806).

Goggin, K., Bissonnette, C., Grenier, C., Volkov, L. and Roucou, X. (2007). Aggregation of cellular prion protein is initiated by proximity-induced dimerization. *Journal of Neurochemistry.* **102** (1195-1205).

Goldmann, W. (1993). PrP gene and its association with spongiform encephalopathies. *British Medical Bulletin.* **49** (839-859).

Gonzalez-Iglesias, R., Pajares, M. A., Ocal, C., Espinosa, J. C., Oesch, B. and Gasset, M. (2002). Prion protein interaction with glycosaminoglycan occurs with the formation of oligomeric complexes stabilized by Cu(II) bridges. *Journal of Molecular Biology.* **319** (527-540).

Govaerts, C., Wille, H., Prusiner, S. B. and Cohen, F. E. (2004). Evidence for assembly of prions with left-handed beta-helices into trimers. *Proceedings of the National Academy of Sciences of the United States of America.* **101** (8342-8347).

Graner, E., Mercadante, A. F., Zanata, S. M., Forlenza, O. V., Cabral, A. L., Veiga, S. S., Juliano, M. A., Roesler, R., Walz, R., Minetti, A., Izquierdo, I., Martins, V. R. and Brentani, R. R. (2000a). Cellular prion protein binds laminin and mediates neuritogenesis. *Brain Research. Molecular Brain Research.* **76** (85-92).

Graner, E., Mercadante, A. F., Zanata, S. M., Martins, V. R., Jay, D. G. and Brentani, R. R. (2000b). Laminin-induced PC-12 cell differentiation is inhibited following laser inactivation of cellular prion protein. *FEBS Letters.* **482** (257-260).

Gregori, L., Kovacs, G. G., Alexeeva, I., Budka, H. and Rohwer, R. G. (2008). Excretion of transmissible spongiform encephalopathy infectivity in urine. *Emerging Infectious Diseases.* **14** (1406-1412).

Griffith, J. S. (1967). Self-replication and scrapie. *Nature.* **215** (1043-1044).

Groenning, M., Norrman, M., Flink, J. M., van de Weert, M., Bukrinsky, J. T., Schluckebier, G. and Frokjaer, S. (2007a). Binding mode of Thioflavin T in insulin amyloid fibrils. *Journal of Structural Biology.* **159** (483-497).

Groenning, M., Olsen, L., van de Weert, M., Flink, J. M., Frokjaer, S. and Jorgensen, F. S. (2007b). Study on the binding of Thioflavin T to beta-sheet-rich and non-beta-sheet cavities. *Journal of Structural Biology.* **158** (358-369).

Guentchev, M., Siedlak, S. L., Jarius, C., Tagliavini, F., Castellani, R. J., Perry, G., Smith, M. A. and Budka, H. (2002). Oxidative damage to nucleic acids in human prion disease. *Neurobiology of Disease.* **9** (275-281).

Guijarro, J. I., Sunde, M., Jones, J. A., Campbell, I. D. and Dobson, C. M. (1998). Amyloid fibril formation by an SH3 domain. *Proceedings of the National Academy of Sciences of the United States of America.* **95** (4224-4228).

Guo, Y., Smith, K., Lee, J., Thiele, D. J. and Petris, M. J. (2004). Identification of methionine-rich clusters that regulate copper-stimulated endocytosis of the human Ctr1 copper transporter. *Journal of Biological Chemistry.* **279** (17428-17433).

Haass, C. and Selkoe, D. J. (2007). Soluble protein oligomers in neurodegeneration: lessons from the Alzheimer's amyloid beta-peptide. *Nature Reviews Molecular Cell Biology.* **8** (101-112).

Hadlow, W. J., Kennedy, R. C. and Race, R. E. (1982). Natural infection of Suffolk sheep with scrapie virus. *Journal of Infectious Diseases.* **146** (657-664).

Haig, D. A. and Clarke, M. C. (1968). The effect of beta-propiolactone on the scrapie agent. *Journal of General Virology.* **3** (281-283).

Haigh, C. L., Edwards, K. and Brown, D. R. (2005). Copper binding is the governing determinant of prion protein turnover. *Molecular and Cellular Neurosciences.* **30** (186-196).

Haigh, C. L., Lewis, V. A., Vella, L. J., Masters, C. L., Hill, A. F., Lawson, V. A. and Collins, S. J. (2009). PrP^{C} -related signal transduction is influenced by copper, membrane integrity and the alpha cleavage site. *Cell Research.* **19** (1062-1078).

Haik, S., Faucheux, B. A., Sazdovitch, V., Privat, N., Kemeny, J. L., Perret-Liaudet, A. and Hauw, J. J. (2003). The sympathetic nervous system is involved in variant Creutzfeldt-Jakob disease. *Nature Medicine.* **9** (1121-1123).

Halliwell, B. (2006). Proteasomal dysfunction: a common feature of neurodegenerative diseases? Implications for the environmental origins of neurodegeneration. *Antioxid Redox Signal*. **8** (2007-2019).

Haraguchi, T., Fisher, S., Olofsson, S., Endo, T., Groth, D., Tarentino, A., Borchelt, D. R., Teplow, D., Hood, L., Burlingame, A. and *et al*. (1989). Asparagine-linked glycosylation of the scrapie and cellular prion proteins. *Archives of Biochemistry and Biophysics.* **274** (1-13).

Harper, J. D. and Lansbury, P. T., Jr. (1997). Models of amyloid seeding in Alzheimer's disease and scrapie: mechanistic truths and physiological consequences of the time-dependent solubility of amyloid proteins. *Annual Review of Biochemistry.* **66** (385-407).

Harrison, P. M., Bamborough, P., Daggett, V., Prusiner, S. B. and Cohen, F. E. (1997). The prion folding problem. *Current Opinion in Structural Biology.* **7** (53-59).

Herms, J., Tings, T., Gall, S., Madlung, A., Giese, A., Siebert, H., Schurmann, P., Windl, O., Brose, N. and Kretzschmar, H. (1999). Evidence of presynaptic location and function of the prion protein. *Journal of Neuroscience.* **19** (8866-8875).

Hernandez, F. and Avila, J. (2008). Tau aggregates and tau pathology. *Journal of Alzheimer's Disease.* **14** (449-452).

Hesketh, S., Sassoon, J., Knight, R. and Brown, D. R. (2008). Elevated manganese levels in blood and CNS in human prion disease. *Molecular and Cellular Neurosciences.* **37** (590-598).

Hesketh, S., Sassoon, J., Knight, R., Hopkins, J. and Brown, D. R. (2007). Elevated manganese levels in blood and central nervous system occur before onset of clinical signs in scrapie and bovine spongiform encephalopathy. *Journal of Animal Science.* **85** (1596-1609).

Hetz, C. A. and Soto, C. (2006). Stressing out the ER: a role of the unfolded protein response in prion-related disorders. *Current Molecular Medicine.* **6** (37-43).

Hetz, C., Castilla, J. and Soto, C. (2007). Perturbation of endoplasmic reticulum homeostasis facilitates prion replication. *Journal of Biological Chemistry.* **282** (12725-12733).

Hetz, C., Russelakis-Carneiro, M., Maundrell, K., Castilla, J. and Soto, C. (2003). Caspase-12 and endoplasmic reticulum stress mediate neurotoxicity of pathological prion protein. *EMBO Journal.* **22** (5435-5445).

Hijazi, N., Kariv-Inbal, Z., Gasset, M. and Gabizon, R. (2005). PrP^{Sc} incorporation to cells requires endogenous glycosaminoglycan expression. *Journal of Biological Chemistry.* **280** (17057-17061).

Hijazi, N., Shaked, Y., Rosenmann, H., Ben-Hur, T. and Gabizon, R. (2003). Copper binding to PrP^{C} may inhibit prion disease propagation. *Brain Research.* **993** (192-200).

Hill, A. F., Butterworth, R. J., Joiner, S., Jackson, G., Rossor, M. N., Thomas, D. J., Frosh, A., Tolley, N., Bell, J. E., Spencer, M., King, A., Al-Sarraj, S., Ironside, J. W., Lantos, P. L. and Collinge, J. (1999). Investigation of variant Creutzfeldt-Jakob disease and other human prion diseases with tonsil biopsy samples. *Lancet.* **353** (183-189).

Hill, A. F., Desbruslais, M., Joiner, S., Sidle, K. C., Gowland, I., Collinge, J., Doey, L. J. and Lantos, P. (1997). The same prion strain causes vCJD and BSE. *Nature*. **389** (448-450, 526).

Hoffmann, C., Ziegler, U., Buschmann, A., Weber, A., Kupfer, L., Oelschlegel, A., Hammerschmidt, B. and Groschup, M. H. (2007). Prions spread via the autonomic nervous system from the gut to the central nervous system in cattle incubating bovine spongiform encephalopathy. *Journal of General Virology.* **88** (1048-1055).

Hornshaw, M. P., McDermott, J. R. and Candy, J. M. (1995a). Copper binding to the N-terminal tandem repeat regions of mammalian and avian prion protein. *Biochemical and Biophysical Research Communications.* **207** (621-629).

Hornshaw, M. P., McDermott, J. R., Candy, J. M. and Lakey, J. H. (1995b). Copper binding to the N-terminal tandem repeat region of mammalian and avian prion protein: structural studies using synthetic peptides. *Biochemical and Biophysical Research Communications.* **214** (993-999).

Horonchik, L., Tzaban, S., Ben-Zaken, O., Yedidia, Y., Rouvinski, A., Papy-Garcia, D., Barritault, D., Vlodavsky, I. and Taraboulos, A. (2005). Heparan sulfate is a cellular receptor for purified infectious prions. *Journal of Biological Chemistry.* **280** (17062-17067).

Hosszu, L. L., Jackson, G. S., Trevitt, C. R., Jones, S., Batchelor, M., Bhelt, D., Prodromidou, K., Clarke, A. R., Waltho, J. P. and Collinge, J. (2004). The residue 129 polymorphism in human prion protein does not confer susceptibility to Creutzfeldt-Jakob disease by altering the structure or global stability of PrP^{C}. *Journal of Biological Chemistry.* **279** (28515-28521).

Hsiao, K. K., Scott, M., Foster, D., Groth, D. F., DeArmond, S. J. and Prusiner, S. B. (1990). Spontaneous neurodegeneration in transgenic mice with mutant prion protein. *Science*. **250** (1587-1590).

Hu, Z., Bonifas, J. M., Beech, J., Bench, G., Shigihara, T., Ogawa, H., Ikeda, S., Mauro, T. and Epstein, E. H., Jr. (2000). Mutations in ATP2C1, encoding a calcium pump, cause Hailey-Hailey disease. *Nature Genetics.* **24** (61-65).

Huang, F. P., Farquhar, C. F., Mabbott, N. A., Bruce, M. E. and MacPherson, G. G. (2002). Migrating intestinal dendritic cells transport PrP(Sc) from the gut. *Journal of General Virology.* **83** (267-271).

Hunter, N. (2003). Scrapie and experimental BSE in sheep. *British Medical Bulletin.* **66** (171-183).

Hunter, N., Goldmann, W., Marshall, E. and O'Neill, G. (2000). Sheep and goats: natural and experimental TSEs and factors influencing incidence of disease. *Archives of Virology, Supplement*. **16** (181-188).

Hutter, G., Heppner, F. L. and Aguzzi, A. (2003). No superoxide dismutase activity of cellular prion protein *in vivo*. *Biological Chemistry.* **384** (1279-1285).

Iwamaru, Y., Takenouchi, T., Ogihara, K., Hoshino, M., Takata, M., Imamura, M., Tagawa, Y., Hayashi-Kato, H., Ushiki-Kaku, Y., Shimizu, Y., Okada, H., Shinagawa, M., Kitani, H. and Yokoyama, T. (2007). Microglial cell line established from prion protein-overexpressing mice is susceptible to various murine prion strains. *Journal of Virology.* **81** (1524-1527).

Jackson, G. S., Hill, A. F., Joseph, C., Hosszu, L., Power, A., Waltho, J. P., Clarke, A. R. and Collinge, J. (1999a). Multiple folding pathways for heterologously expressed human prion protein. *Biochimica et Biophysica Acta.* **1431** (1-13).

Jackson, G. S., Hosszu, L. L., Power, A., Hill, A. F., Kenney, J., Saibil, H., Craven, C. J., Waltho, J. P., Clarke, A. R. and Collinge, J. (1999b). Reversible conversion of monomeric human prion protein between native and fibrilogenic conformations. *Science.* **283** (1935-1937).

Jackson, G. S., Murray, I., Hosszu, L. L., Gibbs, N., Waltho, J. P., Clarke, A. R. and Collinge, J. (2001). Location and properties of metal-binding sites on the human prion protein. *Proceedings of the National Academy of Sciences of the United States of America.* **98** (8531-8535).

Jeffrey, M. and Wells, G. A. (1988). Spongiform encephalopathy in a nyala (Tragelaphus angasi). *Veterinary Pathology.* **25** (398-399).

Jimenez-Huete, A., Lievens, P. M., Vidal, R., Piccardo, P., Ghetti, B., Tagliavini, F., Frangione, B. and Prelli, F. (1998). Endogenous proteolytic cleavage of normal and disease-associated isoforms of the human prion protein in neural and non-neural tissues. *American Journal of Pathology.* **153** (1561-1572).

Jobling, M. F., Huang, X., Stewart, L. R., Barnham, K. J., Curtain, C., Volitakis, I., Perugini, M., White, A. R., Cherny, R. A., Masters, C. L., Barrow, C. J., Collins, S. J., Bush, A. I. and Cappai, R. (2001). Copper and zinc binding modulates the aggregation and neurotoxic properties of the prion peptide PrP106-126. *Biochemistry.* **40** (8073-8084).

Jones, C. E., Abdelraheim, S. R., Brown, D. R. and Viles, J. H. (2004). Preferential Cu2+ coordination by His96 and His111 induces beta-sheet formation in the unstructured amyloidogenic region of the prion protein. *Journal of Biological Chemistry.* **279** (32018-32027).

Jones, S., Batchelor, M., Bhelt, D., Clarke, A. R., Collinge, J. and Jackson, G. S. (2005). Recombinant prion protein does not possess SOD-1 activity. *Biochemical Journal.* **392** (309-312).

Kaimann, T., Metzger, S., Kuhlmann, K., Brandt, B., Birkmann, E., Holtje, H. D. and Riesner, D. (2008). Molecular model of an alpha-helical prion protein dimer and its monomeric subunits as derived from chemical cross-linking and molecular modeling calculations. *Journal of Molecular Biology.* **376** (582-596).

Kalastavadi, T. and True, H. L. (2008). Prion protein insertional mutations increase aggregation propensity but not fiber stability. *BMC Biochemistry.* **9** (7).

Kanaani, J., Prusiner, S. B., Diacovo, J., Baekkeskov, S. and Legname, G. (2005). Recombinant prion protein induces rapid polarization and development of synapses in

embryonic rat hippocampal neurons *in vitro*. *Journal of Neurochemistry.* **95** (1373-1386).

Kanu, N., Imokawa, Y., Drechsel, D. N., Williamson, R. A., Birkett, C. R., Bostock, C. J. and Brockes, J. P. (2002). Transfer of scrapie prion infectivity by cell contact in culture. *Current Biology.* **12** (523-530).

Katamine, S., Nishida, N., Sugimoto, T., Noda, T., Sakaguchi, S., Shigematsu, K., Kataoka, Y., Nakatani, A., Hasegawa, S., Moriuchi, R. and Miyamoto, T. (1998). Impaired motor coordination in mice lacking prion protein. *Cellular and Molecular Neurobiology.* **18** (731-742).

Kaufman, R. J., Swaroop, M. and Murtha-Riel, P. (1994). Depletion of manganese within the secretory pathway inhibits O-linked glycosylation in mammalian cells. *Biochemistry*. **33** (9813-9819).

Kayed, R. and Glabe, C. G. (2006). Conformation-dependent anti-amyloid oligomer antibodies. *Methods in Enzymology.* **413** (326-344).

Kayed, R., Head, E., Sarsoza, F., Saing, T., Cotman, C. W., Necula, M., Margol, L., Wu, J., Breydo, L., Thompson, J. L., Rasool, S., Gurlo, T., Butler, P. and Glabe, C. G. (2007). Fibril specific, conformation dependent antibodies recognize a generic epitope common to amyloid fibrils and fibrillar oligomers that is absent in prefibrillar oligomers. *Molecular Neurodegeneration.* **2** (18).

Kayed, R., Head, E., Thompson, J. L., McIntire, T. M., Milton, S. C., Cotman, C. W. and Glabe, C. G. (2003). Common structure of soluble amyloid oligomers implies common mechanism of pathogenesis. *Science.* **300** (486-489).

Kazlauskaite, J., Young, A., Gardner, C. E., Macpherson, J. V., Venien-Bryan, C. and Pinheiro, T. J. (2005). An unusual soluble beta-turn-rich conformation of prion is involved in fibril formation and toxic to neuronal cells. *Biochemical and Biophysical Research Communications.* **328** (292-305).

Kenward, A. G., Bartolotti, L. J. and Burns, C. S. (2007). Copper and zinc promote interactions between membrane-anchored peptides of the metal binding domain of the prion protein. *Biochemistry.* **46** (4261-4271).

Kim, N. H., Choi, J. K., Jeong, B. H., Kim, J. I., Kwon, M. S., Carp, R. I. and Kim, Y. S. (2005). Effect of transition metals (Mn, Cu, Fe) and deoxycholic acid (DA) on the conversion of PrP^{C} to PrPres. *FASEB Journal.* **19** (783-785).

Kim, N. H., Park, S. J., Jin, J. K., Kwon, M. S., Choi, E. K., Carp, R. I. and Kim, Y. S. (2000). Increased ferric iron content and iron-induced oxidative stress in the brains of scrapie-infected mice. *Brain Research.* **884** (98-103).

Kimberlin, R. H. and Walker, C. A. (1986). Pathogenesis of scrapie (strain 263K) in hamsters infected intracerebrally, intraperitoneally or intraocularly. *Journal of General Virology.* **67** (Pt 2) (255-263).

Kimberlin, R. H. and Walker, C. A. (1989a). The role of the spleen in the neuroinvasion of scrapie in mice. *Virus Research.* **12** (201-211).

Kimberlin, R. H. and Walker, C. A. (1989b). Pathogenesis of scrapie in mice after intragastric infection. *Virus Research.* **12** (213-220).

Kimberlin, R. H., Hall, S. M. and Walker, C. A. (1983). Pathogenesis of mouse scrapie. Evidence for direct neural spread of infection to the CNS after injection of sciatic nerve. *Journal of the Neurological Sciences.* **61** (315-325).

Kirkwood, J. K., Wells, G. A., Wilesmith, J. W., Cunningham, A. A. and Jackson, S. I. (1990). Spongiform encephalopathy in an arabian oryx (Oryx leucoryx) and a greater kudu (Tragelaphus strepsiceros). *Veterinary Record.* **127** (418-420).

Klajnert, B., Cortijo-Arellano, M., Bryszewska, M. and Cladera, J. (2006a). Influence of heparin and dendrimers on the aggregation of two amyloid peptides related to Alzheimer's and prion diseases. *Biochemical and Biophysical Research Communications.* **339** (577-582).

Klajnert, B., Cortijo-Arellano, M., Cladera, J. and Bryszewska, M. (2006b). Influence of dendrimer's structure on its activity against amyloid fibril formation. *Biochemical and Biophysical Research Communications.* **345** (21-28).

Klajnert, B., Cortijo-Arellano, M., Cladera, J., Majoral, J. P., Caminade, A. M. and Bryszewska, M. (2007). Influence of phosphorus dendrimers on the aggregation of the prion peptide PrP 185-208. *Biochemical and Biophysical Research Communications.* **364** (20-25).

Klein, M. A., Frigg, R., Raeber, A. J., Flechsig, E., Hegyi, I., Zinkernagel, R. M., Weissmann, C. and Aguzzi, A. (1998). PrP expression in B lymphocytes is not required for prion neuroinvasion. *Nature Medicine.* **4** (1429-1433).

Klewpatinond, M. and Viles, J. H. (2007). Fragment length influences affinity for Cu2+ and Ni2+ binding to His96 or His111 of the prion protein and spectroscopic evidence for a multiple histidine binding only at low pH. *Biochemical Journal.* **404** (393-402).

Klewpatinond, M., Davies, P., Bowen, S., Brown, D. R. and Viles, J. H. (2008). Deconvoluting the Cu2+ binding modes of full-length prion protein. *Journal of Biological Chemistry.* **283** (1870-1881).

Klohn, P. C., Stoltze, L., Flechsig, E., Enari, M. and Weissmann, C. (2003). A quantitative, highly sensitive cell-based infectivity assay for mouse scrapie prions. *Proceedings of the National Academy of Sciences of the United States of America.* **100** (11666-11671).

Klyubin, I., Walsh, D. M., Cullen, W. K., Fadeeva, J. V., Anwyl, R., Selkoe, D. J. and Rowan, M. J. (2004). Soluble Arctic amyloid beta protein inhibits hippocampal long-term potentiation *in vivo*. *European Journal of Neuroscience.* **19** (2839-2846).

Koperek, O., Kovacs, G. G., Ritchie, D., Ironside, J. W., Budka, H. and Wick, G. (2002). Disease-associated prion protein in vessel walls. *American Journal of Pathology.* **161** (1979-1984).

Korth, C., Kaneko, K. and Prusiner, S. B. (2000). Expression of unglycosylated mutated prion protein facilitates PrP(Sc) formation in neuroblastoma cells infected with different prion strains. *Journal of General Virology.* **81** (2555-2563).

Kovacs, G. G. and Budka, H. (2009). Molecular pathology of human prion diseases. *International Journal of Molecular Sciences.* **10** (976-999).

Kovacs, G. G., Gelpi, E., Strobel, T., Ricken, G., Nyengaard, J. R., Bernheimer, H. and Budka, H. (2007). Involvement of the endosomal-lysosomal system correlates with regional pathology in Creutzfeldt-Jakob disease. *Journal of Neuropathology and Experimental Neurology.* **66** (628-636).

Kovacs, G. G., Kalev, O., Gelpi, E., Haberler, C., Wanschitz, J., Strohschneider, M., Molnar, M. J., Laszlo, L. and Budka, H. (2004). The prion protein in human neuromuscular diseases. *Journal of Pathology.* **204** (241-247).

Kovacs, G. G., Preusser, M., Strohschneider, M. and Budka, H. (2005). Subcellular localization of disease-associated prion protein in the human brain. *American Journal of Pathology.* **166** (287-294).

Kralovicova, S., Fontaine, S. N., Alderton, A., Alderman, J., Ragnarsdottir, K. V., Collins, S. J. and Brown, D. R. (2009). The effects of prion protein expression on metal metabolism. *Molecular and Cellular Neurosciences.* **41** (135-147).

Krasemann, S., Zerr, I., Weber, T., Poser, S., Kretzschmar, H., Hunsmann, G. and Bodemer, W. (1995). Prion disease associated with a novel nine octapeptide repeat insertion in the PRNP gene. *Brain Research. Molecular Brain Research.* **34** (173-176).

Krebs, B., Dorner-Ciossek, C., Schmalzbauer, R., Vassallo, N., Herms, J. and Kretzschmar, H. A. (2006). Prion protein induced signaling cascades in monocytes. *Biochemical and Biophysical Research Communications.* **340** (13-22).

Kretzschmar, H. A., Stowring, L. E., Westaway, D., Stubblebine, W. H., Prusiner, S. B. and Dearmond, S. J. (1986). Molecular cloning of a human prion protein cDNA. *DNA.* **5** (315-324).

Kristiansen, M., Deriziotis, P., Dimcheff, D. E., Jackson, G. S., Ovaa, H., Naumann, H., Clarke, A. R., van Leeuwen, F. W., Menendez-Benito, V., Dantuma, N. P., Portis, J. L., Collinge, J. and Tabrizi, S. J. (2007). Disease-associated prion protein oligomers inhibit the 26S proteasome. *Molecular Cell.* **26** (175-188).

Kristiansen, M., Messenger, M. J., Klohn, P. C., Brandner, S., Wadsworth, J. D., Collinge, J. and Tabrizi, S. J. (2005). Disease-related prion protein forms aggresomes in neuronal cells leading to caspase activation and apoptosis. *Journal of Biological Chemistry.* **280** (38851-38861).

Kruger, D., Thomzig, A., Lenz, G., Kampf, K., McBride, P. and Beekes, M. (2009). Faecal shedding, alimentary clearance and intestinal spread of prions in hamsters fed with scrapie. *Veterinary Research.* **40** (4).

Kunzi, V., Glatzel, M., Nakano, M. Y., Greber, U. F., Van Leuven, F. and Aguzzi, A. (2002). Unhampered prion neuroinvasion despite impaired fast axonal transport in transgenic mice overexpressing four-repeat tau. *Journal of Neuroscience.* **22** (7471-7477).

Kupfer, L., Eiden, M., Buschmann, A. and Groschup, M. H. (2007). Amino acid sequence and prion strain specific effects on the *in vitro* and *in vivo* convertibility of ovine/murine and bovine/murine prion protein chimeras. *Biochimica et Biophysica Acta.* **1772** (704-713).

Kurschner, C. and Morgan, J. I. (1995). The cellular prion protein (PrP) selectively binds to Bcl-2 in the yeast two-hybrid system. Brain Research. *Molecular Brain Research.* **30** (165-168).

Ladogana, A., Casaccia, P., Ingrosso, L., Cibati, M., Salvatore, M., Xi, Y. G., Masullo, C. and Pocchiari, M. (1992). Sulphate polyanions prolong the incubation period of scrapie-infected hamsters. *Journal of General Virology.* **73** (Pt 3) (661-665).

Lafaye, P., Achour, I., England, P., Duyckaerts, C. and Rougeon, F. (2009). Single-domain antibodies recognize selectively small oligomeric forms of amyloid beta, prevent Abeta-induced neurotoxicity and inhibit fibril formation. *Molecular Immunology.* **46** (695-704).

Lander, A. D. (1994). Targeting the glycosaminoglycan-binding sites on proteins. *Chemistry and Biology.* **1** (73-78).

Lasmezas, C. I., Deslys, J. P., Robain, O., Jaegly, A., Beringue, V., Peyrin, J. M., Fournier, J. G., Hauw, J. J., Rossier, J. and Dormont, D. (1997). Transmission of the BSE agent to mice in the absence of detectable abnormal prion protein. *Science.* **275** (402-405).

Latarjet, R., Muel, B., Haig, D. A., Clarke, M. C. and Alper, T. (1970). Inactivation of the scrapie agent by near monochromatic ultraviolet light. *Nature*. **227** (1341-1343).

Lauren, J., Gimbel, D. A., Nygaard, H. B., Gilbert, J. W. and Strittmatter, S. M. (2009). Cellular prion protein mediates impairment of synaptic plasticity by amyloid-beta oligomers. *Nature.* **457** (1128-1132).

Lawson, V. A., Priola, S. A., Meade-White, K., Lawson, M. and Chesebro, B. (2004). Flexible N-terminal region of prion protein influences conformation of protease-resistant prion protein isoforms associated with cross-species scrapie infection *in vivo* and *in vitro*. *Journal of Biological Chemistry.* **279** (13689-13695).

Leach, S. P., Salman, M. D. and Hamar, D. (2006). Trace elements and prion diseases: a review of the interactions of copper, manganese and zinc with the prion protein. *Animal Health Research Reviews.* **7** (97-105).

Lee, H. S., Brown, P., Cervenakova, L., Garruto, R. M., Alpers, M. P., Gajdusek, D. C. and Goldfarb, L. G. (2001). Increased susceptibility to Kuru of carriers of the PRNP 129 methionine/methionine genotype. *Journal of Infectious Diseases.* **183** (192-196).

Lekishvili, T., Sassoon, J., Thompsett, A. R., Green, A., Ironside, J. W. and Brown, D. R. (2004). BSE and vCJD cause disturbance to uric acid levels. *Experimental Neurology.* **190** (233-244).

Lesne, S., Kotilinek, L. and Ashe, K. H. (2008). Plaque-bearing mice with reduced levels of oligomeric amyloid-beta assemblies have intact memory function. *Neuroscience*. **151** (745-749).

LeVine, H., 3rd. (1993). Thioflavine T interaction with synthetic Alzheimer's disease beta-amyloid peptides: detection of amyloid aggregation in solution. *Protein Science.* **2** (404-410).

Lewis, P. A., Tattum, M. H., Jones, S., Bhelt, D., Batchelor, M., Clarke, A. R., Collinge, J. and Jackson, G. S. (2006). Codon 129 polymorphism of the human prion protein influences the kinetics of amyloid formation. *Journal of General Virology.* **87** (2443-2449).

Li, A., Christensen, H. M., Stewart, L. R., Roth, K. A., Chiesa, R. and Harris, D. A. (2007). Neonatal lethality in transgenic mice expressing prion protein with a deletion of residues 105-125. *EMBO Journal.* **26** (548-558).

Li, R., Liu, T., Wong, B. S., Pan, T., Morillas, M., Swietnicki, W., O'Rourke, K., Gambetti, P., Surewicz, W. K. and Sy, M. S. (2000). Identification of an epitope in the C terminus of normal prion protein whose expression is modulated by binding events in the N terminus. *Journal of Molecular Biology*. **301** (567-573).

Li, X. L., Dong, C. F., Wang, G. R., Zhou, R. M., Shi, Q., Tian, C., Gao, C., Mei, G. Y., Chen, C., Xu, K., Han, J. and Dong, X. P. (2009). Manganese-induced changes of the biochemical characteristics of the recombinant wild-type and mutant PrPs. *Medical Microbiology and Immunology*. In press

Liang, J., Bai, F., Luo, G., Wang, J., Liu, J., Ge, F., Pan, Y., Yao, L., Du, R., Li, X., Fan, R., Zhang, H., Guo, X., Wu, K. and Fan, D. (2007). Hypoxia induced

overexpression of PrP(C) in gastric cancer cell lines. *Cancer Biology and Therapy*. **6** (769-774).

Liemann, S. and Glockshuber, R. (1999). Influence of amino acid substitutions related to inherited human prion diseases on the thermodynamic stability of the cellular prion protein. *Biochemistry.* **38** (3258-3267).

Linding, R., Schymkowitz, J., Rousseau, F., Diella, F. and Serrano, L. (2004). A comparative study of the relationship between protein structure and beta-aggregation in globular and intrinsically disordered proteins. *Journal of Molecular Biology*. **342** (345-353).

Linert W., Jameson, G.N.L., Jameson, R.F., Jellinger, K.A. (2006). The chemical interplay between catecholamines and metal ions in neurological diseases. In: Sigel A, Sigel H, Sigel RKO (eds) *Metal ions in life sciences, vol 1*. Wiley and Sons, Hoboken, NJ. (281–320).

Liu, A., Riek, R., Zahn, R., Hornemann, S., Glockshuber, R. and Wuthrich, K. (1999). Peptides and proteins in neurodegenerative disease: helix propensity of a polypeptide containing helix 1 of the mouse prion protein studied by NMR and CD spectroscopy. *Biopolymers*. **51** (145-152).

Liu, M. L., Li, Y. X., Zhou, X. M. and Zhao, D. M. (2008). Copper(II) Inhibits *In vitro* Conformational Conversion of Ovine Prion Protein Triggered by Low pH. *The Journal of Biochemistry*. **143** (333-337).

Llewelyn, C. A., Hewitt, P. E., Knight, R. S., Amar, K., Cousens, S., Mackenzie, J. and Will, R. G. (2004). Possible transmission of variant Creutzfeldt-Jakob disease by blood transfusion. *Lancet*. **363** (417-421).

Lopes, M. H., Hajj, G. N., Muras, A. G., Mancini, G. L., Castro, R. M., Ribeiro, K. C., Brentani, R. R., Linden, R. and Martins, V. R. (2005). Interaction of cellular prion and stress-inducible protein 1 promotes neuritogenesis and neuroprotection by distinct signaling pathways. *Journal of Neuroscience*. **25** (11330-11339).

Lowe, J., McDermott, H., Kenward, N., Landon, M., Mayer, R. J., Bruce, M., McBride, P., Somerville, R. A. and Hope, J. (1990). Ubiquitin conjugate immunoreactivity in the brains of scrapie infected mice. *Journal of Pathology*. **162** (61-66).

Lu, B. Y. and Chang, J. Y. (2002). Isolation and characterization of a polymerized prion protein. *Biochemical Journal*. **364** (81-87).

Lu, D. C., Soriano, S., Bredesen, D. E. and Koo, E. H. (2003). Caspase cleavage of the amyloid precursor protein modulates amyloid beta-protein toxicity. *Journal of Neurochemistry*. **87** (733-741).

Lu, X., Wintrode, P. L. and Surewicz, W. K. (2007). Beta-sheet core of human prion protein amyloid fibrils as determined by hydrogen/deuterium exchange. *Proceedings of the National Academy of Sciences of the United States of America*. **104** (1510-1515).

Luhrs, T., Zahn, R. and Wuthrich, K. (2006). Amyloid formation by recombinant full-length prion proteins in phospholipid bicelle solutions. *Journal of Molecular Biology*. **357** (833-841).

Ma, J. and Lindquist, S. (2001). Wild-type PrP and a mutant associated with prion disease are subject to retrograde transport and proteasome degradation. *Proceedings of the National Academy of Sciences of the United States of America*. **98** (14955-14960).

Maas, E., Geissen, M., Groschup, M. H., Rost, R., Onodera, T., Schatzl, H. and Vorberg, I. M. (2007). Scrapie infection of prion protein-deficient cell line upon ectopic expression of mutant prion proteins. *Journal of Biological Chemistry*. **282** (18702-18710).

Mabbott, N. A., Brown, K. L., Manson, J. and Bruce, M. E. (1997). T-lymphocyte activation and the cellular form of the prion protein. *Immunology*. **92** (161-165).

Mabbott, N. A., Mackay, F., Minns, F. and Bruce, M. E. (2000a). Temporary inactivation of follicular dendritic cells delays neuroinvasion of scrapie. *Nature Medicine*. **6** (719-720).

Mabbott, N. A., Williams, A., Farquhar, C. F., Pasparakis, M., Kollias, G. and Bruce, M. E. (2000b). Tumor necrosis factor alpha-deficient, but not interleukin-6-deficient, mice resist peripheral infection with scrapie. *Journal of Virology*. **74** (3338-3344).

Madore, N., Smith, K. L., Graham, C. H., Jen, A., Brady, K., Hall, S. and Morris, R. (1999). Functionally different GPI proteins are organized in different domains on the neuronal surface. *EMBO Journal*. **18** (6917-6926).

Maignien, T., Lasmezas, C. I., Beringue, V., Dormont, D. and Deslys, J. P. (1999). Pathogenesis of the oral route of infection of mice with scrapie and bovine spongiform encephalopathy agents. *Journal of General Virology*. **80** (Pt 11) (3035-3042).

Malaisé, M., Schatzl, H. M. and Burkle, A. (2008). The octarepeat region of prion protein, but not the TM1 domain, is important for the antioxidant effect of prion protein. *Free Radical Biology and Medicine.* **45** (1622-1630).

Manson, J., West, J. D., Thomson, V., McBride, P., Kaufman, M. H. and Hope, J. (1992). The prion protein gene: a role in mouse embryogenesis? *Development*. **115** (117-122).

Manuelidis, L. (2007). A 25 nm virion is the likely cause of transmissible spongiform encephalopathies. *Journal of Cellular Biochemistry*. **100** (897-915).

Margalit, H., Fischer, N. and Ben-Sasson, S. A. (1993). Comparative analysis of structurally defined heparin binding sequences reveals a distinct spatial distribution of basic residues. *Journal of Biological Chemistry.* **268** (19228-19231).

Margittai, M. and Langen, R. (2004). Template-assisted filament growth by parallel stacking of tau. *Proceedings of the National Academy of Sciences of the United States of America.* **101** (10278-10283).

Marijanovic, Z., Caputo, A., Campana, V. and Zurzolo, C. (2009). Identification of an intracellular site of prion conversion. *PLoS Pathogens*. **5** (e1000426).

Marsh, R. F. and Bessen, R. A. (1993). Epidemiologic and experimental studies on transmissible mink encephalopathy. *Developments in Biological Standardization*. **80** (111-118).

Marsh, R. F. and Hadlow, W. J. (1992). Transmissible mink encephalopathy. *Revue Scientifique et Technique*. **11** (539-550).

Martins, S. M., Frosoni, D. J., Martinez, A. M., De Felice, F. G. and Ferreira, S. T. (2006). Formation of soluble oligomers and amyloid fibrils with physical properties of the scrapie isoform of the prion protein from the C-terminal domain of recombinant murine prion protein mPrP-(121-231). *Journal of Biological Chemistry.* **281** (26121-26128).

Martins, V. R., Graner, E., Garcia-Abreu, J., de Souza, S. J., Mercadante, A. F., Veiga, S. S., Zanata, S. M., Neto, V. M. and Brentani, R. R. (1997). Complementary hydropathy identifies a cellular prion protein receptor. *Nature Medicine.* **3** (1376-1382).

Maskevich, A. A., Stsiapura, V. I., Kuzmitsky, V. A., Kuznetsova, I. M., Povarova, O. I., Uversky, V. N. and Turoverov, K. K. (2007). Spectral properties of thioflavin T in solvents with different dielectric properties and in a fibril-incorporated form. *Journal of Proteome Research*. **6** (1392-1401).

Mathiason, C. K., Hays, S. A., Powers, J., Hayes-Klug, J., Langenberg, J., Dahmes, S. J., Osborn, D. A., Miller, K. V., Warren, R. J., Mason, G. L. and Hoover, E. A. (2009). Infectious prions in pre-clinical deer and transmission of chronic wasting disease solely by environmental exposure. *PLoS One.* **4** (e5916).

Mathiason, C. K., Powers, J. G., Dahmes, S. J., Osborn, D. A., Miller, K. V., Warren, R. J., Mason, G. L., Hays, S. A., Hayes-Klug, J., Seelig, D. M., Wild, M. A., Wolfe, L. L., Spraker, T. R., Miller, M. W., Sigurdson, C. J., Telling, G. C. and Hoover, E. A. (2006). Infectious prions in the saliva and blood of deer with chronic wasting disease. *Science*. **314** (133-136).

Mayer-Sonnenfeld, T., Zeigler, M., Halimi, M., Dayan, Y., Herzog, C., Lasmezas, C. I. and Gabizon, R. (2005). The metabolism of glycosaminoglycans is impaired in prion diseases. *Neurobiology of Disease.* **20** (738-743).

Maynard, C. J., Bush, A. I., Masters, C. L., Cappai, R. and Li, Q. X. (2005). Metals and amyloid-beta in Alzheimer's disease. *International Journal of Experimental Pathology.* **86** (147-159).

Mays, C. E., Kang, H. E., Kim, Y., Shim, S. H., Bang, J. E., Woo, H. J., Cho, Y. H., Kim, J. B. and Ryou, C. (2008). CRBL cells: establishment, characterization and susceptibility to prion infection. *Brain Research*. **1208** (170-180).

Mazzoni, I. E., Ledebur, H. C., Jr., Paramithiotis, E. and Cashman, N. (2005). Lymphoid signal transduction mechanisms linked to cellular prion protein. *Biochemistry and Cell Biology.* **83** (644-653).

McBride, P. A. and Beekes, M. (1999). Pathological PrP is abundant in sympathetic and sensory ganglia of hamsters fed with scrapie. *Neuroscience Letters.* **265** (135-138).

McKenzie, D., Bartz, J., Mirwald, J., Olander, D., Marsh, R. and Aiken, J. (1998). Reversibility of scrapie inactivation is enhanced by copper. *Journal of Biological Chemistry.* **273** (25545-25547).

McKinley, M. P., Bolton, D. C. and Prusiner, S. B. (1983). A protease-resistant protein is a structural component of the scrapie prion. *Cell*. **35** (57-62).

McKinley, M. P., Taraboulos, A., Kenaga, L., Serban, D., Stieber, A., DeArmond, S. J., Prusiner, S. B. and Gonatas, N. (1991). Ultrastructural localization of scrapie prion proteins in cytoplasmic vesicles of infected cultured cells. *Laboratory Investigation.* **65** (622-630).

McLennan, N. F., Brennan, P. M., McNeill, A., Davies, I., Fotheringham, A., Rennison, K. A., Ritchie, D., Brannan, F., Head, M. W., Ironside, J. W., Williams, A. and Bell, J. E. (2004). Prion protein accumulation and neuroprotection in hypoxic brain damage. *American Journal of Pathology.* **165** (227-235).

Mead, S. (2006). Prion disease genetics. *European Journal of Human Genetics.* **14** (273-281).

Menendez-Benito, V., Verhoef, L. G., Masucci, M. G. and Dantuma, N. P. (2005). Endoplasmic reticulum stress compromises the ubiquitin-proteasome system. *Human Molecular Genetics.* **14** (2787-2799).

M'Gowan, J. P. (1918) *Journal of Comparative Pathology and Therapy.* **31**, 278.

Milhavet, O., Casanova, D., Chevallier, N., McKay, R. D. and Lehmann, S. (2006). Neural stem cell model for prion propagation. *Stem Cells.* **24** (2284-2291).

Milhavet, O., McMahon, H. E., Rachidi, W., Nishida, N., Katamine, S., Mange, A., Arlotto, M., Casanova, D., Riondel, J., Favier, A. and Lehmann, S. (2000). Prion infection impairs the cellular response to oxidative stress. *Proceedings of the National Academy of Sciences of the United States of America.* **97** (13937-13942).

Milhavet, O., McMahon, H. E., Rachidi, W., Nishida, N., Katamine, S., Mange, A., Arlotto, M., Casanova, D., Riondel, J., Favier, A. and Lehmann, S. (2000). Prion infection impairs the cellular response to oxidative stress. *Proceedings of the National Academy of Sciences of the United States of America.* **97** (13937-13942).

Miller, M. W., Williams, E. S., Hobbs, N. T. and Wolfe, L. L. (2004). Environmental sources of prion transmission in mule deer. *Emerging Infectious Diseases.* **10** (1003-1006).

Mironov, A., Jr., Latawiec, D., Wille, H., Bouzamondo-Bernstein, E., Legname, G., Williamson, R. A., Burton, D., DeArmond, S. J., Prusiner, S. B. and Peters, P. J. (2003). Cytosolic prion protein in neurons. *Journal of Neuroscience.* **23** (7183-7193).

Mitteregger, G., Korte, S., Shakarami, M., Herms, J. and Kretzschmar, H. A. (2009). Role of copper and manganese in prion disease progression. *Brain Research.* **1292** (155-164).

Mobley, W. C., Neve, R. L., Prusiner, S. B. and McKinley, M. P. (1988). Nerve growth factor increases mRNA levels for the prion protein and the beta-amyloid protein precursor in developing hamster brain. *Proceedings of the National Academy of Sciences of the United States of America.* **85** (9811-9815).

Moore, R. A., Hayes, S. F., Fischer, E. R. and Priola, S. A. (2007). Amyloid formation via supramolecular peptide assemblies. *Biochemistry.* **46** (7079-7087).

Moore, R. A., Taubner, L. M. and Priola, S. A. (2009). Prion protein misfolding and disease. Current Opinion in Structural *Biology*. **19** (14-22).

Morales, R., Abid, K. and Soto, C. (2007). The prion strain phenomenon: molecular basis and unprecedented features. Biochimica et Biophysica Acta. **1772** (681-691).

Morel, E., Andrieu, T., Casagrande, F., Gauczynski, S., Weiss, S., Grassi, J., Rousset, M., Dormont, D. and Chambaz, J. (2005). Bovine prion is endocytosed by human enterocytes via the 37 kDa/67 kDa laminin receptor. *American Journal of Pathology.* **167** (1033-1042).

Morillas, M., Vanik, D. L. and Surewicz, W. K. (2001). On the mechanism of alpha-helix to beta-sheet transition in the recombinant prion protein. *Biochemistry*. **40** (6982-6987).

Morrissey, M. P. and Shakhnovich, E. I. (1999). Evidence for the role of PrP(C) helix 1 in the hydrophilic seeding of prion aggregates. *Proceedings of the National Academy of Sciences of the United States of America.* **96** (11293-11298).

Mouillet-Richard, S., Ermonval, M., Chebassier, C., Laplanche, J. L., Lehmann, S., Launay, J. M. and Kellermann, O. (2000). Signal transduction through prion protein. *Science*. **289** (1925-1928).

Mouillet-Richard, S., Schneider, B., Pradines, E., Pietri, M., Ermonval, M., Grassi, J., Richards, J. G., Mutel, V., Launay, J. M. and Kellermann, O. (2007). Cellular prion protein signaling in serotonergic neuronal cells. *Annals of the New York Academy of Sciences.* **1096** (106-119).

Multhaup, G., Mechler, H. and Masters, C. L. (1995). Characterization of the high affinity heparin binding site of the Alzheimer's disease beta A4 amyloid precursor protein (APP) and its enhancement by zinc(II). *Journal of Molecular Recognition.* **8** (247-257).

Muramoto, T., Kitamoto, T., Tateishi, J. and Goto, I. (1992). The sequential development of abnormal prion protein accumulation in mice with Creutzfeldt-Jakob disease. *American Journal of Pathology.* **140** (1411-1420).

Nadal, R. C., Davies, P., Brown, D. R. and Viles, J. H. (2009). Evaluation of Copper²⁺ Affinities for the Prion Protein. *Biochemistry*. In press.

Naiki, H., Higuchi, K., Hosokawa, M. and Takeda, T. (1989). Fluorometric determination of amyloid fibrils *in vitro* using the fluorescent dye, thioflavin T1. *Analytical Biochemistry.* **177** (244-249).

Nakamura, T. and Lipton, S. A. (2009). Cell death: protein misfolding and neurodegenerative diseases. *Apoptosis*. **14** (455-468).

Nazor, K. E., Seward, T. and Telling, G. C. (2007). Motor behavioral and neuropathological deficits in mice deficient for normal prion protein expression. *Biochimica et Biophysica Acta.* **1772** (645-653).

Nelson, R., Sawaya, M. R., Balbirnie, M., Madsen, A. O., Riekel, C., Grothe, R. and Eisenberg, D. (2005). Structure of the cross-beta spine of amyloid-like fibrils. *Nature*. **435** (773-778).

Nguyen, J., Baldwin, M. A., Cohen, F. E. and Prusiner, S. B. (1995). Prion protein peptides induce alpha-helix to beta-sheet conformational transitions. *Biochemistry*. **34** (4186-4192).

Nieznanski, K., Rutkowski, M., Dominik, M. and Stepkowski, D. (2005). Proteolytic processing and glycosylation influence formation of porcine prion protein complexes. *Biochemical Journal.* **387** (93-100).

Nishida, N., Harris, D. A., Vilette, D., Laude, H., Frobert, Y., Grassi, J., Casanova, D., Milhavet, O. and Lehmann, S. (2000). Successful transmission of three mouse-adapted scrapie strains to murine neuroblastoma cell lines overexpressing wild-type mouse prion protein. Journal of *Virology*. **74** (320-325).

Nishida, Y., Sodeyama, N., Toru, Y., Toru, S., Kitamoto, T. and Mizusawa, H. (2004). Creutzfeldt-Jakob disease with a novel insertion and codon 219 Lys/Lys polymorphism in PRNP. *Neurology*. **63** (1978-1979).

Norstrom, E. M. and Mastrianni, J. A. (2006). The charge structure of helix 1 in the prion protein regulates conversion to pathogenic PrP^{Sc}. *Journal of Virology*. **80** (8521-8529).

Novitskaya, V., Bocharova, O. V., Bronstein, I. and Baskakov, I. V. (2006a). Amyloid fibrils of mammalian prion protein are highly toxic to cultured cells and primary neurons. *Journal of Biological Chemistry.* **281** (13828-13836).

Novitskaya, V., Makarava, N., Bellon, A., Bocharova, O. V., Bronstein, I. B., Williamson, R. A. and Baskakov, I. V. (2006b). Probing the conformation of the prion protein within a single amyloid fibril using a novel immunoconformational assay. *Journal of Biological Chemistry.* **281** (15536-15545).

Novitskaya, V., Makarava, N., Sylvester, I., Bronstein, I. B. and Baskakov, I. V. (2007). Amyloid fibrils of mammalian prion protein induce axonal degeneration in NTERA2-derived terminally differentiated neurons. *Journal of Neurochemistry.* **102** (398-407).

Nunomura, A., Hofer, T., Moreira, P. I., Castellani, R. J., Smith, M. A. and Perry, G. (2009). RNA oxidation in Alzheimer disease and related neurodegenerative disorders. *Acta Neuropathol*. **118** (151-166).

Nunomura, A., Perry, G., Aliev, G., Hirai, K., Takeda, A., Balraj, E. K., Jones, P. K., Ghanbari, H., Wataya, T., Shimohama, S., Chiba, S., Atwood, C. S., Petersen, R. B. and Smith, M. A. (2001). Oxidative damage is the earliest event in Alzheimer disease. *Journal of Neuropathology and Experimental Neurology.* **60** (759-767).

Oesch, B., Westaway, D., Walchli, M., McKinley, M. P., Kent, S. B., Aebersold, R., Barry, R. A., Tempst, P., Teplow, D. B., Hood, L. E. and *et al*. (1985). A cellular gene encodes scrapie PrP 27-30 protein. *Cell*. **40** (735-746).

Orem, N. R., Geoghegan, J. C., Deleault, N. R., Kascsak, R. and Supattapone, S. (2006). Copper (II) ions potently inhibit purified PrPres amplification. *Journal of Neurochemistry.* **96** (1409-1415).

Ostapchenko, V. G., Makarava, N., Savtchenko, R. and Baskakov, I. V. (2008). The polybasic N-terminal region of the prion protein controls the physical properties of both the cellular and fibrillar forms of PrP. *Journal of Molecular Biology.* **383** (1210-1224).

Ouidja, M. O., Petit, E., Kerros, M. E., Ikeda, Y., Morin, C., Carpentier, G., Barritault, D., Brugere-Picoux, J., Deslys, J. P., Adjou, K. and Papy-Garcia, D. (2007). Structure-activity studies of heparan mimetic polyanions for anti-prion therapies. *Biochemical and Biophysical Research Communications*. **363** (95-100).

Paitel, E., Alves da Costa, C., Vilette, D., Grassi, J. and Checler, F. (2002). Overexpression of PrP^{C} triggers caspase 3 activation: potentiation by proteasome

inhibitors and blockade by anti-PrP antibodies. *Journal of Neurochemistry.* **83** (1208-1214).

Pan, K. M., Baldwin, M., Nguyen, J., Gasset, M., Serban, A., Groth, D., Mehlhorn, I., Huang, Z., Fletterick, R. J., Cohen, F. E. and *et al*. (1993). Conversion of alpha-helices into beta-sheets features in the formation of the scrapie prion proteins. *Proceedings of the National Academy of Sciences of the United States of America.* **90** (10962-10966).

Pan, K. M., Stahl, N. and Prusiner, S. B. (1992). Purification and properties of the cellular prion protein from Syrian hamster brain. *Protein Science.* **1** (1343-1352).

Pan, T., Wong, B. S., Liu, T., Li, R., Petersen, R. B. and Sy, M. S. (2002). Cell-surface prion protein interacts with glycosaminoglycans. *Biochemical Journal.* **368** (81-90).

Paquet, S., Langevin, C., Chapuis, J., Jackson, G. S., Laude, H. and Vilette, D. (2007). Efficient dissemination of prions through preferential transmission to nearby cells. *Journal of General Virology.* **88** (706-713).

Pattison, I. H. and Jebbett, J. N. (1971a). Histopathological similarities between scrapie and cuprizone toxicity in mice. *Nature*. **230** (115-117).

Pattison, I. H. and Jebbett, J. N. (1971b). Clinical and histological observations on cuprizone toxicity and scrapie in mice. *Research in Veterinary Science.* **12** (378-380).

Pattison, I. H. and Millson, G. C. (1962). Distribution of the scrapie agent in the tissues of experimentally inoculated goats. *Journal of Comparative Pathology.* **72** (233-244).

Pattison, I. H., Hoare, M. N., Jebbett, J. N. and Watson, W. A. (1974). Further observations on the production of scrapie in sheep by oral dosing with foetal membranes from scrapie-affected sheep. *British Veterinary Journal.* **130** (lxv-lxvii).

Pattison, I. H., Jones, K. M. and Jebbett, J. N. (1971c). Detection of the scrapie agent in tissues of normal mice with special reference to the possibility of accidental laboratory contamination. *Research in Veterinary Science.* **12** (30-39).

Pauly, P. C. and Harris, D. A. (1998). Copper stimulates endocytosis of the prion protein. *Journal of Biological Chemistry.* **273** (33107-33110).

Peden, A. H., Head, M. W., Ritchie, D. L., Bell, J. E. and Ironside, J. W. (2004). Preclinical vCJD after blood transfusion in a PRNP codon 129 heterozygous patient. *Lancet*. **364** (527-529).

Perera, W. S. and Hooper, N. M. (2001). Ablation of the metal ion-induced endocytosis of the prion protein by disease-associated mutation of the octarepeat region. *Current Biology.* **11** (519-523).

Petrozzi, L., Ricci, G., Giglioli, N. J., Siciliano, G. and Mancuso, M. (2007). Mitochondria and neurodegeneration. *Bioscience Reports.* **27** (87-104).

Pham, N., Yin, S., Yu, S., Wong, P., Kang, S. C., Li, C. and Sy, M. S. (2008). Normal cellular prion protein with a methionine at position 129 has a more exposed helix 1 and is more prone to aggregate. *Biochemical and Biophysical Research Communications.* **368** (875-881).

Piccardo, P., Manson, J. C., King, D., Ghetti, B. and Barron, R. M. (2007). Accumulation of prion protein in the brain that is not associated with transmissible disease. *Proceedings of the National Academy of Sciences of the United States of America.* **104** (4712-4717).

Pieri, L., Bucciantini, M., Nosi, D., Formigli, L., Savistchenko, J., Melki, R. and Stefani, M. (2006). The yeast prion Ure2p native-like assemblies are toxic to mammalian cells regardless of their aggregation state. *Journal of Biological Chemistry.* **281** (15337-15344).

Polano, M., Bek, A., Benetti, F., Lazzarino, M. and Legname, G. (2009). Structural Insights into Alternate Aggregated Prion Protein Forms. *Journal of Molecular Biology.* In press.

Poling, A., Morgan-Paisley, K., Panos, J. J., Kim, E. M., O'Hare, E., Cleary, J. P., Lesne, S., Ashe, K. H., Porritt, M. and Baker, L. E. (2008). Oligomers of the amyloid-beta protein disrupt working memory: confirmation with two behavioral procedures. *Behavioural Brain Research*. **193** (230-234).

Pratico, D. and Sung, S. (2004). Lipid peroxidation and oxidative imbalance: early functional events in Alzheimer's disease. *Journal of Alzheimer's Disease.* **6** (171-175).

Priola, S. A. and Chesebro, B. (1998). Abnormal properties of prion protein with insertional mutations in different cell types. *Journal of Biological Chemistry.* **273** (11980-11985).

Priola, S. A., Caughey, B., Wehrly, K. and Chesebro, B. (1995). A 60-kDa prion protein (PrP) with properties of both the normal and scrapie-associated forms of PrP. *Journal of Biological Chemistry.* **270** (3299-3305).

Prohaska, J. R. and Gybina, A. A. (2004). Intracellular copper transport in mammals. *Journal of Nutrition.* **134** (1003-1006).

Prusiner, S. B. (1982). Novel proteinaceous infectious particles cause scrapie. *Science.* **216** (136-144).

Prusiner, S. B., Groth, D., Serban, A., Koehler, R., Foster, D., Torchia, M., Burton, D., Yang, S. L. and DeArmond, S. J. (1993). Ablation of the prion protein (PrP) gene in mice prevents scrapie and facilitates production of anti-PrP antibodies. *Proceedings of the National Academy of Sciences of the United States of America.* **90** (10608-10612).

Prusiner, S. B., McKinley, M. P., Bowman, K. A., Bolton, D. C., Bendheim, P. E., Groth, D. F. and Glenner, G. G. (1983). Scrapie prions aggregate to form amyloid-like birefringent rods. *Cell*. **35** (349-358).

Prusiner, S. B., Scott, M. R., DeArmond, S. J. and Cohen, F. E. (1998). Prion protein biology. *Cell*. **93** (337-348).

Pushie, M. J., Ross, A. R. and Vogel, H. J. (2007). Mass spectrometric determination of the coordination geometry of potential copper(II) surrogates for the mammalian prion protein octarepeat region. *Analytical Chemistry.* **79** (5659-5667).

Qin, K., Yang, D. S., Yang, Y., Chishti, M. A., Meng, L. J., Kretzschmar, H. A., Yip, C. M., Fraser, P. E. and Westaway, D. (2000). Copper(II)-induced conformational changes and protease resistance in recombinant and cellular PrP. Effect of protein age and deamidation. *Journal of Biological Chemistry.* **275** (19121-19131).

Qin, K., Yang, Y., Mastrangelo, P. and Westaway, D. (2002). Mapping Cu(II) binding sites in prion proteins by diethyl pyrocarbonate modification and matrix-assisted laser desorption ionization-time of flight (MALDI-TOF) mass spectrometric footprinting. *Journal of Biological Chemistry.* **277** (1981-1990).

Quaglio, E., Chiesa, R. and Harris, D. A. (2001). Copper converts the cellular prion protein into a protease-resistant species that is distinct from the scrapie isoform. *Journal of Biological Chemistry.* **276** (11432-11438).

Race, B., Meade-White, K., Oldstone, M. B., Race, R. and Chesebro, B. (2008). Detection of prion infectivity in fat tissues of scrapie-infected mice. *PLoS Pathogens.* **4** (e1000232).

Race, B., Meade-White, K., Race, R. and Chesebro, B. (2009). Prion infectivity in fat of deer with chronic wasting disease. *Journal of Virology.* **83** (9608-9610).

Race, R. E., Fadness, L. H. and Chesebro, B. (1987). Characterization of scrapie infection in mouse neuroblastoma cells. *Journal of General Virology.* **68** (Pt 5) (1391-1399).

Rachidi, W., Chimienti, F., Aouffen, M., Senator, A., Guiraud, P., Seve, M. and Favier, A. (2009). Prion protein protects against zinc-mediated cytotoxicity by modifying intracellular exchangeable zinc and inducing metallothionein expression. *Journal of Trace Elements in Medicine and Biology.* **23** (214-223).

Rachidi, W., Mange, A., Senator, A., Guiraud, P., Riondel, J., Benboubetra, M., Favier, A. and Lehmann, S. (2003). Prion infection impairs copper binding of cultured cells. *Journal of Biological Chemistry.* **278** (14595-14598).

Raymond, G. J., Hope, J., Kocisko, D. A., Priola, S. A., Raymond, L. D., Bossers, A., Ironside, J., Will, R. G., Chen, S. G., Petersen, R. B., Gambetti, P., Rubenstein, R.,

Smits, M. A., Lansbury, P. T., Jr. and Caughey, B. (1997). Molecular assessment of the potential transmissibilities of BSE and scrapie to humans. *Nature.* **388** (285-288).

Rayner, M. H. and Suzuki, K. T. (1995). A simple and effective method for the removal of trace metal cations from a mammalian culture medium supplemented with 10% fetal calf serum. *Biometals.* **8** (188-192).

Redecke, L., von Bergen, M., Clos, J., Konarev, P. V., Svergun, D. I., Fittschen, U. E., Broekaert, J. A., Bruns, O., Georgieva, D., Mandelkow, E., Genov, N. and Betzel, C. (2007). Structural characterization of beta-sheeted oligomers formed on the pathway of oxidative prion protein aggregation *in vitro*. *Journal of Structural Biology.* **157** (308-320).

Reixach, N., Deechongkit, S., Jiang, X., Kelly, J. W. and Buxbaum, J. N. (2004). Tissue damage in the amyloidoses: Transthyretin monomers and nonnative oligomers are the major cytotoxic species in tissue culture. *Proceedings of the National Academy of Sciences of the United States of America.* **101** (2817-2822).

Renne, T., Dedio, J., David, G. and Muller-Esterl, W. (2000). High molecular weight kininogen utilizes heparan sulfate proteoglycans for accumulation on endothelial cells. *Journal of Biological Chemistry.* **275** (33688-33696).

Requena, J. R., Groth, D., Legname, G., Stadtman, E. R., Prusiner, S. B. and Levine, R. L. (2001). Copper-catalyzed oxidation of the recombinant SHa(29-231) prion protein. *Proceedings of the National Academy of Sciences of the United States of America.* **98** (7170-7175).

Requena, J. R., Dimitrova, M. N., Legname, G., Teijeira, S., Prusiner, S. B. and Levine, R. L. (2004). Oxidation of methionine residues in the prion protein by hydrogen peroxide. *Archives of Biochemistry and Biophysics.* **432** (188-195).

Rezaei, H., Choiset, Y., Eghiaian, F., Treguer, E., Mentre, P., Debey, P., Grosclaude, J. and Haertle, T. (2002). Amyloidogenic unfolding intermediates differentiate sheep prion protein variants. *Journal of Molecular Biology.* **322** (799-814).

Rezaei, H., Eghiaian, F., Perez, J., Doublet, B., Choiset, Y., Haertle, T. and Grosclaude, J. (2005). Sequential generation of two structurally distinct ovine prion protein soluble oligomers displaying different biochemical reactivities. *Journal of Molecular Biology.* **347** (665-679).

Ricchelli, F., Buggio, R., Drago, D., Salmona, M., Forloni, G., Negro, A., Tognon, G. and Zatta, P. (2006). Aggregation/fibrillogenesis of recombinant human prion protein and Gerstmann-Straussler-Scheinker disease peptides in the presence of metal ions. *Biochemistry.* **45** (6724-6732).

Richt, J. A., Kasinathan, P., Hamir, A. N., Castilla, J., Sathiyaseelan, T., Vargas, F., Sathiyaseelan, J., Wu, H., Matsushita, H., Koster, J., Kato, S., Ishida, I., Soto, C., Robl,

J. M. and Kuroiwa, Y. (2007). Production of cattle lacking prion protein. *Nature Biotechnology.* **25** (132-138).

Riek, R., Hornemann, S., Wider, G., Billeter, M., Glockshuber, R. and Wuthrich, K. (1996). NMR structure of the mouse prion protein domain PrP(121-321). *Nature.* **382** (180-182).

Riek, R., Hornemann, S., Wider, G., Glockshuber, R. and Wuthrich, K. (1997). NMR characterization of the full-length recombinant murine prion protein, mPrP(23-231). *FEBS Letters.* **413** (282-288).

Rivera-Milla, E., Oidtmann, B., Panagiotidis, C. H., Baier, M., Sklaviadis, T., Hoffmann, R., Zhou, Y., Solis, G. P., Stuermer, C. A. and Malaga-Trillo, E. (2006). Disparate evolution of prion protein domains and the distinct origin of Doppel- and prion-related loci revealed by fish-to-mammal comparisons. *FASEB Journal.* **20** (317-319).

Roucou, X., Guo, Q., Zhang, Y., Goodyer, C. G. and LeBlanc, A. C. (2003). Cytosolic prion protein is not toxic and protects against Bax-mediated cell death in human primary neurons. *Journal of Biological Chemistry.* **278** (40877-40881).

Rowan, M. J., Klyubin, I., Wang, Q., Hu, N. W. and Anwyl, R. (2007). Synaptic memory mechanisms: Alzheimer's disease amyloid beta-peptide-induced dysfunction. *Biochemical Society Transactions.* **35** (1219-1223).

Rubenstein, R., Carp, R. I. and Callahan, S. M. (1984). *In vitro* replication of scrapie agent in a neuronal model: infection of PC12 cells. *Journal of General Virology.* **65** (Pt 12) (2191-2198).

Rudyk, H., Vasiljevic, S., Hennion, R. M., Birkett, C. R., Hope, J. and Gilbert, I. H. (2000). Screening Congo Red and its analogues for their ability to prevent the formation of PrP-res in scrapie-infected cells. *Journal of General Virology.* **81** (1155-1164).

Ryder, S., Dexter, G., Bellworthy, S. and Tongue, S. (2004). Demonstration of lateral transmission of scrapie between sheep kept under natural conditions using lymphoid tissue biopsy. *Research in Veterinary Science.* **76** (211-217).

Sabuncu, E., Petit, S., Le Dur, A., Lan Lai, T., Vilotte, J. L., Laude, H. and Vilette, D. (2003). PrP polymorphisms tightly control sheep prion replication in cultured cells. *Journal of Virology.* **77** (2696-2700).

Safar, J. G., Lessard, P., Tamguney, G., Freyman, Y., Deering, C., Letessier, F., Dearmond, S. J. and Prusiner, S. B. (2008). Transmission and detection of prions in feces. *Journal of Infectious Diseases.* **198** (81-89).

Safar, J., Roller, P. P., Gajdusek, D. C. and Gibbs, C. J., Jr. (1993). Thermal stability and conformational transitions of scrapie amyloid (prion) protein correlate with infectivity. *Protein Science.* **2** (2206-2216).

Sakaguchi, S., Katamine, S., Nishida, N., Moriuchi, R., Shigematsu, K., Sugimoto, T., Nakatani, A., Kataoka, Y., Houtani, T., Shirabe, S., Okada, H., Hasegawa, S., Miyamoto, T. and Noda, T. (1996). Loss of cerebellar Purkinje cells in aged mice homozygous for a disrupted PrP gene. *Nature.* **380** (528-531).

Sakaguchi, S., Katamine, S., Shigematsu, K., Nakatani, A., Moriuchi, R., Nishida, N., Kurokawa, K., Nakaoke, R., Sato, H., Jishage, K. and *et al*. (1995). Accumulation of proteinase K-resistant prion protein (PrP) is restricted by the expression level of normal PrP in mice inoculated with a mouse-adapted strain of the Creutzfeldt-Jakob disease agent. *Journal of Virology.* **69** (7586-7592).

Sakurai-Yamashita, Y., Sakaguchi, S., Yoshikawa, D., Okimura, N., Masuda, Y., Katamine, S. and Niwa, M. (2005). Female-specific neuroprotection against transient brain ischemia observed in mice devoid of prion protein is abolished by ectopic expression of prion protein-like protein. *Neuroscience.* **136** (281-287).

Santuccione, A., Sytnyk, V., Leshchyns'ka, I. and Schachner, M. (2005). Prion protein recruits its neuronal receptor NCAM to lipid rafts to activate p59fyn and to enhance neurite outgrowth. *Journal of Cell Biology***. 169** (341-354).

Sasaki, K., Minaki, H. and Iwaki, T. (2009). Development of oligomeric prion-protein aggregates in a mouse model of prion disease. *Journal of Pathology.* **219** (123-130).

Satoh, J., Obayashi, S., Misawa, T., Sumiyoshi, K., Oosumi, K. and Tabunoki, H. (2009). Protein microarray analysis identifies human cellular prion protein interactors. *Neuropathology and Applied Neurobiology.* **35** (16-35).

Schatzl, H. M., Laszlo, L., Holtzman, D. M., Tatzelt, J., DeArmond, S. J., Weiner, R. I., Mobley, W. C. and Prusiner, S. B. (1997). A hypothalamic neuronal cell line persistently infected with scrapie prions exhibits apoptosis. *Journal of Virology.* **71** (8821-8831).

Schmitt-Ulms, G., Legname, G., Baldwin, M. A., Ball, H. L., Bradon, N., Bosque, P. J., Crossin, K. L., Edelman, G. M., DeArmond, S. J., Cohen, F. E. and Prusiner, S. B. (2001). Binding of neural cell adhesion molecules (N-CAMs) to the cellular prion protein. *Journal of Molecular Biology.* **314** (1209-1225).

Schneider, B., Mutel, V., Pietri, M., Ermonval, M., Mouillet-Richard, S. and Kellermann, O. (2003). NADPH oxidase and extracellular regulated kinases 1/2 are targets of prion protein signaling in neuronal and nonneuronal cells. *Proceedings of the National Academy of Sciences of the United States of America.* **100** (13326-13331).

Schonberger, O., Horonchik, L., Gabizon, R., Papy-Garcia, D., Barritault, D. and Taraboulos, A. (2003). Novel heparan mimetics potently inhibit the scrapie prion protein and its endocytosis. *Biochemical and Biophysical Research Communications.* **312** (473-479).

Schulz-Schaeffer, W. J., Tschoke, S., Kranefuss, N., Drose, W., Hause-Reitner, D., Giese, A., Groschup, M. H. and Kretzschmar, H. A. (2000). The paraffin-embedded tissue blot detects PrP(Sc) early in the incubation time in prion diseases. *American Journal of Pathology.* **156** (51-56).

Scott, M. R., Will, R., Ironside, J., Nguyen, H. O., Tremblay, P., DeArmond, S. J. and Prusiner, S. B. (1999). Compelling transgenetic evidence for transmission of bovine spongiform encephalopathy prions to humans. *Proceedings of the National Academy of Sciences of the United States of America.* **96** (15137-15142).

Shaked, G. M., Meiner, Z., Avraham, I., Taraboulos, A. and Gabizon, R. (2001). Reconstitution of prion infectivity from solubilized protease-resistant PrP and nonprotein components of prion rods. *Journal of Biological Chemistry.* **276** (14324-14328).

Shearer, J., Soh, P. and Lentz, S. (2008). Both Met(109) and Met(112) are utilized for Cu(II) coordination by the amyloidogenic fragment of the human prion protein at physiological pH. *Journal of Inorganic Biochemistry.* **102** (2103-2113).

Shewmaker, F., Wickner, R. B. and Tycko, R. (2006). Amyloid of the prion domain of Sup35p has an in-register parallel beta-sheet structure. *Proceedings of the National Academy of Sciences of the United States of America.* **103** (19754-19759).

Shiraishi, N., Inai, Y. and Ihara, Y. (2009). Proteinase K-resistant aggregates of recombinant prion protein PrP-(23-98) are toxic to cultured cells. *Protein & Peptide Letters.* **16** (91-96).

Shiraishi, N., Inai, Y., Bi, W. and Nishikimi, M. (2005). Fragmentation and dimerization of copper-loaded prion protein by copper-catalysed oxidation. *Biochemical Journal.* **387** (247-255).

Shiraishi, N., Utsunomiya, H. and Nishikimi, M. (2006). Combination of NADPH and copper ions generates proteinase K-resistant aggregates from recombinant prion protein. *Journal of Biological Chemistry.* **281** (34880-34887).

Shyng, S. L., Heuser, J. E. and Harris, D. A. (1994). A glycolipid-anchored prion protein is endocytosed via clathrin-coated pits. *Journal of Cell Biology.* **125** (1239-1250).

Shyng, S. L., Huber, M. T. and Harris, D. A. (1993). A prion protein cycles between the cell surface and an endocytic compartment in cultured neuroblastoma cells. *Journal of Biological Chemistry.* **268** (15922-15928).

Shyng, S. L., Lehmann, S., Moulder, K. L. and Harris, D. A. (1995a). Sulfated glycans stimulate endocytosis of the cellular isoform of the prion protein, PrP^C, in cultured cells. *Journal of Biological Chemistry.* **270** (30221-30229).

Shyng, S. L., Moulder, K. L., Lesko, A. and Harris, D. A. (1995b). The N-terminal domain of a glycolipid-anchored prion protein is essential for its endocytosis via clathrin-coated pits. *Journal of Biological Chemistry.* **270** (14793-14800).

Shyu, W. C., Chen, C. P., Saeki, K., Kubosaki, A., Matusmoto, Y., Onodera, T., Ding, D. C., Chiang, M. F., Lee, Y. J., Lin, S. Z. and Li, H. (2005). Hypoglycemia enhances the expression of prion protein and heat-shock protein 70 in a mouse neuroblastoma cell line. *Journal of Neuroscience Research.* **80** (887-894).

Shyu, W. C., Kao, M. C., Chou, W. Y., Hsu, Y. D. and Soong, B. W. (2000). Heat shock modulates prion protein expression in human NT-2 cells. *Neuroreport.* **11** (771-774).

Shyu, W. C., Lin, S. Z., Saeki, K., Kubosaki, A., Matsumoto, Y., Onodera, T., Chiang, M. F., Thajeb, P. and Li, H. (2004). Hyperbaric oxygen enhances the expression of prion protein and heat shock protein 70 in a mouse neuroblastoma cell line. *Cellular and Molecular Neurobiology.* **24** (257-268).

Sigurdson, C. J., Spraker, T. R., Miller, M. W., Oesch, B. and Hoover, E. A. (2001). PrP(CWD) in the myenteric plexus, vagosympathetic trunk and endocrine glands of deer with chronic wasting disease. *Journal of General Virology.* **82** (2327-2334).

Sigurdsson, E. M., Brown, D. R., Alim, M. A., Scholtzova, H., Carp, R., Meeker, H. C., Prelli, F., Frangione, B. and Wisniewski, T. (2003). Copper chelation delays the onset of prion disease. *Journal of Biological Chemistry.* **278** (46199-46202).

Sikorska, B., Liberski, P. P., Sobow, T., Budka, H. and Ironside, J. W. (2009). Ultrastructural study of florid plaques in variant Creutzfeldt-Jakob disease: a comparison with amyloid plaques in kuru, sporadic Creutzfeldt-Jakob disease and Gerstmann-Straussler-Scheinker disease. *Neuropathology and Applied Neurobiology.* **35** (46-59).

Silveira, J. R., Raymond, G. J., Hughson, A. G., Race, R. E., Sim, V. L., Hayes, S. F. and Caughey, B. (2005). The most infectious prion protein particles. *Nature.* **437** (257-261).

Simoneau, S., Rezaei, H., Sales, N., Kaiser-Schulz, G., Lefebvre-Roque, M., Vidal, C., Fournier, J. G., Comte, J., Wopfner, F., Grosclaude, J., Schatzl, H. and Lasmezas, C. I. (2007). *In vitro* and *in vivo* neurotoxicity of prion protein oligomers. *PLoS Pathogens.* **3** (e125).

Singh, A., Isaac, A. O., Luo, X., Mohan, M. L., Cohen, M. L., Chen, F., Kong, Q., Bartz, J. and Singh, N. (2009a). Abnormal brain iron homeostasis in human and animal prion disorders. *PLoS Pathogens.* **5** (e1000336).

Singh, A., Kong, Q., Luo, X., Petersen, R. B., Meyerson, H. and Singh, N. (2009b). Prion protein (PrP) knock-out mice show altered iron metabolism: a functional role for PrP in iron uptake and transport. *PLoS One.* **4** (e6115).

Singh, A., Mohan, M. L., Isaac, A. O., Luo, X., Petrak, J., Vyoral, D. and Singh, N. (2009c). Prion protein modulates cellular iron uptake: a novel function with implications for prion disease pathogenesis. *PLoS One.* **4** (e4468).

Singh, N., Zanusso, G., Chen, S. G., Fujioka, H., Richardson, S., Gambetti, P. and Petersen, R. B. (1997). Prion protein aggregation reverted by low temperature in transfected cells carrying a prion protein gene mutation. *Journal of Biological Chemistry.* **272** (28461-28470).

Snow, A. D. and Wight, T. N. (1989). Proteoglycans in the pathogenesis of Alzheimer's disease and other amyloidoses. *Neurobiology of Aging.* **10** (481-497).

Snow, A. D., Kisilevsky, R., Willmer, J., Prusiner, S. B. and DeArmond, S. J. (1989). Sulfated glycosaminoglycans in amyloid plaques of prion diseases. *Acta Neuropathol.* **77** (337-342).

Snow, A. D., Wight, T. N., Nochlin, D., Koike, Y., Kimata, K., DeArmond, S. J. and Prusiner, S. B. (1990). Immunolocalization of heparan sulfate proteoglycans to the prion protein amyloid plaques of Gerstmann-Straussler syndrome, Creutzfeldt-Jakob disease and scrapie. *Laboratory Investigation.* **63** (601-611).

Sokolowski, F., Modler, A. J., Masuch, R., Zirwer, D., Baier, M., Lutsch, G., Moss, D. A., Gast, K. and Naumann, D. (2003). Formation of critical oligomers is a key event during conformational transition of recombinant syrian hamster prion protein. *Journal of Biological Chemistry.* **278** (40481-40492).

Solassol, J., Crozet, C. and Lehmann, S. (2003). Prion propagation in cultured cells. *British Medical Bulletin.* **66** (87-97).

Solforosi, L., Criado, J. R., McGavern, D. B., Wirz, S., Sanchez-Alavez, M., Sugama, S., DeGiorgio, L. A., Volpe, B. T., Wiseman, E., Abalos, G., Masliah, E., Gilden, D., Oldstone, M. B., Conti, B. and Williamson, R. A. (2004). Cross-linking cellular prion protein triggers neuronal apoptosis *in vivo*. *Science.* **303** (1514-1516).

Soto, C. and Estrada, L. D. (2008). Protein misfolding and neurodegeneration. *Archives of Neurology.* **65** (184-189).

Speare, J. O., Rush, T. S., 3rd, Bloom, M. E. and Caughey, B. (2003). The role of helix 1 aspartates and salt bridges in the stability and conversion of prion protein. *Journal of Biological Chemistry.* **278** (12522-12529).

Stahl, N., Borchelt, D. R. and Prusiner, S. B. (1990). Differential release of cellular and scrapie prion proteins from cellular membranes by phosphatidylinositol-specific phospholipase C. *Biochemistry.* **29** (5405-5412).

Stanczak, P. and Kozlowski, H. (2007). Can chicken and human PrPs possess SOD-like activity after beta-cleavage? *Biochemical and Biophysical Research Communications.* **352** (198-202).

Stockel, J., Safar, J., Wallace, A. C., Cohen, F. E. and Prusiner, S. B. (1998). Prion protein selectively binds copper(II) ions. *Biochemistry.* **37** (7185-7193).

Stohr, J., Weinmann, N., Wille, H., Kaimann, T., Nagel-Steger, L., Birkmann, E., Panza, G., Prusiner, S. B., Eigen, M. and Riesner, D. (2008). Mechanisms of prion protein assembly into amyloid. *Proceedings of the National Academy of Sciences of the United States of America.* **105** (2409-2414).

Stuermer, C. A., Langhorst, M. F., Wiechers, M. F., Legler, D. F., Von Hanwehr, S. H., Guse, A. H. and Plattner, H. (2004). PrP^{C} capping in T cells promotes its association with the lipid raft proteins reggie-1 and reggie-2 and leads to signal transduction. *FASEB Journal.* **18** (1731-1733).

Sugiura, M., Kawasaki, T. and Yamashina, I. (1982). Purification and characterization of UDP-GalNAc:polypeptide N-acetylgalactosamine transferase from an ascites hepatoma, AH 66. *Journal of Biological Chemistry.* **257** (9501-9507).

Sun, Y., Makarava, N., Lee, C. I., Laksanalamai, P., Robb, F. T. and Baskakov, I. V. (2008). Conformational stability of PrP amyloid fibrils controls their smallest possible fragment size. *Journal of Molecular Biology.* **376** (1155-1167).

Sunyach, C., Cisse, M. A., da Costa, C. A., Vincent, B. and Checler, F. (2007). The C-terminal products of cellular prion protein processing, C1 and C2, exert distinct influence on p53-dependent staurosporine-induced caspase-3 activation. *Journal of Biological Chemistry.* **282** (1956-1963).

Sunyach, C., Jen, A., Deng, J., Fitzgerald, K. T., Frobert, Y., Grassi, J., McCaffrey, M. W. and Morris, R. (2003). The mechanism of internalization of glycosylphosphatidylinositol-anchored prion protein. *EMBO Journal.* **22** (3591-3601).

Supattapone, S., Nguyen, H. O., Cohen, F. E., Prusiner, S. B. and Scott, M. R. (1999). Elimination of prions by branched polyamines and implications for therapeutics. *Proceedings of the National Academy of Sciences of the United States of America.* **96** (14529-14534).

Tahiri-Alaoui, A. and James, W. (2005). Rapid formation of amyloid from alpha-monomeric recombinant human PrP *in vitro*. *Protein Science.* **14** (942-947).

Tahiri-Alaoui, A., Gill, A. C., Disterer, P. and James, W. (2004). Methionine 129 variant of human prion protein oligomerizes more rapidly than the valine 129 variant:

implications for disease susceptibility to Creutzfeldt-Jakob disease. *Journal of Biological Chemistry.* **279** (31390-31397).

Tahiri-Alaoui, A., Sim, V. L., Caughey, B. and James, W. (2006). Molecular heterosis of prion protein beta-oligomers. A potential mechanism of human resistance to disease. *Journal of Biological Chemistry.* **281** (34171-34178).

Tank, E. M., Harris, D. A., Desai, A. A. and True, H. L. (2007). Prion protein repeat expansion results in increased aggregation and reveals phenotypic variability. *Molecular and Cellular Biology.* **27** (5445-5455).

Taraboulos, A., Raeber, A. J., Borchelt, D. R., Serban, D. and Prusiner, S. B. (1992). Synthesis and trafficking of prion proteins in cultured cells. Molecular Biology of the Cell. 3 (851-863).

Taylor, D. R. and Hooper, N. M. (2007). Role of lipid rafts in the processing of the pathogenic prion and Alzheimer's amyloid-beta proteins. *Seminars in Cell and Developmental Biology.* **18** (638-648).

Taylor, D. R., Watt, N. T., Perera, W. S. and Hooper, N. M. (2005). Assigning functions to distinct regions of the N-terminus of the prion protein that are involved in its copper-stimulated, clathrin-dependent endocytosis. *Journal of Cell Science.* **118** (5141-5153).

Telling, G. C. (2004). The mechanism of prion strain propagation. *Genome Biology.* **5** (222).

Teplow, D. B., Lazo, N. D., Bitan, G., Bernstein, S., Wyttenbach, T., Bowers, M. T., Baumketner, A., Shea, J. E., Urbanc, B., Cruz, L., Borreguero, J. and Stanley, H. E. (2006). Elucidating amyloid beta-protein folding and assembly: A multidisciplinary approach. *Accounts of Chemical Research.* **39** (635-645).

Terry, L. A., Marsh, S., Ryder, S. J., Hawkins, S. A., Wells, G. A. and Spencer, Y. I. (2003). Detection of disease-specific PrP in the distal ileum of cattle exposed orally to the agent of bovine spongiform encephalopathy. *Veterinary Record.* **152** (387-392).

Thackray, A. M., Fitzmaurice, T. J., Hopkins, L. and Bujdoso, R. (2006). Ovine plasma prion protein levels show genotypic variation detected by C-terminal epitopes not exposed in cell-surface PrP^{C}. *Biochemical Journal.* **400** (349-358).

Thackray, A. M., Hopkins, L. and Bujdoso, R. (2007a). Proteinase K-sensitive disease-associated ovine prion protein revealed by conformation-dependent immunoassay. *Biochemical Journal.* **401** (475-483).

Thackray, A. M., Hopkins, L., Klein, M. A. and Bujdoso, R. (2007b). Mouse-adapted ovine scrapie prion strains are characterized by different conformers of PrP^{Sc}. *Journal of Virology.* **81** (12119-12127).

Thackray, A. M., Klein, M. A. and Bujdoso, R. (2003a). Subclinical prion disease induced by oral inoculation. *Journal of Virology.* **77** (7991-7998).

Thackray, A. M., Klein, M. A., Aguzzi, A. and Bujdoso, R. (2002a). Chronic subclinical prion disease induced by low-dose inoculum. *Journal of Virology.* **76** (2510-2517).

Thackray, A. M., Knight, R., Haswell, S. J., Bujdoso, R. and Brown, D. R. (2002b). Metal imbalance and compromised antioxidant function are early changes in prion disease. *Biochemical Journal.* **362** (253-258).

Thackray, A. M., Madec, J. Y., Wong, E., Morgan-Warren, R., Brown, D. R., Baron, T. and Bujdoso, R. (2003b). Detection of bovine spongiform encephalopathy, ovine scrapie prion-related protein (PrP^{Sc}) and normal PrP^{C} by monoclonal antibodies raised to copper-refolded prion protein. *Biochemical Journal.* **370** (81-90).

Thackray, A. M., McKenzie, A. N., Klein, M. A., Lauder, A. and Bujdoso, R. (2004a). Accelerated prion disease in the absence of interleukin-10. *Journal of Virology.* **78** (13697-13707).

Thackray, A. M., Ryder, S. J. and Bujdoso, R. (2005). Modification of blood cell PrP epitope exposure during prion disease. *Biochemical Journal.* **390** (563-571).

Thackray, A. M., Yang, S., Wong, E., Fitzmaurice, T. J., Morgan-Warren, R. J. and Bujdoso, R. (2004b). Conformational variation between allelic variants of cell-surface ovine prion protein. *Biochemical Journal.* **381** (221-229).

Thompsett, A. R., Abdelraheim, S. R., Daniels, M. and Brown, D. R. (2005). High affinity binding between copper and full-length prion protein identified by two different techniques. *Journal of Biological Chemistry.* **280** (42750-42758).

Thomzig, A., Cardone, F., Kruger, D., Pocchiari, M., Brown, P. and Beekes, M. (2006). Pathological prion protein in muscles of hamsters and mice infected with rodent-adapted BSE or vCJD. *Journal of General Virology.* **87** (251-254).

Thomzig, A., Schulz-Schaeffer, W., Kratzel, C., Mai, J. and Beekes, M. (2004). Preclinical deposition of pathological prion protein PrP^{Sc} in muscles of hamsters orally exposed to scrapie. *Journal of Clinical Investigation.* **113** (1465-1472).

Thomzig, A., Schulz-Schaeffer, W., Wrede, A., Wemheuer, W., Brenig, B., Kratzel, C., Lemmer, K. and Beekes, M. (2007). Accumulation of pathological prion protein PrP^{Sc} in the skin of animals with experimental and natural scrapie. *PLoS Pathogens.* **3** (e66).

Tobler, I., Gaus, S. E., Deboer, T., Achermann, P., Fischer, M., Rulicke, T., Moser, M., Oesch, B., McBride, P. A. and Manson, J. C. (1996). Altered circadian activity rhythms and sleep in mice devoid of prion protein. *Nature.* **380** (639-642).

Toni, M., Massimino, M. L., Griffoni, C., Salvato, B., Tomasi, V. and Spisni, E. (2005). Extracellular copper ions regulate cellular prion protein (PrP^C) expression and metabolism in neuronal cells. *FEBS Letters.* **579** (741-744).

Torok, M., Milton, S., Kayed, R., Wu, P., McIntire, T., Glabe, C. G. and Langen, R. (2002). Structural and dynamic features of Alzheimer's Abeta peptide in amyloid fibrils studied by site-directed spin labeling. *Journal of Biological Chemistry.* **277** (40810-40815).

Treiber, C., Pipkorn, R., Weise, C., Holland, G. and Multhaup, G. (2007). Copper is required for prion protein-associated superoxide dismutase-I activity in Pichia pastoris. *FEBS Journal.* **274** (1304-1311).

Treiber, C., Simons, A. and Multhaup, G. (2006). Effect of copper and manganese on the de novo generation of protease-resistant prion protein in yeast cells. *Biochemistry.* **45** (6674-6680).

Tsiroulnikov, K., Rezaei, H., Dalgalarrondo, M., Chobert, J. M., Grosclaude, J. and Haertle, T. (2006). Cu(II) induces small-size aggregates with amyloid characteristics in two alleles of recombinant ovine prion proteins. *Biochimica et Biophysica Acta.* **1764** (1218-1226).

Tuzi, N. L., Cancellotti, E., Baybutt, H., Blackford, L., Bradford, B., Plinston, C., Coghill, A., Hart, P., Piccardo, P., Barron, R. M. and Manson, J. C. (2008). Host PrP glycosylation: a major factor determining the outcome of prion infection. *PLoS Biology.* **6** (e100).

Tzaban, S., Friedlander, G., Schonberger, O., Horonchik, L., Yedidia, Y., Shaked, G., Gabizon, R. and Taraboulos, A. (2002). Protease-sensitive scrapie prion protein in aggregates of heterogeneous sizes. *Biochemistry.* **41** (12868-12875).

Unterberger, U., Voigtlander, T. and Budka, H. (2005). Pathogenesis of prion diseases. *Acta Neuropathol.* **109** (32-48).

Van Baelen, K., Vanoevelen, J., Missiaen, L., Raeymaekers, L. and Wuytack, F. (2001). The Golgi PMR1 P-type ATPase of Caenorhabditis elegans. Identification of the gene and demonstration of calcium and manganese transport. *Journal of Biological Chemistry.* **276** (10683-10691).

van den Berghe, P. V., Folmer, D. E., Malingre, H. E., van Beurden, E., Klomp, A. E., van de Sluis, B., Merkx, M., Berger, R. and Klomp, L. W. (2007). Human copper transporter 2 is localized in late endosomes and lysosomes and facilitates cellular copper uptake. *Biochemical Journal.* **407** (49-59).

van Keulen, L. J., Schreuder, B. E., Vromans, M. E., Langeveld, J. P. and Smits, M. A. (2000). Pathogenesis of natural scrapie in sheep. *Archives of Virology, Supplement.* **16** (57-71).

van Keulen, L. J., Vromans, M. E. and van Zijderveld, F. G. (2002). Early and late pathogenesis of natural scrapie infection in sheep. *Acta Pathologica, Microbiologica et Immunologica Scandinavica.* **110** (23-32).

Vascellari, M., Nonno, R., Mutinelli, F., Bigolaro, M., Di Bari, M. A., Melchiotti, E., Marcon, S., D'Agostino, C., Vaccari, G., Conte, M., De Grossi, L., Rosone, F., Giordani, F. and Agrimi, U. (2007). PrP^{Sc} in salivary glands of scrapie-affected sheep. *Journal of Virology.* **81** (4872-4876).

Vassallo, N., Herms, J., Behrens, C., Krebs, B., Saeki, K., Onodera, T., Windl, O. and Kretzschmar, H. A. (2005). Activation of phosphatidylinositol 3-kinase by cellular prion protein and its role in cell survival. *Biochemical and Biophysical Research Communications.* **332** (75-82).

Vella, L. J., Sharples, R. A., Lawson, V. A., Masters, C. L., Cappai, R. and Hill, A. F. (2007). Packaging of prions into exosomes is associated with a novel pathway of PrP processing. *Journal of Pathology.* **211** (582-590).

Vendrely, C., Valadie, H., Bednarova, L., Cardin, L., Pasdeloup, M., Cappadoro, J., Bednar, J., Rinaudo, M. and Jamin, M. (2005). Assembly of the full-length recombinant mouse prion protein I. Formation of soluble oligomers. *Biochimica et Biophysica Acta.* **1724** (355-366).

Vey, M., Pilkuhn, S., Wille, H., Nixon, R., DeArmond, S. J., Smart, E. J., Anderson, R. G., Taraboulos, A. and Prusiner, S. B. (1996). Subcellular colocalization of the cellular and scrapie prion proteins in caveolae-like membranous domains. *Proceedings of the National Academy of Sciences of the United States of America.* **93** (14945-14949).

Vieira, M. N., Forny-Germano, L., Saraiva, L. M., Sebollela, A., Martinez, A. M., Houzel, J. C., De Felice, F. G. and Ferreira, S. T. (2007). Soluble oligomers from a non-disease related protein mimic Abeta-induced tau hyperphosphorylation and neurodegeneration. *Journal of Neurochemistry.* **103** (736-748).

Viles, J. H., Cohen, F. E., Prusiner, S. B., Goodin, D. B., Wright, P. E. and Dyson, H. J. (1999). Copper binding to the prion protein: structural implications of four identical cooperative binding sites. *Proceedings of the National Academy of Sciences of the United States of America.* **96** (2042-2047).

Vilette, D. (2008). Cell models of prion infection. *Veterinary Research.* **39** (10).

Vilette, D., Andreoletti, O., Archer, F., Madelaine, M. F., Vilotte, J. L., Lehmann, S. and Laude, H. (2001). Ex vivo propagation of infectious sheep scrapie agent in heterologous epithelial cells expressing ovine prion protein. *Proceedings of the National Academy of Sciences of the United States of America.* **98** (4055-4059).

Villa, V., Corsaro, A., Thellung, S., Paludi, D., Chiovitti, K., Venezia, V., Nizzari, M., Russo, C., Schettini, G., Aceto, A. and Florio, T. (2006). Characterization of the

proapoptotic intracellular mechanisms induced by a toxic conformer of the recombinant human prion protein fragment 90-231. *Annals of the New York Academy of Sciences.* **1090** (276-291).

Voigtlander, T., Unterberger, U., Touma, C., Palme, R., Polster, B., Strohschneider, M., Dorner, S. and Budka, H. (2006). Prominent corticosteroid disturbance in experimental prion disease. *European Journal of Neuroscience.* **23** (2723-2730).

von Poser-Klein, C., Flechsig, E., Hoffmann, T., Schwarz, P., Harms, H., Bujdoso, R., Aguzzi, A. and Klein, M. A. (2008). Alteration of B-cell subsets enhances neuroinvasion in mouse scrapie infection. *Journal of Virology.* **82** (3791-3795).

Vorberg, I., Raines, A. and Priola, S. A. (2004). Acute formation of protease-resistant prion protein does not always lead to persistent scrapie infection *in vitro*. *Journal of Biological Chemistry.* **279** (29218-29225).

Wadsworth, J. D., Hill, A. F., Joiner, S., Jackson, G. S., Clarke, A. R. and Collinge, J. (1999). Strain-specific prion-protein conformation determined by metal ions. *Nature Cell Biology.* **1** (55-59).

Wadsworth, J. D., Joiner, S., Hill, A. F., Campbell, T. A., Desbruslais, M., Luthert, P. J. and Collinge, J. (2001). Tissue distribution of protease resistant prion protein in variant Creutzfeldt-Jakob disease using a highly sensitive immunoblotting assay. *Lancet.* **358** (171-180).

Walsh, D. M., Klyubin, I., Fadeeva, J. V., Cullen, W. K., Anwyl, R., Wolfe, M. S., Rowan, M. J. and Selkoe, D. J. (2002). Naturally secreted oligomers of amyloid beta protein potently inhibit hippocampal long-term potentiation *in vivo*. *Nature.* **416** (535-539).

Walter, E. D., Stevens, D. J., Visconte, M. P. and Millhauser, G. L. (2007). The prion protein is a combined zinc and copper binding protein: Zn2+ alters the distribution of Cu2+ coordination modes. *Journal of the American Chemical Society.* **129** (15440-15441).

Wang, J., Markesbery, W. R. and Lovell, M. A. (2006). Increased oxidative damage in nuclear and mitochondrial DNA in mild cognitive impairment. *Journal of Neurochemistry.* **96** (825-832).

Warner, R. G., Hundt, C., Weiss, S. and Turnbull, J. E. (2002). Identification of the heparan sulfate binding sites in the cellular prion protein. *Journal of Biological Chemistry.* **277** (18421-18430).

Watt, N. T. and Hooper, N. M. (2003). The prion protein and neuronal zinc homeostasis. *Trends in Biochemical Sciences.* **28** (406-410).

Watt, N. T., Routledge, M. N., Wild, C. P. and Hooper, N. M. (2007). Cellular prion protein protects against reactive-oxygen-species-induced DNA damage. *Free Radical Biology and Medicine.* **43** (959-967).

Watzlawik, J., Skora, L., Frense, D., Griesinger, C., Zweckstetter, M., Schulz-Schaeffer, W. J. and Kramer, M. L. (2006). Prion protein helix1 promotes aggregation but is not converted into beta-sheet. *Journal of Biological Chemistry.* **281** (30242-30250).

Weise, J., Crome, O., Sandau, R., Schulz-Schaeffer, W., Bahr, M. and Zerr, I. (2004). Upregulation of cellular prion protein (PrP^C) after focal cerebral ischemia and influence of lesion severity. *Neuroscience Letters.* **372** (146-150).

Weise, J., Sandau, R., Schwarting, S., Crome, O., Wrede, A., Schulz-Schaeffer, W., Zerr, I. and Bahr, M. (2006). Deletion of cellular prion protein results in reduced Akt activation, enhanced postischemic caspase-3 activation, and exacerbation of ischemic brain injury. *Stroke.* **37** (1296-1300).

Weissmann, C. (1991). A 'unified theory' of prion propagation. *Nature.* **352** (679-683).

Weissmann, C., Bueler, H., Fischer, M., Sailer, A., Aguzzi, A. and Aguet, M. (1994a). PrP-deficient mice are resistant to scrapie. *Annals of the New York Academy of Sciences.* **724** (235-240).

Weissmann, C., Bueler, H., Fischer, M., Sauer, A. and Aguet, M. (1994b). Susceptibility to scrapie in mice is dependent on PrP^C. *Philosophical Transactions of the Royal Society of London. Series B: Biological Sciences.* **343** (431-433).

Wells, G. A., Scott, A. C., Johnson, C. T., Gunning, R. F., Hancock, R. D., Jeffrey, M., Dawson, M. and Bradley, R. (1987). A novel progressive spongiform encephalopathy in cattle. *Veterinary Record.* **121** (419-420).

Whittal, R. M., Ball, H. L., Cohen, F. E., Burlingame, A. L., Prusiner, S. B. and Baldwin, M. A. (2000). Copper binding to octarepeat peptides of the prion protein monitored by mass spectrometry. *Protein Science.* **9** (332-343).

Whittle, I. R., Knight, R. S. and Will, R. G. (2006). Unsuccessful intraventricular pentosan polysulphate treatment of variant Creutzfeldt-Jakob disease. *Acta Neurochirurgica.* **148** (677-679; discussion 679).

Will, R. G., Ironside, J. W., Zeidler, M., Cousens, S. N., Estibeiro, K., Alperovitch, A., Poser, S., Pocchiari, M., Hofman, A. and Smith, P. G. (1996). A new variant of Creutzfeldt-Jakob disease in the UK. *Lancet.* **347** (921-925).

Wille, H., Zhang, G. F., Baldwin, M. A., Cohen, F. E. and Prusiner, S. B. (1996). Separation of scrapie prion infectivity from PrP amyloid polymers. *Journal of Molecular Biology.* **259** (608-621).

Williams, E. S. and Miller, M. W. (2003). Transmissible spongiform encephalopathies in non-domestic animals: origin, transmission and risk factors. *Revue Scientifique et Technique.* **22** (145-156).

Williams, E. S. and Young, S. (1980). Chronic wasting disease of captive mule deer: a spongiform encephalopathy. *Journal of Wildlife Diseases.* **16** (89-98).

Willoughby, K., Kelly, D. F., Lyon, D. G. and Wells, G. A. (1992). Spongiform encephalopathy in a captive puma (Felis concolor). *Veterinary Record.* **131** (431-434).

Wojcik, C. (2002). Regulation of apoptosis by the ubiquitin and proteasome pathway. *Journal of Cellular and Molecular Medicine.* **6** (25-48).

Wojda, U., Salinska, E. and Kuznicki, J. (2008). Calcium ions in neuronal degeneration. *IUBMB Life*. **60** (575-590).

Wong, B. S., Brown, D. R., Pan, T., Whiteman, M., Liu, T., Bu, X., Li, R., Gambetti, P., Olesik, J., Rubenstein, R. and Sy, M. S. (2001a). Oxidative impairment in scrapie-infected mice is associated with brain metals perturbations and altered antioxidant activities. *Journal of Neurochemistry.* **79** (689-698).

Wong, B. S., Chen, S. G., Colucci, M., Xie, Z., Pan, T., Liu, T., Li, R., Gambetti, P., Sy, M. S. and Brown, D. R. (2001b). Aberrant metal binding by prion protein in human prion disease. *Journal of Neurochemistry.* **78** (1400-1408).

Wong, B. S., Clive, C., Haswell, S. J., Williamson, R. A., Burton, D. R., Gambetti, P., Sy, M. S., Jones, I. M. and Brown, D. R. (2000a). Copper has differential effect on prion protein with polymorphism of position 129. *Biochemical and Biophysical Research Communications.* **269** (726-731).

Wong, B. S., Liu, T., Li, R., Pan, T., Petersen, R. B., Smith, M. A., Gambetti, P., Perry, G., Manson, J. C., Brown, D. R. and Sy, M. S. (2001c). Increased levels of oxidative stress markers detected in the brains of mice devoid of prion protein. *Journal of Neurochemistry.* **76** (565-572).

Wong, B. S., Pan, T., Liu, T., Li, R., Gambetti, P. and Sy, M. S. (2000c). Differential contribution of superoxide dismutase activity by prion protein *in vivo*. *Biochemical and Biophysical Research Communications.* **273** (136-139).

Wong, B. S., Venien-Bryan, C., Williamson, R. A., Burton, D. R., Gambetti, P., Sy, M. S., Brown, D. R. and Jones, I. M. (2000b). Copper refolding of prion protein. *Biochemical and Biophysical Research Communications.* **276** (1217-1224).

Wong, C., Xiong, L. W., Horiuchi, M., Raymond, L., Wehrly, K., Chesebro, B. and Caughey, B. (2001d). Sulfated glycans and elevated temperature stimulate PrP(Sc)-dependent cell-free formation of protease-resistant prion protein. *EMBO Journal.* **20** (377-386).

Wong, E., Thackray, A. M. and Bujdoso, R. (2004). Copper induces increased beta-sheet content in the scrapie-susceptible ovine prion protein PrPVRQ compared with the resistant allelic variant PrPARR. *Biochemical Journal.* **380** (273-282).

Wright, J. A., McHugh, P. C., Stockbridge, M., Lane, S., Kralovicova, S. and Brown, D. R. (2009a). Activation and repression of prion protein expression by key regions of intron 1. *Cellular and Molecular Life Sciences.* In Press

Wright, J. A., Wang, X. and Brown, D. R. (2009b). Unique copper-induced oligomers mediate alpha-synuclein toxicity. *FASEB Journal.* **23** (2384-2393).

Wyatt, J. M., Pearson, G. R., Smerdon, T. N., Gruffydd-Jones, T. J., Wells, G. A. and Wilesmith, J. W. (1991). Naturally occurring scrapie-like spongiform encephalopathy in five domestic cats. *Veterinary Record.* **129** (233-236).

Yang, S., Thackray, A. M., Fitzmaurice, T. J. and Bujdoso, R. (2008). Copper-induced structural changes in the ovine prion protein are influenced by a polymorphism at codon 112. *Biochimica et Biophysica Acta.* **1784** (683-692).

Yedidia, Y., Horonchik, L., Tzaban, S., Yanai, A. and Taraboulos, A. (2001). Proteasomes and ubiquitin are involved in the turnover of the wild-type prion protein. *EMBO Journal.* **20** (5383-5391).

Yin, S., Pham, N., Yu, S., Li, C., Wong, P., Chang, B., Kang, S. C., Biasini, E., Tien, P., Harris, D. A. and Sy, M. S. (2007). Human prion proteins with pathogenic mutations share common conformational changes resulting in enhanced binding to glycosaminoglycans. *Proceedings of the National Academy of Sciences of the United States of America.* **104** (7546-7551).

Yin, S., Yu, S., Li, C., Wong, P., Chang, B., Xiao, F., Kang, S. C., Yan, H., Xiao, G., Grassi, J., Tien, P. and Sy, M. S. (2006). Prion proteins with insertion mutations have altered N-terminal conformation and increased ligand binding activity and are more susceptible to oxidative attack. *Journal of Biological Chemistry.* **281** (10698-10705).

Yost, C. S., Lopez, C. D., Prusiner, S. B., Myers, R. M. and Lingappa, V. R. (1990). Non-hydrophobic extracytoplasmic determinant of stop transfer in the prion protein. *Nature.* **343** (669-672).

Yu, S., Yin, S., Li, C., Wong, P., Chang, B., Xiao, F., Kang, S. C., Yan, H., Xiao, G., Tien, P. and Sy, M. S. (2007). Aggregation of prion protein with insertion mutations is proportional to the number of inserts. *Biochemical Journal.* **403** (343-351).

Yu, S., Yin, S., Pham, N., Wong, P., Kang, S. C., Petersen, R. B., Li, C. and Sy, M. S. (2008). Ligand binding promotes prion protein aggregation--role of the octapeptide repeats. *FEBS Journal.* **275** (5564-5575).

Yun, S. W., Gerlach, M., Riederer, P. and Klein, M. A. (2006). Oxidative stress in the brain at early preclinical stages of mouse scrapie. *Experimental Neurology.* **201** (90-98).

Zabel, M., Greenwood, C., Thackray, A. M., Pulford, B., Rens, W. and Bujdoso, R. (2009). Perturbation of T-cell development by insertional mutation of a PrP transgene. *Immunology.* **127** (226-236).

Zahn, R., Liu, A., Luhrs, T., Riek, R., von Schroetter, C., Lopez Garcia, F., Billeter, M., Calzolai, L., Wider, G. and Wuthrich, K. (2000). NMR solution structure of the human prion protein. *Proceedings of the National Academy of Sciences of the United States of America.* **97** (145-150).

Zanata, S. M., Lopes, M. H., Mercadante, A. F., Hajj, G. N., Chiarini, L. B., Nomizo, R., Freitas, A. R., Cabral, A. L., Lee, K. S., Juliano, M. A., de Oliveira, E., Jachieri, S. G., Burlingame, A., Huang, L., Linden, R., Brentani, R. R. and Martins, V. R. (2002). Stress-inducible protein 1 is a cell surface ligand for cellular prion that triggers neuroprotection. *EMBO Journal.* **21** (3307-3316).

Zeidler, M., Stewart, G., Cousens, S. N., Estibeiro, K. and Will, R. G. (1997). Codon 129 genotype and new variant CJD. *Lancet*. **350** (668).

Zeng, F., Watt, N. T., Walmsley, A. R. and Hooper, N. M. (2003). Tethering the N-terminus of the prion protein compromises the cellular response to oxidative stress. *Journal of Neurochemistry.* **84** (480-490).

Zhou, L. X., Du, J. T., Zeng, Z. Y., Wu, W. H., Zhao, Y. F., Kanazawa, K., Ishizuka, Y., Nemoto, T., Nakanishi, H. and Li, Y. M. (2007). Copper (II) modulates *in vitro* aggregation of a tau peptide. *Peptides.* **28** (2229-2234).

Zhu, F., Davies, P., Thompsett, A. R., Kelly, S. M., Tranter, G. E., Hecht, L., Isaacs, N. W., Brown, D. R. and Barron, L. D. (2008). Raman optical activity and circular dichroism reveal dramatic differences in the influence of divalent copper and manganese ions on prion protein folding. *Biochemistry.* **47** (2510-2517).

Ziegler, J., Sticht, H., Marx, U. C., Muller, W., Rosch, P. and Schwarzinger, S. (2003). CD and NMR studies of prion protein (PrP) helix 1. Novel implications for its role in the PrP^{C} -->PrP^{Sc} conversion process. *Journal of Biological Chemistry*. **278** (50175-50181).

Zlotnik, I. and Stamp, J. T. (1965). Scrapie in a Dorset Down ram. A confirmation of the histological diagnosis by means of intracerebral inoculation of mice with formol fixed brain tissue. *Veterinary Record.* **77** (1178-1179).

National Creutzfeldt-Jakob disease Surveillance Unit for the United Kingdom (NCJDSU). Last updated 7th September 2009. http://www.cjd.ed.ac.uk/figures.htm. Accessed 15th September 2009.

The European and Allied Countries Collaborative Study Group of CJD (EUROCJD). Last updated 8th August 2008. http://www.eurocjd.ed.ac.uk/EUROINDEX.htm. Accessed 15th September 2009.

Appendix I

Sequences for pET3a-mPrP(23-231). pET3a-mPrP(Δ51-89), pET3a-mPrP(Δ67-90). Alignments were performed using CLUSTALW (http://align.genome.jp/). All ambiguous bases (N) were double checked to ensure they were correct.

I. pET3a-mPrP(23-231) sequencing results. Alignment was performed using mPrP 23-231 sequence from mPrP (NM_0011170).

```
CLUSTAL W (1.81) multiple sequence alignment


mPrP_23-231_      ------------------------------------------------------------ATGA
23-231_sequencing     NNANNNNNNNNNNNNNNANTNNNNNNNNTTNNNTTTAANAAGGAGATATACATATGA
                                                                           ****

mPrP_23-231_      AAAAGCGGCCAAAGCCTGGAGGGTGGAACACCGGTGGAAGCCGGTATCCCGGGCAGGGAA
23-231_sequencing AAAAGCGGCCAAAGCCTGGAGGGTGGAACACCGGTGGAAGCCGGTATCCCGGGCAGGGAA
                  ************************************************************

mPrP_23-231_      GCCCTGGAGGCAACCGTTACCCACCTCAGGGTGGCACCTGGGGGCAGCCCCACGGTGGTG
23-231_sequencing GCCCTGGAGGCAACCGTTACCCACCTCAGGGTGGCACCTGGGGGCAGCCCCACGGTGGTG
                  ************************************************************

mPrP_23-231_      GCTGGGGACAACCCCATGGGGGCAGCTGGGGACAACCTCATGGTGGTAGTTGGGGTCAGC
23-231_sequencing GCTGGGGACAACCCCATGGGGGCAGCTGGGGACAACCTCATGGTGGTAGTTGGGGTCAGC
                  ************************************************************

mPrP_23-231_      CCCATGGCGGTGGATGGGGCCAAGGAGGGGGTACCCATAATCAGTGGAACAAGCCCAGCA
23-231_sequencing CCCATGGCGGTGGATGGGGCCAAGGAGGGGGTACCCATAATCAGTGGAACAAGNCCAGCA
                  ************************************************** ******

mPrP_23-231_      AACCAAAAACCAACCTCAAGCATGTGGCAGGGGCTGCGGCAGCTGGGGCAGTAGTGGGGG
23-231_sequencing AACCAAAAACCAACCTCAAGCATGTGGCAGGGGCTGCGGCAGCTGGGGCAGTAGTGGGGG
                  ************************************************************

mPrP_23-231_      GCCTTGGTGGCTACATGCTGGGGAGCGCCATGAGCAGGCCCATGATCCATTTTGGCAACG
23-231_sequencing GCCTTGGTGGCTACATGCTGGGGAGCGCCATGAGCAGGCCCATGATCCATTTTGGCAACG
                  ************************************************************

mPrP_23-231_      ACTGGGAGGACCGCTACTACCGTGAAAACATGTACCGCTACCCTAACCAAGTGTACTACA
23-231_sequencing ACTGGGAGGACCGCTACTACCGTGAAAACATGTACCGCTACCCTAACCAAGTGTACTACA
                  ************************************************************

mPrP_23-231_      GGCCAGTGGATCAGTACAGCAACCAGAACAACTTCGTGCACGACTGCGTCAATATCACCA
23-231_sequencing GGCCAGTGGATCAGTACAGCAACCAGAACAACTTCGTGCACGACTGCGTCAATATCACCA
                  ************************************************************

mPrP_23-231_      TCAAGCAGCACACGGTCACCACCACCACCAAGGGGGAGAACTTCACCGAGACCGATGTGA
23-231_sequencing NNAAGCAGCACACGGTCACCACCACCACCAAGGGGGAGAACTTCACCGAGACCGATGTGA
                    **********************************************************

mPrP_23-231_      AGATGATGGAGCGCGTGGTGGAGCAGATGTGCGTCACCCAGTACCAGAAGGAGTCCCAGG
23-231_sequencing AGATGATGGAGCGCGNGGTGGAGCAGATGTGCGNCACCCAGTACCAGAAGGAGTCCCAGG
                  ************** ***************** ************************

mPrP_23-231_      CCTATTACGACGGGAGAAGATCCAGCTAG
23-231_sequencing CCTATTACGACGGGAGAAGATCCAGCTAG
                  ****************************
```

II. Sequence alignments for pET3a-mPrP(Δ51-89) in blue, and pET3a-mPrP(Δ67-90) in red as compared to the wild type pET3a-mPrP(23-231). Start and stop codons are highlighted in underlined bold.

```
pET3a-mPrP_d51-89_      NNNTTNNNNNTANCTTTAAGAAGGAGATATACATAT
pET3a-mPrP_d67-90_      NNNNNTTGTTTAACTTTAAGAAGGAGATATACATAT
mPrP_23-231_            TNNNNNNNNTTNNNTTTAANAAGGAGATATACATAT
                                                **************

GAAAAAGCGGCCAAAGCCTNNNNNNNNGNAACACCGGTGGAAGCCGGTATCCCGGGCAGGG
GAAAAAGCGGCCAAAGCCTGGANNNNGGAACACCGGTGGAAGCCGGTATCCCGGGCAGGG
GAAAAAGCGGCCAAAGCCTGGAGGGTGGAACACCGGTGGAAGCCGGTATCCCGGGCAGGG
******************        * ********************************

NNNNCCTGGAGGCAACCGTTACCCA-----------------------------------
NAGNCCTGGAGGCAACCGTTACCCACCTCAGGGTGGCACCTGGGGGCAGCCCCACGGTGG
AAGCCCTGGAGGCAACCGTTACCCACCTCAGGGTGGCACCTGGGGGCAGCCCCACGGTGG
**********

------------------------------------------------------------
TGGCTGGGGACAA-----------------------------------------------
TGGCTGGGGACAACCCCATGGGGGCAGCTGGGGACAACCTCATGGTGGTAGTTGGGGTCA
*************

------------------------GGAGGGGGTACCCATAATCAGTGGAACAAGCCCAG
------------------------GGAGGGGGTACCCATAATCAGTGGAACAAGCCCAG
GCCCCATGGCGGTGGATGGGGCCAAGGAGGGGGTACCCATAATCAGTGGAACAAGNCCAG
                         ****************************** ****

CAAACCAAAAACCAACCTCAAGCATGTGGCAGGGGCTGCGGCAGCTGGGGCAGTAGTGGG
CAAACCAAAAACCAACCTCAAGCATGTGGCAGGGGCTGCGGCAGCTGGGGCAGTAGTGGG
CAAACCAAAAACCAACCTCAAGCATGTGGCAGGGGCTGCGGCAGCTGGGGCAGTAGTGGG
************************************************************

GGGCCTTGGTGGCTACATGCTGGGGAGCGCCATGAGCAGGCCCATGATCCATTTTGGCAA
GGGCCTTGGTGGCTACATGCTGGGGAGCGCCATGAGCAGGCCCATGATCCATTTTGGCAA
GGGCCTTGGTGGCTACATGCTGGGGAGCGCCATGAGCAGGCCCATGATCCATTTTGGCAA
************************************************************

CGACTGGGAGGACCGCTACTACCGTGAAAACATGTACCGCTACCCTAACCAAGTGTACTA
CGACTGGGAGGACCGCTACTACCGTGAAAACATGTACCGCTACCCTAACCAAGTGTACTA
CGACTGGGAGGACCGCTACTACCGTGAAAACATGTACCGCTACCCTAACCAAGTGTACTA
************************************************************

CAGGCCAGTGGATCAGTACAGCAACCAGAACAACTTCGTGCACGACTGCGTCAATATCAC
CAGGCCAGTGGATCAGTACAGCAACCAGAACAACTTCGTGCACGACTGCGTCAATATCAC
CAGGCCAGTGGATCAGTACAGCAACCAGAACAACTTCGTGCACGACTGCGTCAATATCAC
************************************************************

CATCAAGCAGCACACGGTCACCACCACCACCAAGGGGGAGAACTTCACCGAGACCGATGT
CATCAAGCAGCACACGGTCACCACCACCACCAAGGGGGAGAACTTCACCGAGACCGATGT
CANNAAGCAGCACACGGTCACCACCACCACCAAGGGGGAGAACTTCACCGAGACCGATGT
**  ********************************************************

GAAGATGATGGAGCGCGTGGTGGAGCAGATGTGCGTCACCCAGTACCAGAAGGAGTCCCA
GAAGATGATGGAGCGCGTGGTGGAGCAGATGTGCGTCACCCAGTACCAGAAGGAGTCCCA
GAAGATGATGGAGCGCGNGGTGGAGCAGATGTGCGNCACCCAGTACCAGAAGGAGTCCCA
**************** **************** ************************

GGCCTATTACGACGGGAGAAGATCCAGCTAGTAAGGATCCGGCTGCTAACA
GGCCTATTACGACGGGAGAAGATCCAGCTAGTAAGGATCCGGCTGCTAACA
```

GGCCTATTACGACGGGAGAAGATCCAGC**TAG**TAAGGATCCGGCTGCTAACA
****